MAR 15 1929

BUREAU OF STANDARDS JOURNAL OF RESEARCH

Vol. 2 MARCH, 1929 No. 3

CONTENTS

RP. No.	TITLE AND AUTHOR	Page
45	Apparatus and methods for the separation, identification, and determination of the chemical constituents of petroleum. Edward Washburn, Johannes H. Bruun, and Mildred M. Hicks	467
46	Recombination spectra of ions and electrons in cæsium and helium. F. L. Mohler and C. Boeckner	489
47	The spectral absorption of certain monoazo dyes. I. The effect of position isomerism on the spectral absorption of methyl derivatives of benzeneazophenol. Wallace R. Brode	501
48	Transmission of sound through wall and floor structures. V. L. Chrisler and W. F. Snyder	541
49	Discharge coefficients of square-edged orifices for measuring the flow of air. H. S. Bean, E. Buckingham, and P. S. Murphy	561

BUREAU OF STANDARDS JOURNAL OF RESEARCH

CONTENTS OF VOLUME 1

Price of bound volume, $2.75

July, 1928 (Vol. 1, No. 1)

RP1. Accelerated tests of organic protective coatings. Percy H. Walker and E. F. Hickson. Price 5 cents.

RP2. Measurement of the tread movement of pneumatic tires and a discussion of the probable relation to tread wear. W. L. Holt and C. M. Cook. Price 5 cents.

RP3. Absolute methods in reflectometry. H. J. McNicholas. Price 10 cents.

RP4. Interferometer measurements of wave lengths in the vacuum arc spectra of titanium and other elements. C. C. Kiess. Price 5 cents.

RP5. Analysis of bauxite and of refractories of high alumina content. G. E. F. Lundell and J. I. Hoffman. Price 5 cents.

August, 1928 (Vol. 1, No. 2)

RP6. Some measurements of the transmission of ultra-violet radiation through various kinds of fabrics. W. W. Coblentz, R. Stair, and C. W. Schoffstall. Price 5 cents.

RP7. Tinting strength of pigments. H. D. Bruce. Price 5 cents.

RP8. Wave-length measurements in the arc and spark spectra of hafnium. William F. Meggers. Price 5 cents.

RP9. Tests of the effect of brackets in reinforced concrete rigid frames. Frank E. Richart. Price 25 cents.

RP10. Accelerated laboratory corrosion test methods for zinc-coated steel. Edward C. Groesbeck and William A. Tucker. Price 35 cents.

September, 1928 (Vol. 1, No. 3)

RP11. Standard solar wave lengths (3592-7148A). Keivin Burns, William F. Meggers, and C. C. Kiess. Price 5 cents.

RP12. Wave lengths and Zeeman effects in yttrium spectra. William F. Meggers. Price 10 cents.

RP13. Wear and mechanical properties of railroad bearing bronzes at different temperatures. H. J. French, S. J. Rosenberg, W. LeC. Harbaugh, and H. C. Cross. Price 35 cents.

RP14. Steel for casehardening—normal and abnormal steel. S. Epstein and H. S. Rawdon. Price 35 cents.

RP15. Strain markings in mild steel under tension. H. S. Rawdon. Price 15 cents.

Research papers are available as separates for purchase from the Superintendent of Documents United States Government Printing Office, Washington, D. C.

[Continued on page 3 of cover]

DEPARTMENT OF COMMERCE
BUREAU OF STANDARDS
George K. Burgess, Director

BUREAU OF STANDARDS JOURNAL OF RESEARCH

March, 1929
Vol. 2, No. 3

$2.75 PER YEAR ON SUBSCRIPTION
Sold only by the Superintendent of Documents, U. S. Government Printing Office
Washington, D. C.

UNITED STATES
GOVERNMENT PRINTING OFFICE
WASHINGTON
1929

For a list of previous research papers appearing in Volumes 1 and 2, BUREAU OF STANDARDS JOURNAL OF RESEARCH, see pages 2, 3, and 4 of the cover

APPARATUS AND METHODS FOR THE SEPARATION, IDENTIFICATION, AND DETERMINATION OF THE CHEMICAL CONSTITUENTS OF PETROLEUM

By Edward W. Washburn, Johannes H. Bruun, and Mildred M. Hicks

ABSTRACT

This paper contains a description of the following apparatus and methods:

1. A rectifying still with a 20-plate column and with means for independently controlling and measuring the temperatures of the plates. The still is designed for distillation in a stream of an inert gas (CO_2) with or without boiling.

2. All-glass rectifying stills for vacuum distillation. They are heated by immersion in an electrically heated bath of nickel shot.

3. Various types of molecular stills by means of which distillation can be carried out at any temperature at which the vapor pressure at the distilling surface is not lower than the degree of vacuum attainable.

4. Methods and apparatus for fractionation by crystallization or melting.

5. An apparatus for combustion analysis, with special provisions for purifying the oxygen employed and with all rubber connections eliminated. With the aid of this apparatus the formula for any hydrocarbon up to C_{100} can be determined.

The change in the iodine number of a petroleum oil produced by heating it for different periods and at different temperatures up to 370° C. in (*a*) air and (*b*) H_2, N_2, and CO_2, respectively, has been determined, and it is shown that in the absence of air this change is greatly reduced.

Evidence is presented showing that the hazards from exposed mercury surfaces in a laboratory are eliminated as soon as the mercury surface becomes contaminated with a continuous layer of a heavy oil or grease.

CONTENTS

PART 1

Page

I. Introduction 468

PART 2

II. A rectifying still for distillation in a current of inert gas 470
1. The distillation train 470
2. Distillation of the gas oil 472

PART 3

III. The effect of high temperatures upon petroleum in the presence of hydrogen, nitrogen, or carbon dioxide 473

PART 4

IV. Glass rectifying stills for vacuum distillation 476

PART 5

Page
V. Molecular stills 476
1. The essential features of the molecular still 477
2. Types of construction 477
3. History of the molecular still 478
4. Rate of distillation 478
5. Selection of the cooling agent 480
6. Azeotropic mixtures 481
7. Illustrative experiments 482

PART 6

VI. Methods of fractionation by crystallization or melting and of determining freezing-point curves 483

PART 7

VII. Apparatus for combustion analysis 487

PART 8

VIII. Summary 487

PART 1

I. INTRODUCTION

By Edward W. Washburn

In cooperation with the American Petroleum Institute, the Bureau of Standards is conducting an investigation, the object of which is the development of methods for fractionating petroleum into its chemical constituents and for identifying these constituents. An examination of the literature on the composition of petroleum discloses the reported existence of a large number of different hydrocarbons to which formulas and values of physical properties have been assigned. A study of the evidence presented in identification of these "compounds," however, impresses one chiefly because of its inadequacy. In fact, with the exception of some of the lower boiling constituents, most of the compounds whose existence has been reported must be classed as purely fictitious in the light of the evidence at present available.[1]

Most of the previous work on the problem of the constitution of petroleum has rested almost entirely upon the results of fractional distillation, a process which is in many instances inadequate for effecting complete separation of the mixture into its constituents. In attacking the problem anew it was decided to fractionate by both distillation and crystallization, so that constant boiling mixtures might be broken up by crystallization and constant freezing mixtures by distillation. In this way complete separation can ultimately be

[1] See, for example, Burrell, Ind. Eng. Chem., **20**, p. 602; 1928.

attained. The purpose of the present paper is to describe the apparatus and methods employed.

In undertaking the present investigation it was decided to take advantage of the initial fractionation resulting from a commercial straight-run distillation of a petroleum sample from a single pool. Since the lower boiling fractions of such a distillation have been investigated to some extent by other investigators, it was decided to start the present work with what is known commercially as the gas-oil fraction. Through the courtesy of Dr. W. Van Der Gracht, of the Marland Oil Co., of Oklahoma, a petroleum sample from the Oklahoma field was subjected to a straight-run distillation, and all of the fractions resulting therefrom were sent to the bureau. The general characteristics of these fractions are presented in Table 1.[2]

TABLE 1.—*Distillation of petroleum from No. 6 well of the South Ponca Field, Kay County, Okla.*

WILCOX SAND

Property	Naphtha		Kerosene	Gas oil [1]	Wax distillate	Bottoms (color, brown)
Yield ..... per cent..	16.4	22.9	15.4	16.0	18.1	10.2
Gravity ..... °API..	64.8	52.0	41.5	34.6	29.1	18.1
Boiling point:						
Initial ..... °F..	126	214				
End ..... do....	358	436				
Flash point ..... do....			158	225	325	545
Fire point ..... do....			180	275	390	620
Saybolt sec					106 at 100° F.	207 at 210° F.
Congelation ..... °F..					80	92

[1] Contained 0.28 per cent S.

The first step in the further fractionation of the gas-oil fraction required a still of such capacity as to necessitate construction from metal. It was impossible to carry out the distillation by boiling under atmospheric pressure, since decomposition occurs at the temperatures required. The usual recourse under such circumstances is to employ vacuum distillation. A vacuum distillation, however, possesses certain disadvantages. In the first place the lowest boiling fraction contains hydrocarbons which are gases at ordinary temperatures and pressures, and this fraction would be lost in a vacuum distillation unless a collecting pump were employed. In the second place it is difficult to construct a still with gasket connections, for operation at relatively high temperatures, which will remain absolutely vacuum tight throughout the considerable period of time covered by the distillation. The presence of very slight leaks would, it is true, not interfere with the maintenance of the necessary vacuum, since the vacuum pump could easily take care of them. Such slight leaks,

[2] Since the receipt of this material a second lot of 1,000 gallons from the same well has been obtained and 500 gallons are to be subjected to a commercial straight-run low-temperature distillation with 2 per cent cuts. Work upon the further fractionation of the lowest boiling of these fractions is now under way.

however, whose presence would be difficult to detect during the distillation, would result in the introduction of traces of oxygen into the still, and oxygen has a pronounced effect in promoting the cracking of hydrocarbon vapors at high temperatures.

In order, therefore, to avoid the use of vacuum distillation, it was decided to carry out the process in a series of isothermal steps in each of which the temperature of the liquid in the still pot is kept constant (and low enough to avoid cracking) while distillation is compelled to proceed by passing through the liquid a fine stream of bubbles of previously heated oxygen-free carbon dioxide. Then, after passing through condensers, this carbon dioxide is absorbed by a solution of KOH, above which remains the fraction composed of the uncondensed hydrocarbon gases. Previous studies, described below, demonstrated that under these conditions cracking is reduced to a minimum. Obviously, in this process the pressure both inside and outside the still is approximately atmospheric, being slightly higher on the inside so that no leakage into the still can occur.

In constructing the still it was decided to provide the plates in the rectifying column with separate heaters and thermocouples so that the temperatures of these plates could be independently controlled and measured.

PART 2

II. A RECTIFYING STILL FOR DISTILLATION IN A CURRENT OF INERT GAS

By Johannes H. Bruun and Mildred M. Hicks

1. THE DISTILLATION TRAIN

The elements of the train will be described in the order of passage of the inert gas from its storage cylinder to its final absorption. (See fig. 1.)

(*a*) The Purification Train.—The CO_2 from its storage cylinder, *1*, passes first through two drying tubes, *2*, filled with "dehydrite" ($MgClO_4.3H_2O$), then through a flow meter, *3*, into a pyrex glass tube, *4*, filled with copper shavings and heated electrically to 650° C. Glass or copper-to-glass seals are used for all connections in this part of the train.

(*b*) The Manometer and Safety Valves.—The CO_2 from the furnace tube passes first through a cooling coil and then past a mercury manometer, *5*, provided with a safety valve, *6*. (For details, see fig. 2.) This manometer registers the total pressure of the gas, which in turn is determined by the depth of liquid in the still pot plus that on the plates of the rectifying column.

B. S. Journal of Research, RP45

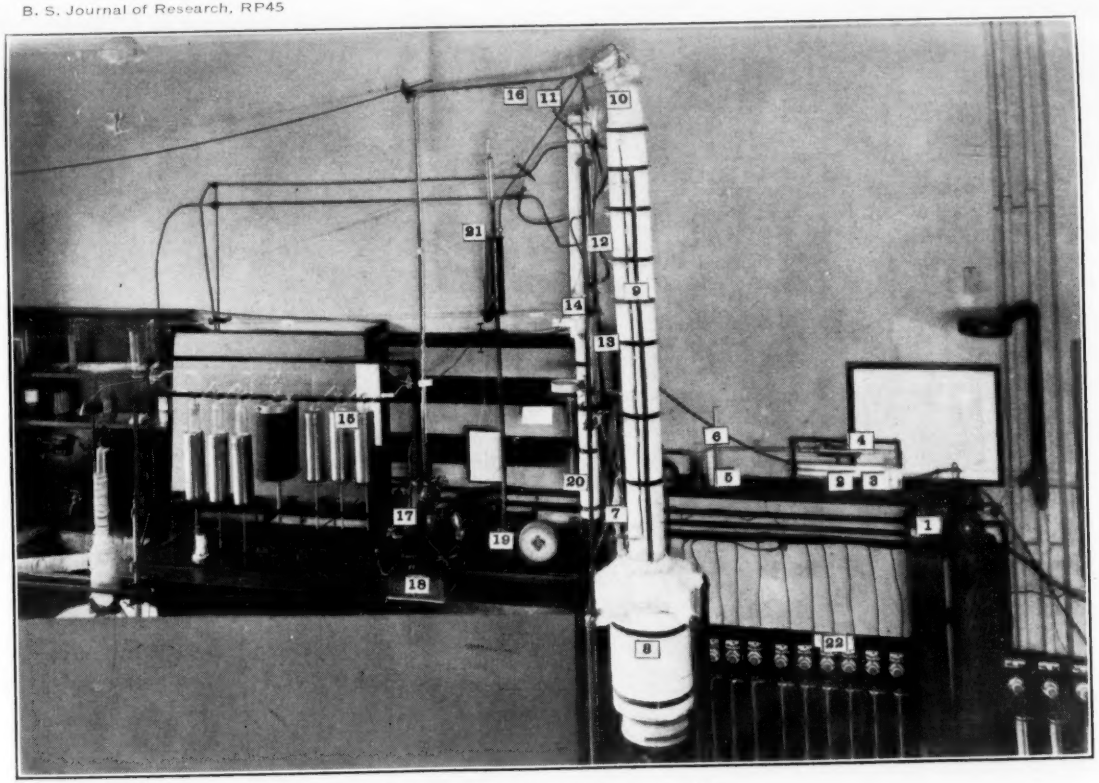

FIG. 1.—*Rectifying-still assembly*

The safety valve acts with either increase or decrease of pressure to prevent any access of air to the gas stream. An automatic shut-off valve prevents any possible back flow of liquid from the still in the event of accidental interruption of gas pressure.

The CO_2 enters the still pot at *7*, first passing through a copper tube provided with an electrical heating coil. At the bottom of the still pot this tube is bent to form a large ring which is perforated so as to break up the gas flow into numerous streams of fine bubbles.

(*c*) THE STILL POT (*8* in fig. 1. For detail, see fig. 3).—The pot holds about 20 liters. It is made of welded steel and is joined to the column by a reinforced bolted flange sealed with a copper-ring gasket. The pot is heated by three independent electric heaters, one at the

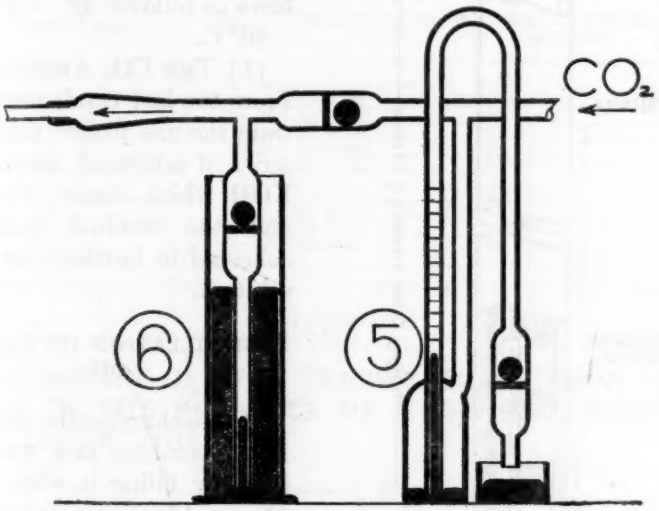

FIG. 2.—*Manometer and safety valve*

bottom and two coiled around the cylinder. A thermocouple is located about 2 inches above the bottom of the pot.

(*d*) THE FRACTIONATING COLUMN.—The column, *9*, contains 20 plates. Each plate is provided with an independent heating coil and alternate plates with thermocouples. These heating coils, together with the insulating covering of the column, serve to maintain the desired temperature conditions in the column and make it possible to clear the column at the end of the distillation. The top of the column contains a reflux condenser, *10*, the temperature of which (as indicated by a thermocouple) is controlled by circulating oil from a special heating and pumping system, *14*, *20*, *19*, and *21*.

(*e*) THE CONDENSERS.—The gas and vapor stream, after leaving the column, passes around a well containing a thermocouple and enters the first condenser, *12*, through a copper tube, *11*, provided with a heating coil to prevent the formation of a solid condensate.

This tube is connected by a copper-to-glass seal to the inner tube of a vertical Liebig condenser, cooled by air or water of controlled temperature. (For detail, see fig. 3.) The condensate from this condenser is received in the graduated tube, *13*, from the top of which the gas stream passes first through a water-cooled condenser, *15*, and then through a series of condensers of decreasing temperatures as follows: 0°, −15°, and −80° C.

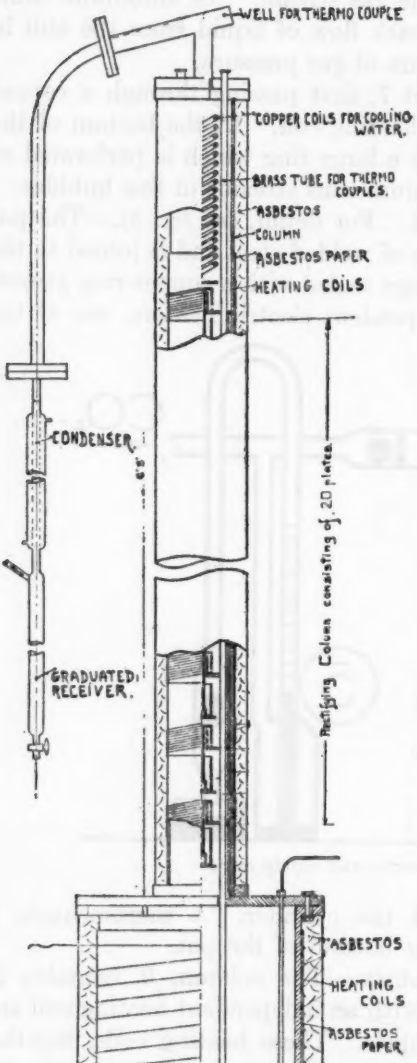

FIG. 3.—*Rectifying-still detail*

(*f*) THE CO_2 ABSORBERS.—From the last condenser of the train the gas passes through a series of saturated solutions of KOH which absorb the CO_2, and the residual gases are collected in bottles over KOH solution.

2. DISTILLATION OF THE GAS OIL

Before charging the still it was first assembled and tested for leaks by filling it with CO_2 at 25 pounds pressure and allowing it to stand for 15 days. At the end of this time the gauge showed a pressure of 25 pounds. The still pot was then charged with gas oil to about three-fourths of its capacity. A stream of dry oxygen-free CO_2 at the rate of 150 cm^3 per minute was first bubbled through the oil for five hours at room temperature in order to remove dissolved air and water. The temperature of the still pot was then gradually raised until all of the plates of the column were filled as shown by the reading

of the manometer. (Fig. 2.) The heating coils of the plates were then adjusted so as to give a controlled gradient of about 70° C. between the bottom and top plates of the column. The temperature of the reflux condenser was set about 2° lower than the temperature of the upper plate. As distillation proceeded, the temperature of the still pot was raised from time to time, with corresponding adjustments of the column, until the temperature of the liquid in the pot reached 350° C. The column was then cleared by gradually raising the temperature of the plates in succession, beginning with the lowest one. Table 2 gives the results of the distillation.

TABLE 2.—*Distillation data*

Serial number of fraction	Time	Temperature, top of column	Temperature, bottom of column	Volume of fraction
	H. *M.*	°*C.*	°*C.*	*cm*³
3	6 --	107 to 221	About 306	910
4A	10 20	222 to 232	307 to 312	910
4B	13 40	233 to 237	313 to 316	565
5	16 40	238 to 252	317 to 321	845
6	19 --	253 to 267	322 to 327	875
7	20 --	268 to 274	328 to 330	860
8	23 --	275 to 279	330 to 335	860
9	31 --	280 to 285	336 to 344	890
10	32 20	286 to 301	345 to 351	910
Bottoms				7,800

PART 3

III. THE EFFECT OF HIGH TEMPERATURES UPON PETROLEUM IN THE PRESENCE OF HYDROGEN, NITROGEN, OR CARBON DIOXIDE

By Johannes H. Bruun

Before the selection of carbon dioxide as the inert gas for use in the distillation procedure just described, experiments were made with different inert gases to determine the effects of these gases upon the tendency of the oil to crack at the temperatures employed in the distillation.

These experiments were carried out in the apparatus shown in Figure 4. The entire assembly is made of pyrex glass. The gas employed is first purified, preheated, and then passed continuously into the oil, which is heated to definite temperatures for different intervals of time. The amount of cracking is estimated by comparing the iodine numbers of the oil before and after subjecting it to this treatment. The inert gas passes from its storage cylinder through a drying tower, *1*, filled with magnesium perchlorate trihydrate and then into an electrically heated furnace, *2*, containing copper shavings for the removal of oxygen (temperature 650° C.).

A cooling coil, *5*, is placed next in the train, and this is followed by a second drying tube, *6*. The gas is then preheated, *7*, and bubbled into the flask containing the oil in contact with copper and brass turnings. A mercury-seal safety valve, *8*, is placed between the heater and the flask, thus taking care of any excess pressure.

The inert gas is first allowed to bubble through the oil at room temperature for two hours in order to free it from dissolved or occluded gases or water vapor. The temperature is read from a thermometer suspended in the flask. The flask is provided with a reflux column kept at room temperature, using an air blast when necessary. A cotton-filled bulb in the gas outlet at the top of the column frees the gas from any oil spray, and the gas is then forced

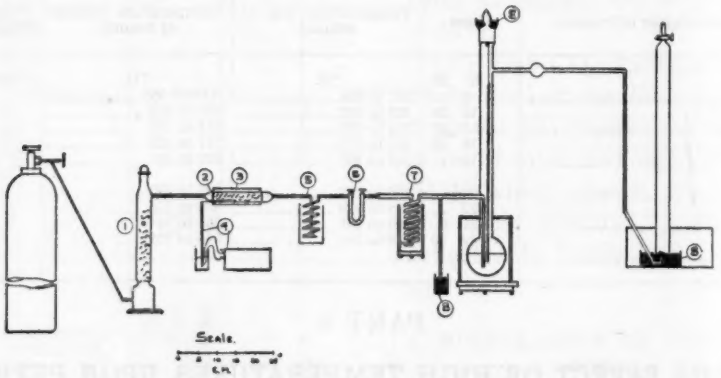

FIG. 4.—*Apparatus for studying cracking behavior*

1, Drying jar with Mg perchlorate trihydrate; *2*, copper tube filled with copper shavings; *3*, electrical heating coils; *4*, potential meter and thermocouple; *5*, cooling coils; *6*, drying tube; *7*, preheater; *8*, mercury seal

through a mercury seal. The hydrogen and nitrogen are allowed to escape, but the carbon dioxide is absorbed in a tower filled with a saturated solution of potassium hydroxide. Using the "wax distillate" from the original distillation (see Table 1), the following results were obtained (Table 3):

TABLE 3.—*Cracking behavior of raw-wax fraction in the presence of various gases*

EFFECT OF NATURE OF GAS—THREE HOURS' HEATING AT 370° C.

Gas	Iodine number		
	Before	After	Increase
N_2	16.0	17.5	1.5
H_2	16.0	17.4	1.4
CO_2	16.0	17.2	1.2

TABLE 3.—*Cracking behavior of raw-wax fraction in the presence of various gases* —Continued

EFFECT OF CO_2—VARIATION WITH TIME OF HEATING AT 370° C.

Time (hours)	Iodine number		
	Before	After	Increase
0.5	16.0	16.4	0.4
3	16.0	17.2	1.2
20	16.5	21.5	5.0

EFFECT OF CO_2—VARIATION WITH TEMPERATURE FOR A 20-HOUR HEATING PERIOD

t (° C.)	Iodine number		
	Before	After	Increase
100	16.5	16.6	0.1
200	16.1	16.1	.0
250	16.7	16.8	.1
315	16.4	16.8	.4
350	16.7	19.4	2.7
370	16.7	21.5	5.0

EFFECT OF BOILING IN CONTACT WITH AIR FOR 20 HOURS WITH A RETURN CONDENSER

B. p. (° C.)		Iodine number		
Initial	After 20 hours	Initial	After 20 hours	Increase
370	330	16.3	59.1	42.8

TABLE 4.—*Cracking behavior of refined wax*[1] *(containing 0.09 per cent sulphur) in the presence of CO_2 during 20 hours' heating at various temperatures*

t (° C.)	Iodine number		
	Before	After	Increase
200	11.4	11.5	0.1
250	11.4	11.4	.0
320	11.4	11.5	.1
360	11.4	16.7	5.3

[1] The raw-wax fraction contained 0.28 per cent S. After washing with concentrated H_2SO_4 this was reduced to 0.09 per cent. At the same time the iodine number fell from 16 to 11.4.

From these results it is clear that in the presence of these inert gases little change in iodine number occurs during prolonged heating up to 320° C., and even at 370° the iodine number increases only one unit at the end of three hours' heating.

PART 4

IV. GLASS RECTIFYING STILLS FOR VACUUM DISTILLATION

By Johannes H. Bruun

The fractions obtained from the disillation in the large still are listed above in Table 2. The next step in the fractionation is to subject these fractions to further distillation in vacuo. For this purpose a series of all-glass stills of successively decreasing size is employed. These stills are all of the same general type which is shown in Figure 5. The rectifying column is vacuum or air jacketed and packed with steel "jack chain."[3]

The air jackets are provided with external heating coils to control the reflux. Thermometers or thermocouples are used for indicating the temperatures of the still pot and of the top of the column. A filling tube permits intermittent feeding of liquid into the still pot without breaking the vacuum and, by closing the stopcock and admitting CO_2 to the receiver and condenser, fractions can be withdrawn from the receiver without breaking the vacuum in the still proper. All stopcocks are partially sealed with mercury seals, and the still is heated by an electrically heated bath of nickel shot. This bath is a good heat conductor, does not oxidize or smoke, and at any time can be rapidly cooled by means of an air blast. The still is connected through a liquid-air trap and an intermediate ballast (a 3-liter flask) to a mercury diffusion pump and McLeod gauge.

For each fraction at least three of the following properties are determined—density, initial freezing point, initial boiling point, refractive index, viscosity—and on the basis of these properties the fractions are combined for further fractionation by distillation, crystallization, or melting. A series of flow charts (illustrated in fig. 6) is kept, showing the complete fractionation history of each fraction. Up to date (August, 1928) the original 15-liter gas-oil fraction has been separated into over 600 different fractions.

A preliminary combustion analysis and molecular weight determination on one of the still impure fractions (fig.15) indicated an empirical formula in the neighborhood of $C_{18}H_{36}$.

PART 5

V. MOLECULAR STILLS

By Edward W. Washburn

The higher melting paraffin waxes can be heated without decomposition only to temperatures at which their vapor pressures are very small. With the usual types of vacuum stills it has not generally been considered feasible to make separations at vapor pressures below a few millimeters; but many substances, which ordinarily are not distilled

[3] Dean, Hill, Smith, and Jacobs, Bureau of Mines, Bulletin 207, p. 9; 1922.

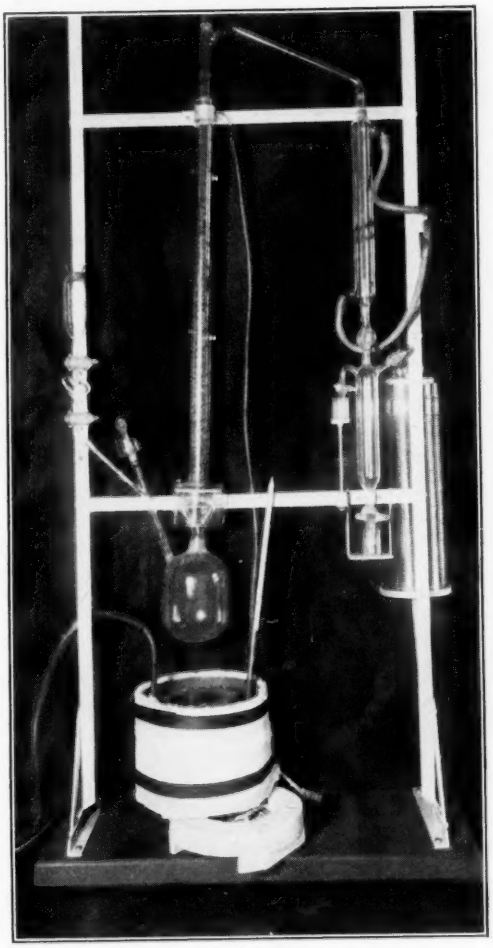

FIG. 5.—*Rectifying still for vacuum distillation*

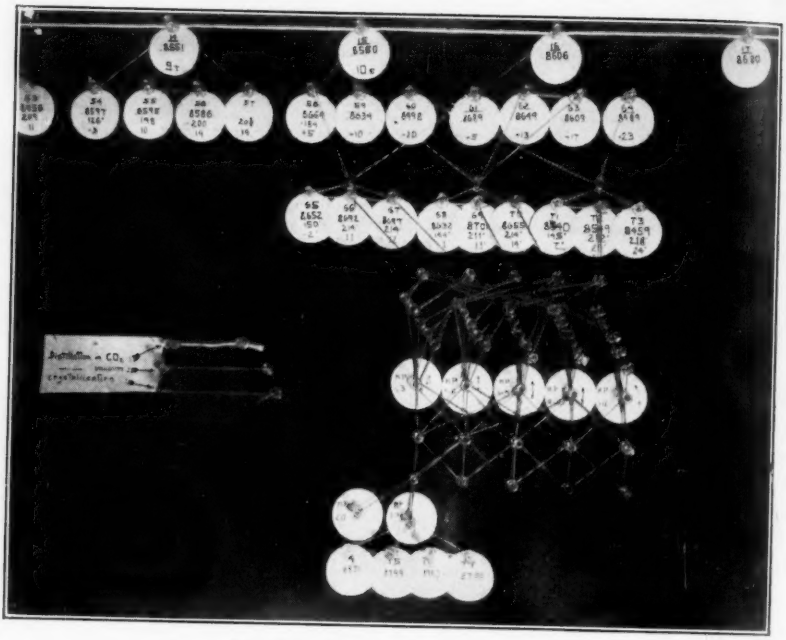

FIG. 6.—*Fractionation flow chart*

FIG. 7.—*Group of molecular stills*

because they can not be heated without decomposition, can be rather easily distilled even at room temperatures by what may be called a "molecular still," a type first used by Brönsted and Hevesy[4] for separating the isotopes of mercury.

1. THE ESSENTIAL FEATURES OF THE MOLECULAR STILL

The essential features of this type of still are the following:

1. A high vacuum. For securing this vacuum, means should be available for producing a vacuum equal to, or preferably better than, the vapor pressure of the substance at the temperature at which it is to be distilled.

2. A large and clean area of evaporating surface.

3. A short distance between the evaporating surface and the condenser.

4. A sufficient temperature difference between the distilling surface and the condensing surface.

With a still constructed according to these principles such materials as mercury, paraffin wax, and calomel, for example, can be distilled at room temperature. It is not necessary that the substance to be distilled be in the liquid state at the distilling temperature, although fractionation without the necessity of provision for artificial stirring is, of course, more rapid with liquids.

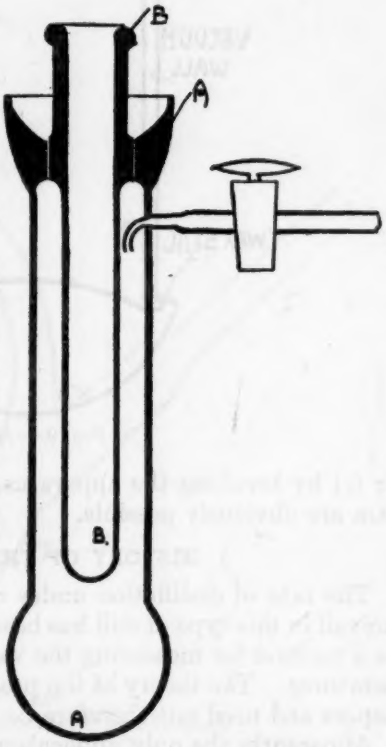

FIG. 8.—*Molecular still*

2. TYPES OF CONSTRUCTION

Various forms of molecular stills are shown in accompanying Figures 7, 8, 9, 10, and 11. In all cases the substance to be distilled is placed in the receptacle *A* and the cooling agent (for example, liquid hydrogen, liquid air, carbon dioxide snow mixed with a suitable liquid, ice and salt, etc., according to the temperature gradient required) is placed in the receptacle *B*. The forms shown in Figures 10 and 11 make it possible to distribute the substance to be distilled in a layer over the interior surface of the vessel *A*, with consequent increase in the rate of distillation. The temperature of the substance in *A* during the distillation is controlled by immersing this part of the apparatus

[4] Brönsted and Hevesy, Phil. Mag., **43**, p. 31; 1922.

in a suitable bath (for example, mercury) provided with a means for regulating its temperature.

The forms shown in Figures 8 and 11 are designed to permit the easy removal of the distillate. In the case of the forms shown in Figures 9 and 10 separation may be effected (*a*) by pipetting out or dissolving out the undistilled residue, (*b*) by freezing the undistilled residue, inverting the apparatus, melting the distillate, and allowing it to flow into a position from which it can be removed by a pipette,

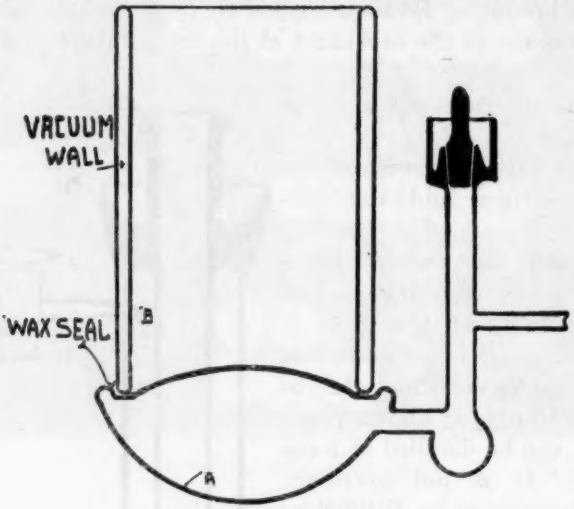

FIG. 9.—*Molecular still*

or (*c*) by breaking the apparatus. Various other forms of construction are obviously possible.

3. HISTORY OF THE MOLECULAR STILL

The rate of distillation under conditions analogous to those which prevail in this type of still has been employed by Langmuir and others as a method for measuring the vapor pressure of metals at high temperatures. The theory of the process is fully discussed in Langmuir's papers and need not therefore be repeated here.[5]

Apparently the only application of the molecular still for purposes of purification by fractional distillation is that described by Brönsted and Hevesy, who used it to separate the isotopes of mercury.[6] It should have, however, a wide range of utility as a general laboratory method, particularly for substances which can not be distilled by the customary methods on account of decomposition.

4. RATE OF DISTILLATION

Under conditions such that no recondensation occurs on the evaporating surface the rate of distillation of a given molecular

[5] See, for example, Jones, Langmuir, and Mackay, Phys. Rev., **30**, p. 201; 1927; and the literature there cited. See also Knudsen, Ann. Phys., **47**, 697; 1915.

[6] See footnote 4, p. 477.

species in a molecular still may be calculated by means of the Langmuir equation

$$n = pS\sqrt{\frac{1}{2\pi MRT}} \qquad (1)$$

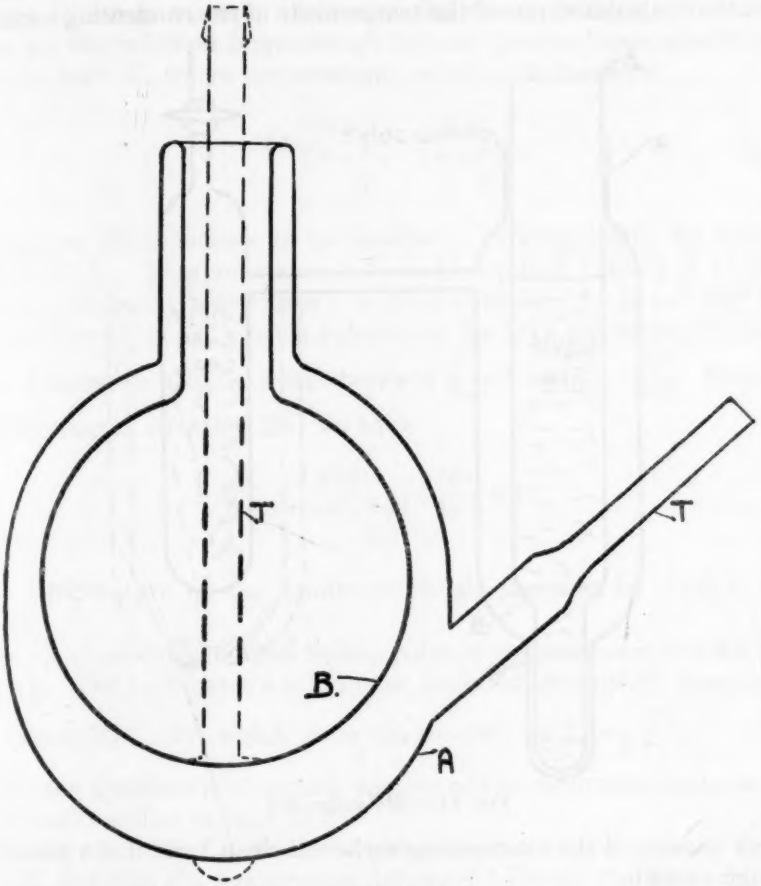

FIG. 10.—*Molecular still. Dewar-flask type*
The tube *T* may be placed in either of the two positions shown

in which n is the number of moles of the substance which distill in one second, p is its vapor pressure at the evaporating surface at $T°$ K., and S is the effective area. M is the molecular weight and R the gas constant. For example, if $M=400$, $p=0.001$ mm Hg, $S=10$ cm^2, and $T=300°$ K., we find

$$n = 0.001 \times 1333 \times 10\sqrt{\frac{1}{2 \times 3.14 \times 8.32 \times 10^7 \times 300 \times 400}}$$

$$= 17 \times 10^{-7} \text{mole/sec.} = 0.7 \text{ mg/sec.}$$

The actual rate of distillation will, in general, be less than the calculated value, owing to some reflection of molecules from the condensing surface, but such reflection will at worst never amount to more than 90 per cent,[7] so that the actual rate will never be less than 0.1 of the calculated rate if the temperature of the condensing surface

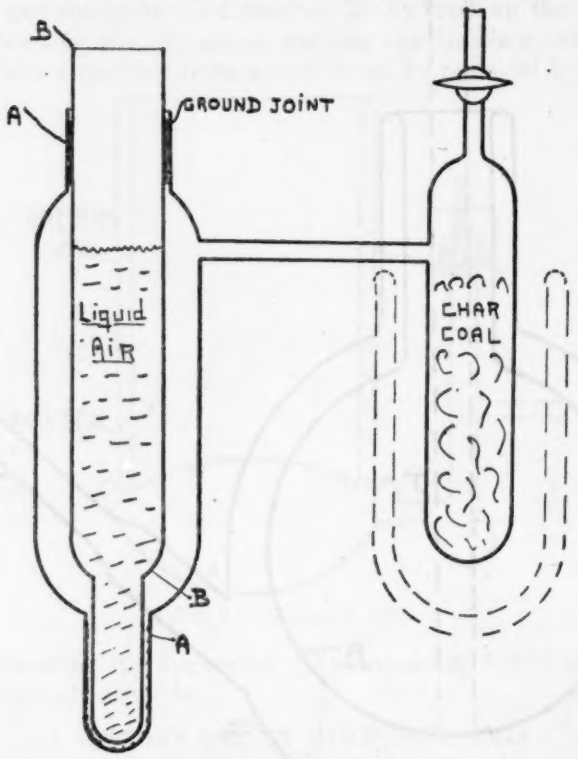

FIG. 11.—*Molecular still*

is low enough, if the evaporating surface is clean,[8] and if the vacuum is high enough.

5. SELECTION OF THE COOLING AGENT

The cooling agent may be selected from the following considerations: p_e = the vapor pressure at the temperature T (°K.) of the evaporating surface, and p_c = the desired vapor pressure at the temperature $(T-\Delta t)$ of the condenser. Let $\frac{p_e}{p_c}=x$. Then

$$\Delta t \lessdot \frac{T \log_{10} x}{\log_{10} x + \phi \frac{T_B}{T}} \text{ approx.} \qquad (2)$$

in which T_B is the normal boiling point in °K. If this is known, the constant ϕ can be obtained from International Critical Tables, vol-

[7] Langmuir, Phys. Rev., **7**, p. 176; 1916; and International Critical Tables, **5**, p. 53.
[8] Clean; that is, free from a layer of lower volatility. *v. infra.*

ume 3, page 246. This relation assumes that the condensate is in the form of a supercooled liquid. In many cases it will be crystalline, in which case the required Δt will be smaller than that given by the above relation.

The following example illustrates the use of relation (2): If we take $x=100$, which is large enough for any practical case, and if we put $T=300°$ K. (room temperature), relation (2) becomes

$$\Delta t \lessdot \frac{300\times 2}{2+\phi\frac{T_B}{T}} = \frac{600}{2+\phi\frac{T_B}{T}} \tag{2a}$$

Suppose the substance to be distilled is anthraquinone, for which $T_B=653°$ K. This substance falls in Group 0 of Table 3 (I. C. T., vol. 3, p. 247) and from Figure 1 (p. 246) we find $\phi=5.0$ at $t_B=380°$ C. From figure 2 (p. 247), using benzene as the type substance, we find that ϕ increases about 0.5 unit between $\frac{T}{T_B}=1$ and $\frac{T}{T_B}=\frac{300}{653}$. Hence, substituting in equation (2a) we have

$$\Delta t \lessdot \frac{600}{2+5.5\times\frac{653}{300}} \lessdot \frac{600}{12.9} \lessdot 46°$$

The temperature of the condenser should therefore be $-19°$ C. or lower.

In many cases the normal boiling point of the substance will not be known. For such cases a safe upper limit for Δt may be computed by taking $T_B \lessdot 1.5T$, which gives (for $x=100$) $\Delta t_{max.}=\frac{2T}{2+1.5\phi}$.

For the distillation of organic compounds at room temperatures it will usually suffice to take $\Delta t \lessdot 60°$.

In this connection it should be pointed out that the ordinary type of still, in which the temperature difference between distilling surface and condensing surface is small and in which the rate of distillation is proportional to the difference between the two vapor pressures, is also capable of practical operation for distillations with vapor pressures as low as 0.05 mm., if the condenser is placed within the distillation chamber as in the apparatus described by Volmer.[9]

6. AZEOTROPIC MIXTURES

If the mixture which is being distilled is an azeotropic mixture, no separation is secured in the ordinary types of stills. In the molecular still, however, fractionation of such a mixture will, in general, result, as Brönsted and Hevesy have pointed out, because from equation

[9] Volmer, Z. angew. Chem., **34**, p. 150; 1921.

(1) it is evident that the rate of evaporation of a given molecular species is determined not alone by its partial vapor pressure, but also by its molecular weight. There is, however, also a condition under which no fractionation will occur in a molecular still, namely, when the ratio $\frac{p_1}{p_2}\left(\frac{M_2}{M_1}\right)^{\frac{1}{2}}$ is equal to the molecular ratio $\frac{n_1}{n_2}$ in the liquid phase, for each of any two molecular species present. Under these conditions the condensate would have the same composition as the original liquid. For mixtures which are ideal solutions this is equivalent to the condition that the ratio $\frac{p_o}{M^{\frac{1}{2}}}$ shall be the same for all molecular species present, p_o being the vapor pressure in the pure state. Since, however, for members of the same homologous series p_o decreases as M increases, fractionation of such mixtures in a molecular still is advantageously affected by the variations in both p_o and M.

The condition that $\frac{n_1}{n_2}=\frac{p_1}{p_2}\left(\frac{M_1}{M_2}\right)^{\frac{1}{2}}$ might, however, conceivably occur quite as frequently as the condition of azeotropism in ordinary distillation. The case that any mixture will satisfy the conditions for distilling in unchanged proportions by both methods is limited to mixtures of substances of equal molecular weights and equal vapor pressures at all temperatures and will never be encountered except with mixtures of two optical isomers. Hence, practically every mixture should be subject to fractionation in either the usual still or the molecular still. It might, of course, be possible that a series of alternate fractionations by the two methods would be necessary to accomplish the most complete separation, if distillation alone is employed.

7. ILLUSTRATIVE EXPERIMENTS

A sample of paraffin wax having an initial freezing range of 54.1 to 51.7° was separated into two fractions by a single distillation at 55° C. in the still shown in Figure 9, using carbon dioxide snow as the cooling agent. The distillate had a freezing range of 48.6 to 48° and the residue a freezing range of 57.1 to 56.5°.

A sample of cane sugar was distilled at 120° C. The distillate was a white solid, sweet in taste and dextro rotatory in aqueous solution.

Another example of the use of stills of the general type shown in Figures 8 and 10 is described in connection with Brönsted and Hevesy's experiments on the isotopic separation of mercury.[10]

Since mercury is a convenient substance for testing the efficiency of a given type of molecular still with reference to the rate of dis-

[10] See footnote 4, p. 477.

tillation obtainable in practice as compared with the rate calculated from equation (1), an experiment was carried out with mercury in the still, shown in Figure 10. The lower part of the still containing the liquid mercury was immersed in a bath of mercury kept at 0° by means of an ice pack. A thermometer inserted through the side arm indicated the average temperature of the distilling surface during the distillation. Liquid air was placed in the inner chamber *B*. The following results were obtained:[11]

Time of distillation	hours	4.0
Area of distillation surface	cm^2	48.0
Temperature of distilling surface	°C	−0.2
Vapor pressure at distilling surface	mm	0.00018
Weight of distillate obtained	g	5.2
Weight of distillate calculated	do	6.2
Efficiency	per cent	84

The test experiments with the molecular still on mercury, paraffin wax, and calomel were carried out by Mildred M. Hicks; those with cane sugar, by Dr. R. T. Leslie and S. T. Schicktanz.

PART 6

VI. METHODS OF FRACTIONATION BY CRYSTALLIZATION OR MELTING AND OF DETERMINING FREEZING-POINT CURVES

By Mildred M. Hicks

In addition to its value as a primary method, fractionation by crystallization or fusion is convenient for breaking up azeotropic mixtures. The fractionation may be carried out either with or without the use of a solvent. For the higher petroleum fractions, such as lubricating oil, petrolatum, or wax, the use of a solvent is usually desirable.

The following solvents have been studied in this connection: Methyl alcohol, glycerol, ethyl ether, acetone, chloroform, carbon

[11] *Note on poison hazards from spilled mercury.*—In recent literature attention has been directed to the dangers of mercury poisoning in rooms containing exposed mercury surfaces resulting from spilled mercury lodged in floor cracks and other crevices from which its removal is difficult. The vapor pressure of pure mercury at room temperatures is of the order 0.001 to 0.003 mm Hg, and if the air of the room were only partially saturated with this mercury vapor, continued exposure thereto might constitute a hazard. One experiment on the rate of distillation of mercury carried out as described above apparently throws some light upon the question.

In this experiment the distillation was carried out for seven hours. Instead, however, of obtaining approximately the theoretical yield of 9 g of distillate, no distillate whatever was obtained. Examination of the mercury surface showed that it was contaminated with a barely visible layer of stopcock grease which was apparently sufficient to completely stop appreciable vaporization in this period of time. It seems probable, therefore, that the hazard from spilled mercury in a laboratory soon disappears by the natural contamination of the mercury surface in a short period of time. In any case a spray of heavy oil on the surface of spilled mercury would appear to be an adequate means of eliminating all hazard in ventilated rooms.

This is also the conclusion reached by Gaede (Ber. Naturforsch. Ges. Freiberg i. Br., **18**, p. 174; 1911), who found that the vapor pressure of Hg at room temperature, as registered in his manometer, fell from 0.0013 mm to zero after admitting air from the room (apparently through a stopcock) and again reevacuating, and then slowly rose to only 0.00007 mm after several hours.

tetrachloride, carbon disulphide, acetic acid, benzene, toluene, petroleum ether, and kerosene. Of these, ethyl ether was found to be one of the best, and it has been the principal one employed thus far. The fractionation may be carried out by any one or more of the following procedures:

1. By cooling the solution.
2. By evaporating the solvent at any controlled temperature.
3. By precipitation with a second solvent.
4. By complete solidification of the solution, followed by equilibrium melting.

All of these procedures have been used, but the fourth one [12] has proved most convenient for most of the work up to the present. In this procedure the solidified solution is placed on a porous support in a vacuum-jacketed funnel fitted with a thermometer and stirrer. The melting mass is stirred so as to maintain equilibrium, and the liquid fractions which drain through are removed from time to time in accordance with the thermometer readings. Some forms of vacuum funnels employed for this purpose are shown in Figure 12.

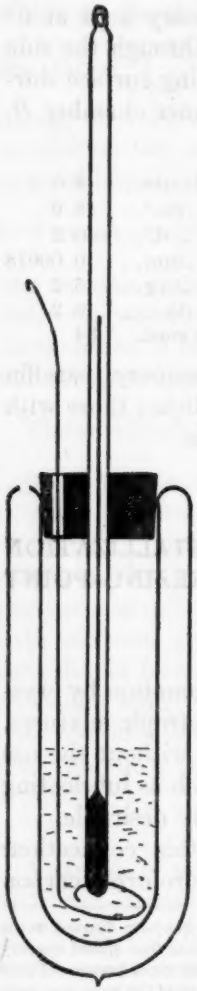

FIG. 13.—*Apparatus for determining time-temperature cooling curves*

The time-temperature cooling curve is a convenient index of the progress of the fractionation. For obtaining this curve the apparatus shown in Figure 13 is employed. Some typical curves obtained in this way are shown in Figures 14, 15, and 16. The values in the F. P. column are the initial freezing points.

It may be stated at this point that in the present investigation there has been found no petroleum fraction which can not be completely and readily obtained in crystalline form. Fractionation by crystallization is therefore possible at any stage of the work except possibly in the case of tarry or asphaltic materials. These have not been studied.

[12] See also Timmermans and Martin, J. chim. phys., 23, p. 6; 1926.

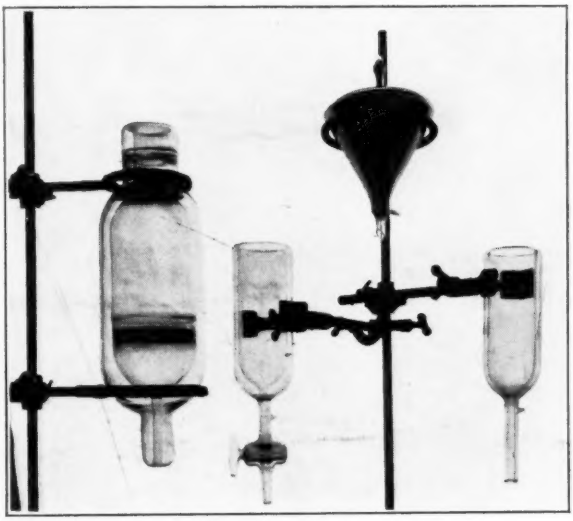

FIG. 12.—*Types of vacuum funnels*

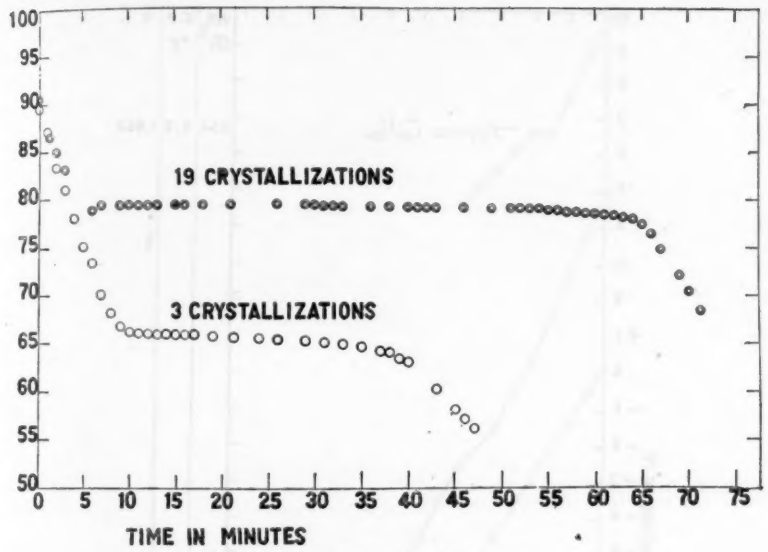

FIG. 14.—*Typical cooling curves*

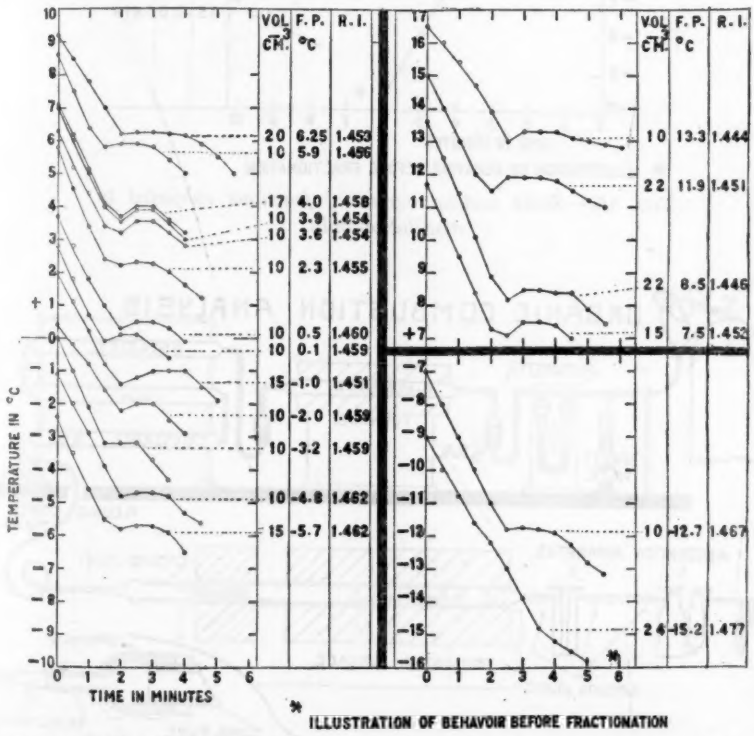

FIG. 15.—*Cooling curves of gas-oil fractions after extensive fractionation by both distillation and crystallization*

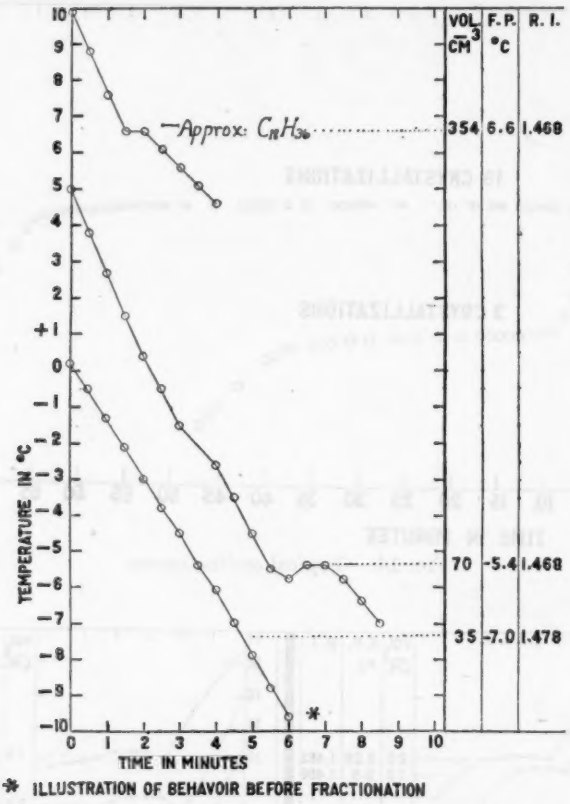

FIG. 16.—*Some cooling curves of fractions subjected to distillation only*

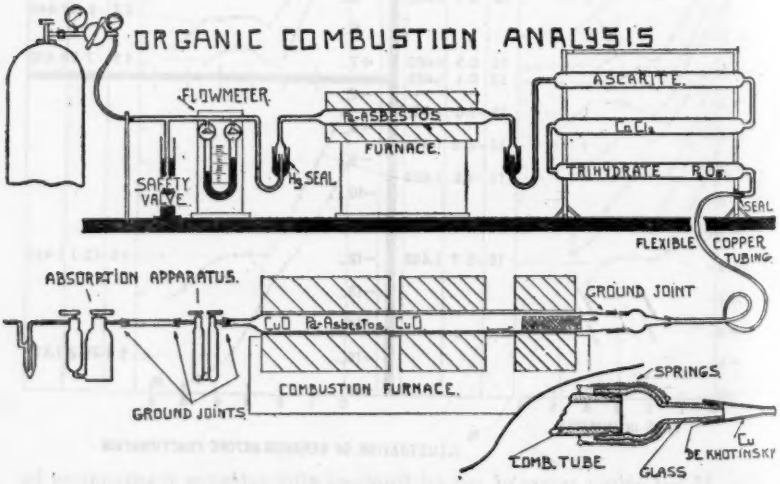

FIG. 18.—*Apparatus for combustion analysis. Detail*

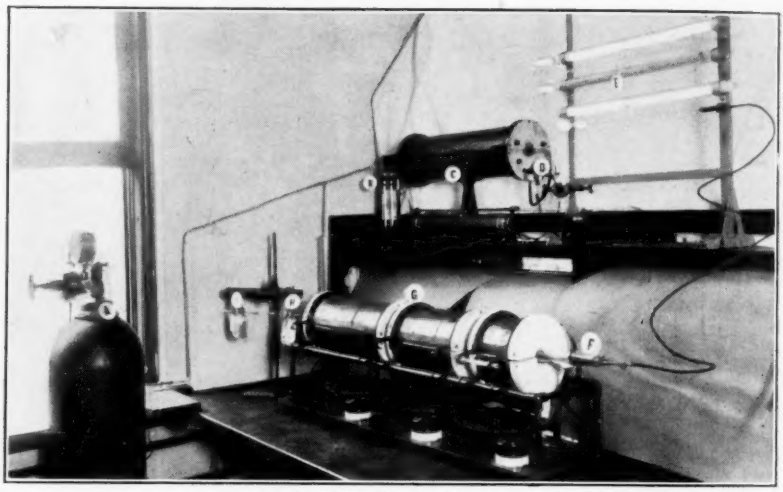

FIG. 17.—*Apparatus for combustion analyses*

A, oxygen tank
B, flow meter
C, furnace for the destruction of organic impurities. Contains a glass tube filled with palladized asbestos
D, mercury seal joint (one on each side of the furnace)
E, purification train filled with $CaCl_2$, ascarite, magnesium perchlorate trihydrate, and P_2O_5. This train, by means of flexible copper tubing is connected to: *F*, ground-glass nonlubricated joint; *G*, the combustion furnace; *H* and *I*, water and CO_2 absorption bulbs (all connections are ground glass-to-glass joints)

PART 7

VII. APPARATUS FOR COMBUSTION ANALYSIS

By Johannes H. Bruun

The combustion apparatus is illustrated in Figures 17 and 18. The only features not usually found in such apparatus are (1) the provisions for insuring the required purity of the oxygen and (2) the use of wax-sealed metal-to-glass or of glass-to-glass joints only, throughout the combustion train.[13] The following results obtained with the apparatus indicate the accuracy with which combustion analyses can be duplicated. With this degree of accuracy in the combustion analysis it is possible, with the aid, when necessary, of a molecular weight determination, to determine with certainty the empirical formula of any hydrocarbon up to C_{100}.

TABLE 5

COMBUSTION OF RESUBLIMED NAPHTHALENE (NOT PURE)

Run	H	Deviation	C	Deviation	Sum
	Per cent		*Per cent*		*Per cent*
1	6.27	0.02	93.61	0.02	99.88
2	6.21	.04	93.66	.03	99.87
3	6.26	.01	93.61	.02	99.87
Average	6.25	.023	93.63	.023	99.87
Theoretical	6.29		93.71		100.00

COMBUSTION OF A GAS-OIL FRACTION (LIQUID)

1	13.66	0.02	86.10	0.03	99.76
2	13.64	.00	86.05	.02	99.69
3	13.61	.03	86.08	.01	99.69
Average	13.64	.017	86.07	.02	99.71

PART 8

VIII. SUMMARY

This paper contains a description of apparatus and methods devised and employed for the fractionation of petroleum into its constituent hydrocarbons. They include the following:

1. A rectifying still with a 20-plate column and with means for independently controlling and measuring the temperatures of the plates. The still is designed for distillation in a stream of an inert gas (CO_2) with or without boiling. It is provided with a purifying train for the CO_2, with a series of condensers with stepped temperatures down to $-80°$ C., and with a final absorber for the CO_2.

[13] For quantitative data relative to the magnitudes of the errors arising from the presence of (*a*) rubber connections, (*b*) stopcock lubricants, and (*c*) impurities in the oxygen, see Lindner (Ber. 60 B: p. 124; 1927) and the literature there cited.

2. A set of all-glass rectifying stills for vacuum distillation. These stills have vacuum or air jacketed columns, mercury-sealed stopcocks, and provision for intermittent feeding of liquid and withdrawal of fractions during the distillation. They are heated by immersion in an electrically heated bath of nickel shot.

3. Various types of molecular stills by means of which distillation can be carried out at any temperature at which the vapor pressure at the distilling surface is not lower than, say, 10^{-6} mm Hg.

4. Methods and apparatus for fractionation by crystallization or melting.

5. An apparatus for combustion analysis, with special provisions for purifying the oxygen employed, and with all rubber connections eliminated. With this apparatus the combustion analysis of a hydrocarbon can be duplicated with the following average precision: Per cent C and H each to about ± 0.05. This makes it possible to determine with certainty the values of n and x in the formula C_nH_{2n+x}, for any hydrocarbon up to C_{100}.

The change in the iodine number of the "wax-distillate" fraction of a petroleum oil produced by heating it for different periods and at different temperatures up to 370° C. in (*a*) air and (*b*) H_2, N_2, and CO_2, respectively, has been determined, and it is shown that in the absence of air the rate of this change is greatly reduced, thus making it possible to distil petroleum at high temperatures without cracking, provided all air is excluded.

Evidence is presented showing that the hazards from exposed mercury surfaces in a laboratory are eliminated as soon as the mercury surface becomes contaminated with a continuous layer of a heavy oil or grease.

ACKNOWLEDGMENT

This paper describes the apparatus and methods which have been developed and are being employed in an investigation on "The separation, identification, and determination of the chemical constituents of commercial petroleum fractions" listed as Project No. 6 of American Petroleum Institute Research. Financial assistance in this work has been received from a research fund of the American Petroleum Institute donated by John D. Rockefeller. This fund is being administered by the institute with the cooperation of the Central Petroleum Committee of the National Research Council.

WASHINGTON, August 4, 1928.

RECOMBINATION SPECTRA OF IONS AND ELECTRONS IN CÆSIUM AND HELIUM

By F. L. Mohler and C. Boeckner

ABSTRACT

METHOD.—Thermionic discharges in cæsium and helium were operated to give strong continuous bands and spectrophotometer measurements of intensity distribution were made in connection with probe wire measurements of electrical conditions.

DISCHARGE CONDITIONS.—Excitation of these spectra is favored by high electron and ion concentrations of the order 10^{13} per cc and low electron speed. Electrons have a Maxwell distribution of average energy between 0.15 and 0.4 volt.

INTENSITY.—Intensity depends on the ion concentration independent of discharge current and voltage. The increase with ion current is less than the square and nearly the first power at high intensity. Intensity increases rapidly with pressure.

INTENSITY DISTRIBUTION.—Measurements of intensity distribution in the 2 *P* band of cæsium and of electron velocity distribution were made under a variety of discharge conditions. Some measurements on the 3 *D* band are given. Photographs and approximate intensity measurements on continuous bands of helium show a strong band beyond $2\,^3P$ and fainter bands beyond $2\,^3S$, $2\,^1P$, and $2\,^1S$.

AFTERGLOW.—By means of a sectored disk and commutator the spectrum of the cæsium afterglow was photographed. It is characterized by a more rapid decrease in intensity of the continuous bands with decreasing wave length.

CONCLUSIONS.—Results on intensity distribution are explained on the basis of simple recombination, although absolute values can not be explained in detail. The relative values of probability of recombination as a function of electron energy are independent of discharge conditions. The form of the functions for the levels 2 *P* and 3 *D* of cæsium are similar. The probability of recombination is proportional to $1/\nu^2\sqrt{\nu-\nu_i}$. This corresponds by the principle of detailed balance to an absorption coefficient beyond the limit proportional to λ^4.

CONTENTS

	Page
I. Introduction	490
II. Apparatus and procedure	491
1. Discharge tubes	491
2. Intensity measurements	491
3. Electrical measurements	491
III. General remarks on discharge conditions	492
IV. Intensity and discharge conditions	493
1. Intensity	493
2. Intensity distribution	494
3. Afterglow of the discharge	496
V. Discussion	497

I. INTRODUCTION

Another paper of the same title[1] describes a type of thermionic discharge in cæsium which shows strong continuous spectra extending to the violet from each series limit. The intensity of the continous bands was enhanced with increased current and vapor pressure in a manner consistent with the hypothesis that the radiation resulted from recombination. The paper included photographs of the spectra in potassium as well as cæsium and visual spectrophotometer measurements of the cæsium bands.

The present paper describes experiments in which probe wire measurements of electrical conditions in the discharge were made in connection with intensity measurements. It includes measurements in cæsium and in helium.

When an electron of velocity v recombines with an ion into an energy level of limiting frequency ν_1, it will radiate a quantum of frequency ν where

$$h\nu = h\nu_1 + \tfrac{1}{2}mv^2 \tag{1}$$

Thus, the intensity $J(\nu)$ at any frequency greater than ν_1 depends on the concentration of electrons of the corresponding speed, $N^-(v)$ on the concentration of ions, N^+, and on a probability factor which is a purely atomic property. The probability can be expressed as the effective collision area times the electron velocity $vq(v\nu_1)$. Equating the quanta emitted and the effective collisions

$$J(\nu)/h\nu\, d\nu = \Sigma N^-(v) \cdot N^+ \cdot vq(v\nu_1)\, dv \tag{2}$$

The summation extends over all limits of frequency less than ν, but in practice one level is usually predominant at any one frequency.

Unfortunately, inherent difficulties in the electrical measurements leave the values of the concentrations uncertain, so that only relative values of $q(v\nu_1)$ are derived. There is a possibility that under the experimental conditions the random Stark effect of neighboring ions will seriously alter the values of this. A recent theoretical paper on Stark Effect and Series Limits[2] discusses the results obtained in the earlier paper[3] and shows that the limits of separate atoms may be diffused over a range of several hundred angstroms. Paschen[4] has made use of the Stark effect broadening of lines to estimate the ion concentration in helium discharges showing recombination bands.

[1] F. L. Mohler, Phys. Rev., **31**, p. 187; 1928.
[2] Robertson and Dewey, Phys. Rev., **31**, p. 973; 1928.
[3] See footnote 1.
[4] Paschen, Berlin Ber., p. 135; 1926.

II. APPARATUS AND PROCEDURE

1. DISCHARGE TUBES

Most of the work has been done with a quartz tube with a flat window at one end. A hot wire cathode (either tungsten or oxide coated platinum) was near the axis of a cylindrical anode with the ends closed except for slits for viewing the discharge. The probe was usually a platinum wire 4 to 10 mm in length and 0.5 mm in diameter, placed parallel to the axis within a centimeter of the cathode. In a general survey of discharge conditions a variety of probes have been tried, and in one tube the probe could be moved by an external magnet.

The cæsium tubes were sealed off the pumps after outgassing, while in work with helium the gas was either circulated through charcoal in liquid air or at least kept in contact with the charcoal trap during the experiment.

2. INTENSITY MEASUREMENTS

A method described in the first paper has been adapted to photographic spectrophotometry. A region of the discharge close to the probe was focused on the plane of the filament of an incandescent lamp, and this was focused on the slit of the spectrograph. Quartz fluorite achromats were used and the lamp was a quartz tube with flat end plates containing a tungsten hairpin filament. This was calibrated in terms of color temperature versus current by an optical pyrometer. The procedure was to match the filament and discharge visually or by trial and then take a series of exposures, changing the lamp current by convenient steps. The photographs showed the wave lengths at which a match was obtained, and the intensity at these wave lengths could be computed by Wien's law.

In some work the intensity of the cæsium 2 P band was measured by sighting an optical pyrometer with a green glass in the eyepiece directly on the discharge. The glass transmitted a narrow spectrum range near the head of this band.

3. ELECTRICAL MEASUREMENTS

The usual method of measuring probe characteristics was used except that because of the rapid variation in current it was necessary to correct the applied potential for the voltage drop across the leads and milliammeter. Voltages were measured relative to the anode.

The theory developed by Mott-Smith and Langmuir [5] has been applied. At negative potentials such that only positive ions reach the probe the current I^+ is given by the equation

$$I^+ = N^+ ea\sqrt{eV_o^+/3\pi M} \qquad (3)$$

[5] Mott-Smith and Langmuir, Phys. Rev., 28, p. 727; 1926.

where N^+ is the concentration, V_o^+ the average kinetic energy, and M the mass of the ions; a is the area of the sheath around the wire and changes with the voltage in accord with the space charge equation. On the basis of published tables, a can be evaluated from the value of I^+ at any applied potential V.[6]

As the negative potential is reduced, electrons reach the probe and, in general, these fall in several velocity groups, the slowest of these groups being by far the largest. Assuming that this group has a Maxwell distribution, the current contributed by it is:

$$I^- = a_o N^- e \sqrt{eV_o/3\pi m}\ \epsilon^{-3V/2V_o} \tag{4}$$

$$\log I_2 - \log I_1 = 3/2 \log \epsilon\ (V_1 - V_2)/V_o \tag{5}$$

where N^- is the concentration and V_o is the average energy of the electrons; a_o is the area of the probe, while V_1, V_2, I_1, I_2 are specific values of V and I. The plot of log I against V is a straight line if there is a Maxwell distribution, and the slope of this determines V_o. The linear relation ends at $V=o$, and the coordinates of this discontinuity give the space potential and N^-. Note that V_o^+ of (3) is not measured and N^+ is not directly determined.

III. GENERAL REMARKS ON DISCHARGE CONDITIONS

The continuous spectra were excited in cæsium with currents between 0.1 and 1.5 amps., applied potentials between 2 and 10 volts, and a vapor pressure of 0.05 mm or more. In helium comparable currents were used at from 20 to 50 volts with a pressure between 2 and 15 mm. Under these conditions the potential drop is concentrated in a thin sheath around the cathode, while a diffuse glow extending toward the anode shows the continuous bands. The region of diffuse glow is characterized by high ion concentration and extremely low electron speed. Semilog plots of the electron current are linear, which indicates that most of the electrons fall in a single group with a Maxwellian distribution. The average energy is between 0.1 and 0.4 volts. Attempts to extend the current voltage curves through the space potential were generally unsuccessful. Except with extremely small probes the probe current robs the discharge before the space potential is reached. With small probes the currents tend to drift and become unsteady, presumably because of overheating.

Results obtained with larger probes permit accurate determinations of the average electron energy and the positive ion current, and it has seemed advisable to limit our attention to these measurements for the present rather than to sacrifice precision.

[6] Langmuir and Blodgett, Phys. Rev., **22**, p. 347; 1923.

The change in positive ion current with voltage was relatively small and could be accounted for by the space charge equation. In some cases a well-defined group of high-speed electrons was detected with a maximum energy of 10 to 15 volts in helium and of 2 to 3 volts in cæsium.

In spite of the incomplete data some estimate can be made of the space potential N^+ and N^-. In the highly ionized force-free space N^+ and N^- must be nearly equal. The average energy of the ions, V_o^+, will be intermediate between that of the gas atoms and that of the electrons, in an average case between 0.07 and 0.2 volt. This gives an uncertainty of about twofold in the value of N^+ in equation (3), and I^- at the space potential can be computed with the same uncertainty assuming $N^- = N^+$. The linear semilog plot can be extrapolated to this value of I^-, and as the electron current doubles in a range of about a tenth of a volt the space potential is determined with an uncertainty of less than 0.2 volt. Measurements with a movable probe in a cæsium discharge of 0.3 amp. at 5 volts gave the following results: At 6 mm from the cathode the average electron energy V_o was 0.35 volt, and assuming an ion velocity corresponding to 1,000° K., N^+ was 1.5×10^{13} per cc. The space potential V_s was about $+1.3$ volts relative to the anode. Close to the anode $V_o = 0.22$ volt, $N^+ = 1.3\times10^{11}$ and $V_s = +0.4$. With a discharge of 0.1 amp. at 6 mm from the cathode, $V_o = 0.22$ volt, $N^+ = 0.4\times10^{13}$ and $V_s = +1.0$, while near the anode $V_o = 0.19$ volt, $N^+ = 0.27\times10^{11}$ and $V_s = +0.2$. In general, V_o increases near the cathode and increases as the ion concentration increases. Because of the slightly positive space potential, ions diffuse to the anode as well as to the cathode, while slow electrons are to some extent imprisoned in the space.

IV. INTENSITY AND DISCHARGE CONDITIONS

1. INTENSITY

Measurements covering a wide range of current and voltage were made by sighting the optical pyrometer, with a green glass in the eyepiece, directly at a cæsium discharge. Figure 1 gives a plot of the measurements of intensity against ion current, I^+, at a vapor pressure of 0.25 mm. The intensity seems to increase nearly linearly beyond the current range of Figure 1, but the probe measurements become unreliable. The plot shows that within the limits of experimental error the intensity is determined by I^+ and is independent of the particular discharge current and voltage used to give I^+. Spectrophotometer measurements in cæsium and helium are in agreement with these results. In helium, as in cæsium, the variation of intensity is much less than the square of the current and at least at the higher intensities is nearly proportional to the first power.

The intensity increases rapidly with the pressure for both cæsium and helium. The relation has not been studied quantitatively, but exposures at 2, 3, and 4 mm of helium show an intensity ratio of roughly 1 to 4 to 8.

2. INTENSITY DISTRIBUTION

It follows from equation (2) that on the basis of measurements of electron velocity distribution and intensity distribution in a continuous band one can derive relative values of the probability of recombination as a function of the electron velocity. The 2 *P* band of cæsium falls in a convenient region for intensity measurements and has been studied most carefully.

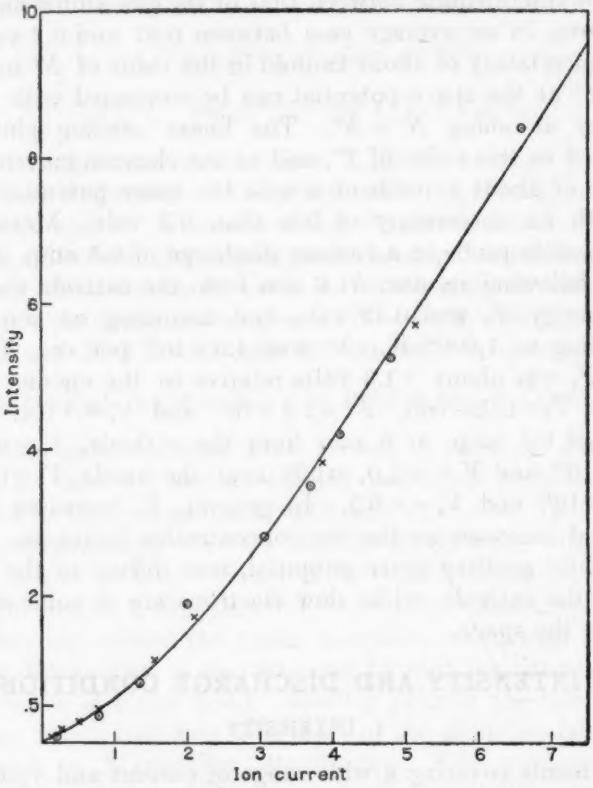

FIG. 1.—*Intensity near 2 P limit of cæsium versus ion current to probe*

Crosses show measurements with discharges at 5 volts and currents between 0.015 and 0.2 amp. Circles give measurements at voltages between 7.8 and 1.5.

A set of photographs and visual intensity matches combined with probe wire measurements were made under constant discharge conditions. The ion current was kept constant by slight variations in

the discharge current or voltage. The chief experimental difficulty was the variation in vapor pressure during the series of exposures which usually required about six hours.

Figures 2 to 4 show two sets of data on electron current, intensity distribution, and probability of recombination obtained under different conditions. For set *I* the cæsium temperature was 190° C., and the discharge was operated at about 7 volts and 0.9 amp. to give an ion current of 14 m. a. and an ion concentration of roughly 8×10^{13} per cc. For set *II* the cæsium temperature was 198° C., discharge voltage 4 volts, current 0.55 amp., ion current 1.4 m. a., and concentration 0.8×10^{13}. Figure 2 is a semilog plot of the electron currents against the voltage for the two cases, and it shows that there is a strictly Maxwell distribution about an average energy of 0.345 volt for set *I* and 0.281 volt for set *II*. Figure 3 is a semilog plot of intensity as a function of wave length. This method of plotting was chosen as the most convenient for interpolation. The difference in form of the two curves is rather small but well beyond the probable error. Dividing the number of quanta at a given wave length by the relative number of electrons at the corresponding speed and multiplying by λ^2/v to transform to proper variables gives a number proportional to $v\ q\ (v,\ 2P)$. Figure 4 shows the two sets of computed values reduced to the same scale by a single arbitrary constant. Six other sets of data have been obtained, and the resulting $v\ q\ (v)$ values fall close to this curve, although the precision was not always as good as in the cases illustrated. The average electron energy varied from 0.28 to 0.38 volt while the ion concentration ranged from 0.8 to 15×10^{13}.

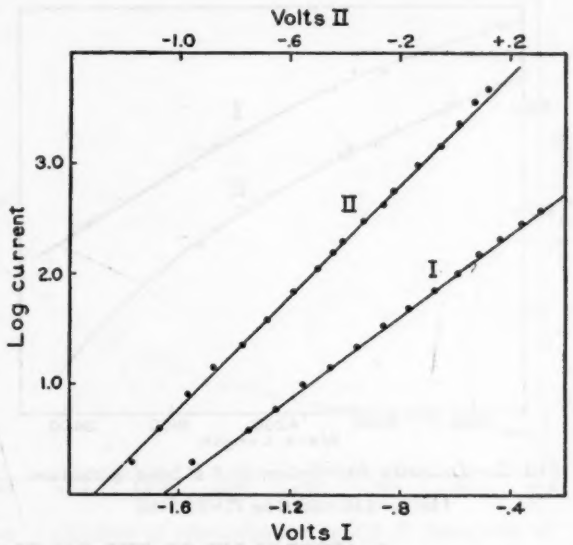

FIG. 2.—*Electron velocity distribution curves*
I gives $V_0=0.345$ volt; *II* gives $V_0=0.281$ volt

Visual spectrophotometer measurements have been made on the 3 *D* band, together with measurements of electron velocity. Similar

intensity measurements are illustrated in the first paper.[7] Line spectra and the 2 P band seriously limit the range and precision of the measurements. These data are included in Figure 6.

The spectrograms of the helium discharge closely resemble published photographs by Paschen[8] of the spectrum of the hollow cathode discharge. Continuous bands can be detected beyond the limits $2\,{}^1P$, $2\,{}^3P$, $2\,{}^1S$, and $2\,{}^3S$ though the $2\,{}^1P$ band is obscured by molecular bands and the $2\,{}^1S$ band is masked by the stronger $2\,{}^3P$ band. The degree of purity of the gas is an important factor. A trace of mercury suppresses the helium molecular bands and facilitates observation of the continuous bands, but traces of other common impurities mask the continuous bands completely. Figure 5 is a plot of the intensity distribution based on spectrophotometer measurements. The estimates of intensity on the red side of $2\,{}^3P$ and on the violet side of $2\,{}^3S$ are extremely uncertain. The discharge conditions for this set of measurements were pressure 4 mm, discharge at 50 volts and 0.5 amp., average electron energy 0.25 volt, ion concentration 10.[13]

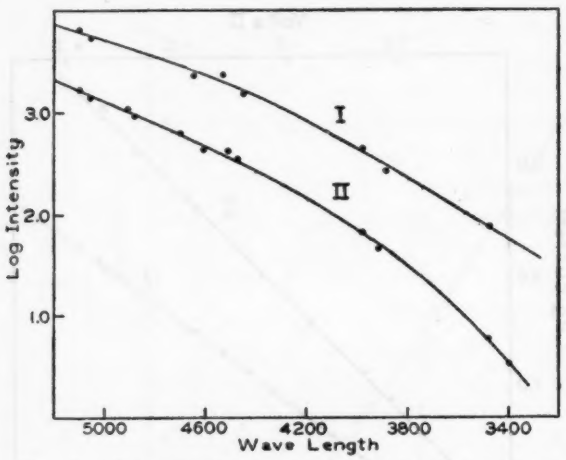

FIG. 3.—*Intensity distribution in 2 P band of cæsium*

I for V_o=0.345 volt; *II* for V_o=0.281 volt

3. AFTERGLOW OF THE DISCHARGE

A sectored disk and commutator were arranged so as to cut off the discharge and permit study of the spectrum of the afterglow. Only qualitative results have been obtained so far. An exposure to the cæsium afterglow was made with a discharge of one ampere and disk speed of 1,500 r. p. m., giving a time interval of about 10^{-3} second between cutting off the discharge and uncovering the spectroscope slit. Comparison exposures on the direct discharge were made on the same plate. Higher series lines are somewhat stronger in the afterglow as was found by Miss Hayner in her study of the mercury afterglow,[9] but the contrast is less marked in this case as the recombination radiation is predominant even in the direct discharge. For the same reason recombination intensity does not reach a maximum

[7] See footnote 1, p. 490. [8] See footnote 4, p. 490. [9] Hayner, Zeits. f. Phys., 35, p. 356; 1926.

after the cut-off but seems to fade continuously. The most striking difference between the discharge and afterglow is that the continuous bands fade toward the violet much more rapidly. The intensity at 4,700 A, relative to that at the 2 *P* limit, is about half as great as in the spectrum of the direct discharge. This can be explained on the basis of electron velocity, which will quickly drop after the discharge is cut off. Assuming that the average electron energy in the discharge is 0.3 volt (2,300° K.), we estimate from the intensity change that the electron energy or temperature in the afterglow is roughly 0.1 volt, or 800° K. As there will be 10^6 electron collisions in 10^{-3}

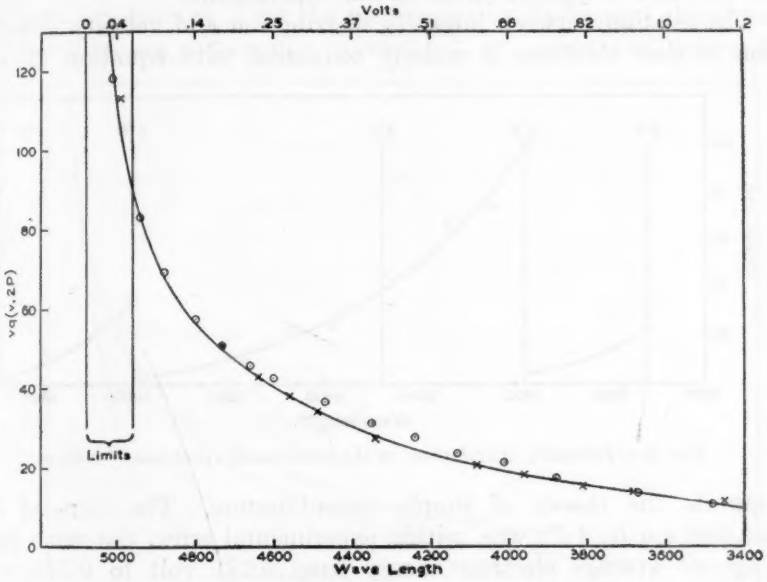

FIG. 4.—*The relative probability of recombination into 2 P from data of Figures 2 and 3*

Crosses refer to set *I* and circles to set *II*. Abscisas are in wave lengths below and corresponding voltage values above

seconds, it is not surprising that electrons have nearly reached equilibrium with the gas at 500° K.

V. DISCUSSION

The relation between intensity and ion current as illustrated in Figure 1, as well as the increase of intensity with pressure, can not as yet be satisfactorily explained. On the basis of the simplifying assumptions which were introduced in the discussion of discharge conditions, one would predict from equation (2) that the intensity should increase as the square of the ion current and be independent of the pressure. The observed increase is much less than the square. Thus, in Figure 1 the highest observed intensity is about a fifth of the com-

puted value.[10] The assumptions may well introduce an uncertainty of the order of twofold but there remains an unexplained discrepancy. As regards the effect of pressure, presumably the ion concentration is increased by the combined effect of lower ion temperature and changed probe characteristics, but this can scarcely account for the magnitude of the intensity change. Franck has proposed the theory that an atom may recombine in the process of ionization by collision[11] with the emission of continuous radiation. The intensity in this case would depend only on the number of collisions with high-speed electrons. We could find no correlation between the intensity and the presence of such electrons in our experiments.

The relation between intensity distribution and velocity distribution of slow electrons is entirely consistent with equation (2) and

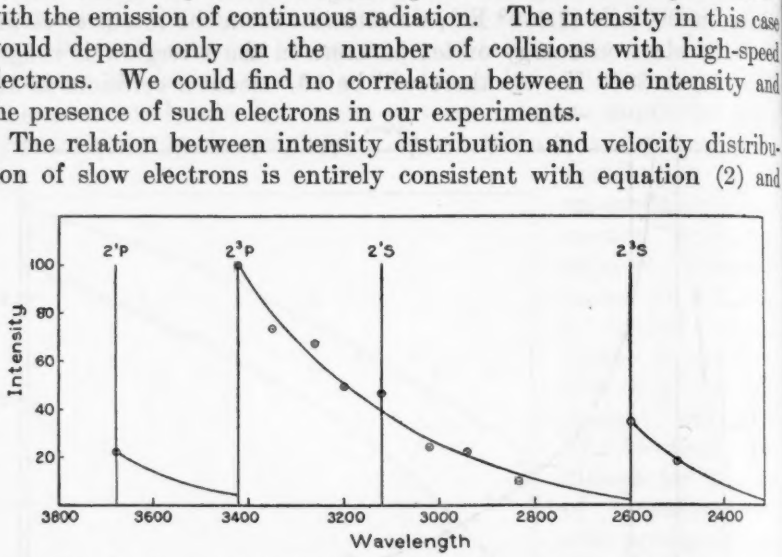

FIG. 5.—*Intensity distribution in the continuous spectrum of helium*

supports the theory of simple recombination. The form of the function $v\ q\ (v, 2\ P)$ was, within experimental error, the same for a range of average electron energy from 0.281 volt to 0.375 volt. (Electron temperature 2,180° to 2,900° K.) It is also significant that the form of the $v\ q\ (v)$ curve is independent of the ion concentration which varied from 0.8×10^{13} to 15×10^{13}. We conclude that the influence of random Stark effect on the intensity distribution is not a serious source of error. The experimental conditions also covered quite a range of pressure and discharge voltage.

There is a general relation based on the principle of detailed balance between the probability of recombination $v\ q\ (v\ \nu_1)$ and the probability of absorption $B\ (\nu\ \nu_1)$ at the frequency ν corresponding to V.[12]

$$v\ q\ (v\ \nu_1) = K_1\ B\ \cdot\ \nu^2/\sqrt{\nu-\nu_1} \qquad (6)$$

The B, of course, applies to atoms initially in the state ν_1 and is quite unmeasurable except where this is the normal state. In the X-ray

[10] Later measurements with a spectrophotometer show that at low currents the intensity is proportional to the square of the current and the lower portion of the curve of Figure 1 is inaccurate.

[11] Franck, Zeits. f. Phys., **47**, p. 509; 1928.

[12] Milne, Phil. Mag., **47**, p. 209; 1924.

range B is proportional to ν^{-4}, and theoretical derivations show that in hydrogenic atoms it will approximate to the same law. Oppenheimer [13] finds by the methods of wave mechanics that the value of the exponent for atomic hydrogen varies from -4.3 at the limit to a minimum value of -3.5 for the normal level, and other levels vary slightly from this. The ν^{-4} absorption law in equation (6) gives:

$$v\,q(v) = K_2/\nu\sqrt{\nu-\nu_1} \qquad (7)$$

He [14] has also derived the relation that $v\,q\,(v)$ is proportional to $(\nu-\nu_1)^{-3/2}$ near the limit. This result and his absorption law are not consistent with equation (6).

Direct measures of B for the continuous bands beyond absorption series limits are apparently invalidated by superposed molecular

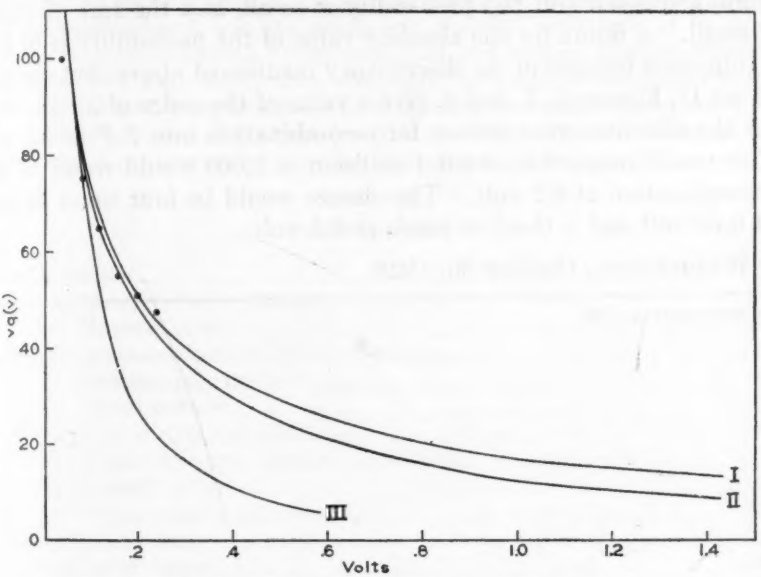

FIG. 6.—*Relative probability of recombination*

I, Theoretical curve derived from ν^{-4} law for B
II, $v\,q$ (v 2 P) from Figure 4. Dots $v\,q$ (v 3 D)
III, $v\,q$ (v, 1 S) derived from photoionization measurements

absorption,[15] but measurements of photoionization may be free from this objection and independent measurements on the 1 S band of cæsium are in satisfactory agreement.[16] [17] The curve of Figure 4 is drawn according to the equation

$$vq\ (v,\ 2\ P) = K/\nu^2\sqrt{\nu-\nu_1} \qquad (8)$$

[13] Oppenheimer, Zeits. f. Phys., **41**, p. 268; 1927.
[14] Oppenheimer, Phys. Rev., **31**, p. 349; 1928.
[15] Harrison and Slater, Phys. Rev., **26**, p. 176; 1925.
[16] Mohler, Foote and Chenault, Phys. Rev., **28**, p. 37; 1926.
[17] Little, Phys. Rev., **30**, p. 109; 1927.

which fits the observations exactly. This gives B proportional to ν^{-5}, and the absorption coefficient varies as ν^{-4} or λ^4. The factor $\sqrt{\nu-\nu_1}$ is predominant in giving the shape of the curve, so that the power of ν is not determined with precision. In Figure 6, *II* is the curve of Figure 4, while *I* is derived from the ν^{-4} law for B. The difference is probably greater than the experimental error. The dots in Figure 6 are derived from the less accurate intensity measurements on the 3 D band. Curve *III* is derived from observed values of photoionization,[18] and there is a serious discrepancy between this and Curve *II* which can not be explained. The $V^{-3/2}$ law of Oppenheimer gives a curve much steeper than *III*.

Curve *II* of Figure 6 shows that the probability of recombination increases very rapidly as the electron energy decreases below 0.3 volt, while above 0.5 volt the probability is small, and the rate of change is small. A figure for the absolute value of the probability is of little significance because of the discrepancy mentioned above, but the data of set *II*, Figures 2, 3, and 4, give a value of the order of 2×10^{-19} cm^2 for the effective cross section for recombination into 2 P at 0.2 volt. This would mean that about 1 collision in 5,000 would result in such recombination at 0.2 volt. The chance would be four times as great at 0.05 volt and a third as much at 0.5 volt.

WASHINGTON, October 30, 1928.

[18] See footnote 16, p. 499.

THE SPECTRAL ABSORPTION OF CERTAIN MONOAZO DYES

I. THE EFFECT OF POSITION ISOMERISM ON THE SPECTRAL ABSORPTION OF METHYL DERIVATIVES OF BENZENEAZOPHENOL

By Wallace R. Brode

ABSTRACT

Quantitative measurements of the spectral absorption of solutions of azobenzene, benzeneazophenol, and the mono- and dimethyl derivatives of benzeneazophenol in alcohol, aqueous hydrochloric acid, and aqueous sodium hydroxide are recorded and their relationships discussed. Although the differences found in the spectral absorption of alcohol solutions or of hydrochloric acid solutions of the position isomers studied are small, marked differences are found in the absorption of 3 per cent aqueous sodium hydroxide solutions.

CONTENTS

	Page
I. Introduction	501
1. Outline of investigation	501
2. Nomenclature	502
II. Spectrophotometric methods and apparatus	504
1. Photographic method	504
2. Visual method	507
III. Preparation of dyes and solutions	509
1. Preparation and purification of dyes	509
2. Analysis of dyes	509
3. Preparation of solutions	509
IV. Experimental data	511
V. Discussion of results	514
1. Alcohol solutions	514
2. Hydrochloric acid solutions	515
3. Sodium hydroxide solutions	518
VI. Summary	525

I. INTRODUCTION

1. OUTLINE OF INVESTIGATION

Probably no other single physical measurement is so characteristic of an organic compound as its spectral absorption. It is a means of identification and a measure of the purity and amount of the compound in the observed solution. The advantages of spectrophotometric analysis are particularly apparent in the examination of dyestuffs, where color is an important factor. The high molecular weight

of the average commercial dyestuff, together with its complex chemical structure and the presence of organic and inorganic impurities, renders more difficult the determination of either its chemical or its other physical properties.

It is natural, therefore, that the dye laboratory of the Bureau of Standards should include the measurement of spectral absorption among the observations which are being made in connection with the collection of accurate quantitative data on the physical and chemical properties of dyestuffs.[1] Through the cooperation of the colorimetry section of the Bureau of Standards, apparatus is available for the accurate measurement of spectral absorption. This apparatus, to a large extent, eliminates the instrumental and personal errors present in many of the earlier researches in this field.

The present paper is chiefly concerned with the relation between the spectral absorption and chemical constitution of the mono- and dimethyl derivatives of benzeneazophenol, in which but one methyl group is present in a benzene ring. These dyes have been prepared and purified, and accurate quantitative measurements have been made of their spectral absorption in three solvents. The solvents used were 95 per cent ethyl alcohol, concentrated hydrochloric acid (35 per cent), and a 3 per cent aqueous solution of sodium hydroxide. Since this work deals with only one type of substituting group, the methyl radical, no conclusions can be drawn on the general effect of substitution, and the discussion of the results will necessarily have to be limited to a recapitulation of the data presented without predicting the possible effects of other substituting groups.

In earlier papers data have been presented on the spectral absorption of azobenzene [2] and benzeneazophenol [3] in various solvents, and only such data on these compounds as may be essential to the clarity of the discussion and the correlation of the effects observed will be presented in this paper.

2. NOMENCLATURE

The nomenclature recommended in the report of a committee of the Optical Society of America [4] has in large part been followed. Scientific Paper No. 440 [5] and Technologic Paper No. 338 [6] of the Bureau of Standards have also been consulted in drawing up this set of definitions. The terms most used, symbolized by **T**, **t**, **k**, *c*, *b*,

[1] Appel, The Work of the Bureau of Standards on Dyes, Ind. and Eng. Chem., **18**, p. 1341; 1926.
[2] Brode, J. Am. Chem. Soc., **48**, p. 1984; 1926.
[3] Brode, J. Phys. Chem., **30**, p. 56; 1926.
[4] Progress Committee on Spectrophotometry, J. O. S. A. and R. S. I., **10**, p. 177, 1925.
[5] Gibson, McNicholas, Tyndall, Frehafer, and Mathewson, The Spectral Transmissive Properties of Dyes: 1. Seven Permitted Food Dyes, in the Visible, Ultra-violet, and Near Infra-red. B. S. Sci. Papers, **18**, No. 440; June, 1922.
[6] Peters and Phelps, Color in the Sugar Industry: 1. Color Nomenclature in the Sugar Industry. B. S. Tech. Papers, **21**, No. 338; March, 1927.

λ, and f, are few in number, but in order to precisely define them other terms are necessarily given.

The following terms relate to the rectilinear propagation of homogeneous radiant energy through a cell with plane, parallel sides (glass or quartz end plates) perpendicular to the direction of propagation, and containing a substance in homogeneous solution in a solvent:

$T_{sol.}$ = the *transmission* of this cell and its contents and is defined as the ratio of the radiant energy passing the last surface of the cell to that incident on the first surface.

$T_{sov.}$ = the transmission of the same or a duplicate cell containing solvent only.

$\mathsf{T}_{sol.}$ = the *transmittance* of the solution contained in the cell and is defined as the ratio of the radiant energy incident on the second inner surface of the cell to that passing the first inner surface.

$\mathsf{T}_{sov.}$ = the transmittance of the solvent only.

$\mathsf{T} = \frac{T_{sol.}}{T_{sov.}} = \frac{\mathsf{T}_{sol.}}{\mathsf{T}_{sov.}}$ = the transmittancy [7] of the dye in solution.

The transmittancy, T, of a dye solution is the quantity obtained from the actual measurements. Since the transmission of the cell containing the solution is always compared with that of a duplicate cell containing the solvent, losses by reflection from the ends of the cell and by absorption by the solvent are compensated. The negative logarithm of the transmittancy, $-\log \mathsf{T}$, is a quantity which is a direct measure of the absorption of the dissolved material. It is this quantity, often called the extinction coefficient in chemical papers, which is plotted in the graphs accompanying this paper.

$\mathbf{t}$ = *specific transmissivity;* that is, transmittancy reduced to unit conditions as regards thickness and concentration.

b = thickness of the absorbing solution. In the present paper 0.5 cm is taken as the unit of thickness, since all of the solutions reported were measured in a cell of that length.

c = concentration of the dissolved material. A concentration of 1.5×10^{-4} gram molecule per liter of solution has been used as the unit in this paper.

$\mathbf{t} = cb\sqrt{\mathsf{T}}$. This is an expression of Beer's law.

$\mathbf{k} = -\log \mathbf{t} = \frac{1}{cb}(-\log \mathsf{T})$ = the specific absorptive index. [8]

The specific absorptive index $\mathbf{k}$ is the characteristic quantity for any solution at any wave length or frequency in the spectrum.

---

[7] Transmittancy is generally designated in chemical publications as $\frac{I}{I_o}$, where I and I_o correspond to $T_{sol.}$ and $T_{sov.}$

[8] The report on spectrophotometry, ref. 4, and B. S. Sci. Paper No. 440, ref. 5, call this specific transmissive index, but see B. S. Tech. Paper No. 338, ref. 6, p. 265.

As shown above, it is obtained from the observed transmittancy, T, by simply dividing the negative logarithm of this number by the product of the concentration and thickness of the solution measured.

λ = wave length, the unit of which in this paper is the millimicron, $m\mu = 10^{-9}$ m.

ν = frequency,[9] the unit of which in this paper is the fresnel, f = vibrations ÷ seconds $\times 10^{12}$.

The spectral absorption data are presented graphically and in tables. The graph form has $-\log_{10} T$ from 0.00 to 2.00 as ordinates and frequency from 350 f to 1,400 f as abscissas. It should be noted that $-\log_{10} T$ is plotted downward on the graph and, therefore, that the greater the absorption the farther a point will be from the top of the graph. The spectral absorption curve obtained by drawing a smooth curve through observed values plotted on the graph delimits narrow regions of relatively high absorption which are called absorption bands. An absorption band is located in the spectrum by its position of maximum absorption; that is, the frequency of a band is taken to be the frequency of maximum absorption. Similarly, the magnitude of a band is the value of the specific absorptive index at the frequency of maximum absorption. For purposes of discussion, the observed bands are numbered, starting with the one of lowest frequency. In case a band is composed of smaller ones, the components are lettered in order from the low-frequency to the high-frequency side. The principal band is the one of greatest magnitude.

II. SPECTROPHOTOMETRIC METHODS AND APPARATUS

1. PHOTOGRAPHIC METHOD

The observations in the ultra-violet and extending into the visible portion of the spectrum were made by the Hilger sector photometer method. This method requires the use of three distinct pieces of apparatus—a source of continuous radiant energy, a sector photometer, and a quartz spectrograph. (Fig. 1.)[10]

The source of radiant energy is a vertical high voltage spark under water, obtained by the use of a Tesla coil. The spark between the tungsten electrodes is approximately 12 mm in length and gives a continuous spectrum from the visible throughout the ultra-violet as far as the system will record. Distilled water is run through the spark chamber during operation.

The sector photometer consists essentially of two quartz wedge lenses, on one side of which are the rotating sectors and on the other

[9] This is the *true* frequency. The term wave number or oscillation frequency often used is defined as $\frac{10^3}{\lambda}$.

[10] The author is indebted to the colorimetry section of the Bureau of Standards for placing this entire apparatus at his disposal.

side a holder for the two absorption cells. The quartz spectrograph is a Fuess instrument, with lenses of 74 cm focal length giving a dispersion of 13.9 cm between 600 and 1,200 *f*. A slit width of 0.15

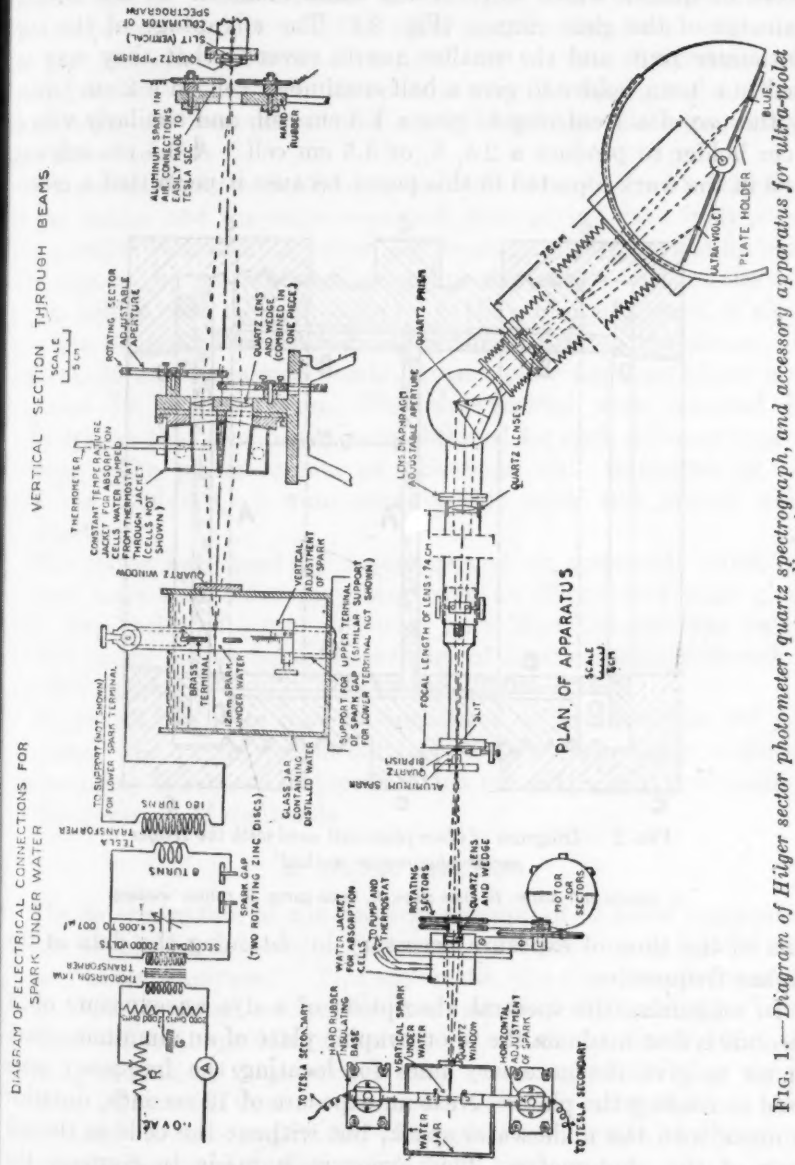

FIG. 1.—*Diagram of Hilger sector photometer, quartz spectrograph, and accessory apparatus for ultra-violet spectroradiometry*

mm was used, corresponding to 3.7 *f* at a frequency of 1,200 *f*. A quartz biprism is placed directly in front of the slit of the spectrograph, with its refracting edge perpendicular to the slit, and serves to bring the two beams from the photometer adjacent to each other.

The cells used in this work were a special modification of those described in Scientific Paper No. 440 [11] of the Bureau of Standards. The essential difference is the use of half centimeter rings, and cover pieces of quartz which were of the same diameter as the outside diameter of the glass rings. (Fig. 2.) The advantage of the half centimeter rings and the smaller quartz cover is that they may be used in a 1 cm holder to give a half centimeter cell, in a 2 cm holder by the use of a 1 cm ring to give a 1.5 cm cell, and similarly with a 4 cm holder to produce a 2.5, 3, or 3.5 cm cell. A 0.5 cm cell was used in the work reported in this paper because it permitted a reduc-

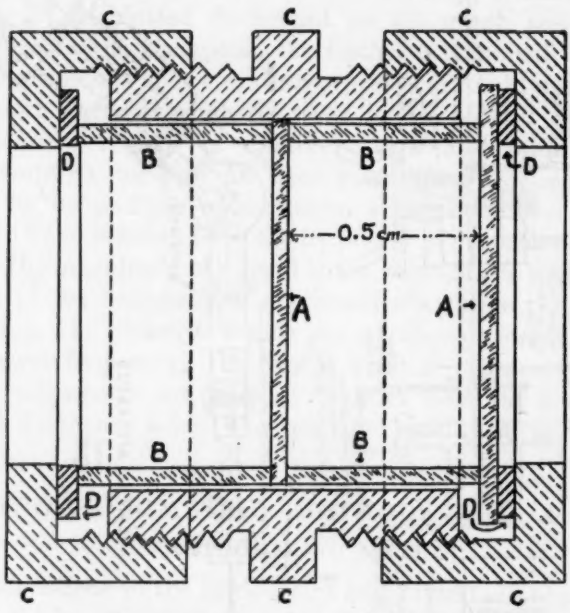

FIG. 2.—*Diagram of absorption cell used with the Hilger sector photometer method*

A, Quartz end plates; *B*, glass rings; *C*, brass parts; *D*, rubber washers

tion in the time of exposure necessary in obtaining the data at the higher frequencies.

In measuring the spectral absorption of a dye an exposure of 20 seconds is first made on the photographic plate of an aluminum spark in air to give the necessary lines for locating the frequency scale used in reading the plate. Next an exposure of 16 seconds, duration is made with the underwater spark, but without the cells in the cell rack of the photometer. This exposure is made to compare the intensities of the two beams, which must be the same throughout the observed spectrum. The cell containing the solvent is now placed in one of the openings in the holder and the cell containing

[11] See footnote 5, p. 502.

the solution in the other. A series of exposures is then made, varying the ratio of the apertures for each exposure.

There results on the photographic plate a series of pairs of contiguous spectra. One member of each pair has undergone absorption in certain regions and the other member has been reduced in density throughout its whole length. At certain frequencies the photographic densities of the spectra may be equal, and at these frequencies the transmittancy is known from the relative apertures of the sectors.

When enough exposures have been made, the cells are interchanged in the holder and the series repeated, thus giving data from which the possible instrumental error has been very largely eliminated.[12] The next to the last exposure is another comparison without the cells in the holder, and the last exposure is the aluminum spark in air to give the necessary reference lines for the reading of the plates. In general, 25 exposures were made on each plate and two plates were required for each solution. The observations were repeated for each dye, so that four plates were obtained for each different type of solvent. The plates known as "Eastman 36" (prepared by the Eastman Kodak Co.) were used in this work and proved quite satisfactory.

The plates were read by superimposing an accurately ruled frequency scale and observing them over an illuminated milk glass. The frequencies of equal densities were then located, the values plotted in the curves being the average of several readings of each of the four exposures.

In general, the data may be considered accurate within $\pm 3\,f$ in frequency and within ± 0.03 unit in $-\log_{10}$ transmittancy, although the accuracy is somewhat dependent on the shape, size, and position in the spectrum of the bands.

2. VISUAL METHOD

The determination of the spectral absorption of these compounds in the visible portion of the spectrum was made on a Keuffel and Esser "Color Analyzer." This apparatus, like the ultra-violet apparatus, uses rotating sectors for the variation of intensity. These are rotated with sufficient rapidity to eliminate flicker, and the opening of one of these sectors may be varied while they are in motion. The cells were for the most part the same as those used with the ultra-violet apparatus, although in some cases another type, previously described by the author,[13] was used.

[12] See B. S. Sci. Paper No. 440, ref. 5, and also note R. Davis, Experimental Study of the Relation Between Intermittent and Nonintermittent Sector-Wheel Photographic Exposures, B. S. Sci. Papers, **21**, No. 528, pp. 95–140; 1926.

[13] Brode, J. Am. Chem. Soc., **46**, p. 584; 1924.

The visual method was used for the alkaline and acid solutions, but not for the alcohol solutions. The visual observations for the most part supplement the photographic observations, as the majority of the bands observed have their maxima in the ultra-violet. The points recorded on the graphs in this paper are the average of all the observations for that particular value of $-\log_{10} T$, including the photographic and visual results when data were obtained for the same point by both methods. The maxima of all the curves were

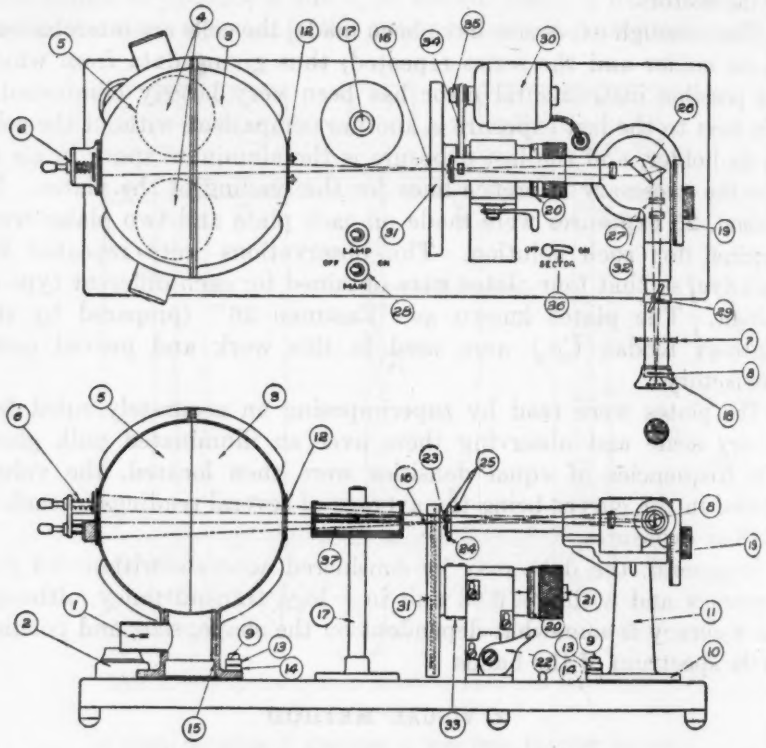

FIG. 3.—*The Keuffel & Esser "Color Analyzer"*

A complete description of this apparatus is given in a booklet issued by the company

determined solely by the photographic method. The visual method was essential, however, in determining the shape of the first absorption band near its base, where it was often beyond the range of the photographic method.

The method used was to set the rotating sectors at values of $-\log_{10} T$ and then to adjust the wave-length scale of the constant deviation prism until a match was obtained. The accuracy of this method is dependent on the shape, magnitude, and position of the band, the uncertainty being between ± 2 to 4 $m\mu$ in wave length (2 to 4 *f*) and within ± 0.04 unit in $-\log_{10} T$.

III. PREPARATION OF DYES AND SOLUTIONS

1. PREPARATION AND PURIFICATION OF DYES

The dyes were prepared from materials of a chemically pure grade and were crystallized from alcohol. In general, one-sixth molar quantities and the same methods of diazotization and coupling were used for all of the dyes. The directions given by Fierz [14] for the diazotizing of aniline were used for all of the amines. The couplings were made according to the general directions for basic coupling given by Fierz and by Cain.[15] Mechanical stirring was used throughout the diazotization and coupling to insure complete reactions. The dyes were prepared separately at different times, and no general observations were made as to the relative ease of diazotization or coupling. In all cases coupling was effected without difficulty. The dyes were purified by at least three separate crystallizations from alcohol. The structural formulas of the dyes prepared are given in Figure 4.

2. ANALYSIS OF DYES

The dyes were analyzed according to the Kolthoff [16] modification of the Knecht and Hibbert [17] titanous chloride method. The titration results and the observed melting points, together with the melting points given in the literature [18] for these dyes, are recorded in the accompanying table. (Table 1.)

TABLE 1.—*Analysis and melting points*

Dye	Analysis by $TiCl_3$	Melting points	
		Observed	Literature
	Per cent	° *C.*	° *C.*
Azobenzene	100.0	68	68
Benzeneazophenol	99.6	152	152
Benzeneazo-*o*-cresol	99.2	128	128–130
Benzeneazo-*m*-cresol	98.5	107	109
o-Tolueneazophenol	99.5	102	102–3
m-Tolueneazophenol	98.3	140	144–5
p-Tolueneazophenol	100.8	151	151
o-Tolueneazo-*o*-cresol	99.6	132	132
o-Tolueneazo-*m*-cresol	100.5	113	111
m-Tolueneazo-*o*-cresol	98.0	114	115
m-Tolueneazo-*m*-cresol	99.5	106	106–7
p-Tolueneazo-*o*-cresol	100.2	162	163
p-Tolueneazo-*m*-cresol	99.7	135	135

3. PREPARATION OF SOLUTIONS

All of the dyes are soluble in alcohol and were measured in this solvent, in strong hydrochloric acid, and in dilute sodium hydroxide

[14] Fierz, Farbenchemie, Schulthess, Zürich; 1920.
[15] Cain, Synthetic Dyestuffs, Griffin & Co., London; 1923.
[16] Kolthoff, Rec. Trav. Chim., 45, p. 169; 1926.
[17] Knecht and Hibbert, New Reduction Methods in Volumetric Analysis, Longmans, New York; 1925.
[18] Beilstein, Handbuch der Organischen Chemie, 4; 1899; Ergänzungsband, 4; 3d ed.; 1906.

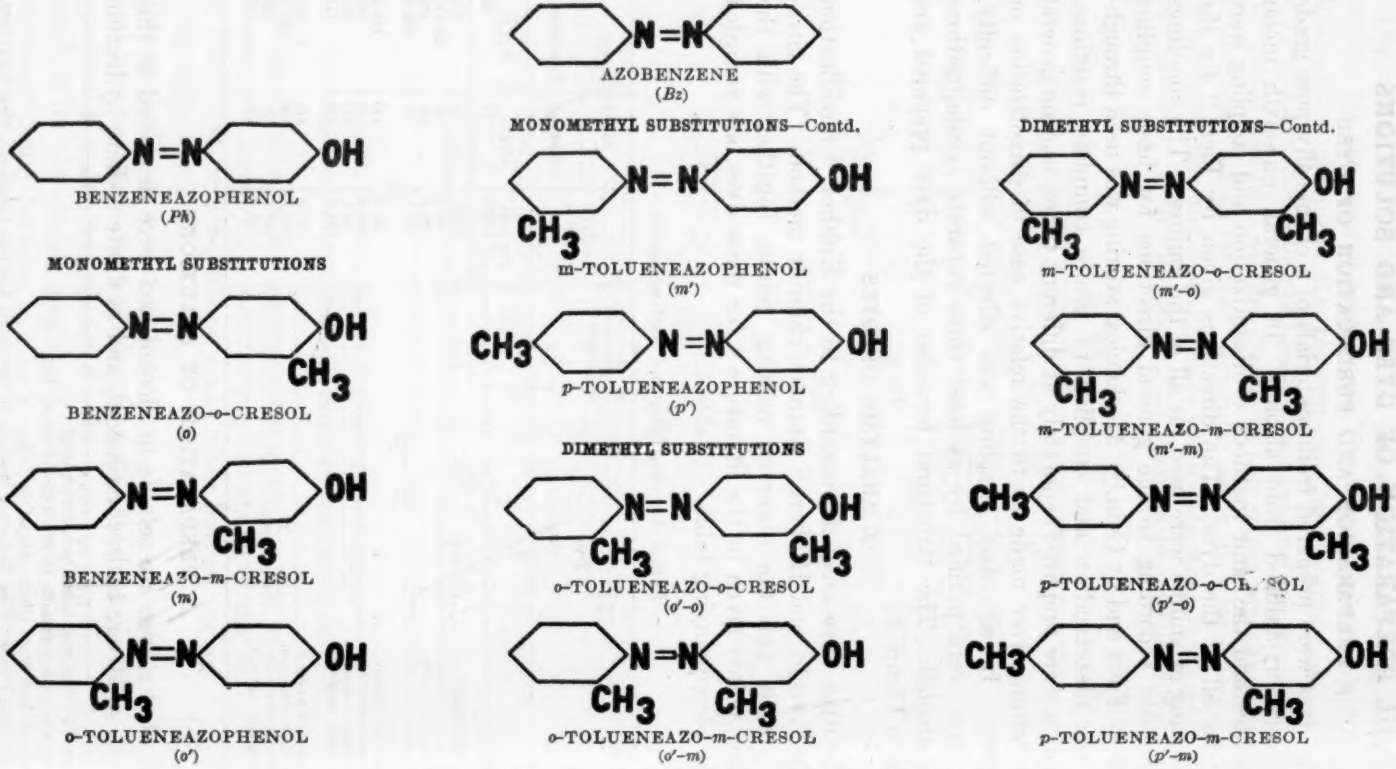

FIG. 4.—*Structural formulas of the compounds studied*

lution, with the exception of azobenzene, which could be measured alcohol and hydrochloric acid solutions only. The alcohol solutions were prepared as follows: 0.7200 g of benzeneazophenol or 8450 g of its various methyl and dimethyl derivatives was dissolved 95 per cent ethyl alcohol at room temperature and diluted to 500 l at 20° C. (solution A). The alcohol was of good commercial ality and showed practically no selective absorption in the spectral gions studied. Fifty ml of solution A was diluted with alcohol to 0 ml (solution B) and 25 ml of solution B diluted to 250 ml (solution). Thus solution C, which was measured, contained 2.88 cg per er of benzeneazophenol, or 3.38 cg per liter of the mono- and methyl dyes.

The acid solutions were made by diluting 5 ml of solution B to 100 l with the usual laboratory 35 per cent C. P. hydrochloric acid. he concentration of the dye in these solutions was then 1.44 cg per er of solution in the case of benzeneazophenol and 1.69 cg per liter the other dyes. It should be noted that these solutions and the kaline solutions described below contained a small amount of ohol.

The alkaline solutions were made by diluting 10 ml of solution B d 10 ml of a 30 per cent solution of C. P. stick sodium hydroxide in stilled water to 100 ml with distilled water. The concentration of e dye in the alkaline solutions was the same as in the alcohol lutions. The concentration of the sodium hydroxide in the solutions measured was 3 per cent.

The alcohol and hydrochloric acid solutions of azobenzene were epared in the same manner as the above solutions, using 0.825 g the pure compound. The measured solutions contained 3.30 cg dye per liter in alcohol and 1.65 cg per liter in hydrochloric acid.

IV. EXPERIMENTAL DATA

The experimental data obtained in the determination of the spectral sorption of azobenzene, benzeneazophenol, and all the mono- and methyl derivatives of benzeneazophenol, in which there is not more an one methyl substitution in a benzene ring, dissolved in alcohol, ncentrated hydrochloric acid, and 3 per cent aqueous sodium droxide, are given graphically in Figures 12 to 37 and numerically Tables 2 to 6. The data in the graphs are plotted on a form previously described, and in each case the name of the compound, the lvent, the concentration of the dye, and the cell length are given. he points on the graphs are the average of all the observations made. he spectral absorptions of the dyes in alcohol and in hydrochloric id are presented on the same graphs. In all cases the band of lower equency is the principal one of the curve for the hydrochloric acid lution. It should be noted that the concentration of the dye in

FIG. 4.—*Structural formulas of the compounds studied*

hydrochloric acid is one-half the concentration of the same dye in alcohol. The spectral absorption of the dyes in an aqueous solution of sodium hydroxide, as well as that of benzeneazophenol in an alcoholic solution of sodium hydroxide, are plotted on separate graphs because of the unusual behavior of the dyes in these solvents. As an aid in the general comparison of the various curves, most of them are given on a greatly reduced scale in Figures 5, 6, 7, and 8. In comparing the curves in these figures it should be remembered that only with compounds having the same molecular weight is the concentration the same.

TABLE 2.—*Frequencies of the absorption bands of solutions of compounds in 95 per cent ethyl alcohol*

[Values given in vibrations per 10^{-12} second]

Compound [1]	Band I [2]	Band II	Band III	$\frac{f_I}{f_{II}}$	$\frac{f_{III}}{f_{II}}$
Bz	670	947	1,410	0.71	1.49
Ph	635	855	1,280	.74	1.50
o	627	843	1,257	.74	1.49
m	655	840	1,265	.78	1.51
o'	667	847	1,260	.78	1.48
m'	635	855	1,274	.74	1.49
p'	655	850	1,255	.77	1.48
o'-o	605	839	1,240	.72	1.48
o'-m	650	833	1,240	.78	1.49
m'-o	650	843	1,260	.77	1.48
m'-m	650	836	1,255	.78	1.50
p'-o	652	838	1,245	.78	1.48
p'-m	670	831	1,250	.81	1.50

[1] The names of the compounds represented by these abbreviations are given in Figure 4.
[2] The accuracy of these values is considerably lower than in the other cases, because of the size and shape of the bands.

TABLE 3.—*Specific absorptive indices of the absorption bands; that is, at the frequencies given in Tables 2 and 4, of solutions of the compounds studied in 95 per cent ethyl alcohol and in concentrated hydrochloric acid*

Compound [1]	Centigrams per liter	Solvents					
		Alcohol			Hydrochloric acid		
		Bands					
		I [2]	II	III	I	II [2]	III
Bz	2.731	0.06	1.28	1.10	2.20	0.82	(1.10)
Ph	2.971	.12	1.91	1.00	2.96	.16	.51
o	3.182	.11	1.82	.89	2.77	----------	.62
m	3.182	.09	1.76	.80	2.82	.13	.61
o'	3.182	.09	1.75	.89	2.71	.22	.64
m'	3.182	.08	1.83	.95	2.80	.17	.81
p'	3.182	.07	1.95	.98	3.12	.16	.65
o'-o	3.392	.09	1.78	.84	2.75	.16	.54
o'-m	3.392	.13	1.76	.84	2.76	.22	.63
m'-o	3.392	.10	1.87	.98	3.02	.27	.80
m'-m	3.392	.10	1.77	.79	2.94	.18	.74
p'-o	3.392	.08	1.95	.99	3.12	----------	.84
p'-m	3.392	.09	1.97	.84	3.32	----------	.66

[1] The names of the compounds represented by these abbreviations are given in Figure 4.
[2] The accuracy of these values is considerably lower than in the other cases, because of the size and shape of this band.

TABLE 4.—*Frequencies of the absorption bands of solutions of the compounds in concentrated hydrochloric acid*

[Values given in vibrations per 10^{-12} second]

Compound [1]	Band I	Band II [2]	Band III [2]	$\frac{f\,II}{f\,I}$	$\frac{f\,III}{f\,I}$
Bz	725	1,070	----------	1.48	----------
Ph	644	922	1,207	1.43	1.87
o	628	----------	1,185	----------	1.89
m	636	927	1,172	1.46	1.84
o'	628	890	1,176	1.42	1.87
m'	632	920	1,185	1.46	1.88
p'	625	910	1,185	1.46	1.90
o'-o	619	870	1,160	1.41	1.87
o'-m	628	927	1,195	1.48	1.90
m'-o	630	922	1,190	1.46	1.89
m'-m	629	900	1,210	1.43	1.92
p'-o	617	----------	1,172	----------	1.90
p'-m	613	----------	1,187	----------	1.94

[1] The names of the compounds represented by these abbreviations are given in Figure 4.
[2] The accuracy of these values is considerably lower than in the other cases, because of the size and shape of the bands.

TABLE 5.—*Frequencies of the absorption bands of solutions of the compounds studied in a 3 per cent aqueous solution of sodium hydroxide*

[Values given in vibrations per 10^{-12} second]

Compound [1]	Band I				Band II
	A		B		
	A (observed)	A′ (analysis)	B (observed)	B′ (analysis)	Observed [2]
Ph	697	676	760	778	1,140
o	673	672	763	770	1,107
m	675	672	737	760	1,110
o'	695	672	743	764	1,170
m'	698	672	765	770	1,150
p'	698	672	773	770	1,181
o'-o	[3] (690)	668	----------	755	1,128
o'-m	665	665	729	752	1,150
m'-o	670	667	745	750	1,110
m'-m	670	666	738	755	1,120
p'-o	661	664	757	748	1,110
p'-m	668	664	735	752	1,138

[1] The names of the compounds represented by these abbreviations are given in Figure 4.
[2] The accuracy of these values is considerably lower than in the other observed cases, because of the flat shape of this band and its position in the far ultra-violet near the limit of observation.
[3] Approximate values.

TABLE 6.—*Specific absorptive indices of the absorption bands; that is, at the frequencies given in Table 5, of solutions of the compounds studied in a 3 per cent aqueous solution of sodium hydroxide*

Compound [1]	Bands						
	I						II
	A (observed)	B (observed)	A′ (analysis)	B′ (analysis)	A′+B′	$\frac{A'}{A'+B'}$	
Ph	1.70	1.56	1.53	1.29	2.82	0.543	0.60
o	1.84	1.38	1.82	.85	2.67	.682	.68
m	1.55	1.67	1.38	1.29	2.67	.518	.65
o′	1.48	1.63	1.18	1.40	2.58	.457	.61
m′	1.69	1.55	1.50	1.26	2.76	.543	.66
p′	1.77	1.60	1.57	1.32	2.89	.542	.66
o′–o	[2](1.63)	[2](1.51)	1.47	1.06	2.53	.581	.65
o′–m	1.14	1.63	1.06	1.34	2.40	.442	.61
m′–o	1.96	1.50	1.92	.90	2.82	.680	.71
m′–m	1.53	1.71	1.40	1.31	2.71	.517	.61
p′–o	2.05	1.26	2.05	1.02	3.07	.668	.72
p′–m	1.64	1.86	1.52	1.42	2.94	.517	.73

[1] The names of the compounds represented by these abbreviations are given in Figure 4.
[2] Approximate values.

In Tables 2, 4, and 5 are given the observed values for the frequencies of the absorption bands.

In Tables 3 and 6 are given the specific absorptive indices, **k**, of the compounds studied at the frequencies of the bands. (See Tables 2, 4, and 5.) These values of **k** are the corresponding values of $-\log_{10}\mathsf{T}$ taken from the graphs reduced to unit thickness and concentration. For convenience, the measured thickness 0.5 cm has been taken as the unit of thickness and 1.5×10^{-4} g molecule per liter of solution as the unit of concentration. The latter is equivalent to 2.731 cg of azobenzene, 2.971 cg of benzeneazophenol, 3.182 cg of the monomethyl-benzeneazophenols, and 3.392 cg of the dimethyl-benzeneazophenols per liter of solution. With this unit of concentration the calculated values, **k**, are usually rather near the observed values, $-\log_{10}\mathsf{T}$. However, Beer's law was found to be applicable to the solutions over a much wider range of concentrations than are involved in the calculations of **k**. The values of **k**, Tables 3 and 6, represent then the absorption of molecular equivalents of the dyes in the different solvents at the frequencies of maximum absorption.

V. DISCUSSION OF RESULTS

1. ALCOHOL SOLUTIONS

The spectral absorptions of azobenzene and benzeneazophenol have been discussed in previous articles [19] and will be referred to only in relation to the absorption of the derivatives with which this paper is concerned.

[19] See footnotes 2 and 3, p. 502.

Table 2 gives the positions of the absorption bands of the solutions of the dyes in 95 per cent ethyl alcohol. There are three bands which are similar in character for all the compounds. The first band is small, the second prominent and narrow, and the third intermediate in size and shape between the other two. The numerical relationship between the positions of the bands of the individual compounds is given in the table. It will be seen that the frequency of the first band is 0.76 ± 0.05 time that of the second and the frequency of the third 1.49 ± 0.02 times that of the second. This gives a whole number relationship between the frequencies of the bands of very nearly 3, 4, and 6 times some fundamental frequency. The introduction of the OH group into azobenzene, of the CH_3 group into benzeneazophenol, and of the CH_3 group into methylbenzeneazophenol is accompanied by a shift in the position of the bands to lower frequencies in most but not all cases. The relationship between the positions of the bands is apparently not altered by these changes in constitution.

The specific absorptive indices of the absorption bands shown by the alcohol solutions are listed in Table 3. The introduction of OH into azobenzene is accompanied by an increase in the index of the second band and a decrease in that of the third band. The specific absorptive indices of the second and third bands of the methyl and dimethyl derivatives are all smaller than the corresponding values of benzeneazophenol with the exception of the *p'*-substituted compounds, whose indices for the second band are larger than those of benzeneazophenol. The ratio of the index of the third band to that of the second is 0.86 for azobenzene, 0.52 for benzeneazophenol, and varies between 0.46 and 0.52 for the methyl and dimethyl derivatives. Thus, there is no decided shift in the relative absorption of the second and third bands in going from benzeneazophenol to its methyl derivatives, although there are variations in the absorptive indices. The variations in the specific absorptive indices of the first band are not significant, because the band is too small to be accurately measured.

2. HYDROCHLORIC ACID SOLUTIONS

Hydrochloric acid may behave not only as a solvent, but as a reagent. Addition compounds of this acid with some of the dyes discussed in this paper have been isolated, and it is probable that similar compounds may exist in the solutions measured. No attempt has been made to study the formation of such compounds, but a comparison of the spectral absorption of the hydrochloric acid solutions with that of the corresponding alcohol solutions indicates that the effect of the acid is not merely one of a solution, but is chemical in nature, and is not directly associated with the hydroxyl group.

Table 4 gives the positions of the absorption bands of the solutions of the dyes in concentrated hydrochloric acid. There are three bands, similar in character for all of the compounds studied but entirely different from those of the compounds dissolved in alcohol. The first

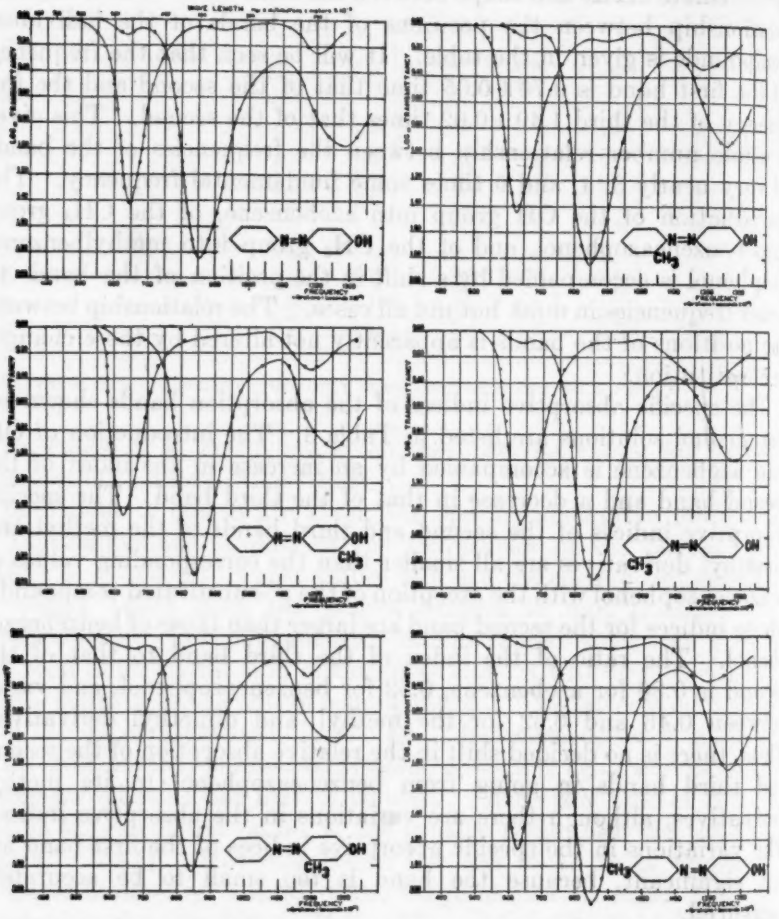

FIG. 5.—*The spectral absorption of solutions of benzeneazophenol and its monomethyl derivatives in 95 per cent ethyl alcohol (the right-hand principal bands) and in concentrated hydrochloric acid (the left-hand principal bands)*

The names of the compounds, the formulas of which are shown in the above graphs, are given in Figure 4. For data on these compounds plotted on a larger scale, giving cell thickness and concentration, see Figures 13, 16, 18, 20, 22, and 24

band is prominent and narrow, the second band is very small, and the third intermediate between the other two. The second band is located at a frequency approximately 1.45 times that of the first. The third band is located at a frequency 1.89 ± 0.06 times that of the first.

Substitution is accompanied by a shift in the position of the bands to lower frequencies except in three of the dimethyl derivatives.

The specific absorptive indices of the bands are listed in Table 3. The indices of the first band are considerably larger than those of the

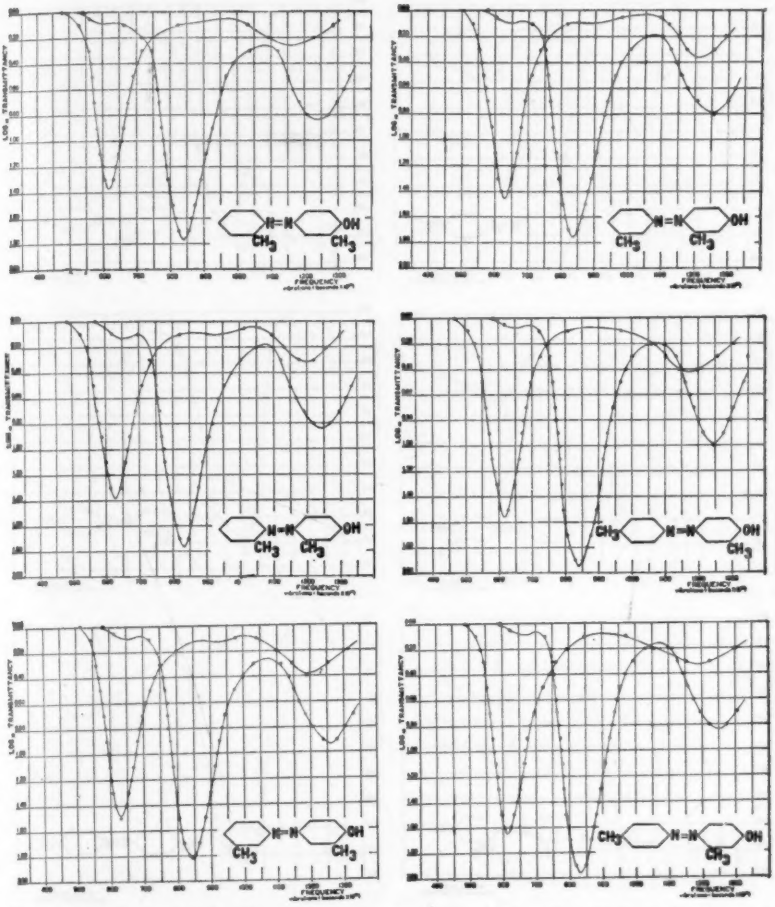

FIG. 6.—*The spectral absorption of solutions of the dimethyl derivatives of benzeneazophenol, in which but one methyl substitution occurs in a benene ring, in 95 per cent ethyl alcohol (the right-hand principal bands) and in concentrated hydrochloric acid (left-hand principal bands)*

The names of the compounds, the formulas of which are shown in the above graphs, are given in Figure 4. For data on these compounds, plotted on a larger scale, giving concentration and cell thickness, see Figures 26, 28, 30, 32, 34, and 36

principal band of the alcohol solution in each instance. The introduction of the OH group into azobenzene and of the methyl groups into benzeneazophenol is accompanied by changes in the specific absorptive index of the first band analogous to those of the second band of the corresponding alcohol solutions.

3. SODIUM HYDROXIDE SOLUTIONS[20]

The action of a solution of sodium hydroxide is chemical in nature and is directly connected with the hydroxyl group in the molecule, so that data on azobenzene can not be obtained.

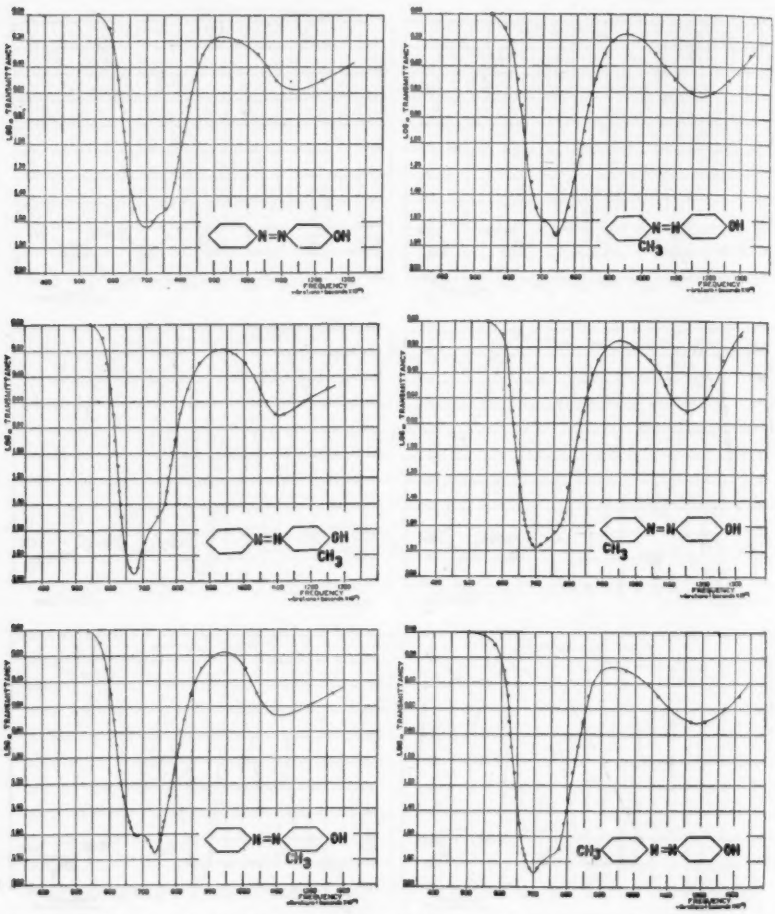

FIG. 7.—*The spectral absorption of solutions of benzeneazophenol and its monomethyl derivatives in a 3 per cent aqueous sodium hydroxide solution*

The names of the compounds, the formulas of which are shown in the above graphs, are given in Figure 4. For data on these compounds, plotted on a larger scale, giving cell thickness and concentration, see Figures 14, 17, 19, 21, 23, and 25

The absorption spectrum of benezeneazophenol in a 3 per cent aqueous solution of sodium hydroxide has two principal bands. The first band is more than twice as strong as the second and, like those already described in this paper, is asymmetric with a larger portion of the base on the high-frequency side. It differs, however, from

[20] A portion of this section was presented before the Philadelphia meeting of the American Chemical Society, September, 1926.

the other bands studied in that it is broad at the peak and unsymmetrical, with an indication of being composed of two bands close together, the component of lower frequency being slightly stronger than the other. Confirmation of the presence of two overlapping bands is to be found in the data for the methyl derivatives of the dye

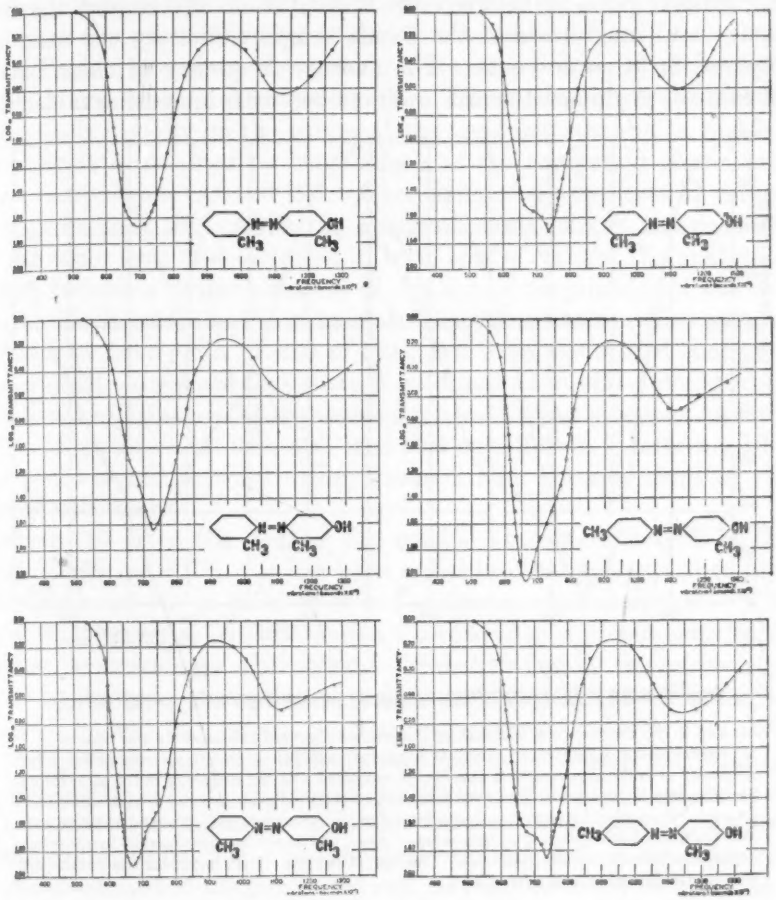

FIG. 8.—*The spectral absorption of solutions of the dimethyl derivatives of benzeneazophenol, in which but one methyl substitution occurs in a benzene ring, in a 3 per cent aqueous solution of sodium hydroxide*

The names of the compounds, the formulas of which are shown in the above graphs, are given in Figure 4. For data on these compounds, plotted on a larger scale, giving cell thickness and concentration, see Figures 27, 29, 31, 33, 35, and 37

described below. The second principal band is located at 1,140 f and is broad and flat in character.

The general characteristics of the spectral absorption of the mono- and dimethyl derivatives of benzeneazophenol are the same as those of the parent substance; that is, (1) two principal bands, the first being more intense than the second; and (2) the first band appears to

be composed of two components which together produce the observed band. Since this principal band appears to be composed of two parts and varies considerably in shape with different compounds, it is difficult to draw any conclusions with regard to the relation between either frequency or amount of absorption and chemical constitution. The general relation between the substitution effects and the frequency and magnitude of the bands is approximately the same as observed in other solvents. The average frequency of these bands appears to be shifted toward lower values with increasing molecular

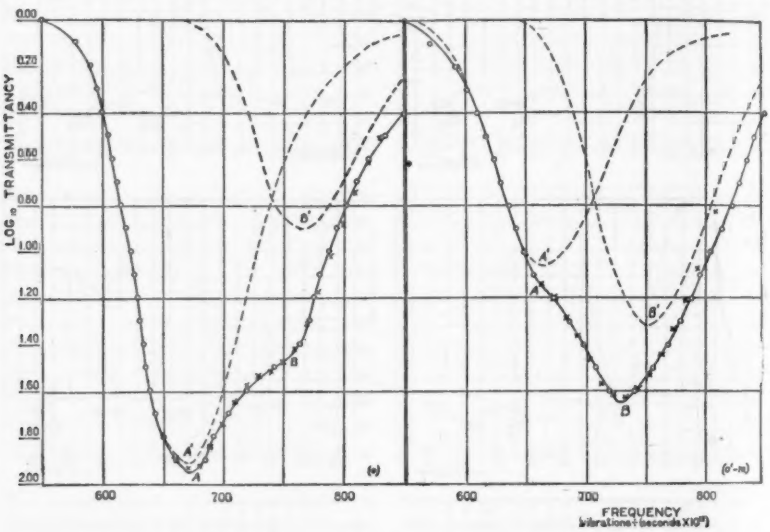

FIG. 9.—*The analysis of two observed curves into component curves*

Note that in the above curves, which show the greatest observed difference in the ratio of A′ to B′, the frequency differences of A′ and B′ is approximately the same in both cases. The shift in frequency of both components in case (*b*), as compared with the frequency of the same components in case (*a*), is approximately the same as that observed in alcohol and in hydrochloric acid solutions, when a second methyl radical is introduced into the molecule. The above curves represent the spectral absorption of (*a*) benzeneazo-*o*-cresol, and (*b*) *o*-tolueneazo-*m*-cresol in a 3 per cent aqueous solution of sodium hydroxide. (See figs. 17 and 29.) The *x* marks on the graphs indicate values calculated from A′ and B′

weight. The spectral absorption of compounds with *p′*-substitutions is greater than that with the other substitutions or of the unsubstituded parent compound. By a method of analysis [21] it has been

[21] The analysis of these curves into their elements is based on two assumptions—(1) that each composite curve has but two components and (2) that these two components have the same shape when calculated to the same height of band. The basis of the first assumption is that the general characteristics of all of these bands are such as to indicate but two main components. The observed bands may be composed of a large number of lesser components or even lines, but, for the purposes of analysis and study, it may be assumed that these lesser components are equivalent in their aggregate to only two effective bands. The second assumption is based on the following facts. In the other solvents studied the general shape of each curve and the frequency relations between the bands were the same for all of the compounds. It is therefore reasonable to expect the same general relationships when an aqueous solution of sodium hydroxide is used as a solvent.

If these assumptions are accepted, then each of the observed composite curves can be analyzed into two component curves definite in shape and position. It does not follow, however, that all composite curves

possible to determine approximately the frequency and magnitude of the component bands which constitute the observed principal band. These data are given in Tables 5 and 6, together with approximate values obtained directly from the compound curves. The smaller band observed in the neighborhood of $1{,}150\,f$ is extremely flat and varies considerably in shape with the particular compound, which indicates the possibility that it also is a compound band.

In Table 6 are given the specific absorptive indices of the components A and B of the principal bands. These values include observations made directly on the curves at the apparent maxima (A and B), and the data obtained by the analysis of the compound curves into their components (A′ and B′). Comparing these two sets of values, it may be seen that, while the apparent deviations in the data are of the same type and direction in both sets of values, the analytical values furnish a better estimate of the actual magnitudes of the two bands which compose the principal absorption bands. The general indications from both groups of data and from the varied shapes of the original curves are that there is an apparent equilibrium between two forms of vibration of the molecule, representing, possibly, slightly different molecular states, and that this equilibrium is influenced by the position of the substituting group in the benzene rings of the parent substance.

Figure 10 gives the sum of the specific absorptive indices of the components (A′+B′). It has been noted in other solvents that substitution in the the *p′*-position causes an increase in absorption. This generalization holds equally true in the case of an aqueous solution of sodium hydroxide as the solvent. Substitution in the *o′*-position tends to decrease absorption as well as influence the relative magnitudes of A′ and B′.

The spectral absorption of benzeneazophenol, the parent substance, in an aqueous solution of sodium hydroxide represents what we may call a neutral equilibrium in which band A is of slightly greater magnitude than band B. This neutral equilibrium does not represent an equal amount of the two forms and may undoubtedly be influenced by changes in the character of either the basic substance or the solvent. For example, in the absorption spectrum of benzeneazophenol in an alcoholic solution of sodium hydroxide (fig. 15) the equilibrium has been shifted with an increase in B and a corresponding decrease in A. Two other curves closely resemble the neutral curve of benzene-

can be so analyzed. The fact that all of the curves studied may be so analyzed lends additional weight to the assumptions. The suitability of the theory is further attested by the facts that (1) the frequency differences of the component bands in all cases are approximately the same, (2) there is an apparent equilibrium between the two component bands, dependent on the position of the substitution, so that as one band is increased the other band is decreased a corresponding amount. The general relations between the magnitudes of the bands, both observed and calculated (Table 6), are of the same general type. The analytical data, however, show more clearly the relative proportions of the two components in any one band.

azophenol, namely, those of the spectral absorption of the *m'*- (fig. 23) and *p'*- (fig. 25) substituted compounds. These two, together with the unsubstituted parent substance, constitute the neutral group or series. In the case of the *m'*-substituted compounds there appears to be practically no effect of any kind on either the equilibrium between A and B or the specific absorptive indices of these bands. In the case of the *p'*-substituted compounds there is an increase in absorption, but the relative shapes of the bands and the ratio between A and B are the same as in the original compound without the *p'*-substitution.

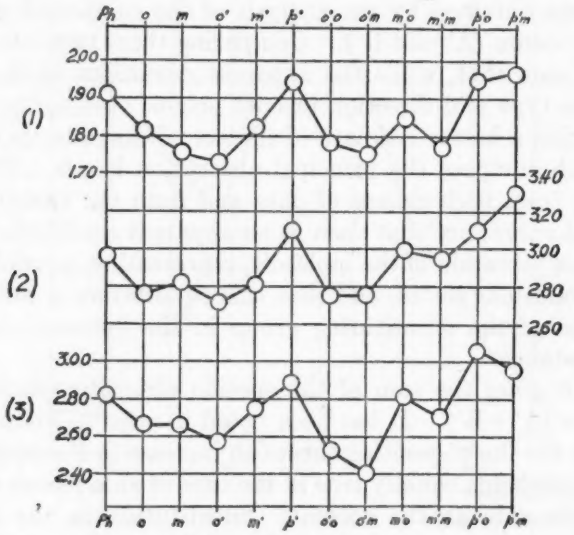

FIG. 10.—*Specific absorptive indices at the frequencies of maximum absorption of the principal bands of solutions of the compounds studied in (1) ethyl alcohol, (2) concentrated hydrochloric acid, and (3) a 3 per cent aqueous solution of sodium hydroxide (A'+B')*

(The abbreviated symbols for the compounds are explained in fig. 4)

Substitution in the *o*-position (*o* to the hydroxyl group) (fig. 17) causes a marked increase in the A band and a corresponding decrease in the B band, or, in other words, a shift of the equilibrium toward the A state.

Substitution in the *m*-position (fig. 19) causes a shift of the equilibrium in the opposite direction; that is, an increase in the B band with a corresponding decrease in the A band. The degree of shift of this equilibrium from the neutral state, however, is not as great as in the case of the *o*-substitution.

Substitution in the *o'*-position (fig. 21) causes an increase in the B band with a decrease in the A band of about the same difference from the neutral ratio, but in the opposite direction to that caused

by the *o*-substitution. In addition, there is a suppression of both of the bands, so that the sum of the specific absorptive indices of bands A and B is considerably smaller than in the other cases. (Fig. 10.)

The general effect of di-substitution on the specific absorptive indices of the two component bands is a combination of two separate directing forces. In the case of the *o'*, *o*-substituted compound (fig. 27) the effects are opposite in character and to a large extent neutralize each other. The *o*-substitution appears to have a slightly stronger influence than the *o'*-substitution, as the percentage of A present is slightly greater than in the neutral equilibrium. (Fig. 11.) How-

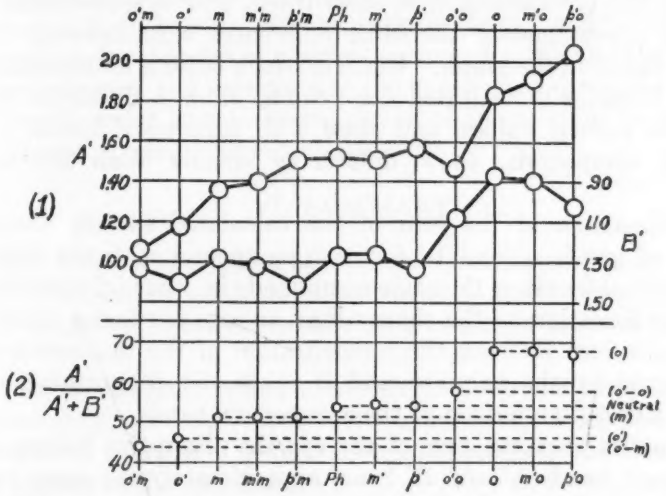

FIG. 11.—(*1*) *Specific absorptive indices of the components of the principal bands of solutions of the compounds studied in a 3 per cent aqueous solution of sodium hydroxide.* A' *= upper series,* B' *= lower series.* (*2*) *Percentage of the* A' *component,* $\frac{A'}{A'+B'}$, *of the principal bands of solutions of the compounds studied in a 3 per cent aqueous solution of sodium hydroxide*

(The abbreviated symbols for the compounds are explained in fig. 4)

ever, the effect of the *o'*-substitution on the suppression of the bands seems to be only slightly influenced by the oppositely directed force of the *o*-substitution. In the *o'*, *m*-substituted compound (fig. 29) the substituting positions influence in the same direction from the neutral equilibrium or level, so that there is an addition of the two effects and a slightly greater suppression of the bands due to the *o'*-substitution. The effect of the introduction of the second substitution in the *m'*-position on the spectral absorption of the compound is practically nil within the accuracy of the observations. There is possibly a slight increase in the specific absorptive indices of the bands of the *m'*, *o*-substituted compound over that of the *o*-substi-

tuted compound alone, and a slight lowering of the ratio of A to B. In the spectral absorption of the *m'*, *m*-substituted compound there is an indication of the same effect, although it is less prominent than in the *m'*, *o*-substituted compound. The influence of substitution in the *p'*-position, as mentioned before, seems to be merely to increase the absorption, an effect quite independent of the solvent used.

In the graph (fig. 11) giving the specific absorptive indices of components A' and B', those of B' are plotted on an inverted scale, since from general observation it may be seen that as one band increases the other decreases. It is to be noticed that in cases which are normal, such as the unsubstituted, *m*-substituted, and *m'*-substituted compounds, approximately the same differences exist between the A' and B' values in the graph. Cases in which there is an intensification of the bands, *p'*-substituted compounds, show a difference greater than the normal values, and cases with suppressed bands, *o'*-substituted compounds, show differences smaller than the normal values.

A comparison of the sum of the calculated specific absorptive indices of bands A' and B' for each compound with the indices of the principal bands of the same compounds in other solvents (fig. 10) lends confirmation to the theory that, in any particular compound, the equilibrium between the concentration of the tautomeric forms represented by the bands A and B is directly proportional to the specific absorptive indices of their respective bands.

It appears that the sum of the specific absorptive indices of the component bands A' and B' bears approximately the same relation to the indices of the principal bands of the same compounds in other solvents. Hence, for each compound the ratio of $A'/A'+B'$ should give approximately the percentage of the A compound present and at the same time make the necessary corrections or allowances for the *p'*- and *o'*-substitution effects on the specific absorptive indices of both the bands. Table 6 gives these percentage values which, as may be observed, can be arranged in groups (fig. 11) representing different stages or levels in the equilibrium.

Reference should be made to the works of earlier investigators which are closely related to the principal objects of this investigation. The methods and apparatus used by many of these investigators have limited the possible accuracy of their observations to such an extent as to preclude the detection of variations in the shape of the curves of the order observed in the study of the series of compounds described in this paper. Baly,[22] Purvis,[23] and Klingstedt[24] have observed the effect of *p*-substitution on the increase in the magnitude

[22] Baly, J. Chem. Soc., **107**, p. 1058; 1915.
[23] Purvis, J. Chem. Soc., **103**, p. 1088; 1913.
[24] Klingstedt, Compt. rend., **175**, p. 365; 1922.

of the band. This same effect, although not always mentioned, can be noted in the data of other observers. Among the series of data on the absorption spectra of isomeric compounds, where the isomerism consists of the change of the position of substitution in a benzene ring, may be mentioned the following: *o*-, *m*-, and *p*-xylene, *o*-, *m*-, and *p*-nitrotoluene, *o*-, *m*-, and *p*-cresol, and a number of other derivatives, which are for the most part given in the list of references to the absorption spectra of organic compounds published by the British Association for the Advancement of Science.[25] With the exception of the general increase in magnitude of the bands of the *p*-substituted compounds, these data are of little aid in the prediction of the effect of substitution on the absorption bands. Recent work by Henri [26] and his coworkers on the absorption spectra of position isomers, in particular the xylenes, dichlorobenzenes, and toluidines in the vapor state, promises to be of considerable value in the determination of the relation between absorption and chemical constitution.

VI. SUMMARY

1. The spectral absorption of solutions of azobenzene in 95 per cent ethyl alcohol and in concentrated hydrochloric acid has been measured in the visible and in the ultra-violet to a frequency between 1,250 and 1,450 *f*.

2. The spectral absorption of solutions of benzeneazophenol in 95 per cent ethyl alcohol, concentrated hydrochloric acid, and a 3 per cent aqueous solution of sodium hydroxide has been measured in the same regions of the spectrum.

3. The 11 possible mono- and dimethyl derivatives of benzeneazophenol, in which there is but one methyl substitution in a benzene ring, have been prepared, and the spectral absorption of their solutions in the same solvents in the same regions of the spectrum as in the case of the parent compound, benzeneazophenol, has been measured.

4. The spectral absorption of a solution of benzeneazophenol in a 3 per cent alcoholic solution of sodium hydroxide has also been measured.

From the data obtained the following generalizations may be made:

1. An increase in molecular weight is, in most instances, accompanied by a decrease in the frequency of the absorption band of these similarly constituted compounds.

2. In any one solvent there appears to be a definite mathematical relationship between the frequencies of the observed bands. In the various solvents used the mathematical relationships between the

[25] Annual Report of the British Association for the Advancement of Science; 1916.

[26] Henri, Structure des Molécules, Herman, Paris; 1925.

observed absorption bands are quite different, indicating a considerable change in the molecular states of the compounds.

3. The introduction of a hydroxyl group into the *p*-position of the azobenzene molecule, forming benzeneazophenol, results, in addition to a decided shift in the frequency of the bands, in an increase in the magnitude and a narrowing of the principal band and a decrease in magnitude and flattening of the other observed bands. This would indicate a shift of the vibrational intensity of the molecule to the frequency of the principal band.

4. Substitution of a methyl group in the *p'*-position in benzeneazophenol results in an increase in the magnitude of the absorption bands, irrespective of the type of solvent.

5. Substitution of a methyl group in the *o'*-position in benzeneazophenol results in a general decrease in the magnitude of the absorption bands.

6. The principal absorption bands of solutions of benzeneazophenol and its methyl derivatives in a 3 per cent aqueous solution of sodium hydroxide appear to consist of two overlapping bands.

7. The equilibrium which seems to exist between these two components is dependent on the nature of the solvent and the position of the substituting group. An *o*-substitution of the methyl group in the benzeneazophenol molecule causes an increase in the lower frequency component, with a corresponding decrease in the higher frequency component. A *m'*- or *o'*- substitution produces a reverse effect, while the equilibrium is not affected by either a *m'*- or *p'*-substitution.

The data presented in this paper suggest the possibility of a method of structural analysis for the determination of the position of a substituting group in a complex organic molecule and a reverse of this process in the prediction of the spectral absorption of a compound of known structure. Additional data on the effect of substituting groups, including those of nitro, chlorine, bromine, carboxy, and sulphonic acid substitutions, are now being collected with this object in view.

Fundamental data have been presented on the relation between spectral absorption and chemical constitution.

Acknowledgement is made to W. D. Appel, of the dye laboratory of the chemistry division, for his assistance and advice in this work.

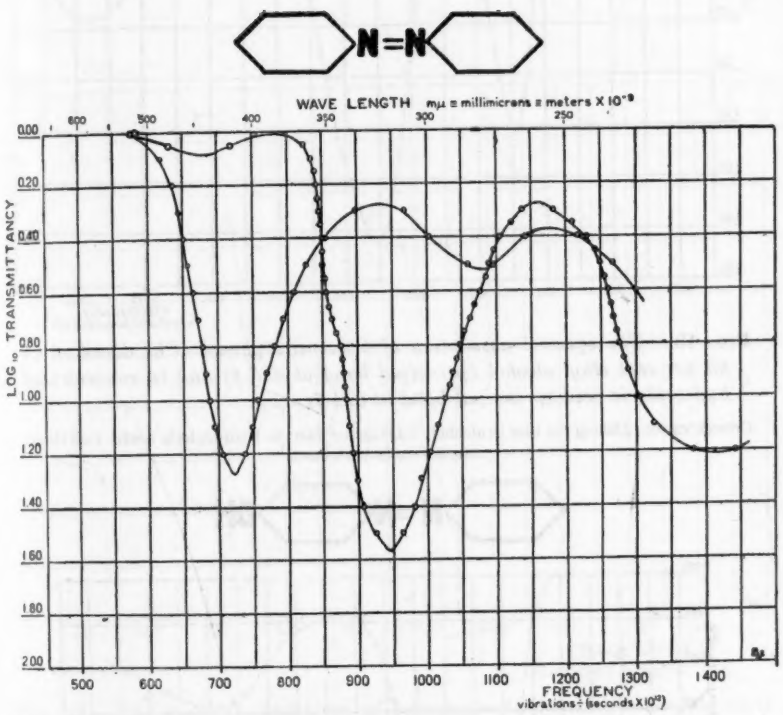

FIG. 12.—*The spectral absorption of azobenzene (Bz) dissolved in 95 per cent ethyl alcohol (principal band at 947 f) and in concentrated hydrochloric acid (principal band at 725 f)*

Concentration, 3.300 eg per liter in alcohol; 1.650 eg per liter in hydrochloric acid. Cell thickness 0.5 cm in both cases

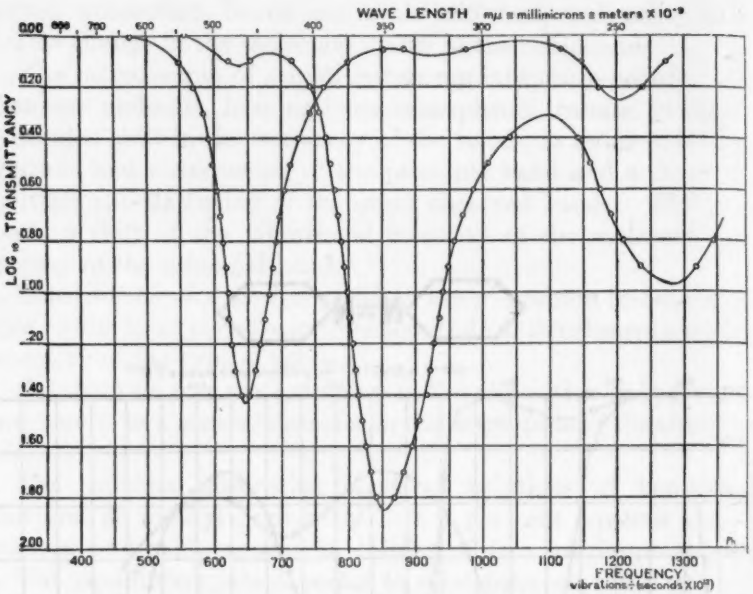

FIG. 13.—*The spectral absorption of benzeneazophenol (Ph) dissolved in 95 per cent ethyl alcohol (principal band at 855 f) and in concentrated hydrochloric acid (principal band at 644 f)*

Concentration, 2.880 cg per liter in alcohol; 1.440 cg per liter in hydrochloric acid. Cell thickness, 0.5 cm in both cases

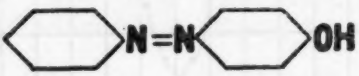

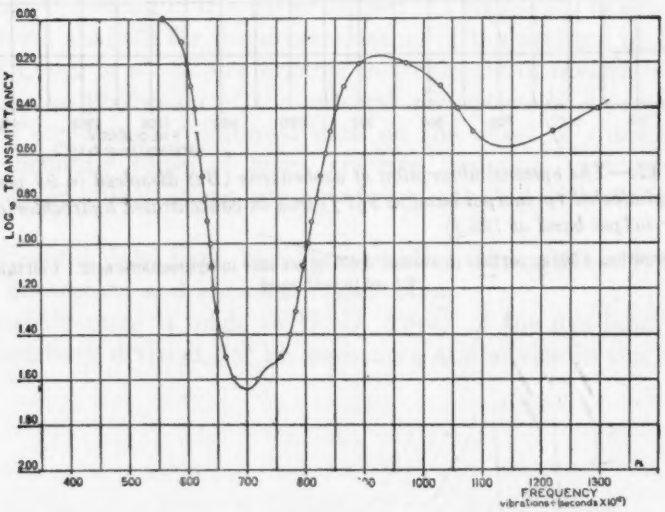

FIG. 14.—*The spectral absorption of benzeneazophenol (Ph) dissolved in a 3 per cent aqueous solution of sodium hydroxide*

Concentration, 2.880 cg per liter. Cell thickness, 0.5 cm

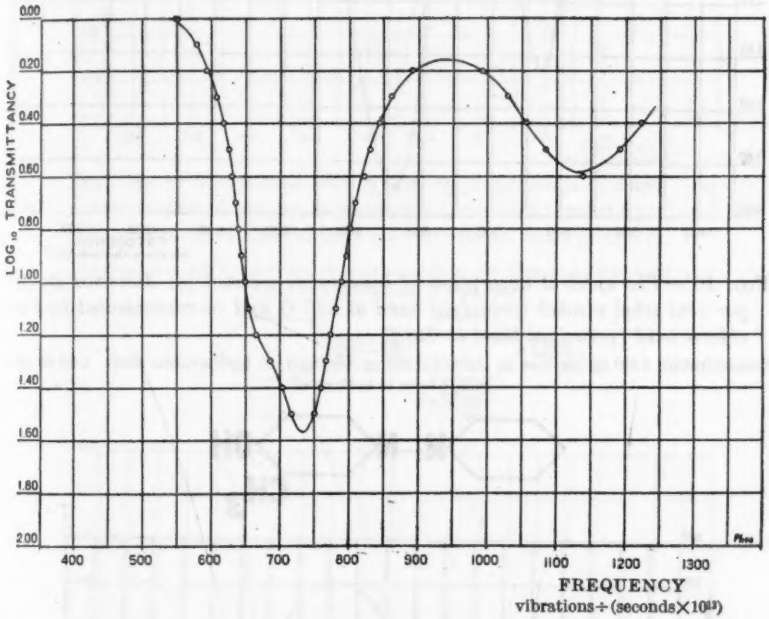

FIG. 15.—*The spectral absorption of benzeneazophenol (Ph) dissolved in a 3 per cent solution of sodium hydroxide in 95 per cent ethyl alcohol*

Concentration, 2.292 cg per liter. Cell thickness, 0.5 cm

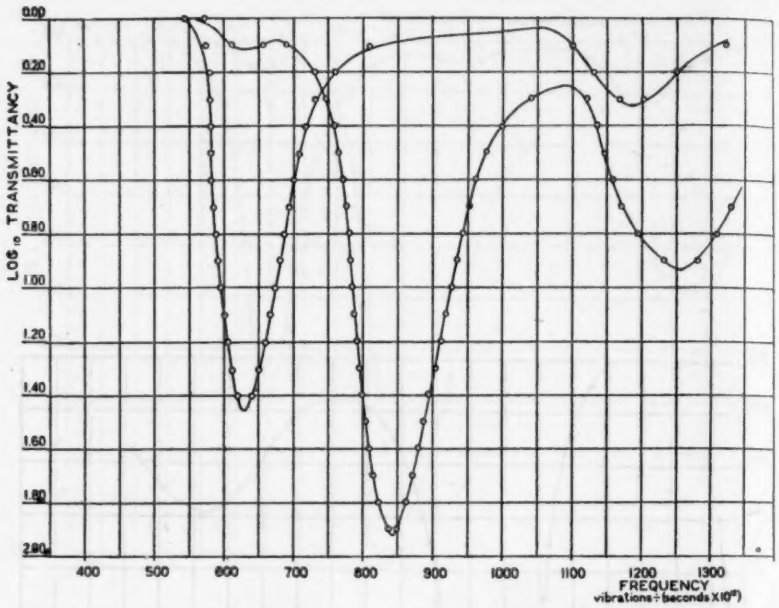

FIG. 16.—*The spectral absorption of benzeneazo-o-cresol (o) dissolved in 95 per cent ethyl alcohol (principal band at 843 f) and in concentrated hydrochloric acid (principal band at 628 f)*

Concentration 3.380 cg per liter in alcohol; 1.690 cg per liter in hydrochloric acid. Cell thickness, 0.5 cm in both cases

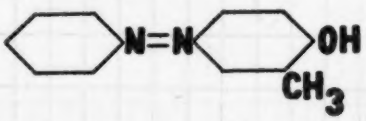

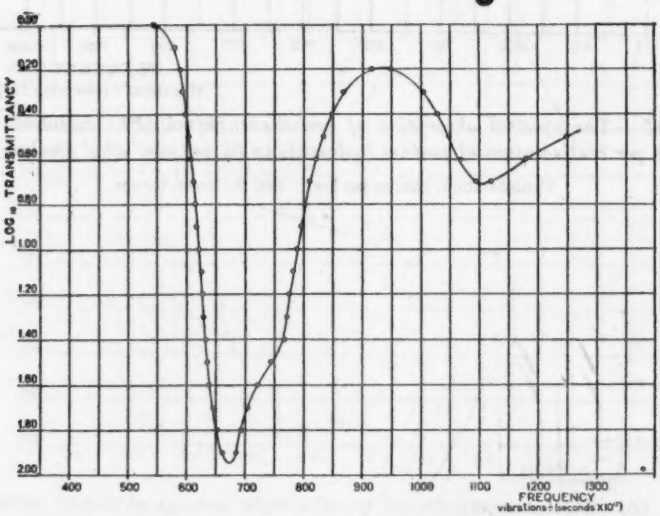

FIG. 17.—*The spectral absorption of benzeneazo-o-cresol (o) dissolved in a 3 per cent aqueous solution of sodium hydroxide*

Concentration, 3.380 cg per liter. Cell thickness, 0.5 cm

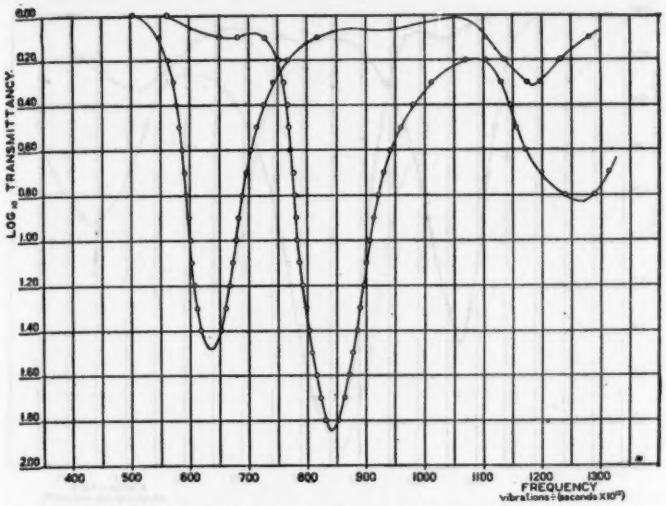

FIG. 18.—*The spectral absorption of benzeneazo-m-cresol (m) dissolved in 95 per cent ethyl alcohol (principal band at 840 f) and in concentrated hydrochloric acid (principal band at 636 f)*

Concentration, 3.380 cg per liter in alcohol; 1.690 cg per liter in hydrochloric acid. Cell thickness, 0.5 cm in both cases

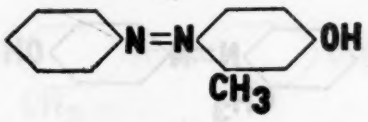

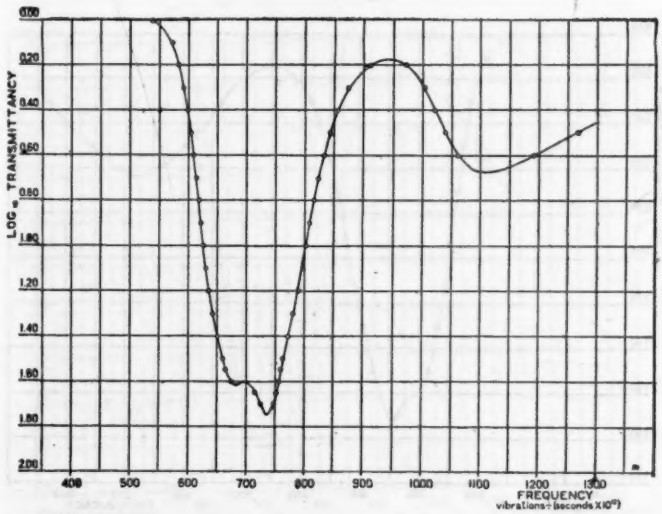

FIG. 19.—*The spectral absorption of benzeneazo-m-cresol (m) dissolved in a 5 per cent aqueous solution of sodium hydroxide*

Concentration, 3.380 cg per liter. Cell thickness, 0.5 cm

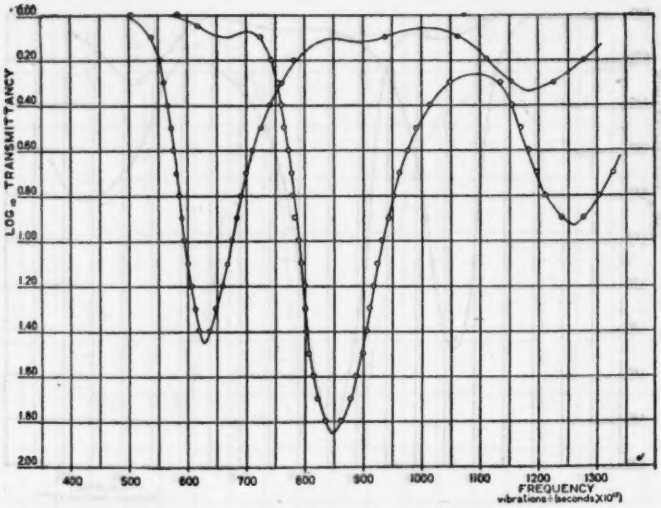

FIG. 20.—*The spectral absorption of o-tolueneazophenol (o′) dissolved in 95 per cent ethyl alcohol (principal band at 847 f) and in concentrated hydrochloric acid (principal band at 628 f)*

Concentration, 3.380 cg per liter in alcohol; 1.690 cg per liter in hydrochloric acid. Cell thickness, 0.5 cm in both cases

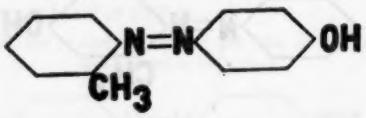

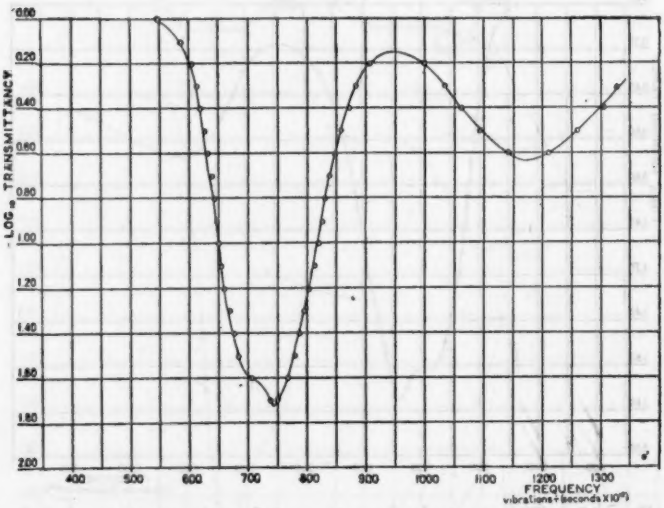

FIG. 21.—*The spectral absorption of o-tolueneazophenol (o′) dissolved in a 3 per cent aqueous solution of sodium hydroxide*

Concentration, 3.380 cg per liter. Cell thickness, 0.5 cm

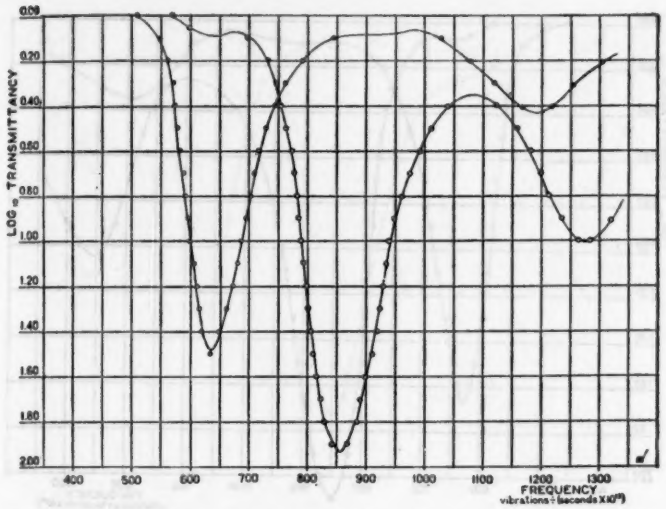

FIG. 22.—*The spectral absorption of m-tolueneazophenol (m') dissolved in 95 per cent ethyl alcohol (principal band at 855 f) and in concentrated hydrochloric acid (principal band at 632 f)*

Concentration, 3.380 cg per liter in alcohol; 1.690 cg per liter in hydrochloric acid. Cell thickness, 0.5 cm in both cases

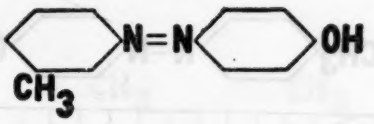

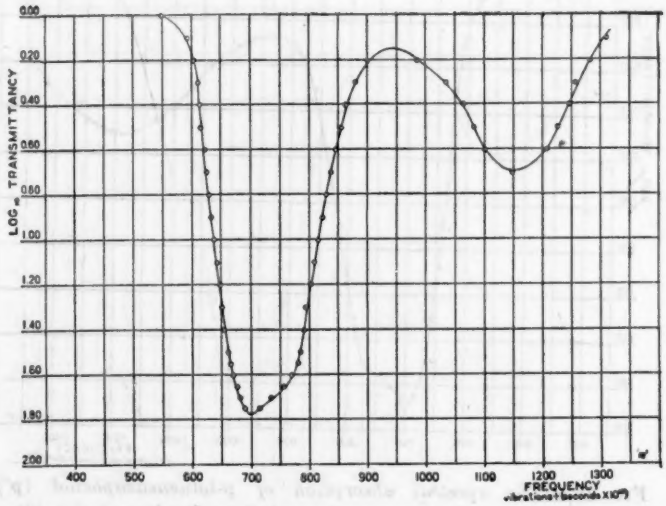

FIG. 23.—*The spectral absorption of m-tolueneazophenol (m') dissolved in a 3 per cent aqueous solution of sodium hydroxide*

Concentration, 3.380 cg per liter. Cell thickness, 0.5 cm

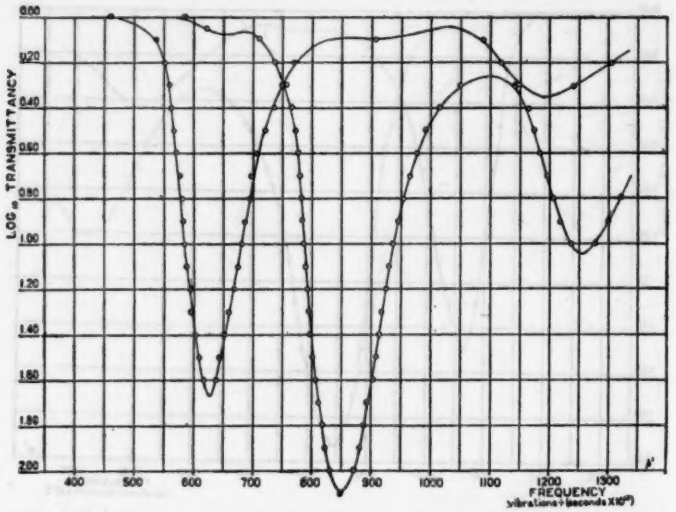

FIG. 24.—*The spectral absorption of p-tolueneazophenol (p') dissolved in 95 per cent ethyl alcohol (principal band at 850 f) and in concentrated hydrochloric acid (principal band at 625 f)*

Concentration, 3.380 cg per liter in alcohol; 1.690 cg per liter in hydrochloric acid. Cell thickness, 0.5 cm in both cases

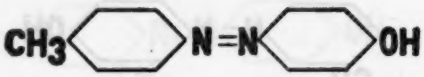

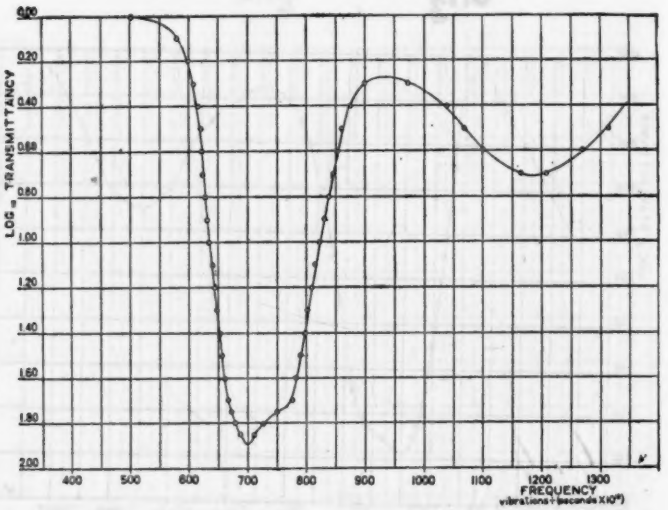

FIG. 25.—*The spectral absorption of p-tolueneazophenol (p') dissolved in a 3 per cent aqueous solution of sodium hydroxide*

Concentration, 3.380 cg per liter. Cell thickness, 0.5 cm

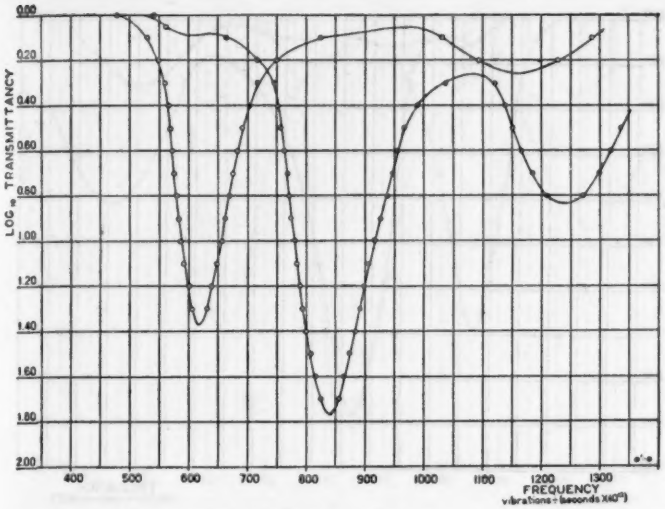

FIG. 26.—*The spectral absorption of o-tolueneazo-o-cresol (o', o) dissolved in 95 per cent ethyl alcohol (principal band at 839 f) and in concentrated hydrochloric acid (principal band at 619 f)*

Concentration, 3.380 cg per liter in alcohol; 1.690 cg per liter in hydrochloric acid. Cell thickness, 0.5 cm in both cases

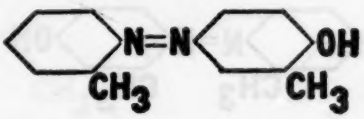

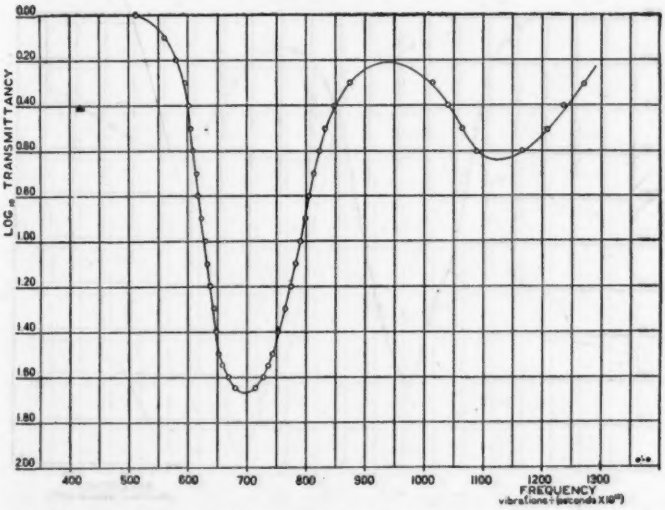

FIG. 27.—*The spectral absorption of o-tolueneazo-o-cresol (o', o) dissolved in a 3 per cent aqueous solution of sodium hydroxide*

Concentration, 3.380 cg per liter. Cell thickness, 0.5 cm

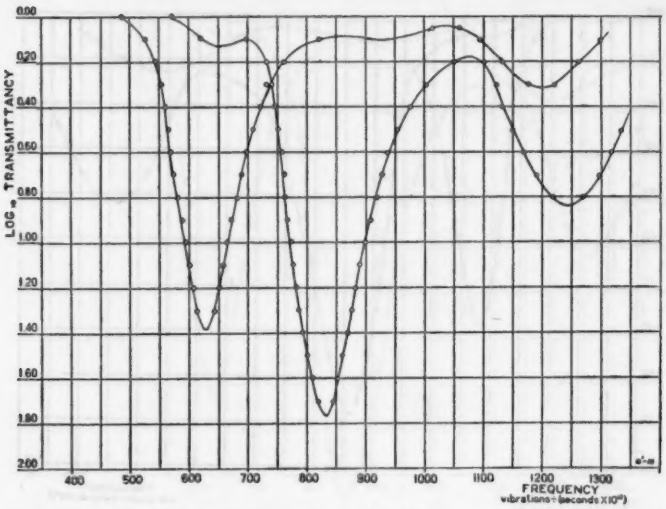

FIG. 28.—*The spectral absorption of o-tolueneazo-m-cresol (o', m) dissolved in 95 per cent ethyl alcohol (principal band at 833 f) and in concentrated hydrochloric acid (principal band at 628 f)*

Concentration, 3.380 cg per liter in alcohol; 1.690 cg per liter in hydrochloric acid. Cell thickness, 0.5 cm in both cases

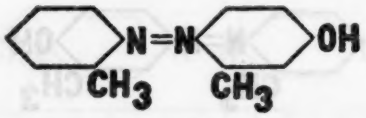

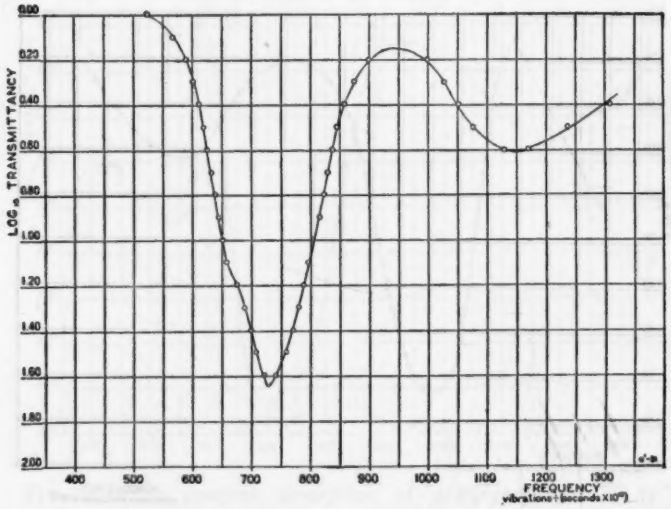

FIG. 29.—*The spectral absorption of o-tolueneazo-m-cresol (o', m) dissolved in a 3 per cent aqueous solution of sodium hydroxide*

Concentration, 3.380 cg per liter. Cell thickness, 0.5 cm

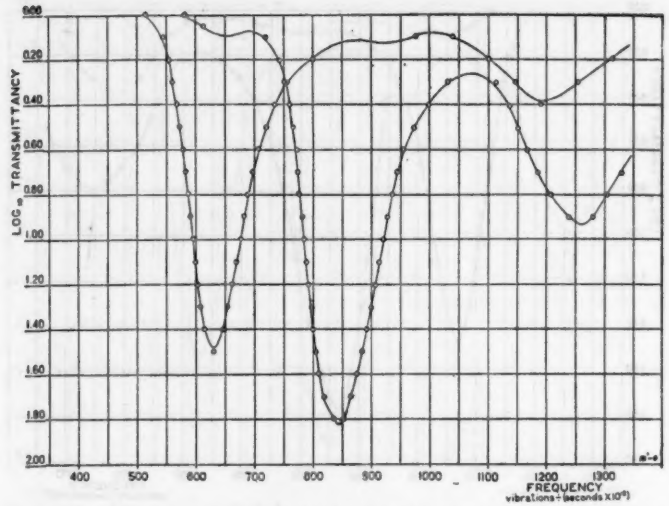

FIG. 30.—*The spectral absorption of m-tolueneazo-o-cresol (m′, o) dissolved in 95 per cent ethyl alcohol (principal band at 843 f) and in concentrated hydrochloric acid (principal band at 630 f)*

Concentration, 3.380 cg per liter in alcohol; 1.690 cg per liter in hydrochloric acid. Cell thickness, 0.5 cm in both cases

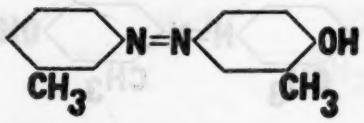

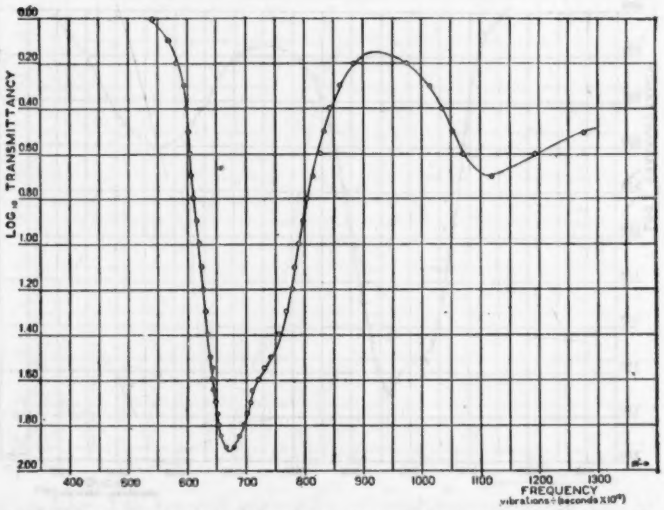

FIG. 31.—*The spectral absorption of m-tolueneazo-o-cresol (m′, o) dissolved in a 3 per cent aqueous solution of sodium hydroxide*

Concentration, 3.380 cg per liter. Cell thickness, 0.5 cm

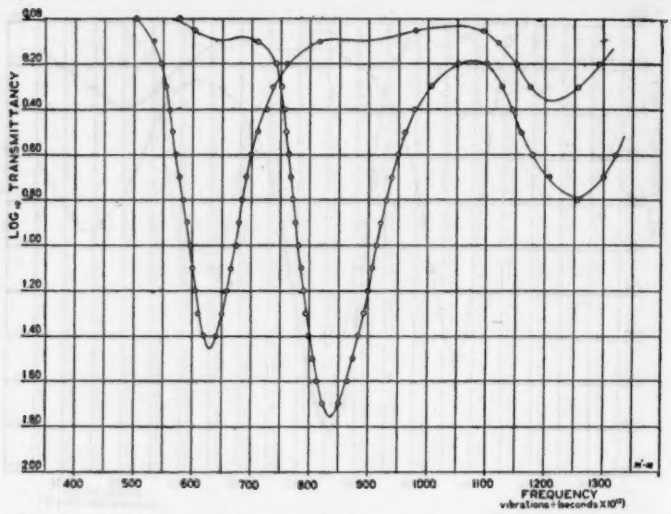

FIG. 32.—*The spectral absorption of m-tolueneazo-m-cresol (m′, m) dissolved in 95 per cent ethyl alcohol (principal band at 836 f) and in concentrated hydrochloric acid (principal band at 629 f)*

Concentration, 3.380 cg per liter in alcohol; 1.690 cg per liter in hydrochloric acid
Cell thickness, 0.5 cm in both cases

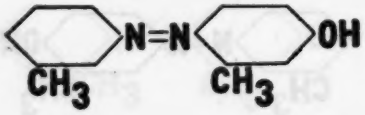

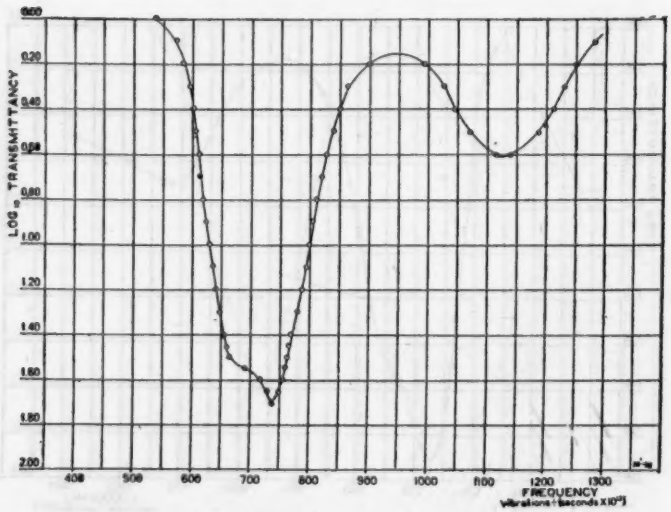

FIG. 33.—*The spectral absorption of m-tolueneazo-m-cresol (m′, m) dissolved in a 3 per cent aqueous solution of sodium hydroxide*

Concentration, 3.380 cg per liter. Cell thickness, 0.5 cm

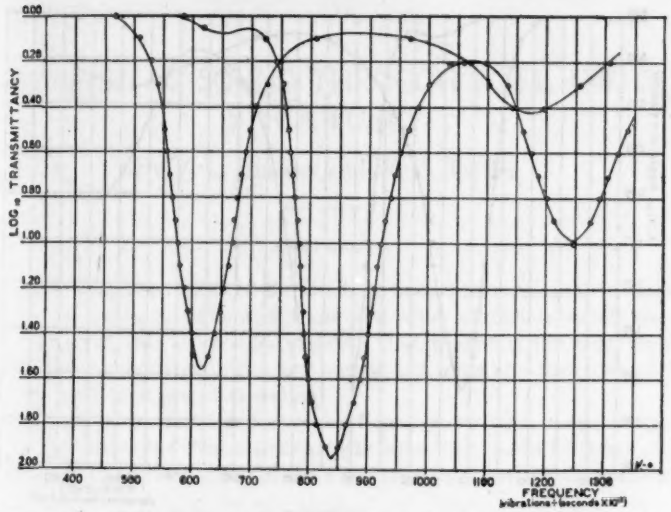

FIG. 34.—*The spectral absorption of p-tolueneazo-o-cresol (p′, o) dissolved in 95 per cent ethyl alcohol (principal band at 838 f) and in concentrated hydrochloric acid (principal band at 617 f)*

Concentration, 3.380 cg per liter in alcohol; 1.690 per liter in hydrochloric acid. Cell thickness, 0.5 cm in both cases

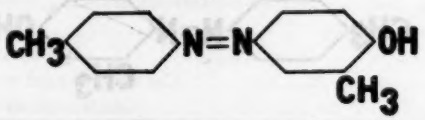

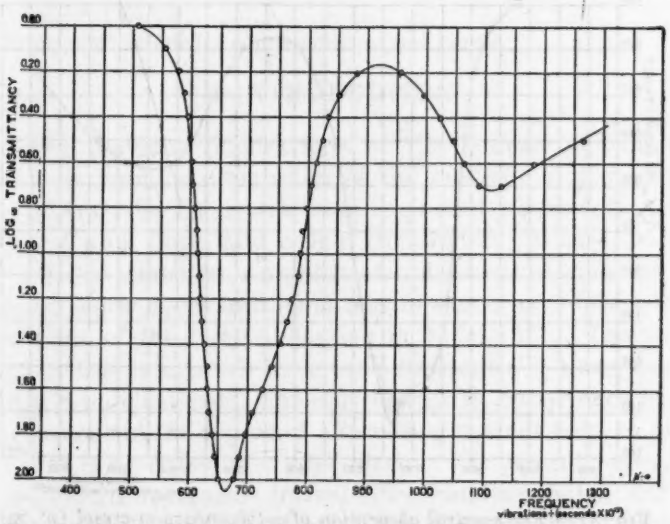

FIG. 35.—*The spectral absorption of p-tolueneazo-o-cresol (p′, o) dissolved in a 3 per cent aqueous solution of sodium hydroxide*

Concentration, 3.380 cg per liter. Cell thickness, 0.5 cm

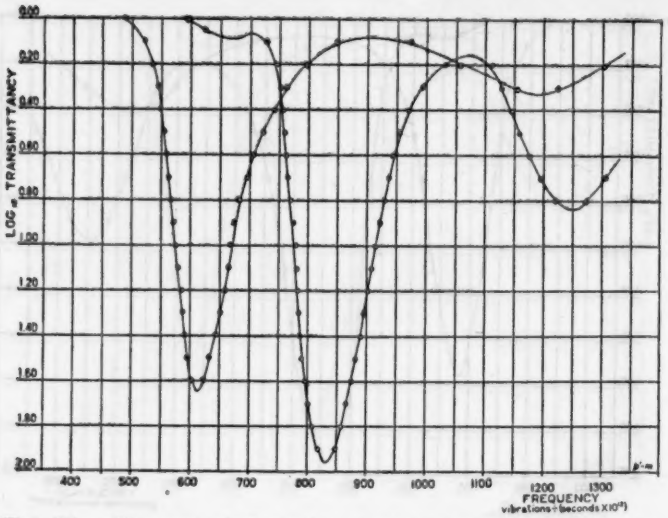

FIG. 36.—*The spectral absorption of p-tolueneazo-m-cresol (p', m) dissolved in 95 per cent ethyl alcohol (principal band at 831 f) and in concentrated hydrochloric acid (principal band at 613 f)*

Concentration, 3.380 cg per liter in alcohol; 1.690 cg per liter in hydrochloric acid. Cell thickness, 0.5 cm in both cases

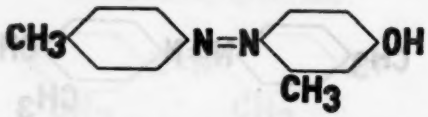

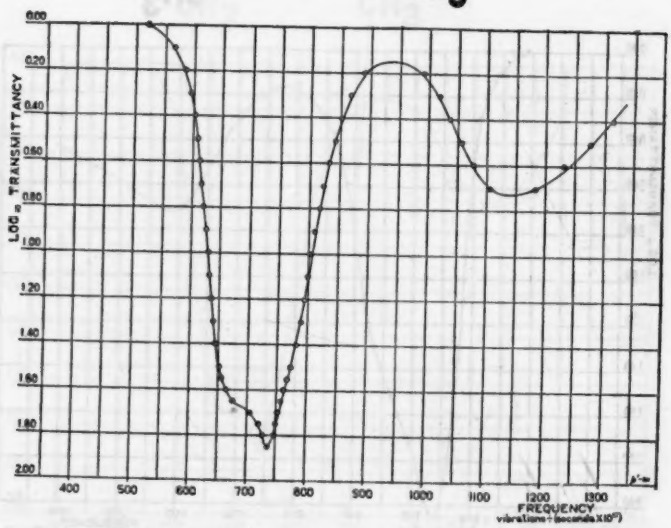

FIG. 37.—*The spectral absorption of p-tolueneazo-m-cresol (p', m) dissolved in a 3 per cent aqueous solution of sodium hydroxide*

Concentration, 3.380 cg per liter. Cell thickness, 0.5 cm

WASHINGTON, September, 1926.

TRANSMISSION OF SOUND THROUGH WALL AND FLOOR STRUCTURES

By V. L. Chrisler and W. F. Snyder

ABSTRACT

This paper contains a report of the work on sound transmission through (1) a large number of masonry walls and floors and other materials which are homogeneous in construction, the results showing that weight is the most important factor under these conditions; (2) a few compound walls and floors which have a masonry core, and (3) a few stud walls.

The results are given for five frequency bands covering a range from 250 to 3,365 cycles per second. Transmission tests were also made for impact noises. Specifications for the construction of the various panels used are appended.

CONTENTS

	Page
I. Introduction	541
II. Methods of measurement	542
III. Method of expressing results (sensation units)	543
IV. Discussion of results	543
1. Air-borne sounds	543
2. Impact or tapping sounds	550
3. General conclusions	551
V. Description of panels	553
VI. General specifications for construction of test panels	556

I. INTRODUCTION

In several previous publications of the Bureau of Standards [1] there is to be found a description of the methods employed in the bureau's laboratories for determining the sound transmission of various types of wall, floor, and ceiling construction, with a statement of the results obtained on a number of test panels of different types. The present paper gives additional results which have been obtained since the issue of the last publication in June, 1927. The methods employed in this later work have been substantially those described in the earlier publications. The only change of importance has been an improvement in the source of alternating current used to produce sound. This is described in a later place in the present paper.

In the modern apartment house, office building, hotel, and other buildings of this nature sound insulation is becoming of increasing

[1] Transmission and Absorption of Sound by Some Building Materials, B. S. Sci. Paper No. 526. Soundproofing of Apartment Houses, B. S. Tech. Paper No. 337. Transmission of Sound through Building Materials, B. S. Sci. Paper No. 552.

importance. This consideration is often difficult to satisfy simultaneously with other important requirements. The rising costs of construction have brought about a tendency to make nonload-bearing walls as thin as possible, and, due to requirements which are necessary to eliminate the fire hazard, the modern fireproof building is liable to be noisy, as sound is easily transferred along steel beams or through thin masonry walls. The problem is to find a type of wall which will have maximum opacity to sound with minimum weight and with a reasonable cost of construction.

To meet this situation, the Bureau of Standards, with the cooperation of a number of manufacturers of building materials, has undertaken an extensive program in which the sound-insulating properties of a large number of structures have been measured in the laboratory. This work has not been confined to heavy partition walls but has been extended to lighter types and to various materials which might be used in such structures. The lightest material used was wrapping paper, while the heaviest structure was a combination tile floor with a cinder fill and concrete finish, weighing 109 pounds to the square foot.

Some of the most interesting results have been obtained with the use of the lighter materials, such as are employed in the construction of airplane cabins. In the study of this aspect of the general problem it has become apparent that some of the conclusions reached in considering heavier building structures do not apply to combinations of lighter material.

II. METHODS OF MEASUREMENT

In much of the work described in the present paper an improved source of alternating current has been used, in the form of a beat-frequency oscillator. As such instruments have lately come on the market, it may be sufficient to give a brief description of the type employed. It contained two circuits, each of radio-frequency. One of these circuits was maintained by means of a piezoelectric crystal of quartz, while the capacity of the other was varied to give beats of the desired audio-frequencies. The width of the frequency bands was controlled by the use of a revolving condenser of suitable capacity, similar to that described in Scientific Paper No. 526.

By means of this apparatus it has been found possible to make measurements at lower frequencies than with the oscillator formerly used. In addition, the frequency band could be made wider at the lower frequencies. A number of measurements made on a series of panels, using both oscillators, showed that the mean reduction factor was not appreciably affected by the width of the band.

III. METHOD OF EXPRESSING RESULTS (SENSATION UNITS)

All results given in this paper and in the previous publications above referred to have been obtained by the use of the telephone receiver as a detector and measurer of sound energy. The indications of this instrument are given on what is called the physical scale, which measures the energy of the sound wave. But the instrument most universally used for detecting sound and estimating its intensity is the human ear, and unfortunately the ear does not respond according to the physical scale. As the intensity of a sound increases steadily on the physical scale, the response of the ear fails to keep pace with it. There appears to be in the ear a regulating or protective mechanism whose nature is not understood, which, like the well-known mechanism of the eye, protects the organ against excessive stimulation. Experiment shows that the response of the ear is proportional to the logarithm of the physical intensity; that is, energies proportional to 10, 100, and 1,000 would produce in the ear effects proportional to 1, 2, and 3, respectively. This logarithmic scale has been termed in previous papers the ear scale and has been used for expressing results because of its natural fitness.

A slight modification of this scale has been employed for some time by telephone engineers [2] and is used in all audiometers made by the Western Electric Co. This scale merely multiplies the numbers of the ear scale by 10, the unit of this new scale being that fractional change in intensity which is approximately the smallest that the average ear can detect. For this reason this unit is called a sensation unit. In the example given above, intensities corresponding to 1, 2, and 3 on the ear scale would be represented by 10, 20, and 30 sensation units. = DECIBELS

It seems advisable that the same units should be used by all engaged in acoustic work, and consequently sensation units have been adopted in this paper. Reduction factors given on the ear scale in previous publications may be converted into sensation units by multiplying by 10.

Wallace Waterfall, in a private communication, has suggested a way of illustrating the values of sensation units in familiar terms. We may call it an ear sensation scale. (Fig. 1.)

IV. DISCUSSION OF RESULTS

1. AIR-BORNE SOUNDS

The present paper gives the results of experiments on the sound transmission of over 70 panels, ranging in weight from a masonry structure of 109 pounds per square foot down to a single thickness of

[2] Fletcher, Bell Telephone Laboratories, Reprint B-152-1; J. Frank. Inst.; September, 1923.

wrapping paper. The results for the principal cases are given graphically in Figure 2, plotting the reduction factor in sensation units against the logarithm of the weight per square foot. The numerical values for all the panels are given in Table 1.

In general, it appears that for panels which are more or less homogeneous in structure the points lie close to a straight line; that is, mass is the predominating factor, but it is quite apparent that mass is not always the only factor in the case. Where the panel departs

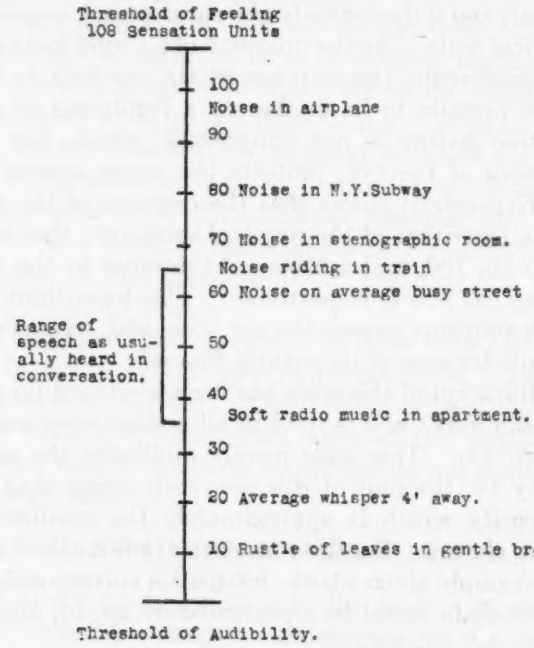

FIG. 1.—*Ear sensation scale*

from homogeneity, as in panels 77 and 78b, structure becomes of importance.

As stated in a previous paper,[3] a partition wall or floor acts in much the same manner as a large diaphragm. It is well known that the amplitude of vibration of a large diaphragm depends upon its mass, stiffness, and damping factor.

Consider panels 79, 80, and 81. These panels differed but slightly in weight, yet No. 79 transmitted quite a little more sound than either No. 80 or No. 81. The principal difference was that the workmanship was not as good in No. 79. The bricks of No. 79 were not as well embedded in the mortar as in the other two, and the vertical joints were not filled. According to McBurney,[4] a panel built like

[3] B. S. Sci. Paper No. 552.

[4] J. W. McBurney, Effect of Workmanship on Strength of Brick Masonry, Am. Architect, 132, p. 613; Nov. 5, 1927.

No. 80 has from 24 to 112 per cent greater wall strength than No. 79. It would appear that this same factor affects the sound transmission to some extent.

Consider floor panels No. 78a and 78b. Panel 78a was a better sound insulator than 78b and yet was considerably lighter. When these measurements were first taken, it seemed probable that some error had been made in the measurements. To verify these results, a second set of measurements was made on No. 78b, with a result exactly the same as before. The concrete finish and cinder fill were then stripped off, leaving the panel in its original condition as No. 78a. The sound-transmission measurements were then repeated, and the average reduction factor found was within 0.7 sensation unit of its original value. This, again, illustrates that simply loading a panel does not necessarily make it a better sound insulator. The cinder fill had almost no mechanical strength and probably increased the rigidity of the panel very little, but it did form an intimate contact between the slab and concrete finish, so that any vibration of the slab was easily transmitted to the finished part of the floor and hence to the receiving room.

Also consider panels 27 and 28 (B. S. Sci. Paper No. 526) and panels 25, 26, 29, and 30 (B. S. Sci. Paper No. 552). These were panels built of clay tile, gypsum tile, and brick. In each case two panels were built as nearly alike as possible, one being finished with gypsum plaster and the other with lime plaster; and in each case the panels finished with gypsum plaster were slightly better sound insulators than those with lime plaster. It should be emphasized that the difference was not enough to be of any practical importance but merely sufficient to be detected in the laboratory.

There were two other interesting panels among the small ones. These were panels 110 and 111, consisting of $\frac{1}{8}$ and $\frac{1}{16}$ inch sheet lead, respectively. Plotting the results for these panels with those for other materials (fig. 2) it will be seen that the points for these panels fall below the curve, indicating that they transmit more sound than a piece of sheet iron or glass of the same weight.

In every case mentioned in the four preceding paragraphs it is to be noticed that the panel which transmits the least sound is the most rigid.

With the small panels where the material was thin it has been found that the method of holding the edges affects the result. If the clamped area extends in from the edge for about 2 inches, the material transmits less sound than when held only by a narrow rim at the edge. This change in transmission is rather too large to be accounted for by such stiffening as might be produced by clamping for 2 inches around the edge. Further work is being done to determine to what extent the boundary conditions will affect the results.

From the above it is evident that the result for sound transmission of various materials is not dependent entirely on the mass, though this

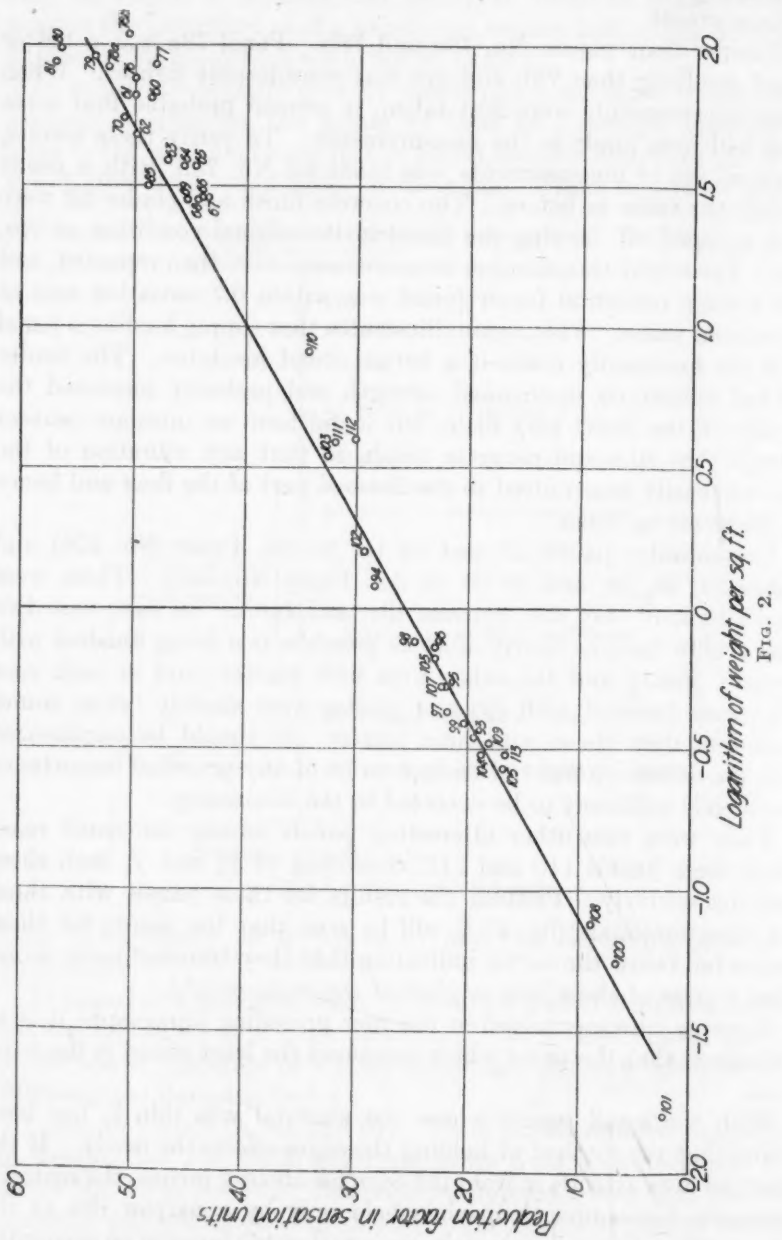

FIG. 2.

is the most important factor. Figure 2 shows that most structures which are more or less homogeneous do have a reduction factor in sensation units which is nearly proportional to the logarithm of the

weight per unit area. From this curve the approximate reduction factor of many new structures may be predicted with a reasonable degree of certainty, provided they are tested under similar conditions. If the conditions of test are radically altered, entirely different results may be expected. To illustrate this, the curves in Figure 3 have been plotted, giving results as determined by Sabine,[5] Heimburger,[6] and the Bureau of Standards. The reduction factors as given by each observer are not directly comparable, as the methods by which they are measured are entirely different. For instance, Sabine makes all of his measurements by the reverberation method, using a small receiving room in which the observer stands with his ear close to the panel. This makes the reduction factor less than it would be if the

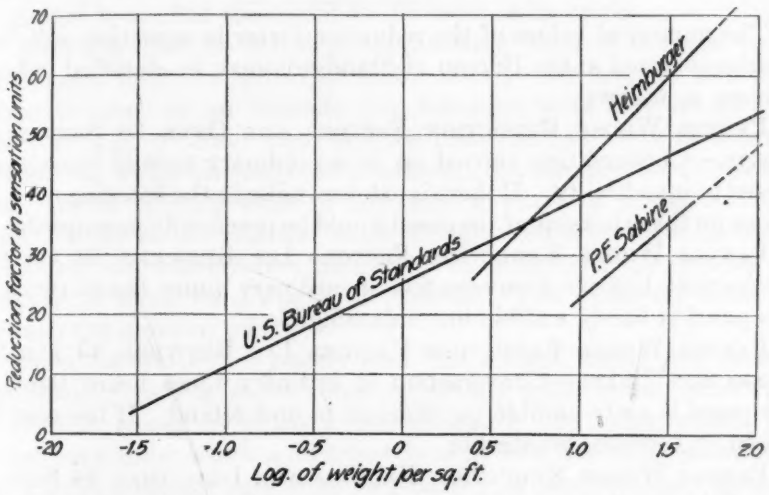

FIG. 3.—*Comparative results at various laboratories on sound transmission of panels*

receiving room were larger and the observer stood at some distance from the panel. Heimburger places a loud-speaker horn close to the panel and surrounds it by a box so that in all probability not more than 4 or 5 square feet of wall surface are appreciably affected by the sound waves. For walls with a thickness of 6 to 8 inches the thickness of the wall becomes comparable to the surface area affected, and the wall acts as if it were much stiffer than if a larger section were used. This increases the reduction factor.

Each method has its advantages, and while the different methods do not give the same absolute results they should agree in the comparison of a number of different panels. The fact that the results depend upon the method, and also the room in which the measurements are made, is unfortunate. The art of measuring sound trans-

[5] Paul E. Sabine, The Armour Eng.; May, 1926.
[6] Gunnar Heimburger, the Am. Architect; Jan. 20, 1928.

mission is not yet on as definite a basis as the measurement of heat conductivity. In consequence, each observer must in some way explain what is meant by the figures which he gives for the reduction factor. Referring to Figure 3 and comparing the ordinates in sensation units for the same abscissas, we obtain the following values from the curves given by the three different observers.

Reduction factor in sensation units

Bureau of Standards	Sabine	Heimburger
32.4	------	29.0
39.5	22.7	44.5
44.2	31.0	54.7
49.0	39.5	65.0
53.7	48.0	75.2

The numerical values of the reduction factor in sensation units for results obtained at the Bureau of Standards may be classified in four groups, as follows:

Panels Whose Reduction Factors are Over 60 Sensation Units.—Conversation carried on in an ordinary tone of voice is reduced to inaudibility. If there is external noise in the listening room, a shout on the other side of the panel would be practically unnoticeable.

Panels Whose Reduction Factors Lie Between 50 and 60 Sensation Units.—Conversation in ordinary tones heard through the panel is barely audible but unintelligible.

Panels Whose Reduction Factors Lie Between 40 and 50 Sensation Units.—Conversation in ordinary tones heard through the panel is quite audible but difficult to understand. If the voice is raised, it becomes intelligible.

Panels Whose Reduction Factors are Less than 40 Sensation Units.—Conversation in ordinary tones heard through the panel is distinctly audible and intelligible.

The above comparisons are based on tests in a listening room in which there was no noise and which was quite reverberant. In a room furnished with rugs, draperies, or other sound-absorbing objects the panels would be apparently more effective than when tested in bare rooms.

A practical demonstration of the above statement was made by lining a large box with highly absorbing material. The average reduction factor of this box was slightly under 40 sensation units. The box was placed in a very reverberant room. A person inside the box could understand everything said by a person outside, while the person outside was unable to understand a single word that was spoken by the person inside unless he raised his voice The reason for this was that the absorbing material in the box lowered the intensity of sound originating within to such an extent that it was no longer sufficient to carry through and be audible after transmission.

For sound generated outside in a reverberant room there was no absorbing material, and in consequence the sound could build up to an intensity level sufficient to carry it through to the person inside the box. In certain cases this principle may be of practical value. If a room contains a number of typewriters, a partition might be built which is insufficient to prevent the sound reaching the other side if the typewriting room is reverberant, but if absorbing material in sufficient quantity be added to the walls of the typewriting room the partition might be satisfactory. The absorbing material in this case would serve two purposes—it would reduce the noise level so that it would be much pleasanter for the operators of the machines; and, due to the reduced noise level, a lighter partition would be sufficient to confine the sound to the room of its origin.

Attention must be called to the masking effect of external noise. If a panel having a reduction factor between 30 and 40 sensation units is taken as an example, the following facts may be noticed. If there is no external noise and the panel acts as the wall between two rooms which are fairly reverberant, it is quite easy for two people who are on opposite sides of the panel to carry on a conversation; but if there is the slightest noise in the room where the person is listening, the conversation becomes a mumble, and the chances are that not a single word will be understood. The louder the noise the greater the masking effect.

From the above it is readily seen that a panel might give entirely satisfactory results under some conditions while under other conditions it would be entirely unsatisfactory. In other words, the conditions under which a structure is to be used are to be considered, as a given structure may seem satisfactory or unsatisfactory as these conditions are favorable or unfavorable.

Returning to the results which were obtained for masonry walls, one fact is at once evident—that for solid masonry a wall to be a good sound insulator must be excessively heavy. In the search for a type of structure which would give more efficient insulation it was found that the insulation was materially increased if the wall were split into layers. For masonry walls it was found that this could be accomplished by using wood furring strips to which was fastened the plaster base and finally the plaster coat. With 4-inch clay tile furred out in this manner on both sides, the sound insulation was, perhaps, a little better than that of an 8-inch brick wall without furring. It should also be noticed that the nature of the plaster base makes little difference, as the results were about the same for metal lath, masonite, and insulite.

Tests were also made to determine whether a change in the method of attaching the furring would make any material difference. In

panel No. 82 the furring strips were wired to the brickwork by wires laid in the mortar when the panel was built. The furring strips thus attached were not perfectly tight at best but could be moved, perhaps, a few hundredths of an inch. Panel No. 83 had the same brick center as No. 82, but the plaster and furring strips were taken off, holes drilled into the brick, and nailing plugs driven into the holes. The furring strips were then nailed on and finished as nearly as possible as in No. 82. The plaster may have been a little thicker, as the panel was slightly heavier. As the amount of sound transmitted was also slightly less, the result indicated that this change in the method of fastening the furring strips did not appreciably affect the sound insulation of the panel.

This surface was then stripped and insulite used as the plaster base, as panel No. 84. With the exception of the change in plaster base, panels Nos. 83 and 84 were made as nearly the same as possible. The sound transmission was about the same, although panel No. 84 was lighter.

Comparison of the transmission of No. 73 with Nos. 71 and 72 apparently indicates that a plaster base of fiber board may give somewhat better sound insulation than metal lath, while No. 74, with a different type of fiber board, shows no improvement. This difference between Nos. 73 and 74 is probably not to be ascribed to the difference in the fiber boards. Panel No. 74 was built about a year after Nos. 71, 72, and 73 and of a different lot of tile. It is possible that this has affected the results. In any case, however, it is apparent that where a slight increase in weight is not objectionable there is little choice between the use of different plaster bases. The important part is the type of structure.

For structures which have wood studs or wood joists there has been very little progress made in improving the sound insulation. A comparison of the results shows that some of the earlier structures tested are as good sound insulators as the later ones.

2. IMPACT OR TAPPING SOUNDS

The preceding discussion has had reference entirely to air-borne sounds. Another type of sound, much harder to control, is produced by vibration communicated directly to the structure. This may be transferred from a machine or caused by impact, as when a chair is dropped or by walking across the floor. In many cases of this kind it seems as if the noise is as loud on one side of the floor or partition as on the other.

To study this type of sound, a special machine was built. (Fig. 4.) It consists, essentially, of five rods which can be raised and allowed to fall by separate cams. The cams are driven by a motor at such a speed that a rod falls approximately every fifth of a second. The

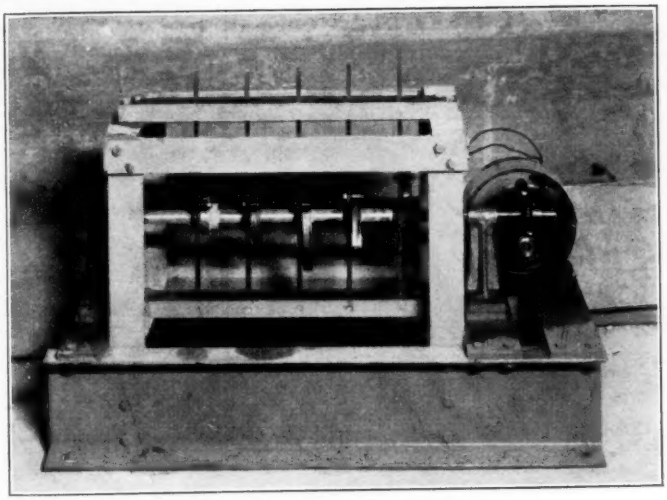

FIG. 4.—*Machine for producing impact sounds*

noise thus produced can be measured in the same manner as the sound from a loud-speaker.

Measurements were taken of the intensity of the sound on both sides of the floor panel. The ratios of the results, expressed as reduction factors in sensation units, are recorded in the column headed "Tapping" in Table 1.

Two sets of these measurements are of special interest. Panel 116a, a type of concrete floor, shows a reduction of only 1.2 sensation unit in the intensity of sound on the two sides—almost indistinguishable by the ear. By adding a floating floor, loosely laid on the concrete (No. 116b), the reduction was increased to 30 sensation units, a noticeable change, but insufficient to prevent the transmission of footsteps. By the further addition of fiber board between the floor and the concrete (No. 116c) the reduction was increased to 33 sensation units, at which footsteps were still audible.

Similar results were obtained with panel No. 117a, which is a combination floor of 4-inch hollow clay partition tile. In its original condition this gives a reduction of 5.1 sensation units, which makes but little difference to the ear. By the addition of a floating floor (117b) the reduction was increased to 34 sensation units, and by the further insertion of fiber board (117c) to 35 sensation units. Even this latter figure was insufficient to deaden the sound of footsteps; but by the final addition of a suspended ceiling below (118) the reduction was raised to 51 sensation units, enough to prevent the sound of footsteps being transmitted under ordinary conditions.

3. GENERAL CONCLUSIONS

When comparing panels, it should be remembered that, owing to the form in which the results are expressed, the improvement of one panel over another should be expressed as a difference of their reduction factors in sensation units and not as a ratio. For instance, if one panel has a reduction factor of 40 sensation units and another of 50 the panel having a reduction factor of 50 will reduce a sound heard through it 10 sensation units more than the one having a reduction factor of 40; but it would not be proper to say that the better panel in this case is one-fourth, or 25 per cent, better than the poorer one. This can be illustrated as follows: Assume the original intensity of the sound as 60 sensation units. The intensity as heard through the best panel would be $60-50=10$ sensation units. As heard through the poorer panel it would $60-40=20$ sensation units. As heard under these conditions the best panel appears to be twice as good as the poorer one. Assume, now, the original intensity of the sound to be changed to 80 sensation units. As heard through the best panel the intensity would be 30 and through the poorer 40. On this basis the best panel would appear to be only 4/3 instead of twice as good as

the poorer one. It is evident, then, that one panel can not be expressed as being a better sound insulator than another by a certain percentage. It will be noticed in both cases, however, that the sound which is heard through the poorer panel is 10 sensation units louder than that heard through the better panel. This holds, no matter what the original intensity of the sound (providing it is audible through the better panel), and is the only correct method of stating the improvement of one panel over another.

TABLE 1

Panel No.	Reduction factor in sensation units at frequency bands—							
	250–251	500–527	1,000–1,065	2,000–2,385	3,000–3,365	Average	Weight per square foot	Log weight per square foot
60	49.4	40.1	37.0	55.2	53.6	48.6	65	1.81
61	49.4	46.3	48.7	53.3	52.2	50.0	66	1.82
62	44.3	44.5	48.9	58.0	53.2	49.8	48	1.68
63	38.8	42.1	46.6	53.5	54.7	47.1	39	1.59
64	41.2	37.4	45.1	52.1	52.7	45.7	37	1.57
65	41.1	42.0	43.7	50.1	45.9	44.6	37	1.57
66	41.1	40.0	41.5	49.9	47.3	44.0	29	1.46
67	42.0	36.7	42.3	50.6	45.7	43.5	29	1.46
68	40.7	35.9	43.3	51.0	51.2	44.4	28	1.45
69	41.7	41.4	43.7	49.8	50.3	45.4	28	1.45
70	48.6	46.3	48.4	55.4	56.5	51.0	55	1.74
71	55.6	52.8	57.3	57.6	64.0	57.5	34	1.53
72	55.7	52.4	53.3	60.2	69.7	58.3	34	1.53
73	55.3	53.2	56.8	68.8	69.6	60.7	28	1.45
74	52.2	51.9	60.9	61.1	61.6	57.5	34	1.53
75	55.2	50.8	50.8	65.8	73.2	59.2	50	1.70
76	46.3	46.8	47.8	54.5	54.4	50.0	76	1.88
77	46.7	47.1	47.4	50.5	49.1	48.2	85	1.93
78a	51.2	46.8	49.6	60.4	54.0	52.4	83	1.92
78b	52.4	48.0	49.9	54.6	48.1	50.6	109	2.04
79	47.7	48.1	55.6	56.3	60.4	53.6	92	1.96
80	47.7	49.4	57.0	59.2	70.0	56.7	97	1.99
81	50.2	47.6	55.5	63.5	69.2	57.2	87	1.94
82	52.1	47.4	56.5	53.9	57.8	53.5	36.5	1.56
83	46.8	44.3	54.4	61.3	69.2	55.2	38.2	1.58
84	48.8	50.5	59.8	55.8	58.2	54.6	33.3	1.52
85	40.0	36.9	48.7	59.1	59.1	48.8	31.6	1.50
86	42.4	38.2	44.7	54.1	61.7	48.2	14.7	1.17
87	37.7		37.2	38.1	34.9	39.0	11.8	1.07
88	42.1		44.1	48.2	42.2	44.2	19.6	1.29
89	40.3		37.0	40.1	36.6	38.5	17	1.23
90	38.3		36.2	44.1	38.7	39.3	17	1.23
91	41.7		44.5	50.6	42.3	44.8	12.3	1.09
92	37.6		41.2	48.4	42.5	42.4	11.8	1.07
93	17.9	13.2	17.7	23.2	25.3	19.5	.35	−.46
94	25.3	20.5	28.8	35.0	31.7	28.3	1.2	.08
95	19.0	17.5	22.0	26.7	25.5	22.1	.52	−.28
96	21.0	20.7	25.5	26.0	21.9	23.0	.73	−.14
97	19.5	17.1	20.7	26.1	25.7	21.8	.43	−.37
98	22.2	20.2	24.1	20.9	27.1	24.9	.75	−.12
99	16.2	15.2	19.7	25.2	25.3	20.3	.39	−.41
100	3.6	3.0	5.9	10.1	10.7	6.7	.055	−1.26
101	1.4	1.5	1.7	3.3	3.7	2.3	.016	−1.80
102	26.2	27.4	30.8	33.0	29.2	29.3	1.6	.204
103	32.6	30.9	33.5	34.2	32.2	32.7	3.5	.54
104	14.2	14.7	18.0	23.5	23.5	18.8	.30	−.52
105	13.4	12.6	15.1	21.5	21.8	16.9	.27	−.57
106	22.4	17.3	23.4	27.4	24.6	23.0	.66	−.18
107	21.4	18.8	22.3	24.6	24.7	22.4	.53	−.28
108	3.7	5.6	7.7	12.6	14.3	8.8	.075	−1.12
109	14.1	12.5	17.6	22.5	23.6	18.1	.33	−.48
110	31.0	27.2	37.5	43.8	32.6	34.4	8.2	.91
111	31.8	33.2	32.0	32.1	32.5	32.0	3.90	.59
112	28.8	32.4	31.8	32.4	28.7	30.2	4.0	.60
113	11.4	13.2	16.9	21.8	20.3	16.7	.30	−.52

TABLE 1—Continued

Panel No.	Reduction factor in sensation units at frequency bands—									
	150–187	250–285	500–547	1,000–1,070	2,000–2,175	3,000–3,165	Average	Weight per square foot	Log weight per square foot	Tapping
114a	47.9	46.8	40.7	50.1	48.8	47.4	47.0			14
114b	47.7	48.3	40.6	50.3	48.9	46.6	47.1			14
114c	57.6	57.5	54.8	62.4	57.6	56.6	57.8			22
114d	57.9	60.1	53.5	62.7	55.7	56.7	57.8			22
115a	52.6	53.6	49.2	54.9	55.3	55.0	53.4	12.6	1.10	22
115b	62.4	65.3	57.3	68.8	62.3	65.0	63.5	16.1	1.21	30
116a	50.9	54.8	58.7	56.5	53.2	56.0	55.0	54.4	1.74	1.2
116b	58.9	57.0	55.4	67.6	65.2	62.5	61.1	58.1	1.76	30
116c	57.9	58.2	55.8	66.3	67.3	62.3	61.3	58.9	1.77	33
117a	56.5	56.6	55.8	57.7	58.8	57.2	57.1	69.8	1.84	5.1
117b	62.7	63.1	61.0	65.9	73.7	67.4	65.6	73.5	1.87	34
117c	63.6	70.3	63.4	63.5	68.7	68.0	66.3	74.2	1.87	35
118	68.0	67.9	65.8	72.1	<76.0	<77.0	<70.0	72.8	1.86	51
119	38.2	39.6	39.2	43.9	49.0	58.8	44.8	17.4	1.24	
120	28.5	28.6	24.0	35.6	47.5	50.7	35.8	5.10	.71	
121	33.9	32.2	29.4	40.8	58.5	63.9	43.1	6.60	.82	
122	50.2	52.2	43.9	57.9	61.0	61.1	54.4	14.2	1.15	
123	46.2	39.5	47.2	57.0	56.3	55.2	50.3	13.3	1.12	
124	34.1	29.9	27.9	41.8	59.3	60.1	42.2	4.94	.69	
125	52.2	52.6	47.4	53.7	58.2	62.7	54.5	16.1	1.21	
126	50.1	52.2	49.4	59.6	60.1	53.8	54.2	13.1	1.12	
127	45.4	45.1	44.7	47.6	57.7	59.0	49.9	20.9	1.32	
128	49.9	53.0	52.0	57.3	62.9	66.2	56.9	21.3	1.33	

The most important fact to know about a panel is not how much better it is than another but whether it will reduce a given sound to inaudibility. To determine this, two things should be known—the intensity of the sound which it is desired to reduce to inaudibility and the minimum intensity of the sounds present in the room where the listener is located. For instance, very slight noises in this room might mask any sound having an intensity of 20 or less sensation units. If the noise which we wish to reduce to inaudibility has an intensity of 70, the wall or partition should have a reduction factor of 50. This will reduce the sound to an intensity of 20 units, and this would be masked by the other noises present so as to be inaudible. If the room is absolutely quiet, it will be necessary to have a partition with a reduction factor of 70 to reduce the sound to inaudibility. Whether a partition is satisfactory or not depends, therefore, upon the intensity of other noises present. Street noises, for instance, may completely mask sounds having intensities of as much as 30 or more sensation units.

V. DESCRIPTION OF PANELS

Panel No.

60. Hollow clay tile panel (2 units 3¾ by 12 by 12 and 8 by 12 by 12), end construction. Plastered both sides with brown coat of gypsum plaster and smooth white finish.

61. Hollow clay tile panel (2 units 3¾ by 5 by 12 and 8 by 5 by 12), side construction. Plastered both sides with brown coast of gypsum plaster, smooth white finish.

Panel No.

62. Hollow clay tile panel constructed of 8 by 12 by 12 tile, 6 cells. Plastered on both sides with brown coat of gypsum plaster, smooth white finish.
63. Hollow clay tile panel constructed of 6 by 12 by 12 load-bearing partition tile, 6 cells. Plastered on both sides with brown coat of gypsum plaster, smooth white finish.
64. Hollow clay tile panel constructed of 6 by 12 by 12 partition tile, medium burned, 3 cells. Plastered both sides with brown coat of gypsum plaster and smooth white finish.
65. Hollow clay tile panel constructed of 6 by 12 by 12 soft partition tile, 3 cells. Plastered on both sides with brown coat of gypsum plaster, smooth white finish.
66. Hollow clay tile panel constructed of 4 by 12 by 12 partition tile, 3 cells. Plastered on both sides with brown coat of gypsum plaster, smooth white finish.
67. Hollow clay tile panel constructed of 4 by 12 by 12 partition tile, 3 cells. The tile in this panel was laid so that none of the flues in the panel were over 2 feet in length. Plastered both sides with brown coat of gypsum plaster, smooth white finish.
68. Hollow clay tile panel constructed of 3 by 12 by 12 partition tile, 3 cells. Plastered both sides with brown coat of gypsum plaster, smooth white finish.
69. Built as near like No. 68 as possible.
70. Hollow clay tile panel constructed of Heath cubes. Plastered both sides with brown coat of gypsum plaster, smooth white finish.
71. Hollow clay tile panel constructed of 4 by 12 by 12 partition tile, 3 cells. Wood furring strips, paper, metal lath, scratch and brown coat of gypsum plaster, smooth white finish.
72. Hollow clay tile panel constructed of 4 by 12 by 12 partition tile, 3 cells, pads, wood furring strips, paper, metal lath, scratch and brown coats of gypsum plaster, smooth white finish.
73. Hollow clay tile panel constructed of 4 by 12 by 12 partition tile, 3 cells, wood furring strips, Masonite, brown coat gypsum plaster, smooth white finish.
74. Hollow clay tile panel constructed of 4 by 12 by 12 partition tile, 3 cells, wood furring strips, Insulite, brown coat of gypsum plaster, smooth white finish.
75. Double partition 3 by 12 by 12 hollow clay tile spaced 1¾ inches between sides. Flax-li-num 1 inch thick and butted tight was placed in the space between the tile. One side of the partition was carried on ½-inch Flax-li-num strips which were 4 inches wide, the strips being placed at the sides and top as well as the bottom.
76. Flat arch floor panel constructed of 8-inch 4-cell tile, plastered with brown coat gypsum plaster and smooth white finish. Two by fours were fastened to the top surface approximately 16 inches on center and the space between filled with cinder concrete. The floor was finished with hardwood flooring.
77. Same as 76, except the floor was finished with 2 inches of cinder concrete and 1 inch cement.
78a. Combination floor panel constructed of 6 by 12 by 12, 3-cell partition tile. The ceiling of this panel was finished with a brown coat of gypsum plaster and a smooth white finish.
78b. This panel was the same as 78a, except 2 inches of cinder concrete and 1 inch cement were added to upper surface.

Panel No.

79. Eight-inch brick panel, New Hampshire brick, poor workmanship, plastered on both sides with brown coat gypsum plaster, smooth white finish.
80. Eight-inch brick panel, New Hampshire brick, good workmanship, plastered on both sides with brown coat gypsum plaster, smooth white finish.
81. Eight-inch brick panel, Mississippi brick, good workmanship, plastered on both sides with brown coat gypsum plaster, smooth white finish.
82. New Hampshire brick laid on edge, furring strips wired, gypsum plaster board, plastered both sides with scratch and brown coat gypsum plaster, smooth white finish.
83. Same as No. 82, except the furring strips were nailed.
84. Same as No. 83, except Insulite was used as a plaster base instead of gypsum plaster board.
85. Same as No. 82, except the plaster was applied directly to the brick surface.
86. Wood studs, ½-inch Flax-li-num nailed to each side, 1 by 2 inch furring strips, wood lath, plastered both sides with scratch and brown gypsum plaster, smooth white finish.
87. Wood studs, Sheet Rock nailed to each side, No. 12 porous gypsum poured into space between studs.
88. Same as No. 87, except No. 30 porous gypsum was used.
89. Same as No. 87, except No. 18 porous gypsum was used.
90. Same as No. 87, except No. 24 porous gypsum was used.
91. Wood studs, Sheet Rock nailed to one side and temporary form on the opposite side. No. 18 porous gypsum was poured in space between studs. After the porous gypsum set the form was removed and the gypsum allowed to dry. When dry, Sheet Rock was nailed on in place of form.
92. Same as No. 91 except Gypsolite was used in place of Sheet Rock and No. 12 porous gypsum in place of No. 18.
93. Single sheet of aluminum 0.025 inch thick.
94. Single sheet of galvanized iron 0.03 inch thick.
95. Single sheet 3-ply plywood ⅛ inch thick.
96. Single sheet 3-ply plywood ¼ inch thick.
97. Single sheet Insulite 5/16 inch thick.
98. Single sheet Insulite ½ inch thick.
99. Single sheet Insulite ¼ inch thick.
100. Single sheet airplane fabric doped and varnished.
101. Single sheet heavy wrapping paper.
102. Single sheet double-strength glass ⅛ inch thick.
103. Single sheet plate glass ¼ inch thick.
104. Single sheet standard Celotex ¼ inch thick.
105. Single sheet carpet lining Celotex ¼ inch thick.
106. Single sheet standard Celotex ½ inch thick.
107. Single sheet carpet lining Celotex ½ inch thick.
108. Single sheet aluminum 0.006 inch thick.
109. Single sheet duralumin 0.020 inch thick.
110. Single sheet of lead ⅛ inch thick.
111. Single sheet of lead 1/16 inch thick.
112. Single sheet galvanized iron 0.03 inch thick, loaded with 2.8 pounds sand per square foot.
113. Single sheet aluminum-coated duralumin.
114a. Floor panel, wood joists. Plaster on wood lath applied to lower side, subflooring and ⅜-inch finish flooring to upper side.
114b. Same as No. 114a, with exception of flooring. One-half inch Insulite between rough and finished floors.

Panel No.

114c. Same as No. 114a, with exception of flooring. Rough flooring, ½-inch Insulite, floating floor consisting of nailing strips rough and finish flooring.

114d. Same as No. 114c, except Insulite was inserted between rough and finished floor in floating floor.

115a. Suspended ceiling, wood joists, ½-inch Insulite plastered applied as ceiling. Rough floor, finish floor applied as flooring.

115b. Same as 115a, with exception of flooring. Rough flooring, ½-inch Insulite and floating floor as in 114c.

116a. Reinforced concrete flat slab type of floor construction. Insulite furred out and applied as ceiling, plaster.

116b. Same as 116a except floating floor added as in 114c.

116c. Same as 116b, except ½-inch Insulite added between concrete slab and floating floor.

117a. Combination floor panel constructed of 4 by 12 by 12 three-cell partition tile. The ceiling was finished with furring strips, ½-inch Insulite, and plaster.

117b. Same as 117a, except floating floor was added as in 114c.

117c. Same as 117b, except ½-inch Insulite was added between masonry slab and floating floor.

118. Same as 117c, except ceiling was stripped off and suspended ceiling attached.

119. Wood studs, wood lath, scratch and brown coats gypsum plaster, smooth white finish.

120. Wood studs, ½-inch Insulite applied to both sides, joints filled.

121. Wood studs, two ½-inch sheets of Insulite applied to both sides, joints filled.

122. Same as No. 121, with addition of scratch and brown coats gypsum plaster, smooth white finish.

123. Same as No. 120, with addition of scratch and brown coats gypsum plaster, smooth white finish.

124. Staggered wood studs, ½-inch Insulite applied to both sides, joints filled.

125. Same as No. 124, with addition of Ecod Fabric, scratch and brown coats gypsum plaster, smooth white finish.

126. Same as No. 124 with addition of scratch and brown coats gypsum plaster, smooth white finish.

127. Wood studs, ½-inch Insulite applied to one side, plastered and back plastered. Metal lath applied to opposite side and plastered with scratch, brown, and finish coats.

128. Wood studs, ½-inch Insulite applied to one side, plastered with brown coat and back plastered, furring strips, ½-inch Insulite, scratch, brown, and finish coats gypsum plaster. The opposite side was covered with metal lath plastered with scratch, brown, and finish coats gypsum plaster.

VI. GENERAL SPECIFICATIONS FOR CONSTRUCTION OF TEST PANELS

1. Erection of Brick.—The brick were laid in mortar composed of 1 part Portland cement, 1/10 part mason's hydrated lime, and 3 parts sand by volume. The surfaces to be plastered were reasonably true and free from dirt or other loose material. The joints were flush with the surface.

2. Erection of Clay Tile.—Unless otherwise specified, the tile were medium burned hollow clay tile and laid in a mortar composed

of 1 part Portland cement, 1 part mason's hydrated lime, and 4 parts sand by volume. The surfaces to be plastered were reasonably true and free from dirt or other loose material. The joints were flush with the surface.

3. Erection of Reinforced Concrete Slab.—The concrete used in the slab was composed of 1 part Portland cement, 2 parts concrete sand, and 4 parts gravel by volume. The slab was 4 inches thick and reinforced with ⅜ inch round deformed rods placed 9 inches on center. Furring strips were applied to one side before the concrete set, nails previously driven through the furring strips being used as a tie.

4. Erection of Combination Floor Slabs.—The concrete mix was the same as in paragraph 3. The rows of tile were spaced about 18 inches on center. The space between the tile was filled with concrete and about 2 inches of concrete was poured on top. In panel 117a each concrete joist was reinforced by two ⅜ inch round rods.

5. Erection of Wood Studs.—(*a*) *Straight studding.*—New straight 2 by 4's were used. They were spaced 16 inches on center and securely nailed to the frame, which consisted of 3 by 4's.

(*b*) *Staggered studding.*—New straight 2 by 4's were used. They were spaced 8 inches on centers, alternate studs having a 2-inch projection. The studs were securely nailed to the cap and base, each of which consisted of a 2 by 6.

6. Erection of Wood Joist.—(*a*) New straight 2 by 4's were used. They were spaced 16 inches on centers and securely nailed to a frame which consisted of 3 by 4's.

(*b*) *Joists for suspended ceiling.*—New straight 2 by 4's were used. The floor joists were spaced so that each one was 4 inches to the right from the centers of a floor joist, and the bottom was 2 inches lower than the bottom of the floor joist.

7. Erection of Wood Lath.—Four-foot laths were used, straight and free from knots. The laths were erected on both sides of the panel, parallel to each other, three-eighths of an inch apart and perpendicular to the direction of the studs. They were cut to such lengths that both ends of each lath came over a support. The end joints between laths were staggered at every seventh lath. Each lath was nailed to each support it crossed. The laths were wetted the day before the scratch coat was applied.

8. Erection of Metal Lath.—This was expanded metal lath, painted, and of medium weight. The sheets were attached with their longer dimensions across the supports. A sheet of lath being 8 feet long, there were no joints between ends. The joints between the sides of the sheets were lapped one full mesh and tied with No. 18 iron wire midway between supports. Each sheet was securely fas-

tened to each support it crossed, the fastenings being spaced about 6 inches apart across the width of the sheet.

9. Erection of Ecod Fabric.—Each sheet was securely fastened to every support it crossed, the fastenings being spaced about 6 inches apart along the studs. All end joints were made over a stud. The side joints were lapped one full mesh.

10. Erection of Insulite.—The insulite used was cut from 4 by 12-foot by ½-inch stock to sizes required for the panels. Each ½-inch layer was nailed to each joist, stud, or furring strip, as the case happened to be, with fourpenny nails approximately 6 inches apart. One-quarter inch joints were allowed between sheets of insulite. Wire mesh was applied over joints on panels to be plastered. On panels which were not plastered the joints were filled.

11. Erection of Masonite.—This was erected in the same manner as insulite, paragraph 10.

12. Erection of Gypsum Plaster Board.—These boards were 32 by 36 by ⅜ inch. Both sides of the panel were covered with these boards, erected so that the 36-inch dimension ran parallel to the furring strips. The boards were cut so that the sides of each board came over the furring strips. The joints were staggered every row. A space of ¼ inch was left all around each board. Both sides and the center of each board were nailed to the furring strips every 6 inches.

13. Erection of Flax-li-num.—The Flax-li-num was erected according to manufacturers' specifications.

14. Erection of Furring Strips.—The furring strips were of wood $1\frac{3}{16}$ inch by 2 inches by 7 feet 2 inches. These strips were either wired or nailed to the panels 16 inches on centers.

15. Scratch Coat Gypsum Plaster.—This coat was composed of 1 part retarded neat gypsum plaster and 2 parts dry sand by weight. The ingredients were thoroughly mixed, first dry and again wet. The exposed surface was reasonably true and was scratched with an appropriate tool. The thickness of this coat was approximately ¼ inch.

16. Brown Coat Gypsum Plaster.—This coat was composed of 1 part retarded neat gypsum plaster to 3 parts dry sand by weight. The ingredients were thoroughly mixed, first dry and again wet, and applied with sufficient pressure to form a good bond. When the plaster base was masonry, insulite, masonite, or gypsum plaster board, this coat was built out until the average thickness of the plaster was ½ inch, rodded and floated to a true, even surface. For wood and metal lath the total thickness of the plaster from the face of the studs or furring strips to the face of the plaster was ⅞ inch.

17. Smooth Finish Coat.—This coat was composed of one bag of finishing hydrated lime to one-half bag of unretarded gypsum plaster. The lime was made into a putty with water at least 24 hours prior to

use. A small amount of this putty was circled out on the plasterer's board, some water put into the circle, and gauging plaster equal to one-half the volume of the putty dusted into the water. The whole was then mixed with a trowel, more water being added if necessary. More material was not mixed at one time than could be used in 30 minutes. The mixture was not retempered, but each batch was started with clean board and tools. This plaster was applied as a thin, even layer over the brown coat. It was watched carefully for the appearance of incipient crystallization. When this occurred, it was immediately troweled down to a smooth, true finish, using considerable pressure on the trowel, and brushing the surface with water if necessary. This coat was as thin as possbile without permitting the brown coat to show through.

18. Erection of Subflooring.—New, straight ¾ by 3½ inch stock was used. It was applied diagonally across the floor joists and well nailed.

19. Erection Finish Flooring.—New, straight ⅜-inch oak stock was used, except for panel No. 76. The oak flooring was applied perpendicular to the joist and securely nailed. For panel No. 76, ¾-inch maple flooring was used and nailed directly to nailing strips without the use of rough flooring.

20. Erection of Floating Floor.—This was made of 1 by 2 inch nailing strips, subflooring nailed at right angles to the nailing strips, and finished flooring nailed at right angles to subflooring.

21. Erection of Suspended Ceiling.—This was made up on a wood frame. Screw eyes were inserted so that it could be suspended with wires from the masonry floor. Insulite was used as a plaster base, and this was plastered in the usual way.

22. Cinder Fill.—This was composed of one bag of Portland cement to 10 cubic feet of cinders. These ingredients were thoroughly mixed, first dry and again wet, then tamped into place on the floor.

23. Concrete Finish on Floors.—This was composed of one bag of Portland cement to 3 cubic feet of dry sand. This was thoroughly mixed and poured over the cinder concrete so as to have an average thickness of 1 inch. The surface was troweled off to give a smooth, level finish.

Washington, October 25, 1928.

DISCHARGE COEFFICIENTS OF SQUARE-EDGED ORIFICES FOR MEASURING THE FLOW OF AIR

By H. S. Bean, E. Buckingham, and P. S. Murphy

ABSTRACT

1. Air at pressures between 1 and 13 atmospheres was passed through square-edged concentric orifices installed in long, straight pipes of 4, 6, and 8 inches nominal diameter, the three pipes being in series. At each orifice the temperature and static pressure were observed, and the fall of pressure through the orifice was measured between pairs of taps located in each of the three ways commonly adopted in commercial orifice meter practice.

2. The rate of flow was measured by throttling the air nearly to atmospheric pressure and discharging it through a flow nozzle on the end of the line. The design, calibration, and peculiarities of behavior of the nozzles are described, and the theory of this method of measurement is discussed in two appendixes. Such nozzles appear to be very satisfactory for use as primary standards.

3. The various quantities known as discharge coefficients and used in orifice meter computations are defined.

4. The experimental results are represented by equations connecting the values of the discharge coefficients with the ratio of orifice to pipe diameter and with the ratio of downstream to upstream static pressure. Tables of numerical values of discharge coefficients are also given.

5. The accuracy of the results and the limitations to their general applicability are discussed.

CONTENTS

		Page
I.	Introduction	562
II.	General plan of the investigation	562
III.	Orifice plates	563
IV.	Compressors and test line	565
V.	Orifice stations	566
VI.	Apparatus for measuring the rate of discharge	567
VII.	Measurement of the rate of discharge	568
VIII.	Remarks on flow nozzles	570
IX.	Discharge coefficients of orfices for liquids	571
X.	Discharge coefficients of orifices for gases	578
XI.	Outline of the methods of computation	581
XII.	Location of the pressure taps	584
	1. Pipe taps	584
	2. Throat taps	585
	3. Flange taps	585
XIII.	Method of analyzing the results	586
XIV.	Results for throat taps	588
XV.	Comments on the results for throat taps	594
XVI.	Results for flange taps	595

14830°—20——1

Page
XVII. Comments on the results for flange taps 598
XVIII. Results for pipe taps 599
XIX. Comments on the results for pipe taps 601
XX. Comparison of the three sets of results 601
XXI. Specimens of the experimental results 605
XXII. Comments on the data in Tables 19 to 22 608
1. Mean values of δ 609
2. Scattering of observed points 609
XXIII. Discussion of the accidental errors 610
XXIV. The effects of viscosity 612
XXV. Geometrical similarity and the influence of pipe diameter 616
XXVI. Equations for use in orifice meter computations 619
XXVII. Numerical examples 621
XXVIII. Remarks on metering other gases 624
XXIX. Summary of conclusions 624
Appendixes 625
A. Theory of the flow nozzle and the impact tube 625
B. Discharge coefficients of the nozzles 642
C. Similar orifices 653

I. INTRODUCTION

During the summers of 1922, 1923, and 1924 experiments on the flow of air through orifices of the type commonly used for metering gases were carried out at Edgewood, Md., as a cooperative project between the Chemical Warfare Service of the United States Army and the Bureau of Standards. The authorities of Edgewood Arsenal contributed the use of a bank of large ammonia compressors with their appurtenances, and of much other engineering material, tools, etc.; and, in addition to furnishing the power needed, they facilitated the work in every way possible. The installation of the piping, apparatus, and instruments and the taking of observations were carried out by members of the staff of the Bureau of Standards.

This paper contains a brief description of the apparatus and methods employed and presents a summary of the more important results of the investigation, together with such comments and discussion as seem appropriate. Several matters which required more extended discussion than appeared desirable in the body of the paper have been treated in appendixes.

II. GENERAL PLAN OF THE INVESTIGATION

In regard to any one orifice, the object of the experiments is to determine the relation between the rate of discharge of air through the orifice, on the one hand, and the temperature and static pressure of the air and the pressure drop or differential across the orifice, on the other. If this relation has been determined and expressed in simple form, the rate of discharge may thereafter be found, by computation or graphically, from observations of the temperature,

static pressure, and differential, and the orifice may thus be utilized as a flow meter for air.

The purpose of the investigation was to obtain experimental data from orifices of various sizes and proportions, working over a wide range of static pressures and rates of flow, so as to get as much systematic general information regarding the properties and behavior of such orifices as was practicable with the facilities and in the time at our disposal.

The circumstances which permitted of using large volumes of air and high static pressures, so as to cover a wide range of working conditions, entailed the disadvantage—which attaches to most large scale as contrasted with laboratory experiments—of making it impossible to secure high precision in the individual experiments. To offset this, the methods adopted made it practicable to work rapidly and make a large number of separate experiments so as, in some degree, to average out the accidental errors.

The principle of the experiments is very simple. A steady stream of compressed air is sent along the pipe in which the orifice to be tested is installed; the temperature, static pressure, and differential are observed by means of instruments near the orifice; and at the same time the rate at which air is flowing along the pipe and through the orifice is measured by some independent means, either ahead of the orifice or farther along the line.

The most obvious method of measurement is to discharge the air into a gas holder and measure the rate of rise, but since no holder of sufficient size was available the rate of discharge was determined by means of flow nozzles, as will be explained later. If the flow of air is not perfectly steady, the capacity between the orifice and the flow nozzle on the end of the line introduces a time lag, so that, though the measurement of the rate of discharge from the nozzle may be accurate, it does not correspond exactly in time to the observations made simultaneously at the orifice. Accidental errors of this sort were unavoidable because the power supply to the compressors was not perfectly steady, and the speed of the compressors could not be held entirely constant.

III. ORIFICE PLATES

The orifices to be reported on here were all of the most familiar type—round, concentric with the pipe, and square-edged at the upstream face of the plate. They were adapted for use in pipes of 8, 6, and 4 inches nominal diameter, and the list in Table 1 gives some of their important dimensions.

TABLE 1.—*List of orifice plates*

D=inside diameter of pipe in inches.
d=diameter of orifice in inches.
$e.\ w.$=width of cylindrical edge of orifice in inches.
$d/D=\beta$=diameter ratio.
$e.\ w./d$=edge-width ratio.

[Letters in column 5 denote the owners of the borrowed plates, as follows: *B*, Bachrach Instrument Co.; *C*, Chemical Warfare Service; *F*, Foxboro Co.; *H*, Hope Natural Gas Co.; *M*, Metric Metal Works]

Diameter of pipe D (inches.)	Serial number of plate	Diameter ratio $\frac{d}{D}=\beta$	Edge-width ratio $\frac{e.\ w.}{d}$	Owner of plate
1	2	3	4	5
7.634	1-8	0.1308	0.128	
	2-8	.1961	.085	
	3-8	.2050	.090	M.
	4-8	.2613	.064	
	5-8	.2778	.061	
	6-8	.3931	.043	
	7-8	.3936	.010	H.
	8-8	.3960	.042	
	9-8	.4015	.046	M.
	10-8	.4996	.031	M.
	11-8	.5245	.008	H.
	12-8	.5254	.032	
	13-8	.5580	.030	
	14-8	.5980	.028	M.
	15-8	.7042	.024	M.
	16-8	.7847	.021	
	17-8	.8023	.021	M.
5.785	1-6	.1080	.212	F.
	2-6	.192	.123	F.
	3-6	.2636	.084	
	4-6	.3026	.067	F.
	5-6	.3453	.065	
	6-6	.411	.048	F.
	7-6	.497	.047	F.
	8-6	.5180	.043	
	9-6	.5190	.042	
	10-6	.562	.039	F.
	11-6	.605	.037	F.
	12-6	.630	.009	B.
	13-6	.6094	.033	
	14-6	.780	.032	F.
	15-6	.801	.007	B.
3.777	1-4	.1992	.186	M.
	2-4	.2642	.084	C.
	3-4	.2651	.067	
	4-4	.2651	.124	
	5-4	.2656	.036	
	6-4	.3295	.105	
	7-4	.3977	.093	M.
	8-4	.3982	.021	H.
	9-4	.5295	.129	
	10-4	.5305	.036	C.
	11-4	.5944	.058	
	12-4	.6125	.056	M.
	13-4	.6624	.012	H.
	14-4	.6651	.049	
	15-4	.8277	.038	M.
	16-4	.8578	.040	

Of these 48 plates, 22 were made at the Bureau of Standards, while the others were loaned to us by the five organizations named in the heading of the table, to all of whom we wish to express our thanks.

The bureau plates were made with great care, and the inclusion of the commercial plates increased the interest of the results by show-

ing that, as a general rule, the behavior of the commercial plates did not differ appreciably from that of similar plates made at the bureau.

The plates were all in good condition, with the corner between the flat upstream face of the plate and the cylindrical edge of the orifice approximately square and smooth. Microscopic examination showed in many cases that this entrance corner was by no means perfect, but with few exceptions the experiments failed to reveal differences of behavior that could be traced to these visible imperfections of finish.

The 12 plates loaned by the Metric Metal Works were ¼ inch thick and were chamfered on the downstream side so as to leave the cylindrical edge of the orifice only ⅛ inch wide. Of the 4 plates loaned by the Hope Natural Gas Co., the two larger were ¾ inch

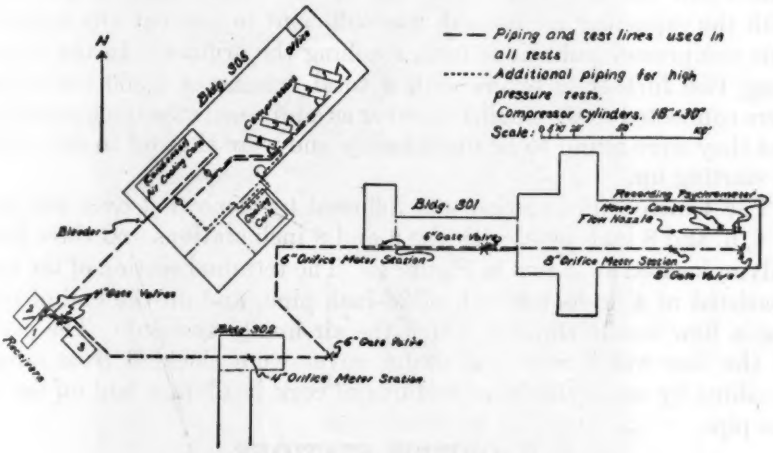

FIG. 1.—*Arrangement of piping for orifice meter tests*

Located in part of 155 mm gas shell filling plant of Edgewood Arsenal, Md.

thick and the two smaller ¼ inch. All 4 were chamfered so as to leave the cylindrical edge of the orifice about $\frac{1}{32}$ inch wide. All the other plates were flat on both sides with the hole bored straight through, the thicknesses of the plates being $\frac{5}{32}$ inch or less.

IV. COMPRESSORS AND TEST LINE

The general arrangement and approximate dimensions of the experimental installation are shown in Figure 1.

Air was supplied by one or more of a set of four 18 by 30 inch ammonia compressors which had a maximum combined output of about 30 cubic feet of free air per second. In most cases the gauge pressure in the test line was limited to 75 lbs./in.^{2} at the first orifice, but a number of runs were also made at pressures up to 275 lbs./in.^{2}

For these high-pressure runs the compressors were compounded, so that three working in parallel discharged through an intercooler to the fourth, acting as a second stage.

From the compressors to the first, or 4-inch orifice station, the air passed successively through: (*a*) Two oil traps of 60 cubic feet capacity, (*b*) a bank of ammonia condenser coils, (*c*) 100 feet of 4-inch pipe, (*d*) a receiver of 450 cubic feet capacity, and (*e*) 130 feet more of 4-inch pipe. This pipe, as well as the following 6 and 8 inch sections of the line, was "extra heavy." The lengths and volumes stated above are, of course, only approximate.

Any desired number of the 48 sections of the condenser coils could be cut out so as to change the resistance, and by this means, together with adjustment of a valve at the outlet from the receiver, a pressure drop of from 10 to 15 lbs./in.^{2} was maintained between the compressor outlet and the first orifice station. This resistance, in conjunction with the capacities mentioned, was sufficient to prevent any appreciable compressor pulsations from reaching the orifices. In the beginning, two further receivers with a total volume of 2,300 cubic feet were connected to the smaller receiver as additional steadying capacity, but they were found to be unnecessary and were shut off to save time in starting up.

The 4-inch orifice station was followed by somewhat over 400 feet of 4, 6, and 8 inch pipe, with the 6 and 8 inch stations and three gate valves, located as shown in Figure 1. The terminal section of the line consisted of a 30-foot length of 36-inch pipe, and on the end of this was a flow nozzle through which the air finally escaped. The parts of the line which were not under cover were shielded from direct sunshine by semicylindrical sections of cork insulation laid on top of the pipe.

V. ORIFICE STATIONS

Except for the difference of pipe diameter all three orifice stations were much alike. Figure 2 is a view of the 8-inch station. The 4 and 8 inch flanges for holding the orifice plates were kindly loaned to us by the Hope Natural Gas Co., and the 6-inch pair was made at the Bureau of Standards.

The side holes for pressure connections, provided at various distances from the orifice plate, were tapped with $\frac{1}{8}$-inch standard threads, and after the internal burr had been removed, brass connectors were screwed in, care being taken that they did not project beyond the inner surface of the pipe. All the upstream holes were connected to a single header through $\frac{5}{16}$-inch copper tubing, each lead including a valve so that any one hole could be used by itself. The downstream holes were similarly connected to a second header, the two headers were connected to the differential gauge, and either header could be connected to the static pressure gauge.

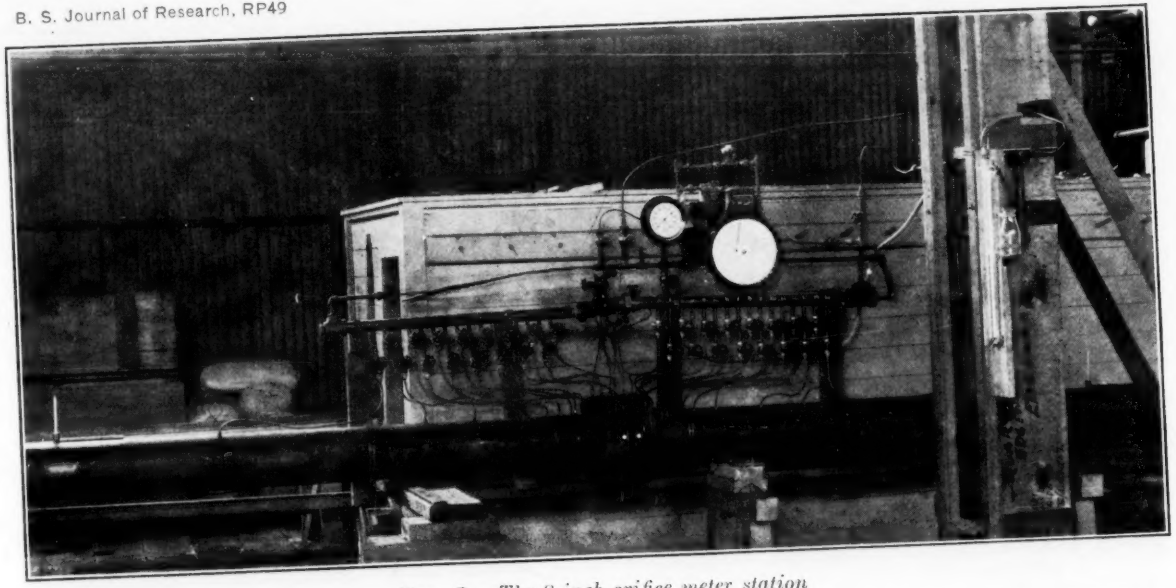

FIG. 2.—*The 8-inch orifice meter station*

The direction of flow was from right to left. The differential manometer is suspended in the frame at the right and a mercury manometer for static pressures is fastened to the outside of the frame. The white dots on the flanges mark the locations of the punch marks

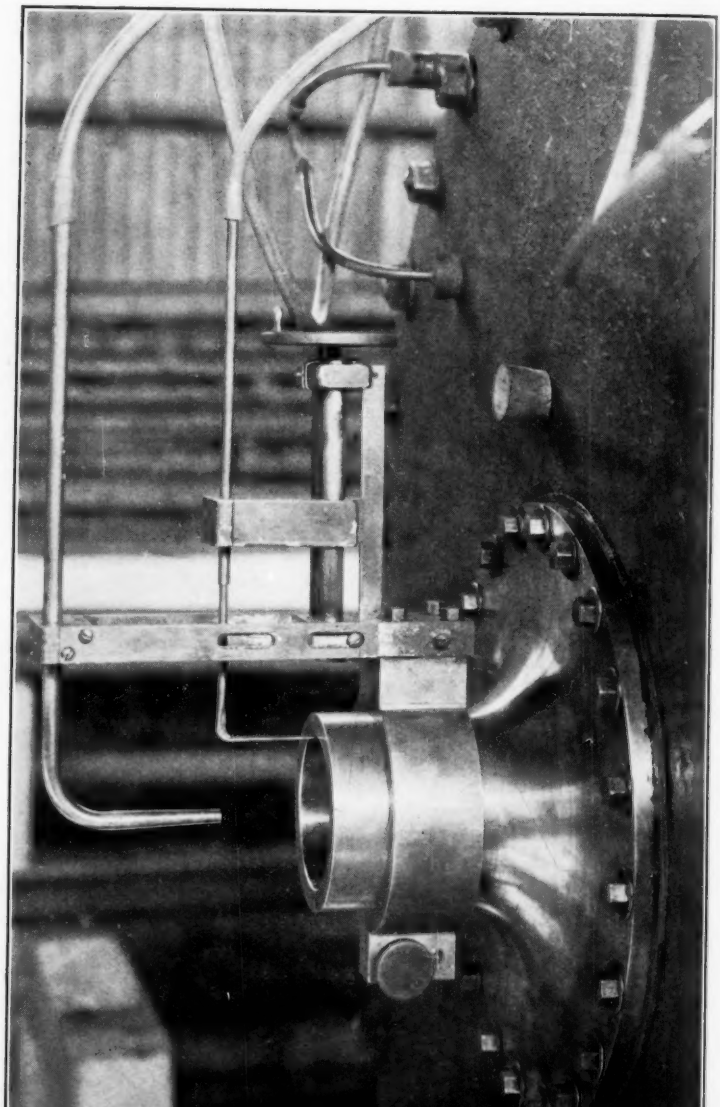

FIG. 3.—*Discharge nozzle and impact tips*

The distance from the center of each side hole to the face of the nearer flange was measured, once for all. A punch mark was made on the flange, and its distance from the face was also measured, the marks on the two flanges being on a line parallel to the axis of the pipe. After a plate of known thickness had been inserted and the bolts drawn up, a measurement of the distance between the two punch marks gave the combined thickness of the two gaskets; and on the permissible assumption that the gaskets were of sensibly equal thickness, the distance of any hole from the upstream face of the orifice plate could be computed.

Static pressures above 100 inches of mercury were read on standardized Bourbon gauges and lower pressures on mercury U-tube manometers. Differentials were read on U-tube manometers containing water, carbon tetrachloride, or mercury.

Wells containing mercurial thermometers were located about 12 pipe diameters upstream and downstream from the orifice plate. They had fins to increase the surface in contact with the air flowing along the pipe.

Thermometers were hung in suitable places for giving the approximate temperatures of the manometer columns, so that temperature corrections could be applied when needed.

VI. APPARATUS FOR MEASURING THE RATE OF DISCHARGE

The rate of flow of air along the line was measured by means of a nozzle and impact tube, according to the method described by S. A. Moss.[1] Figure 1 shows the position of the 36-inch pipe or discharge trunk in relation to the test line, and Figure 3 shows the end of the trunk with a nozzle and impact tubes in place.

Inside the trunk a mercurial thermometer gave the temperature of the air approaching the nozzle, and a recording psychrometer near the entrance end furnished data for finding the humidity. Two honeycombs were used to straighten and regularize the flow along the trunk toward the nozzle.

The large impact tip shown in Figure 3 was ¼ inch in diameter and was fixed on the axis of the jet about 2½ inches out from the end of the nozzle. It was connected to one leg of an open, vertical manometer containing water or oil which served to measure the impact pressure at the center of the jet, and it could also be connected to one leg of an inclined manometer which was employed during calibration.

The small impact tip, about 0.02 inch in diameter, was mounted on a radial cross slide and could be traversed along any radius of the jet, just clearing the end of the nozzle. A scale and vernier permitted of determining its distance from the axis of the nozzle. This small

[1] Trans. Am. Soc. Mech. Engs., **38**, p. 761; 1916.

tip was used only for calibrating the nozzle, and during this operation it was connected to the other leg of the inclined manometer mentioned above. By traversing the small impact tip along various radii of the jet and taking readings of the inclined manometer, while the impact pressure at the large fixed tip remained constant, the distribution of impact pressure over the area of the mouth of the nozzle could be determined.

A mercurial barometer was provided for reducing observed gauge pressures to absolute pressures when necessary.

Nine nozzles were prepared for the investigation and were calibrated, but most of the observations on rates of discharge were made with only four of them. They were of cast bronze smoothly finished and polished inside. The entrance curve leading to the cylindrical throat was a quarter-ellipse with a diameter ratio of 2 to 3, except in one case, where it was a quarter-circle. Table 2 contains a list of the nozzles, with their throat diameters and the approximate ratios of their other dimensions to the throat diameters, the notation being given in Figure 4.

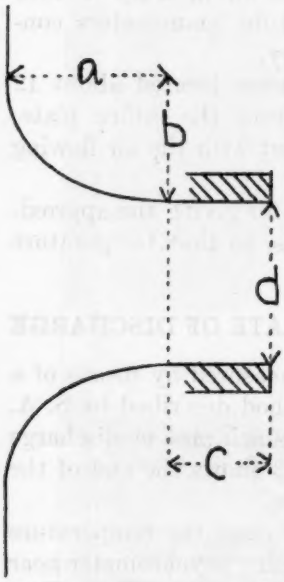

FIG. 4.—*Proportions of flow nozzles*

TABLE 2.—*Dimensions of flow nozzles*

Nozzle	d	$\frac{c}{d}$	$\frac{a}{d}$	$\frac{b}{d}$
	Inches			
D-1	1.764	1	1	⅔
A-1	3.255	1	1	⅔
B-1	4.206	1	1	⅔
C-1	5.006	1	1	⅔
A-2	3.262	½	1	⅔
B-2	4.521	½	1	⅔
C-2	5.003	½	1	⅔
A-3	3.272	1	1	1
A-4	3.258	1	⅔	1

VII. MEASUREMENT OF THE RATE OF DISCHARGE

Air from the test line entered the discharge trunk and after passing through the two honeycombs it approached the nozzle in a slow, regular stream at a speed of not over 4.2 ft./sec. It then expanded to the outside barometric pressure and issued from the parallel-sided mouth of the nozzle as a cylindrical jet at a speed between fifty and four hundred times the speed of approach.

In such a jet the impact pressure is uniform all over the middle part. Near the wall of the nozzle skin friction retards the motion and the impact pressure falls off; but this influence of the wall does

not reach far into the jet because with a short nozzle and high air speed there is no time for it to do so, and the uniform central core of the jet is not affected by it.

From the uniformity of the impact pressure we may conclude that the fall of pressure and the increase of speed have taken place in the same way for all filaments of the core, and that since these filaments have not been affected by proximity to the wall of the nozzle the flow in them has been unresisted and adiabatic; that is, isentropic. The ideal conditions presupposed in the familiar thermodynamic theory of the formation of jets of gas are therefore satisfied, in the core, to a high degree of approximation, and the theoretical equations may be relied upon for computing the rate of discharge per square inch of cross section of the core as is discussed in Appendix A.

The observational data needed for this are the outside barometric pressure, the pressure drop or differential through the nozzle, and the temperature and humidity of the air approaching along the trunk.

The pressure drop through the nozzle is obtained from the central impact tip. If this tip is connected to one leg of the vertical water manometer while the other leg is connected to a static side hole in the wall of the trunk, the manometer shows no difference of pressure. Strictly speaking, it gives the impact pressure of the air moving along the trunk, but this was never more than about 0.004 inch of water and was inappreciable. This relation holds quite accurately—certainly to better than 1 part in 1,000—up to the speed of sound or the critical pressure ratio, though not beyond.

It follows from the foregoing that the pressure in the central impact tip is equal to the pressure of the air ahead of the nozzle in the trunk, so that its excess over the outside barometric pressure, as read on the open manometer, is the same thing as the pressure drop which is driving the air through the nozzle.

The theoretical equation gives the rate of discharge per square inch of section of the core, and if there were no skin friction and the uniform core filled the whole section of the mouth of the nozzle, the total rate of discharge could be found by multiplying the rate per square inch in the core by the measured area of the nozzle mouth, expressed in square inches. The actual rate of discharge is, of course, somewhat less than this because the core does not fill the whole nozzle but is surrounded by a nonuniform sheath in which the speed falls off toward the wall. The actual total rate of discharge is therefore the product of the theoretical rate by a discharge coefficient which is slightly less than unity and the value of which is determined by calibration.

Observations with the small, movable impact tip serve to determine how the speed falls off toward the wall, and when the distribution of

speed in the nonuniform sheath is known, the discharge coefficient can be computed. The process will be further discussed in Appendix B.

VIII. REMARKS ON FLOW NOZZLES

The smoother the internal surface of the nozzle the less will be the tangential retarding drag of skin friction and the nearer will the discharge coefficient be to unity. With a given quality of surface, a large nozzle is relatively smoother than a small one; hence it is to be expected that if the surfaces are finished with equal care, large nozzles will, in general, have higher discharge coefficients than smaller ones of the same shape. This rule may, however, be subject to frequent exceptions, for smoothness of finish is difficult to reproduce at all exactly, and rather small variations in the internal finish of a nozzle may have an appreciable effect on the discharge coefficient.

If the linear speed of the air is increased, each individual particle of air takes less time to pass through the nozzle, and there is less time for the retarding effect of the drag at the wall to be propagated inward toward the center of the jet. The diameter of the uniform core therefore increases, and the discharge coefficient of the nozzle increases with the linear speed of the jet; that is, with the rate of discharge or with the impact pressure in the core.

This variation with speed is quite appreciable, especially at low speeds, and the discharge coefficients of such flow nozzles as were used in this investigation can not be treated as constants except over short ranges of speed. The results of the calibration experiments were represented by curves showing the relation of the discharge coefficient to the central impact pressure, and each time that a nozzle was used to measure the rate of flow of air along the test line, the value of the discharge coefficient to be used in the computations was read from the curve for this nozzle, at the impact pressure observed in the large central impact tip.

An idea of the magnitude of the above-mentioned variations of the discharge coefficient with diameter and impact pressure may be obtained from Table 3. This table contains values of the discharge coefficient read from the calibration curves of the four nozzles which were used in most of the orifice tests, at impact pressures of $h = 1, 2, 5, 12$, and 30 inches of water, corresponding to linear speeds of about 66, 94, 150, 230, and 360 ft./sec.

TABLE 3.—*Discharge coefficients of nozzles*

Nozzle	Throat diameter (inches)	Discharge coefficient at—				
		h=1 inch	h=2 inches	h=5 inches	h=12 inches	h=30 inches
D–1	1.764	0.980	0.983	0.986	0.989	0.991
A–2	3.262	.983	.985	.988	.991	.994
B–2	4.521	.989	.992	.994	.995	----
C–2	5.003	.991	.992	.994	.995	----

The expectation that for similarly finished nozzles the discharge coefficient will increase with the diameter is seen to be confirmed for these nozzles. The values in the table also conform to the rule that the discharge coefficient of a nozzle increases with the rate of discharge, and this gradual increase of the discharge coefficient, as the uniform core of the jet fills a larger and larger fraction of the cross section of the mouth of the nozzle, may be regarded as the normal course of affairs for a nozzle which is suitably designed for the rates of discharge which it is intended to measure; but exceptions to this normal behavior may occur if the approach to the cylindrical throat is too sharply curved. At the entrance end of the nozzle, where the cross section is large and the speed low, the degree of curvature is of little importance; but upon approaching the throat the speed increases and the permissible curvature becomes less.

The curvature of the path of the particles of fluid near the wall of the nozzle gives rise to a centrifugal force directed inward and causes a decrease of pressure near the wall. In the case of a liquid, this may result in a detachment of the jet from the wall, so that the jet contracts and no longer fills the nozzle; and in the case of air, the result is to decrease the diameter of the uniform core at the mouth of the nozzle and so decrease the discharge coefficient.

Since the centrifugal force directed away from the curved wall toward the axis of the nozzle depends on both the curvature of the path and the linear speed along it, both of these are of importance. With a given nozzle, the discharge coefficient may increase with the rate of discharge up to a certain point; but then, if the rate of discharge is increased still more, the effect of too great curvature of the wall may begin to make itself evident by a decrease of the discharge coefficient.

This is what was observed with nozzles A–3 and A–4. With A–3 the earlier part of the calibration curve was of normal shape and very like the curves for the other nozzles, but when the impact pressure had reached about 8 inches of water the discharge coefficient began to fall slowly instead of continuing to increase. With nozzle A–4, in which the curvature near the beginning of the cylindrical throat was considerably sharper, this effect was much more marked and began earlier—when the impact pressure or the drop through the nozzle was only 5 or 6 inches of water.

Calibration curves for all the flow nozzles are given in Appendix B, Figure 12.

IX. DISCHARGE COEFFICIENTS OF ORIFICES FOR LIQUIDS

The most generally useful method of describing the results of such experiments as those now in question is to state the numerical values of the discharge coefficients obtained, and that plan is adopted here.

But a discharge coefficient may be defined in various ways, and the value obtained from a given set of observations depends on how the coefficient is defined; hence, unless this is clearly understood, a table of discharge coefficients has no precise meaning and is useless. It is, therefore, advisable to discuss the meaning of the term "discharge coefficient" somewhat fully.

The differential set up by a fluid flowing through an orifice depends on the density of the fluid as well as on the rate of flow. The density of an ordinary liquid is so little affected by changes of pressure that it may be treated as constant, but the density of a gas depends on the temperature and static pressure in the pipe and, furthermore, it decreases as the gas passes through the orifice from a higher to a lower pressure. For this reason the behavior of gases is somewhat less simple than that of liquids, and it seems well to discuss liquids first.

Let it be supposed that we have means for making a liquid of known density, such as water, flow steadily along a pipe and through an orifice installed in it; and that a pair of pressure taps and a differential gauge are provided for measuring the pressure drop, or differential, from the upstream to the downstream side of the orifice plate. Weighing or measuring tanks are also to be provided, so that the rate of discharge can be determined simultaneously with observations of the differential, and the relation between the two determined by experiments at various rates of flow, with various liquids and various orifices.

The result of such experiments on round, concentric, square-edged orifices has been to show that under most ordinary conditions: (*a*) The rate of discharge M of a given liquid through a particular orifice is nearly proportional to the square root of the differential Δ, or $M \propto \sqrt{\Delta}$, nearly; (*b*) if a given orifice is tested with liquids of different densities, the rate of discharge needed to set up a given differential is nearly proportional to the square root of the density ρ, or $M \propto \sqrt{\rho}$, nearly; (*c*) if a larger or smaller orifice is substituted for the one first used, and if the pipe diameter D and the distances of the pressure taps from the orifice plate are also increased or decreased in the same ratio as the orifice diameter d, the rate of discharge of any one liquid, at a given differential is nearly proportional to the area of the orifice, that is, to the square of its diameter d, or $M \propto d^2$, nearly.

These three conclusions from experiment may be summed up by the statement that if we write

$$B = \frac{M}{d^2\sqrt{\rho\Delta}} \quad \text{or} \quad M = Bd^2\sqrt{\rho\Delta} \tag{1}$$

the value of B is nearly the same for all rates of flow, for all liquids, and for all round, concentric, square-edged orifices of the same diameter ratio d/D, so long as the pressure taps are always placed in the same relative positions with respect to the orifice.

If the experiments are made on orifices of some other diameter ratio, a relation of the same form is obtained, but the value of B is somewhat different, depending on the value of d/D; and if the location of the pressure taps is altered, the value of B is again nearly constant but different from the previous value.

If B were strictly constant under all circumstances, the result of the whole investigation could be stated by giving the one value found for B, and the rate of discharge in any future case could be found by substituting this value in (1), together with the known values of d and ρ, and the observed differential Δ. For an orifice of measured diameter, employed for metering a liquid of known density, the quantity

$$Bd^2\sqrt{\rho} = K \tag{2}$$

would be a known constant, and the computation of the rate of discharge from the observed differential by means of the formula

$$M = K\sqrt{\Delta} \tag{3}$$

would be a very simple operation.

In reality, the three experimental relations stated above are not exact and B is not always quite constant, even for a given diameter ratio and with given relative positions of the pressure taps. It may vary slightly with the absolute size of the orifice, the linear speed of flow, and the density and viscosity of the liquid; but under most conditions of ordinary orifice meter practice these variations are small, and for any one diameter ratio and a given location of the pressure taps B may be treated as a constant.

It is evident from the foregoing that the results of an experimental study of the flow of liquids through any type of orifice, such as the square-edged orifice in a thin plate, might be made conveniently available for application to orifice meter calculations by means of tables or curves giving the values found for B, from which the value to be used in equation (1) in any particular case might be read off, either directly or by interpolation. This is, in substance, the method actually adopted, although the conventional presentation of the subject gives it a slightly different appearance and seems to attach more importance to an obviously very imperfect theory than is at all necessary. The conventional treatment runs about as follows:

The flow of a liquid through an orifice is a mechanical phenomenon and is, of course, subject to the general laws of mechanics; but the motion is so complicated that it is impossible to construct a

complete mathematical theory for describing or accounting for all the details of what happens. Instead of attempting this, we limit ourselves to considering an ideal state of motion which bears some resemblance to the reality, though not a very close one, and which is simple enough that the rate of flow under the ideal conditions can be computed exactly from mechanical principles.

The ideal simplified state of motion is specified as one in which the following conditions are satisfied: (*a*) At the section where the upstream pressure tap is situated, the velocity is uniform and parallel to the axis of the pipe, and the static pressure is also uniform all over the section and equal to the pressure indicated by a gauge connected to the tap; (*b*) at the smallest section of the orifice the velocity of the liquid is perpendicular to the plane of this section—that is, parallel to the axis of the pipe—and both the velocity and the static pressure are uniform all over the section; (*c*) the pressure in the downstream pressure tap is equal to the uniform static pressure in the plane of the orifice; and (*d*) there are no energy losses by turbulence, viscosity, or skin friction.

In the actual motion of a liquid through an orifice installed in a pipe, conditions *a* and *d* are usually nearly fulfilled, and in these respects the ideal state of affairs does not differ very much from what really happens. Conditions *b* and *c* may also be nearly satisfied in practice, if the orifice has a well-rounded entrance or is in the form of a flow nozzle, and if the pressure taps are suitably placed. For such an orifice, the conditions presupposed in the theoretical reasoning are approximately satisfied, and the rate of discharge deduced for the ideal case is fairly close to the true rate found by experiment.

But with a square-edged orifice condition *b* is far from satisfied. In the plane of the orifice the flow is convergent, and neither the velocity nor the static pressure is uniform; the jet is trumpet shaped, with its narrowest section or vena contracta considerably smaller than the orifice and some distance downstream, and the velocity and pressure are nearly uniform at the vena contracta instead of at the orifice. Condition *c* loses its meaning when *b* is not satisfied. The downstream pressure tap may be so placed as to give the pressure in the vena contracta; but it need not be, and often is not, so placed, and the pressure it gives depends to a considerable extent on where it is.

On the whole, it may be said that the ideal state of motion for which the theoretical deductions are exactly true, while it may be nearly realized for well-shaped flow nozzles, is not a good representation of the facts for square-edged orifices. It is therefore not surprising that the "theoretical" rate of discharge turns out to be

quite different from the true rate in the case of square-edged orifices.

Turning, now, to the consideration of the ideal case, let—

D [ins.] = the inside diameter of the pipe;

d [ins.] = the diameter of the orifice;

$\beta = \frac{d}{D}$ = the diameter ratio of the orifice;

ρ[lb./ft.^{3}] = the density of the liquid;

Δ[lb./in.^{2}] = the differential;

S_1[ft./sec.] = the linear speed at the upstream tap;

S_2[ft./sec.] = the linear speed through the orifice;

M_t[lb./sec.] = the theoretical rate of discharge;

M[lb./sec.] = the actually observed rate;

$C = M/M_t$ = the discharge coefficient of the orifice.

Since the rate of flow is the same past the upstream tap as through the orifice and the speed is uniform over each of these sections (conditions a and b), we have

$$M_t = \frac{\pi}{4}\left(\frac{D}{12}\right)^2 \rho S_1 = \frac{\pi}{4}\left(\frac{d}{12}\right)^2 \rho S_2 \tag{4}$$

whence

$$S_1 = \frac{d^2}{D^2} S_2 = \beta^2 S_2 \tag{5}$$

Since there are no energy losses (condition d), the increase of kinetic energy of each cubic foot of the liquid, as its speed increases from S_1 at the upstream tap to S_2 at the plane of the orifice, is equal to the work done on it by the pressure drop Δ. Hence, measuring work and kinetic energy in standard foot pounds, we have

$$\frac{\rho(S_2^2 - S_1^2)}{2 \times 32.174} = 144\Delta \tag{6}$$

or after eliminating S_1 by means of (5) and solving for S_2,

$$S_2 = 96.261\sqrt{\frac{\Delta}{(1-\beta^4)\rho}} \tag{8}$$

Upon substituting this value of S_2 in (4), we have as the expression for the theoretical rate of discharge through the orifice

$$M_t = \frac{0.5250}{\sqrt{1-\beta^4}} d^2 \sqrt{\rho\Delta} \tag{9}$$

where M_t = lb./sec.; d = ins.; ρ = lb./ft.^{3}; and Δ = lb/in^2.

The factor

$$\frac{0.5250}{\sqrt{1-\beta^4}} \tag{10}$$

is independent of the absolute size of the orifice and is a constant for all orifices of any one diameter ratio, so long as the units specified above are retained. A change of units would, in general, require a change in the figure 0.525.

In some unusual circumstances the effects of the departures of the actual from the ideal motion of the liquid may offset one another in such a way that the theoretical rate of discharge computed from (9) agrees with the rate actually observed; but, in general, the two rates are different, often considerably different. The ratio of the two, or

$$C = \frac{M}{M_t} \tag{12}$$

is known as the "discharge coefficient" of the orifice for the given liquid at the differential Δ; and if (12) is written in the form

$$M = CM_t = C\,\frac{0.5250}{\sqrt{1-\beta^4}}\,d^2\sqrt{\rho\Delta} \tag{13}$$

it states that when the discharge coefficient C is known the true rate of discharge may be found by multiplying the theoretical rate by the discharge coefficient.

Upon comparing (13) with (1), we find that

$$B = \frac{0.5250}{\sqrt{1-\beta^4}}\,C \tag{14}$$

and B differs from C only by a constant factor, the value of which is determined by the units and the diameter ratio. Hence, what was said earlier regarding the approximate constancy of B and the convenience of representing experimental results by tables of values of B is equally applicable to the discharge coefficient C. Tables of either quantity may be transformed into tables of the other by means of (14) without further experiment.

The statement of results in terms of C is the method most commonly adopted, and it has the advantage that C is a pure ratio and therefore independent of the units in which rates of discharge are expressed, so long as the same unit is used for both M and M_t. On the other hand, the constant in (14) does depend on what units are used for M, d, ρ, and Δ, and the same is therefore true of B. Accordingly, results stated in terms of B would be directly applicable only to computations made in terms of a particular set of units, whereas a statement in terms of C is applicable, whatever the units used. A further advantage of stating results in terms of the discharge coeffi-

cient C is that it conforms to established practice and so facilitates the comparison of new experimental results with data which may already have been published.

In leading up to the conception of the discharge coefficient, the first step was to specify an ideal state of motion of the liquid which was simple enough to be treated rigorously by the principles of mechanics. This led to equation (9) for the theoretical rate of discharge and to the definition of C by (12). The result is satisfactory because, for a given liquid flowing through a given orifice, the discharge coefficient thus defined is nearly constant, so that equation (13) reduces to the very simple approximate form

$$M = K\sqrt{\Delta} \tag{15}$$

where K is a known constant, to the same order of accuracy as C itself is a known constant.

But there was no necessity of specifying the ideal motion in the particular way adopted, for any other ideal state of motion that was simple enough to be treated rigorously by theoretical principles might equally well have been selected. A different choice would have led to a different expression for the theoretical rate of discharge M_t; and the discharge coefficient defined by (12), in conjunction with the equation for M_t, would have had a different value. It is therefore evident that the discharge coefficient might be defined in various ways, and that the term "discharge coefficient" has no definite significance unless accompanied by a statement of how the "theoretical" rate of discharge is to be computed.

Since the procedure followed above leads to a satisfactorily simple result, there is no object in making a change unless it either simplifies the computation of M_t or leads to more nearly constant values of the discharge coefficient; and in practice, only one other definition of the discharge coefficient is in common use. It is arrived at by adding to the conditions already imposed on the ideal state of motion the further condition that the diameter of the pipe shall be treated as if very much larger than the diameter of the orifice, regardless of what the ratio of the two really is, thus departing still further from the actual state of motion.

Imposing this condition is equivalent to setting $\beta = 0$ in the equations already obtained, without changing anything else, and we get the equations

$$M'_t = 0.5250 d^2\sqrt{\rho\Delta} \tag{16}$$

$$C' = \frac{M}{M'_t} \tag{17}$$

$$M = C' M'_t = C' \times 0.5250 d^2\sqrt{\rho\Delta} \tag{18}$$

in place of (9, 12, 13).

The quantity C' defined by (16, 17) may be called "the discharge coefficient with approach factor included," to distinguish it from C, which is "the discharge coefficient with approach factor not included." When the term "discharge coefficient" is used without qualification, it usually means C and not C'. Comparison of (18) with (13) shows that

$$C = C'\sqrt{1-\beta^4} \tag{19}$$

so that either form of the discharge coefficient may readily be transformed into the other and a table of one is equivalent to tables of both.

When the diameter ratio $d/D=\beta$ is small, C and C' are nearly equal, and it is unnecessary to distinguish them. For example, if $d=0.2D$, $C=0.9992C'$. But if $d=0.5D$, $C=0.9682C'$, and mistaking one for the other would result in an error of over 3 per cent.

X. DISCHARGE COEFFICIENTS OF ORIFICES FOR GASES

The subject of discharge coefficients may be discussed in the same general way for gases as for liquids. By specifying an ideal state of motion that is simple enough for exact treatment on theoretical principles we find the rate at which the gas would flow through the orifice if the ideal conditions could be realized, and we then express the ratio of the actual to the theoretical rate as a discharge coefficient. If the orifice meter is to be a commercial and not merely a laboratory instrument, the computations must be simple, and the discharge coefficient must not vary too much with the rate of discharge; but, aside from these two requirements, the question whether the imaginary ideal motion bears any close resemblance to reality is of no importance whatever.

We start by imposing the same conditions as for liquids, regarding the distribution of velocity and pressure in the vicinity of the orifice and the absence of energy losses. But since the density of a gas depends on its pressure and temperature and changes as the gas flows through the orifice, the ideal state of motion requires further specification, either by making assumptions as to how the gas behaves or by imposing conditions as to how it shall behave in the ideal case.

The most obvious conditions to impose are that the gas shall follow the ideal gas equation $pv=RT$ exactly, and that it shall not gain or lose any heat by contact with the orifice plate or the walls of the pipe. These supplementary conditions, with those previously adopted for liquids, lead to the so-called "adiabatic equation" for the theoretical rate of discharge and to a corresponding definition of the discharge coefficient. This equation is important and useful for some purposes, but it is much too complicated to be used in ordinary practice and it need not be discussed here, though it will be referred to again later.

For the sake of obtaining a simpler result we adopt a condition which makes the ideal state of motion to be treated by theoretical principles much more unlike what really happens, and this condition is that the density of the gas shall remain constant during the flow through the orifice instead of decreasing, as it does, in fact. But imposing this condition is merely saying that the gas shall act like a liquid, and therefore the reasoning to be gone through is an exact repetition of what has already been given for liquids, and the resulting equations are precisely the same in form.

Only one more point remains to be specified. Having said that the density shall be constant, we are still at liberty to say what the constant value shall be and to select any value that is most convenient. In practice, the choice is usually made in one of the two following ways.

Let

p_1[lb./in.^{2}] = the absolute static pressure at the upstream pressure tap;

p_2[lb./in.^{2}] = the absolute static pressure at the downstream pressure tap;

t[° F.] = the temperature of the gas ahead of the orifice, just before the flow starts to converge;

ρ_1[lb./ft.^{3}] = the density of the gas at p_1, t;

ρ_2[lb./ft.^{3}] = the density it would have at p_2, t.

Then, in practice either ρ_1 or ρ_2 is taken as the density to be used in the equations; that is, the gas is treated as a liquid of density either ρ_1 or ρ_2. Introducing these specifications of the density into the equations already obtained for liquids gives us from (13)

$$M = C_1 \frac{0.5250}{\sqrt{1-\beta^4}} d^2 \sqrt{\rho_1 \Delta} \qquad (a)$$

or

$$M = C_2 \frac{0.5250}{\sqrt{1-\beta^4}} d^2 \sqrt{\rho_2 \Delta} \qquad (b)$$

and from (18)

$$M = C_1' \times 0.5250 d^2 \sqrt{\rho_1 \Delta} \qquad (c)$$

or

$$M = C_2' \times 0.5250 d^2 \sqrt{\rho_2 \Delta} \qquad (d)$$

(20)

We thus have four slightly different equations for computing the true rate of flow M from the observed differential Δ, each of which contains and defines one of the four coefficients C_1, C_2, C_1', and C_2'.

It is convenient to have descriptive names for these discharge coefficients, and, to start with, they may all be called "hydraulic" coefficients, to indicate that they are obtained by treating the gas as

a liquid, and to distinguish them from the "adiabatic" discharge coefficient which results from using the adiabatic equation mentioned above. The following designations may now be adopted:

C_1 is "the hydraulic discharge coefficient based on the upstream static pressure, with the approach factor not included";

C_2 is "the hydraulic discharge coefficient based on the downstream static pressure, with the approach factor not included;"

C_1' is "the hydraulic discharge coefficient based on the upstream static pressure, with the approach factor included"; and

C_2' is "the hydraulic discharge coefficient based on the downstream static pressure, with the approach factor included."

These four kinds of discharge coefficients are evidently not independent but connected by relations which permit of computing the value of any one from that of any other. For example, we have from (20) the relations

$$\left.\begin{aligned} C_2 &= C_1\sqrt{\frac{\rho_1}{\rho_2}} && (a)\\ C_1' &= C_1/\sqrt{1-\beta^4} && (b)\\ C_2' &= C_1\sqrt{\frac{\rho_1}{\rho_2}}\Big/\sqrt{1-\beta^4} && (c) \end{aligned}\right\} \quad (21)$$

This is merely another way of saying that the same set of experimental results may equally well be expressed in any one of the four ways, that is, by tables or curves giving values of any one of the four discharge coefficients.

In the foregoing discussion of the meaning and definition of discharge coefficients, the theoretical rate of discharge M_t and the true rate M have been expressed in pounds per second, because when the rates are expressed as mass per unit time the equations have a particularly simple form; but any other units might equally well have been used without changing the values of the C's, because these values are pure ratios and therefore independent of what units may be used for measuring the two rates of discharge.

If other units were adopted, such as gallons per minute for liquids or cubic feet per hour at standard pressure and temperature for gases, equations (20) would have a somewhat different appearance. And, similarly, measuring diameters in feet or centimeters instead of in inches, or measuring differentials in inches of water or mercury instead of in pounds per square inch, would change the value of the numerical factor 0.5250. But no such changes in the units have any effect on the values of the discharge coefficients.

Some of these other forms of equation, equivalent to (20), will be given later with illustrative examples, but that may be postponed until the results of the present experimental investigation have been set forth and discussed.

XI. OUTLINE OF THE METHODS OF COMPUTATION

Of the four kinds of discharge coefficients defined by equations (20), only C_1 was computed directly from the observations, the values of the other three being found subsequently by means of (21). To find the value of C_1, equation (20*a*) is put into the form

$$C_1 = \frac{\sqrt{1-\beta^4}}{0.525 d^2} \cdot \frac{M}{\sqrt{\rho_1 \Delta}} \tag{22}$$

and the values of d, β, M, Δ, and ρ_1, are substituted.

The internal diameter D of each of the three sizes of pipe at its orifice station, and the diameter d of each of the orifices, were measured by ordinary methods which need not be described. The values of the factor $(\sqrt{1-\beta^4}/0.525 d^2)$, which is a constant for each orifice, were then computed once for all.

The values of Δ, M, and ρ_1 varied from one experiment to another and had to be determined from the observations in each case. The differential Δ was read in inches of water, carbon tetrachloride, or mercury and after reduction to pounds per square inch it was ready for substitution in (22); but the values of M and ρ_1 required some preliminary computation.

Since the flow was kept as nearly as possible steady during each experiment, the rate of flow through any orifice inserted in the line was the same as the rate of discharge from the flow nozzle on the end of the discharge trunk and was to be determined from observations there. The quantities required were: (*a*) The outside barometric pressure, (*b*) the impact pressure at the center of the jet, (*c*) the temperature of the air in the discharge trunk ahead of the nozzle, and (*d*) the wet bulb depression read from the chart of the recording psychrometer in the trunk. The calibration curve of the nozzle having been determined by separate experiments, the value of M could be computed from the observations just mentioned.

The remaining quantity needed for substitution in (22) is the density ρ_1, which is, by definition, to be computed for the upstream static pressure p_1 and the temperature t of the air just ahead of the orifice. Since the air was not dry but contained a small admixture of water vapor, the humidity had to be known so that allowance might be made for the effect of the vapor.

Thep ressure p_1 is the sum of the static gauge pressure at the upstream tap and the outside barometric pressure. The static gauge was usually connected to the upstream tap and the pressure there observed directly, although since the differential was always observed at the same time, the static gauge might equally well have been connected to the downstream tap.

The temperature t was taken to be the mean of the temperatures t_1 and t_2 read at the upstream and downstream thermometer wells,

each about 12 pipe diameters distant from the orifice plate. An error of 1° F. in the value of t causes an error of 1/1,000 or less in the value of C_1, and since this was small in comparison with the other accidental errors of the experiments, an accuracy of ± 1 degree was sufficient.

When the outside air was much hotter or colder than the air in the pipe, the resulting heat leakage was sometimes enough to make t_1 and t_2 differ by 2° or more, but in most of the experiments the difference was much less than this, and either t_1 or t_2 could be used in place of the mean value without causing any significant change in C_1. In runs where this was found to be the case, further readings of one of the thermometers were usually dispensed with.

In addition to the values of p_1 and t, which would have sufficed if the air had been perfectly dry, it was necessary to know what fraction of the mixture consisted of water vapor. After the air entered the test line it had no opportunity to take up more water, and the vapor content could not increase. On the other hand, the pressure was continually falling, while the temperature remained nearly constant, so that the vapor in the expanding mixture was becoming more dilute and further from saturation and there was no tendency for water to be precipitated. Hence, the composition of the moist air remained unchanged along the line and was the same at each orifice as in the discharge trunk where the psychrometer was situated.

A sufficiently accurate measure of the vapor content of the air is provided by the value of the ratio π/p, where p is the total pressure of the mixture and π is the partial pressure of the water vapor in it. The value of π/p was found for the air in the discharge trunk from the observed pressure, temperature, and wet bulb depression. The hygrometric tables in the "Smithsonian Meteorological Tables" were used for this purpose. The value of π/p thus found was applicable to the air at higher pressures upstream, for reasons stated above.

The values of p_1, t, and π/p being known, it was possible to compute the value of ρ_1 from known data on the properties of dry air and water vapor. The following values were used:

The density of dry air containing the normal amount of carbon dioxide, at 32° F., and at the pressure of 1 atmosphere or 14.696 lbs./in.^{2}, was taken to be 0.08072 lb./ft.^{3} The coefficient of expansion at the constant pressure of 1 atmosphere was taken to be 1/490 of the volume at 32°, per degree. This is very close to the mean value over the range 32° to 122°. Values of the (pv) product, needed in determining the correction factor which allows for the departure from Boyle's law, were taken from the "Wärmetabellen" issued by the Physikalisch-Technische Reichsanstalt. The specific gravity of water vapor, referred to dry air at the same pressure and temperature, was assumed to be 18/29.

On the basis of the foregoing data, if air followed Boyle's law exactly, the density of dry air at t°F. and p_1 lb./in.^{2} would be

$$0.08072 \times \frac{p_1}{14.696} \times \frac{490}{458+t} = 2.6914 \frac{p_1}{458+t} \text{ lb./ft.}^3 \quad (23)$$

Within the range of pressure and temperature covered in these experiments, the value of the (pv) product at any one temperature is not quite constant but decreases slightly as the pressure is raised. Hence, the density at any pressure p_1 is greater than the Boyle's law value given by (23) in the ratio

$$\frac{(pv) \text{ at } t° \text{ and } 14.7 \text{ lb./in.}^2}{(pv) \text{ at } t° \text{ and } p_1 \text{ lb./in.}^2} = Y \quad (24)$$

Since the air is not dry but contains water vapor at the partial pressure π_1, the partial pressure of the dry air in the mixture is only $(p_1 - \pi_1)$. This substitution of water vapor for a part of the dry air, without changing the total pressure, has the same effect on the density as if a fraction π_1/p_1 of the dry air had been made lighter in the ratio 18/29; or as if the fraction π_1/p_1 of the whole number of molecules of air had been removed and replaced by the same number of water molecules, which are only 18/29 as heavy. The density as computed for dry air at p_1, t must, therefore, be multiplied by the correction factor

$$\frac{p_1 - \pi_1 + \frac{18}{29}\pi_1}{p_1} = 1 - 0.38\frac{\pi_1}{p_1} \quad (25)$$

The equation finally obtained from (23, 24, 25) is

$$\rho_1 = 2.6914 \frac{p_1}{458+t} Y \left(1 - 0.38 \frac{\pi_1}{p_1}\right) \quad (26)$$

and this was used for computing the values of ρ_1 to be substituted in (22) for computing the value of C_1.

To facilitate the work of computation, curves giving the values of log Y in terms of p_1 were drawn for each 10° from 32° to 112°. The value of log Y for any values of p_1 and t could then be obtained by interpolation from this set of curves.

Within the range of conditions covered by these experiments the departure of air from Boyle's law increases with rising pressure or falling temperature, but it is never large, and Y remains between 1.00 and 1.01. For example, if $p_1 = 295$ lbs./in.^{2} and $t = 42°$, the correction factor is $Y = 1.0092$. Hence if Y were omitted from (26) the value computed for ρ_1 would be somewhat less than 1 per cent low and the resulting value of C_1, one-half per cent high. But this represents an extreme case, for the pressure was usually much less than 295 lbs./in.^{2} and the temperature was seldom or never as low

as 42°. Hence, in the great majority of instances the effect of the departure from Boyle's law was insignificant and Y could be omitted from (26) without affecting C_1 by as much as 1 in 1,000.

It may be remarked here, however, that in some natural gases the departures from Boyle's law are so much greater than in air that when such a gas is to be metered through an orifice at high pressure, failure to allow for these departures when interpreting the meter readings may result in errors of several per cent.

The humidity correction was also always small. If the air were completely saturated at as high a temperature as 90°, and its absolute pressure were as low as 20 lbs./in.^{2}, the value of the humidity factor would be $1-0.38\pi_1/p_1=0.9868$, so that the correction to C_1 would be nearly 0.7 per cent. But at lower temperatures or higher pressures the possible concentration of water vapor is relatively less and the correction is smaller. In many of the experiments it was negligible.

In computing the value of the correction term $(0.38\pi_1/p_1)$, it is assumed that the air and the water vapor exert their partial pressures independently, each as if the other were not present, and that each of them follows the ordinary gas equation $pv=RT$. These assumptions are, of course, only approximately true; but when the water content is low and the correction small, as it always was, they are quite adequate to the purpose.

XII. LOCATION OF THE PRESSURE TAPS

In addition to the abrupt fall of pressure from the upstream to the downstream side of the orifice plate, there are other variations of pressure along the wall of the pipe near the orifice, particularly on the downstream side, so that the differential observed at any given rate of discharge depends on the distances of the pressure taps from the orifice plate and the observations have no precise meaning unless these distances are specified. This may be done most satisfactorily in terms of the diameter of the pipe as the unit, by stating the values of l_1/D and l_2/D, where l_1 and l_2 are the distances from the upstream face of the orifice plate to the centers of the upstream and downstream taps, and D is the inside diameter of the pipe.

Since there is nothing in the definitions of the discharge coefficients by equations (20) to fix the positions of the pressure taps, any pair of distances might be adopted; but in American practice three particular arrangements have become more or less standard, to the exclusion of others. They may be designated and described as follows.

1. PIPE TAPS

The standard distances, expressed in pipe diameters, are $l_1/D=2.5$ and $l_2/D=8$, but these distances need not be at all exact because in both these regions the pressure varies slowly along the wall of the

pipe and the tap may be displaced some distance from the standard position without any appreciable effect on the discharge coefficient. To the accuracy now attainable in the commercial use of orifice meters, and so long as the diameter ratio of the orifice is not greater than $\beta=0.6$, a tolerance of at least ± 1 pipe diameter is permissible in the distances of the taps from the orifice plate.

2. THROAT TAPS[1]

The standard distances are $l_1/D=1$ and $l_2/D=0.5$.

3. FLANGE TAPS

The standard positions for the pressure holes are 1 inch from the nearer face of the orifice plate, regardless of the thickness of the plate or the diameter of the pipe, so that there are no standard values of l_1/D and l_2/D.

For orifices of diameter ratios up to $\beta=0.6$, installed in 6-inch or larger pipes, it seems probable that holes at any smaller distances from the plate would give sensibly the same differential, and that 1 inch is merely a safe upper limit.[3] But for orifices of larger diameter ratio, or for much smaller pipes, this would no longer be true and the positions of the pressure holes would need to be more accurately specified. It would also be desirable to adopt a standard upper limit to the thickness of the orifice plate, expressed as a fraction of the pipe diameter.

There would be some advantages in abandoning this arrangement in favor of one in which the pressures were taken off right in the corner at the face of the plate through a narrow circumferential slit left between the plate and the end of the pipe, as recommended by Hodgson.[4]

In the present investigation each orifice was tested with three combinations of pressure taps which corresponded, roughly, to those mentioned above; and in each experiment the differentials were read between the three pairs of taps, as nearly as practicable at the same time and under the same conditions of flow. Auxiliary experiments on the longitudinal distribution of pressure for orifices of various diameter ratios made it possible to reduce the values obtained for C_1 to what they would have been with the taps in the standard locations. The

[1] This designation is used here for lack of a better short term. Such appropriateness as it can claim consists in the fact that on the downstream side of orifices of medium diameter ratio the lowest static pressure is usually found at about one-half pipe diameter from the orifice plate, so that this section corresponds in some measure to the throat of a Venturi. The term "Venturi taps" might, perhaps, be an acceptable alternative.

[3] See Holbrook Gaskell, jr., Proc. Inst. Civ. Eng., **197**, p. 250; 1913–14. Horace Judd, Trans. A. S. M. E., **38**, p. 331; 1916. J. M. Spitzglass, Trans. A. S. M. E., **44**, p. 919; 1922.

[4] J. L. Hodgson, The Orifice as a Basis of Flow-Measurement, Inst. Civ. Eng., Selected Engineering Papers, No. 31; 1925.

necessary corrections were usually quite negligible, but they were applied when they were as large as 1 in 1,000. The discharge coefficients to be given are therefore to be regarded as referring to the three standard combinations of pressure taps described above.

XIII. METHOD OF ANALYZING THE RESULTS

The three sets of results, each comprising about 360 separate values of the coefficient C_1, were examined separately but treated in the same general manner. Orifice plates of about the same diameter ratio were grouped together, and the values of C_1 obtained for each group were plotted as ordinates against the values of the pressure ratio $p_2/p_1=r$ as abscissas. A smooth curve was drawn to represent the general run of the points, and the result was a set of curves representing, approximately, the relation

$$C_1=f(r) \qquad (\beta \text{ constant}) \tag{27}$$

for each of the mean values of β pertaining to the several groups of orifices.

Values of C_1 were then read from these smooth curves at $r=1.00$, 0.95, 0.90, . . . etc., and the values for each r were plotted against the values of the diameter ratio β. If the original curves had been consistent with one another, the points of this second or cross plotting would have fallen on a set of smooth curves

$$C_1=f_1(\beta) \qquad (r \text{ constant}) \tag{28}$$

but in reality they were somewhat scattered, showing that the first set of curves required some modifications. By gradual readjustment two consistent sets of smooth curves were obtained, which appeared to represent the aggregate of all the values of C_1 as well as could be done.

Since such a process involves a good deal of judgment on the part of the operator, it was carried through on the throat tap values several times by each of two persons, at considerable intervals of time, and the results were tabulated and compared. For diameter ratios up to $\beta=0.5$, the different independent estimates of the most representative mean value of C_1, at any given value of the pressure ratio r, seldom differed by as much as 0.5 per cent and were usually closer together than that. But for the higher diameter ratios, where the possible range of pressure ratios was short, on account of the limited air supply, and where there were fewer observations, the different estimates sometimes differed by as much as 1.5 per cent.

After a good deal of study it was found that if the results obtained in the 4-inch pipe were set aside for separate discussion, the values

of C_1 for the 6 and 8 inch pipes could be represented satisfactorily by empirical equations of the general form

$$C_1 = \varphi(r, \beta) \tag{29}$$

the particular forms of the equation being different for the different combinations of pressure taps.

In deciding on the form to be adopted for (29), two conditions had to be satisfied. The first was that at any given pressure ratio r the limiting value of C_1 as β approaches zero must be the same for all three pairs of pressure taps. This is evident from the consideration that when β is very small the flow is merely a discharge from one large space into another, with the fluid in each of the spaces so nearly at rest that, aside from gravity, its pressure is sensibly the same on all parts of the wall, and the location of the pressure taps is immaterial. The empirical equations (29) for the three combinations had, therefore, to become identical for $\beta = 0$.

The second condition arises from the fact that when the percentage differential is very small and the pressure ratio $p_2/p_1 = r$ approaches unity, the effects of compressibility vanish and air behaves like a liquid of the same kinematic viscosity.[5] This means that if the influence of viscosity is negligible, as it was in all or nearly all of our experiments, the value of C_1 for a given orifice and for very low percentage differentials must be the same as the discharge coefficient of the orifice for water.

This familiar experimental fact would have provided a desirable check on our limiting values of C_1 for $r = 1$, if accurate values of C as a function of β had been available for water. We did not find any such values for orifices installed in pipes, which appeared to be more trustworthy than an extrapolation from our own values for air, but there is one particular value which seems pretty well fixed.

If the percentage differential is very small, and if the diameter ratio is also very small, the value of C_1 for air must become identical with the value for a submerged jet of water issuing from a round, square-edged orifice in the wall of a large tank. This quantity has been the subject of a great many measurements, and the best determinations [6] show that when the Reynolds number [7] is high enough that viscosity no longer has any appreciable influence, the value is close to 0.597. This agrees well with a natural extrapolation from our observed points to $r = 1$ and $\beta = 0$, and also with the experiments of Bachmann [8] on air. We therefore adopted this figure as a fundamental value to which C_1 must converge when $r = 1$ and $\beta = 0$.

[5] See Section XXIV.
[6] See for example, Hamilton Smith's "Hydraulics," Chap. XI.
[7] See Section XXIV and Appendix C.
[8] H. Bachmann, Dissertation, Darmstadt; 1911.

The results obtained for 8 and 6 inch pipes did not show any systematic differences greater than the accidental differences between ostensibly similar orifices of the same size; but the coefficients for the 4-inch pipe were, on the whole, distinctly higher. The tables of discharge coefficients presently to be given are therefore to be understood as representing our average results from 6 and 8 inch plates only.

XIV. RESULTS FOR THROAT TAPS

Throat taps are, by definition, located one pipe diameter upstream and one-half pipe diameter downstream from the upstream face of the orifice plate. The definitions of the four familiar forms of discharge coefficient, C_1, C_2, C'_1, and C'_2, are given by equations (20) in Section X, above, and the relations between them are given by equations (21).

Our average results for orifices in the 6 and 8 inch pipes are represented by the equation

$$C_1 = 0.5970 + 0.09\beta^4 - 0.115\ (x + x^2)(1 + 1.5\beta^4) \tag{30}$$

in which

$$x = \frac{p_1 - p_2}{p_1} = 1 - r \tag{31}$$

that is, x is the differential, expressed as a fraction of the upstream static pressure.

Values of C_1 computed from (30) are given in Table 4.

TABLE 4.—*Throat taps*

[Values of C_1, the hydraulic discharge coefficient based on the upstream static pressure, with the approach factor not included]

$C_1 = 0.5970 + 0.09\ \beta^4 - 0.115\ (x + x^2)\ (1 + 1.5\ \beta^4)$

β=	0.0	0.2	0.3	0.4	0.5	0.55	0.6
r=							
1.00	0.597	0.597	0.598	0.599	0.602	0.605	0.609
.95	.591	.591	.592	.593	.596	.598	.601
.90	.584	.584	.585	.586	.589	.591	.593
.85	.577	.577	.578	.579	.581	.583	.585
.80	.569	.569	.570	.571	.572	.574	------
.75	.561	.561	.561	.562	.563	------	------
.70	.552	.552	.552	.553	------	------	------
.65	.543	.543	.543	.543	------	------	------
.60	.533	.533	.533	------	------	------	------
.55	.522	.522	------	------	------	------	------
.50	.511	.511	------	------	------	------	------

The shortening of the later columns is due to the limited compressor capacity, which made it impossible to attain high differentials with the larger orifices.

Equation (30) is purely empirical and should not be relied on outside the limits shown by the table. We had some observations on the smaller orifices at pressure ratios as low as $r = 0.3$, and the equation appears to fit these points within the experimental errors, but

there were relatively few of these observations, and we prefer not to trust the equation for pressure ratios lower than shown in the table.

As regards higher values of β, our observations were not satisfactory. Even for the smaller diameter ratios, the accidental errors were large and the resulting points much scattered, when the percentage differential was low; and in no case would the observations at pressure ratios greater than $r=0.95$ have sufficed, by themselves, to determine a curve $C_1=f(r)$. At higher percentage differentials the observations were more consistent and for the plates of small or medium diameter ratios, which could be tested over a large range of values of r, a fairly good determination of the mean curve was possible. But with large diameter ratios the possible range of r was narrower and the scattering worse.

For example, with two orifices for which $\beta=0.6904$ and 0.7042, 13 values of C_1 obtained at pressure ratios greater than $r=0.956$ were distributed irregularly between 0.598 and 0.643. In another case with four orifices, of diameter ratios from 0.780 to 0.802, 15 values of C_1 obtained with pressure ratios down to $r=0.967$, were scattered between 0.610 and 0.664, with one additional value at 0.713.

In both these instances the mean value of C_1 was within one-fourth per cent of the value computed from equation (30) for the mean values of x and β, and it seems probable that, for low percentage differentials, the equation gives a fairly good representation of the facts for 6 and 8 inch pipes up to $\beta=0.8$; but we do not recommend it for use when the diameter ratio of the orifice is greater than $\beta=0.6$, the limit shown in the table.

After the values of C_1 had been obtained those of C_2, C'_1, and C'_2, defined in Section X, were found from them by means of equations (21), and the results corresponding to Table 4 are given in Tables 5, 6, and 7.

TABLE 5.—*Throat taps*

[Values of C_2, the hydraulic discharge coefficient based on the downstream static pressure, with the approach factor not included]

$$C_2=C_1\sqrt{\frac{1}{1-x}}$$

$\beta=$	0.0	0.2	0.3	0.4	0.5	0.55	0.6
$r=$							
1.00	0.597	0.597	0.598	0.599	0.603	0.605	0.609
.95	.606	.606	.607	.608	.611	.614	.617
.90	.616	.616	.617	.618	.621	.623	.626
.85	.626	.626	.627	.628	.630	.632	.634
.80	.637	.637	.637	.638	.640	.642	-------
.75	.648	.648	.648	.649	.650	-------	-------
.70	.660	.660	.660	.661	-------	-------	-------
.65	.673	.673	.673	.673	-------	-------	-------
.60	.688	.688	.688	-------	-------	-------	-------
.55	.704	.704	-------	-------	-------	-------	-------
.50	.722	.722	-------	-------	-------	-------	-------

TABLE 6.—*Throat taps*

[Values of C'_1, the hydraulic discharge coefficient based on the upstream static pressure, with the approach factor included]

$$C'_1 = C_1/\sqrt{1-\beta^4}$$

β=	0.0	0.2	0.3	0.4	0.5	0.55	0.6
r=							
1.00	0.597	0.598	0.600	0.607	0.622	0.635	0.652
.95	.591	.592	.594	.601	.616	.628	.645
.90	.584	.585	.587	.594	.608	.620	.636
.85	.577	.578	.580	.586	.600	.611	.627
.80	.569	.570	.572	.578	.591	.602	------
.75	.561	.562	.564	.569	.582	------	------
.70	.552	.553	.555	.560	------	------	------
.65	.543	.543	.545	.550	------	------	------
.60	.533	.533	.535	------	------	------	------
.55	.522	.522	------	------	------	------	------
.50	.511	.511	------	------	------	------	------

TABLE 7.—*Throat taps*

[Values of C'_2, the hydraulic discharge coefficient based on the downstream static pressure, with the approach factor included]

$$C'_2 = C_2/\sqrt{1-\beta^4}$$

β=	0.0	0.2	0.3	0.4	0.5	0.55	0.6
r=							
1.00	0.597	0.598	0.600	0.607	0.622	0.635	0.652
.95	.606	.607	.609	.616	.631	.644	.661
.90	.616	.617	.619	.626	.641	.653	.671
.85	.626	.627	.629	.636	.651	.663	.680
.80	.637	.637	.640	.646	.661	.673	------
.75	.648	.648	.651	.657	.672	------	------
.70	.660	.661	.663	.669	------	------	------
.65	.673	.674	.676	.682	------	------	------
.60	.688	.688	.690	------	------	------	------
.55	.704	.704	------	------	------	------	------
.50	.722	.723	------	------	------	------	------

Table 8 contains values of a fifth discharge coefficient C_m, defined in analogy with (20) by writing

$$M = C_m \frac{0.5250}{\sqrt{1-\beta^4}} d^2 \sqrt{\rho_m \Delta} \tag{32}$$

in which ρ_m is the density of the air at $t°$ F. and at the mean pressure

$$p_m = \frac{p_1 + p_2}{2} \tag{33}$$

It is connected with C_1 by the equation

$$C_m = C_1 \sqrt{\frac{2}{2-x}} \tag{34}$$

and might be designated as "the mean hydraulic discharge coefficient with approach factor not included."

The corresponding quantity

$$C'_m = C_m/\sqrt{1-\beta^4} \tag{35}$$

might then be called "the mean hydraulic discharge coefficient with approach factor included."

TABLE 8.—*Throat taps*

[Values of C_m, the mean hydraulic discharge coefficient, with the approach factor not included]

$$C_m = C_1\sqrt{\frac{2}{2-\varepsilon}}$$

β=	0.0	0.2	0.3	0.4	0.5	0.55	0.6
r=							
1.00	0.597	0.597	0.598	0.599	0.603	0.605	0.609
.95	.599	.599	.599	.601	.604	.606	.609
.90	.600	.600	.600	.601	.604	.606	.609
.85	.600	.600	.601	.602	.604	.606	.609
.80	.600	.600	.601	.602	.603	.605	-------
.75	.600	.600	.600	.601	.602	-------	-------
.70	.599	.599	.599	.599	-------	-------	-------
.65	.597	.597	.597	.598	-------	-------	-------
.60	.595	.595	.595	-------	-------	-------	-------
.55	.593	.593	-------	-------	-------	-------	-------
.50	.590	.590	-------	-------	-------	-------	-------

Table 9 contains values of the "adiabatic" discharge coefficient C_a found from those of C_1 by means of the relation

$$C_a = C_1\left[\frac{2(1-r)(1-\beta^4 r^{1.2})}{7(r^{1.2}-r^{1.4})(1-\beta^4)}\right]^{\frac{1}{2}} \tag{36}$$

Readers who are interested in this quantity may be assumed to be already familiar with the theoretical considerations on which the definition of C_a is based. They are usually set forth in works on technical thermodynamics and are similar to those involved in the theory of the flow nozzle discussed in Appendix A to the present paper.

TABLE 9.—*Throat taps*

[Values of C_a, the adiabatic discharge coefficient]

β=	0.0	0.2	0.3	0.4	0.5	0.55	0.6
r=							
1.00	0.597	0.597	0.598	0.599	0.603	0.605	0.609
.95	.608	.608	.608	.610	.614	.617	.621
.90	.618	.619	.619	.622	.626	.630	.635
.85	.630	.630	.631	.633	.638	.643	.648
.80	.642	.643	.643	.646	.652	.656	-------
.75	.656	.656	.657	.660	.666	-------	-------
.70	.670	.670	.671	.674	-------	-------	-------
.65	.686	.686	.687	.690	-------	-------	-------
.60	.704	.704	.705	-------	-------	-------	-------
.55	.724	.724	-------	-------	-------	-------	-------

The relations of the various discharge coefficients to one another and to the pressure ratio and diameter ratio may be exhibited most clearly by curves drawn from the tabulated values, either with r as abscissa for constant β, or with β as abscissa for constant r. A few such diagrams may be given.

Figure 5 shows curves drawn with r as abscissa for the limiting diameter ratio $\beta=0$; that is, for a small orifice between two large spaces. Since the differential is independent of the positions of the pressure taps, when β is sufficiently small, these curves are applicable

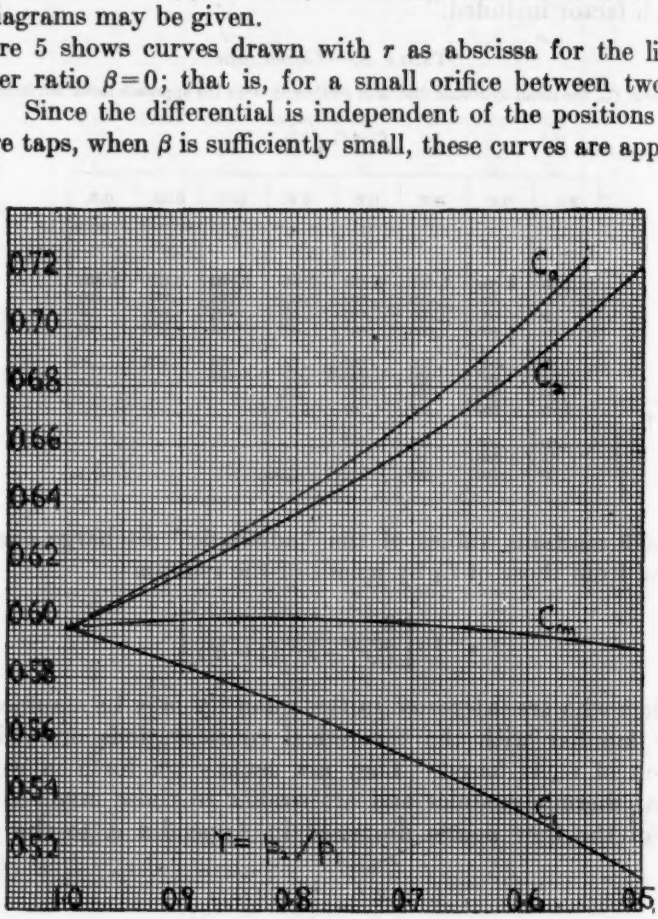

FIG. 5.—*Variation of discharge coefficients with pressure ratio, for small diameter ratios (Tables 4, 5, 8, and 9)*

to all three types of pressure connection. Moreover, when β is very small, the curves for C'_1, C'_2, and C_m' become identical with those for C_1, C_2, and C_m, respectively.

The following points may be noted:

(*a*) As r decreases and the differential becomes a larger and larger fraction of the upstream static pressure, C_1 decreases only about two-thirds as fast as C_2 increases. In other words, the discharge coefficient C_1, based on the density at the upstream pressure, is somewhat less affected by changes of the pressure ratio than is the coefficient C_2, based on the downstream pressure.

(*b*) The values of C_2 are not greatly different from those of the "adiabatic" coefficient C_a.

(*c*) The mean coefficient C_m, defined by (34), is nearly constant over a wide range of pressure ratios. If the indicating and recording mechanism of an orifice meter were so designed as to be actuated by the mean of the two static pressures, the meter could be used without any correction for change of coefficient with pressure ratio, over a much wider range than when only one of the two static pressures is employed. By using a pressure somewhat nearer the lower of the two, the first part of the curve for C_m might be made very close to a horizontal straight line.

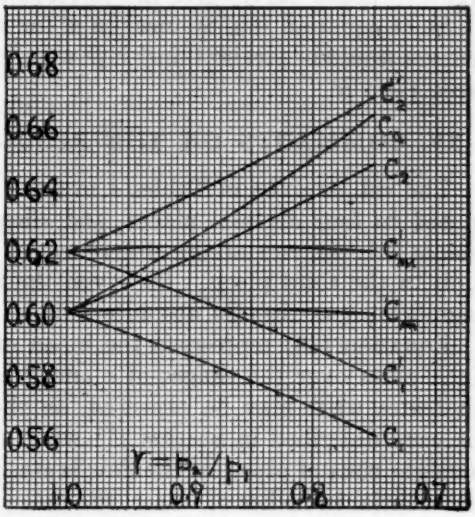

FIG. 6.—*Discharge coefficients for $\beta = 0.5$ and for throat taps (Tables 4 to 9)*

When the diameter ratio is not very small and the differentials measured between the different pairs of taps are appreciably different, the diagrams will be different for the three pairs, and the curves for C'_1, C'_2, and C'_m will not coincide with those for C_1, C_2, and C_m. The curves for throat taps and for the diameter ratio $\beta = 0.5$ are given in Figure 6.

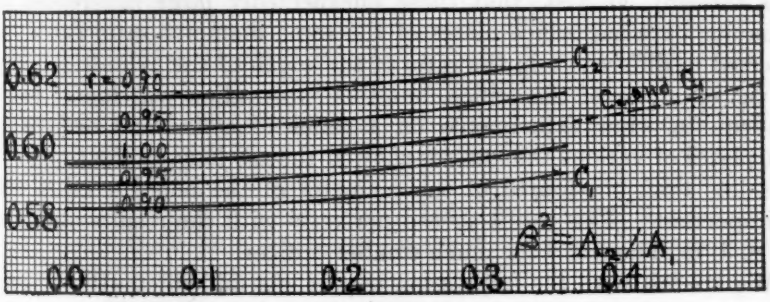

FIG. 7.—*Variation of C_1 and C_2 with area ratio for throat taps*

Another mode of representation is illustrated in Figure 7, in which the abscissa is β^2, or the ratio of the area of the orifice to the cross section of the pipe, and each curve refers to a constant pressure ratio instead of to a constant diameter ratio as in Figures 5 and 6.

The middle curve gives the limiting values of both C_1 and C_2 for vanishingly small differentials, on the supposition that the effects of viscosity are negligible. The two lower curves give the values of C_1 for differentials of 5 and 10 per cent of the unstream pressure, and the two upper curves give the corresponding values of C_2.

Since equation (30) is linear in β^4 for any fixed value of x, all these curves would be straight lines if β^4 were used as abscissa instead of the area ratio β^2.

XV. COMMENTS ON THE RESULTS FOR THROAT TAPS

The values given in Tables 4 to 9 are rounded off from values computed to four decimal places, and since they have not been further smoothed, the run of the differences is sometimes irregular by one unit in the third place. But even the third figure has little general significance as regards absolute values.

Equation (30) represents the mean of our results for the 6 and 8 inch pipes over the ranges of r and β covered by the tables, and it indicates what may be expected, on the average, from such orifices as were described in Section III when (*a*) they are installed in long straight runs of pipe, (*b*) the flow is steady, and (*c*) the product of the differential in inches of water, the mean static pressure in pounds per square inch, and the square of the orifice diameter in inches is not less than 10.[9] But the values of C_1 for individual orifices showed systematic departures of as much as 1 per cent, and occasionally more, from the average represented by equation (30).

These individual pecularities were most marked among the smaller orifices, in which a given degree of imperfection of the upstream corner of the orifice is relatively more important than for larger orifices. It was thought, at first, that these unexpectedly large differences of behavior between orifice plates of the same diameter ratio could be referred to differences in the ratio of the width of the cylindrical edge to the diameter of the orifice, but this explanation was found to be inadequate. For experiments on a series of cylindrical orifices in flat plates of various thicknesses showed that so long as the thickness was less than one-fourth of the diameter of the hole its value was unimportant. This result agreed perfectly with the results obtained by S. J. G. Thomas [10] for much smaller orifices.

We are left with the impression that it is a difficult matter to produce a number of duplicate plates which will all give the same discharge coefficient within ± 0.3 per cent.

The 4-inch plates gave higher values of C_1 than the 6 and 8 inch plates and for any given diameter ratio the mean curve $C_1 = f(x)$

[9] See Section XXIV and Appendix C.
[10] Phil. Mag., 44, p. 969; November, 1922.

for the 4-inch plates would lie about 1.5 per cent higher than the mean curve for the 6 and 8 inch plates, represented by (30).

The values of C_1 for individual 4-inch plates differed from their mean by amounts up to ± 1.5 per cent; that is, they were from nothing up to 3 per cent higher than values computed from (30). One 4-inch plate gave values of C_1 low enough to agree very well with (30). It had been noted, after microscopic examination, as having a "poor edge, rough and ridged," and this imperfection doubtless accounted for its departing so far from the mean of the 4-inch plates. This was one of the bureau plates, of diameter ratio $\beta = 0.3295$.

The range of variation of the values of C_1 for the 4-inch plates from their mean, or ± 1.5 per cent, was somewhat greater than the similar range for the 6 and 8 inch plates about their mean, represented by (30). Moreover, with the 6 and 8 inch plates the departures from the mean were most pronounced for the small values of β; that is, on the whole, for small absolute diameters. Both these facts point to the necessity of greater perfection of workmanship for small than for large orifices, if any standard table of discharge coefficients is to be relied upon.

Possible reasons for the high values of C_1 obtained from the 4-inch plates will be suggested in Section XXV.

XVI. RESULTS FOR FLANGE TAPS

The pair of flanges for holding the 8-inch orifice plates was one loaned to us by the Hope Natural Gas Co., and the holes for the pressure connections were approximately at the standard distances of 1 inch from the nearer face of the plate. In the 6-inch flanges, which were made at the Bureau of Standards, these distances were about three-fourths inch, so that for the 8 and 6 inch pipes the pressure taps were not equally distant from the plate, but at distances proportional to the diameter of the pipe. With pipes as large as 6 inches in diameter, such small variations have no appreciable effect on the differential, or on the discharge coefficient computed from it, unless the diameter ratio is considerably higher than $\beta = 0.6$.

Our average results for orifices in the 6 and 8 inch pipes are represented by the equation

$$C_1 = 0.5970 + 0.12\beta^4 - 0.6\beta^{12} - 0.115(x + x^2)(1 + 1.5\beta^4) \qquad (37)$$

in which, as before,

$$x = \frac{p_1 - p_2}{p_1} = 1 - r \qquad (38)$$

Values of C_1 computed from (37) are shown in Table 10 and the corresponding values of C_2, C'_1, C'_2, and C_m in Tables 11 to 14.

TABLE 10.—*Flange taps*

[Values of C_1, the hydraulic discharge coefficient based on the upstream static pressure, with the approach factor not included]

$$C_1=0.5970+0.12\beta^4-0.6\beta^{12}-0.115(x+x^2)(1+1.5\beta^4)$$

β=	0.0	0.2	0.3	0.4	0.5	0.55	0.6
r=							
1.00	0.597	0.597	0.598	0.600	0.604	0.608	0.611
.95	.591	.591	.592	.594	.598	.601	.604
.90	.584	.585	.585	.587	.591	.593	.596
.85	.577	.577	.578	.579	.583	.585	.588
.80	.569	.570	.570	.571	.574	.576	-------
.75	.561	.561	.562	.563	.565	-------	-------
.70	.552	.552	.553	.553	-------	-------	-------
.65	.543	543	.543	.543	-------	-------	-------
.60	.533	.533	.533	-------	-------	-------	-------
.55	.522	.522	-------	-------	-------	-------	-------
.50	.511	.511	-------	-------	-------	-------	-------

TABLE 11.—*Flange taps*

[Values of C_2, the hydraulic discharge coefficient based on the downstream static pressure, with the approach factor not included]

$$C_2=C_1\sqrt{\frac{1}{1-x}}$$

β=	0.0	0.2	0.3	0.4	0.5	0.55	0.6
r=							
1.00	0.597	0.597	0.598	0.600	0.604	0.608	0.611
.95	.606	.606	.607	.609	.613	.616	.620
.90	.616	.616	.617	.619	.622	.625	.628
.85	.626	.626	.627	.629	.632	.634	.637
.80	.637	.637	.637	.639	.642	.644	-------
.75	.648	.648	.648	.650	.653	-------	-------
.70	.660	.660	.660	.661	-------	-------	-------
.65	.673	.673	.673	.674	-------	-------	-------
.60	.688	.688	.688	-------	-------	-------	-------
.55	.704	.704	-------	-------	-------	-------	-------
.50	.722	.722	-------	-------	-------	-------	-------

TABLE 12.—*Flange taps*

[Values of C'_1, the hydraulic discharge coefficient based on the upstream static pressure, with the approach factor included]

$$C'_1=C_1/\sqrt{1-\beta^4}$$

β=	0.0	0.2	0.3	0.4	0.5	0.55	0.6
r=							
1.00	0.597	0.598	0.600	0.608	0.624	0.637	0.655
.95	.591	.592	.594	.602	.617	.630	.647
.90	.584	.585	.587	.595	.610	.622	.639
.85	.577	.578	.580	.587	.602	.614	.630
.80	.569	.570	.572	.579	.593	.604	-------
.75	.561	.562	.564	.570	.584	-------	-------
.70	.552	.553	.555	.561	-------	-------	-------
.65	.543	.543	.545	.551	-------	-------	-------
.60	.533	.533	.535	-------	-------	-------	-------
.55	.522	.522	-------	-------	-------	-------	-------
.50	.511	.511	-------	-------	-------	-------	-------

TABLE 13.—*Flange taps*

[Values of C'_2, the hydraulic discharge coefficient based on the downstream static pressure, with the approach factor included]

$$C'_2 = C_2/\sqrt{1-\beta^4}$$

β=	0.0	0.2	0.3	0.4	0.5	0.55	0.6
r=							
1.00	0.597	0.598	0.600	0.608	0.624	0.637	0.655
.95	.606	.607	.610	.617	.633	.647	.664
.90	.616	.617	.619	.627	.643	.656	.674
.85	.626	.627	.629	.637	.653	.666	.683
.80	.637	.637	.640	.647	.663	.676	----
.75	.648	.649	.651	.658	.674	----	----
.70	.660	.661	.663	.670	----	----	----
.65	.673	.674	.676	.683	----	----	----
.60	.688	.688	.691	----	----	----	----
.55	.704	.704	----	----	----	----	----
.50	.722	.723	----	----	----	----	----

TABLE 14.—*Flange taps*

[Values of C_m, the mean hydraulic discharge coefficient, with the approach factor not included]

$$C_m = C_1\sqrt{\frac{2}{2-x}}$$

β=	0.0	0.2	0.3	0.4	0.5	0.55	0.60
r=							
1.00	0.597	0.597	0.598	0.600	0.604	0.607	0.611
.95	.599	.599	.599	.601	.605	.608	.612
.90	.600	.600	.600	.602	.606	.609	.612
.85	.600	.600	.601	.602	.606	.608	.611
.80	.600	.600	.601	.602	.605	.607	----
.75	.600	.600	.600	.602	.604	----	----
.70	.599	.599	.599	.600	----	----	----
.65	.597	.598	.598	.598	----	----	----
.60	.595	.595	.596	----	----	----	----
.55	.593	.593	----	----	----	----	----
.50	.590	.590	----	----	----	----	----

Tables of C'_m and C_a may readily be computed by means of equations (37, 34, 35, 36), but since these two forms of the coefficient are not in common use they may be omitted. The table for C_m is given in order to call attention again to the advantage of this quantity. Values of C'_m would have the same property of approximate independence of the pressure ratio for orifices of any one diameter ratio.

Equation (37) satisfies the condition of reducing to identity with (30) when $\beta=0$. Like (30), it is a purely empirical representation of the observed facts, and it does not lay claim to validity outside the limits shown by the tables, although it does, in fact, represent such observations as were made outside these limits with about the same accuracy as equation (30) for the throat tap combination.

Figure 5, for $\beta=0$, is applicable to flange taps, as already remarked. The curves for $\beta=0.5$ would be very like those of Figure 6, and since the information they would convey is all contained in the tables it seems unnecessary to give them.

XVII. COMMENTS ON THE RESULTS FOR FLANGE TAPS

Much the same comments may be made here as in Section XV with regard to throat taps. Equation (37) represents the average results obtained from orifices installed in the 6 and 8 inch pipes, but the values of C_1 for individual orifices departed from the mean in the same way and by about the same amounts as when the differentials were measured between the throat taps.

The 4-inch plates likewise behaved as described in Section XV. One of them agreed with the equation, but the others gave values of C_1 from 0.3 to 3.2 per cent higher than computed from (37), the average excess being about 1.3 per cent.

In one respect the results for flange taps differ from those for throat taps. This difference is shown by Figure 8, in which F is the limiting curve $C_1 = f(\beta^2)$ for $x = 0$ and for flange taps, while T, repeated from Figure 7, is the corresponding curve for throat taps.

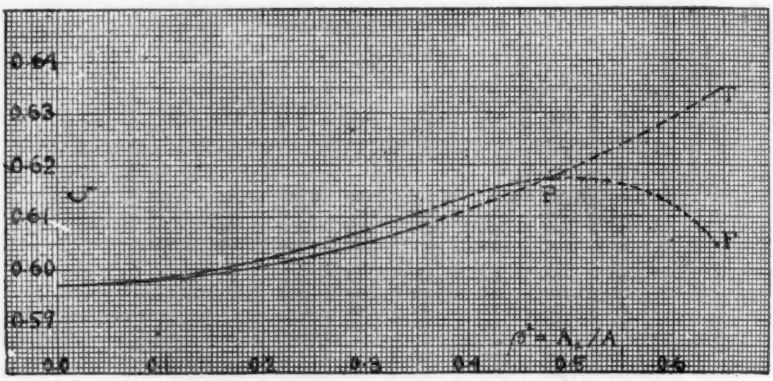

FIG. 8.—*Limiting values of C_1 at low differentials for throat taps (T) and flange taps (F)*

As β increases from very small values, where both arrangements of taps give the same differential, C_1 increases more rapidly for flange than for throat taps, as indicated by the term $0.12\beta^4$ in (37) compared with $0.09\beta^4$ in (30). The pressure is a little higher near the plate than it is one-half pipe diameter downstream, so that the differential is lower and the discharge coefficient higher, and this difference increases with β, up to about $\beta = 0.6$ or $\beta^2 = 0.36$.

But as β increases, the downstream minimum of pressure moves up toward the plate and the pressure at the flange tap falls, relatively to that at the throat tap. The effect of this is that as β continues to increase, the difference between the differentials measured in the two ways increases less rapidly, reaches a maximum, and then falls off, the two values of C_1 approaching each other. At some point,

indicated by P in Figure 8, the curves cross, and thereafter the discharge coefficient is lower for flange than for throat taps.

Assuming that the equations (30) and (37) from which the curves are drawn remain valid for $\beta > 0.6$, and that the dotted portions of the curves are approximately correct, the crossing occurs at about $\beta^2 = 0.475$ or $\beta = 0.69$. For still higher diameter ratios, the value of C_1 for the flange taps decreases and, as shown by our experiments, it is lower at $\beta = 0.79$ than at $\beta = 0.70$, and still lower at $\beta = 0.83$.

These peculiarities of the curve for flange taps are sufficiently well represented by the inclusion of the term $-0.6\beta^{12}$ in (37). More extensive and more accurate experiments would doubtless permit of improving the empirical equations for both flange and throat taps, but the present forms of (30) and (37) seem to be as good as the observations they purport to represent.

XVIII. RESULTS FOR PIPE TAPS

Pipe taps are, by definition, placed 2.5 pipe diameters upstream and 8 pipe diameters downstream from the orifice plate.

Our average results for orifices in the 6 and 8 inch pipes may be represented by the equation

$$C_1 = 0.5970 + 0.006\beta + 0.54\beta^{2.3} + \beta^3 x^2 - 0.115(x + x^2)(1 + 11\beta^3) \quad (39)$$

in which

$$x = \frac{p_1 - p_2}{p_1} = 1 - r \quad (40)$$

Values of C_1 computed from (39) are given in Table 15 and the corresponding values of C_2, C'_1, and C'_2 in Tables 16, 17, and 18.

TABLE 15.—*Pipe taps*

[Values of C_1, the hydraulic discharge coefficient based on the upstream static pressure, with the approach factor not included.]

$C_1 = 0.5970 + 0.006\beta + 0.54\beta^{2.3} + \beta^3 x^2 - 0.115(x + x^2)(1 + 11\beta^3)$

β=	0.0	0.1	0.2	0.3	0.35	0.4	0.45	0.5	0.55	0.6
r=										
1.00	0.597	0.600	0.612	0.633	0.647	0.665	0.686	0.710	0.737	0.767
.95	.591	.594	.605	.625	.639	.655	.674	.696	.720	.748
.90	.584	.588	.598	.617	.629	.645	.661	.681	.703	.727
.85	.577	.580	.590	.608	.619	.633	.648	.665	.684	
.80	.569	.572	.582	.598	.608	.621	.634	.649	.665	
.75	.561	.564	.573	.588	.597	.608	.619	.632		
.70	.552	.555	.563	.577	.585	.594	.604			
.65	.543	.545	.553	.565	.573	.580				
.60	.533	.535	.543	.553	.559					
.55	.522	.525	.532	.541						
.50	.511	.513	.520							

TABLE 16.—*Pipe taps*

[Values of C_2, the hydraulic discharge coefficient based on the downstream static pressure, with the approach factor not included]

$$C_2 = C_1\sqrt{\frac{1}{1-\tau}}$$

β=	0.0	0.1	0.2	0.3	0.35	0.4	0.45	0.5	0.55	0.6
τ=										
1.00	0.597	0.600	0.612	0.633	0.647	0.665	0.686	0.710	0.737	0.767
.95	.606	.610	.621	.641	.655	.672	.691	.714	.739	.767
.90	.616	.619	.630	.650	.663	.679	.697	.718	.741	.766
.85	.626	.629	.640	.659	.672	.686	.703	.722	.743	------
.80	.637	.640	.650	.669	.680	.694	.709	.726	.744	------
.75	.648	.651	.662	.679	.690	.702	.715	------	------	------
.70	.660	.663	.674	.690	.700	.710	.722	------	------	------
.65	.673	.677	.686	.701	.710	.720	------	------	------	------
.60	.688	.691	.701	.715	.722	------	------	------	------	------
.55	.704	.707	.717	.729	------	------	------	------	------	------
.50	.722	.726	.735	------	------	------	------	------	------	------

TABLE 17.—*Pipe taps*

[Values of C'_1, the hydraulic discharge coefficient based on the upstream static pressure, with the approach factor included]

$$C'_1 = C_1/\sqrt{1-\beta^4}$$

β=	0.0	0.1	0.2	0.3	0.35	0.4	0.45	0.5	0.55	0.6
τ=										
1.00	0.597	0.600	0.612	0.635	0.652	0.674	0.700	0.733	0.765	0.822
.95	.591	.594	.605	.627	.643	.663	.688	.718	.748	.801
.90	.584	.588	.598	.619	.634	.653	.675	.703	.730	.779
.85	.577	.580	.591	.610	.624	.641	.662	.687	.711	------
.80	.569	.572	.582	.600	.613	.629	.648	.670	.691	------
.75	.561	.564	.573	.590	.602	.616	.633	.653	------	------
.70	.552	.555	.564	.579	.590	.602	.617	------	------	------
.65	.543	.546	.554	.568	.577	.588	------	------	------	------
.60	.533	.535	.543	.556	.564	------	------	------	------	------
.55	.522	.525	.532	.543	------	------	------	------	------	------
.50	.511	.513	.520	------	------	------	------	------	------	------

TABLE 18.—*Pipe taps*

[Values of C'_2, the hydraulic discharge coefficient based on the downstream static pressure, with the approach factor included]

$$C'_2 = C_2/\sqrt{1-\beta^4}$$

β=	0.0	0.1	0.2	0.3	0.35	0.4	0.45	0.5	0.55	0.6
τ=										
1.00	0.597	0.600	0.612	0.635	0.652	0.674	0.700	0.733	0.765	0.822
.95	.606	.610	.621	.644	.660	.681	.706	.737	.767	.822
.90	.616	.619	.631	.653	.668	.688	.712	.741	.769	.821
.85	.626	.629	.641	.662	.677	.695	.718	.745	.771	------
.80	.637	.640	.651	.671	.685	.703	.724	.749	.773	------
.75	.648	.651	.662	.681	.695	.711	.730	.754	------	------
.70	.660	.663	.674	.692	.705	.720	.737	------	------	------
.65	.673	.677	.687	.704	.716	.729	------	------	------	------
.60	.688	.691	.701	.717	.728	------	------	------	------	------
.55	.704	.707	.717	.732	------	------	------	------	------	------
.50	.722	.726	.736	------	------	------	------	------	------	------

Like equations (30) and (37), equation (39) is not to be regarded as valid beyond the limits of r and β for which values are given in the tables.

XIX. COMMENTS ON THE RESULTS FOR PIPE TAPS

Over the range of r and β covered by the tables, the values of C_1 for individual plates of the 6 and 8 inch sizes departed from the mean values, represented by the empirical equation (39), in the same way as was found to occur with throat and flange taps, though the departures were, if anything, not quite so large.

With the exception already noted, the 4-inch plates gave systematically higher values of C_1 than those computed from (39).

If we exclude from consideration two further plates on which only a very few observations were made, there remain nine of the 4-inch plates having diameter ratios from 0.1992 to 0.6125. For these plates the excess of C_1 over the value computed from (39) ranged from 0.4 per cent to 1.9 per cent, with a mean of 1.1 per cent. For the same set of plates the corresponding figures for throat taps are 0.5 to 2.7, mean 1.4; and for flange taps they are 0.3 to 2.3, mean 1.1.

The figure for any one plate is, of course, an average from the separate values obtained with that plate; and since the observations were seldom numerous enough to determine a curve for a single plate with any great precision, the figures just given for the individual plates must be regarded as uncertain by at least ± 0.3 per cent.

XX. COMPARISON OF THE THREE SETS OF RESULTS

Since the equations which have been devised for representing our results are purely empirical, they might, of course, be somewhat varied, or possibly replaced by others of quite different appearance. But such other equations would have to represent the same facts by giving approximately the same numerical values of C_1 over the specified ranges of r and β, and the equations as they stand provide adequate means for comparing the three kinds of result.

For convenience of comparison, the equations may be reproduced here in the following forms:

For throat taps (30)

$$C_1 = 0.5970 + 0.09\beta^4[-0.115(x+x^2)(1+1.5\beta^4)] \qquad (41)$$

For flange taps (37)

$$C_1 = 0.5970 + 0.09\beta^4 + 0.03\beta^4 - 0.6\beta^{12}[-0.115(x+x^2)(1+1.5\beta^4)] \qquad (42)$$

For pipe taps (39)

$$C_1 = 0.5970 + 0.006\beta + 0.54\beta^{2.3}[-0.115\ (x+x^2)(1+11\beta^3) + \beta^3 x^2] \qquad (43)$$

In each case the terms involving x have been placed within the square brackets [ ], and since these terms vanish when $x=0$, the earlier terms alone give the limiting form of the equation for very low percentage differentials.

The terms within the [ ] represent the changes of C_1, with increasing x, for any fixed value of β. Their presence is necessitated by the fact that the air expands as its pressure falls. If there were no such expansion, these terms would be absent, and the earlier terms therefore, represent, according to an extrapolation from our experimental results, what is to be expected for water—always on the supposition that the effects of viscosity do not become appreciable.

In the limiting case of very small diameter ratios, and therefore negligible speed of flow at all points not close to the orifice, the three equations degenerate into the single form

$$C_1=0.5970-0.115\ (x+x^2) \tag{44}$$

thus satisfying the conditions mentioned in Section XIII.

Equations (41) and (42) are much alike. Of the two additional terms $+0.03\beta^4$ and $-0.6\beta^{12}$, which appear in (43), the first represents the fact that as β increases from very small values the differential between the flange taps is, at first, less than between the throat taps. The second term, which ultimately more than offsets the first, represents the effect of the displacement of the downstream pressure minimum toward the orifice. This displacement is slow and of little importance, so long as β is small, but has a marked influence later on, as was illustrated in Figure 8.

In contrast with (41) and (42), equation (43) is of a very different and more complicated form. This difference reflects the different physical nature and greater complexity of the phenomena which determine the differential when the region in question extends far enough downstream to include the zone of maximum restoration of pressure, instead of stopping at a section 0.5 pipe diameter from the orifice, or approximately at the minimum of static pressure.

In defining the discharge coefficient of an orifice for a liquid we make use, first, of the conception of a "theoretical" jet speed which would occur if the whole observed fall of pressure were due to, or were used up in producing, acceleration of the fluid. In practice, there is very little dissipative resistance, as far as the vena contracta, and the speed of the jet there is nearly equal to the theoretical speed which would be computed from the fall of pressure between the undisturbed stream ahead of the orifice and the vena contracta.

If the theoretical rate of discharge could then be computed from the cross section of the vena contracta, it would agree very closely with the actual discharge, and the discharge coefficient would be nearly unity, as it is for a well-made flow nozzle or Venturi. In practice, the computation has to be made with the area of the orifice

because the cross section of the vena contracta is unknown, and the computed rate of discharge is correspondingly increased. And if the differential used in the computation is the true fall of static pressure from the undisturbed stream ahead of the orifice to the vena contracta, the discharge coefficient obtained will be very nearly identical with the contraction coefficient, defined as the ratio of the cross sectional area of the jet at the vena contracta to the area of the orifice.

In a cylindrical jet the static pressure must be uniform over any section and equal to the pressure just outside. So long as the diameter ratio is not large and the vena contracta is still at some distance from the orifice, the profile of the jet in the vicinity of the vena contracta is not sharply curved, and the relation just mentioned must be approximately true.

In practice, the downstream static pressure is observed at the wall of the pipe and not in, or just outside, the vena contracta. But visual observations with glass pipes [11] have shown that the minimum of pressure at the wall occurs at the same section of the pipe as the vena contracta, and it has commonly been assumed that this minimum pressure is equal to the static pressure in the vena contracta. While this can hardly be very accurately true, it seems probable that it is nearly so for diameter ratios not greater than $\beta = 0.6$; and in the absence of further evidence the assumption may be accepted as nearly true.

From this it follows that if the downstream tap is placed at the point of minimum pressure or maximum differential the discharge coefficient obtained is very nearly equal to the contraction coefficient. And since the minimum pressure is sensibly the same as the pressure at the downstream throat tap, so long as $\beta < 0.6$, we may regard the discharge coefficient with approach factor not included, obtained from observations with throat taps, as a fairly accurate representation of the contraction coefficient.

Except for the disturbing effects of viscosity, which are usually small in practice, the profile of a jet of liquid from a round, square-edged orifice is independent of the speed; the contraction coefficient remains constant; and the discharge coefficient is independent of the magnitude of the differential. But with a gas the phenomena are somewhat different.

Since the static pressure of the jet does not fall to its lowest value until the vena contracta is reached, it is higher in the converging part of the jet between the orifice and the vena contracta than the pressure in the surrounding space. This transverse gradient of pressure causes the gas to expand laterally, as well as forward, with

[11] Experiments by E. G. Bailey, Report of the Special Research Committee on Fluid Meters of the American Society of Mechanical Engineers, 2d ed., pp. 34, 35; 1927.

the result that the section of the vena contracta is larger than it would be for a nonexpanding liquid, and the difference increases as the percentage differential increases.

The effect of this change in the contraction coefficient is clearly shown by the increase of the "adiabatic" discharge coefficient C_a. Except for the ignoring of contraction, the assumptions on which the theoretical "adiabatic" rate of flow is computed corresponds very closely to reality; and if the downstream tap is so placed as to give the static pressure of the jet in the vena contracta, the value obtained for C_a is nearly identical with the contraction coefficient. The curves marked C_a, in Figures 5 and 6, therefore, show approximately how the section of the vena contracta increases relatively to the area of the orifice as the percentage differential increases and the difference of behavior between air and water becomes more and more pronounced.

Turning, now, to the consideration of the pipe tap arrangement, we find a different state of affairs. The assumption that the frictional resistances are negligible, and that changes of static pressure represent changes in speed, is nearly true for the region included between the throat taps; but when extended to the whole region between the pipe taps it becomes totally false, and the bodily transfer of the algebra developed for throat taps to the case of pipe taps, while perfectly legitimate and justifiable on the score of expediency, does not represent any physical reality.

The differential between the pipe taps is merely the over-all loss of static pressure between the two taps, due to dissipative resistance. With a liquid, and supposing the diameter of the pipe to be the same at both taps, there is, on the whole, no acceleration at all and no appreciable change of kinetic energy. And in the case of a gas there is only the—usually quite insignificant—increase of linear speed due to the fact that the density falls with the pressure, and that the product of speed and density must remain constant if the flow is to be steady. The orifice plate interposed between the two taps acts merely as an obstruction which introduces a large resistance and so concentrates a pressure drop great enough for convenient measurement within a short length of pipe—10½ pipe diameters if the taps are in the standard positions.

When the diameter ratio is very small, the kinetic energy of the jet is all dissipated, there is no restoration of pressure, and it is appropriate to regard the orifice as a device for forcibly accelerating the fluid. But when the diameter ratio is large and there is a considerable restoration of pressure, the differential between the pipe taps represents dissipative or frictional resistance and not kinetic resistance to acceleration, except in the sense that if there had been no acceleration anywhere there would have been no increase

of kinetic energy to be dissipated. Hence, it is more natural and in closer accordance with the physical facts to regard an orifice plate of large diameter ratio merely as a ridge projecting inward from the wall of the pipe and introduced for the sake of increasing the resistance of the pipe to flow along it.

There is thus a gradual change of the nature of the phenomena which occur between the orifice and a point eight pipe diameters downstream, as β increases. The discharge coefficient is not susceptible of the same simple interpretation for pipe as for throat or flange taps, and a more complicated and quite different form of equation is required to represent the manner in which it depends upon the diameter ratio and pressure ratio.

XXI. SPECIMENS OF THE EXPERIMENTAL RESULTS

Several matters which deserve mention may best be elucidated by comparing the values of C_1 obtained from the observations on particular orifices with the values given by the empirical equation. For this purpose, data for four of the orifices and for throat taps are presented in Tables 19 to 22, which are all arranged in the same way.

The values of C_1 determined by the observations are listed in column 4, in the order of increasing values of x as shown in column 3.

For each orifice a curve

$$C_1 = f(x) \ (\beta \text{ constant}) \tag{45}$$

was drawn to represent equation (30) with the given β; and for each of the observed values of x in column 3 the value of C_1 was read off. This value, denoted by C_1 (calc.), was then subtracted from the observed value C_1 (obs.), and the difference

$$C_1(\text{obs.}) - C_1(\text{calc.}) = \delta \tag{46}$$

listed in column 5, is the amount by which each observed point is above the curve, or the excess of the observed over the computed value of C_1. The combined errors of drawing the curve and reading from it may sometimes have amounted to ± 5 in the last figure given, but the values of δ are quite accurate enough for our present purpose.

Each table is divided into two parts, of which the first contains the values of C_1(obs.) and δ for $x < 0.02$ and the second all the remaining values. The mean values of δ for the two parts are shown separately, and the general mean is given at the foot of column 5.

TABLE 19.—*Plate No. 1–6 (Foxboro Company)*

[D=5.785 ins.; d=0.6265 ins.; β=0.1083; throat taps]

Flow nozzle used	Initial pressure p_1 lbs./in.²	$\frac{p_1-p_2}{p_1}=x$	C_1 (obs.)	C_1 (obs.) $-C_1$(calc.) $=\delta$	$\delta-0.0018$	$\delta-0.0009$
1	2	3	4	5	6	7
D-1	207.9	0.0151	0.5814	−0.0140	−0.0158	
D-1	86.7	.0180	.6185	+.0234	+.0216	
				+.0047	±.0187	
D-1	139.1	.0522	.5764	−.0144	−.0162	−0.0153
A-2	225.6	.0594	.5826	−.0073	−.0091	−.0082
D-1	16.1	.0864	.5963	+.0100	+.0082	+.0091
D-1	89.3	.1062	.5958	+.0122	+.0104	+.0113
D-1	18.4	.1718	.5806	+.0066	+.0048	+.0057
D-1	20.7	.2877	.5586	+.0041	+.0023	+.0032
A-2	24.2	.3842	.5312	−.0046	−.0064	−.0055
A-2	39.6	(.6100)	(.4862)	(+.0022)		
A-2	64.7	(.7340)	(.4638)	(+.0153)		
General means				+.0009	±.0095	±.0083
				+.0018	±.0098	

We may first examine Table 19, which refers to the smallest of all the orifices tested. The observations are spread over a very wide range of x, but we shall ignore the last two values of C_1 because the values of x at which they were obtained are outside the range for which the empirical equation was developed and over which we regard it as safely applicable.

The general mean at the foot of column 5 shows that, on the average, the values of C_1 found for this orifice were higher than the computed values by about 0.0018 or 0.3 per cent.

Column 6 gives the departures of the individual values of δ from their general mean. The mean of these departures, taken without regard to sign, is ± 0.0098, and this figure may be regarded as a rough measure of the internal inconsistencies of the series.

Column 7 contains the corresponding values for $x>0.02$.

Judged by the criterion of internal consistency, this series is one of our worst, and if there had been none better our results would not have been worth much.

Table 20 contains similar, but more numerous, data for an orifice of diameter ratio $\beta=0.2778$. The last value of C_1 is disregarded for reasons stated above. The general mean at the foot of column 5 shows that, on the average, the values of C_1 for this orifice were lower than the values from equation (30) by about 0.0024 or 0.5 per cent.

The mean departure from the general mean is ± 0.0041 (foot of column 6), so that this series is much more consistent with itself than the series in Table 19.

TABLE 20.—*Plate No. 5–8 (Bureau of Standards)*

[D=7.634 ins.; d=2.121 ins.; β=0.2778; throat taps]

Flow nozzle used	Initial pressure p_1 lb./in.²	$\frac{p_1-p_2}{p_1}=x$	C_1 (obs.)	C_1(obs.) $-C_1$ (calc.) $=\delta$	$\delta+0.0024$	$\delta+0.0027$
1	2	3	4	5	6	7
B-2	222.7	0.0057	0.5947	−0.0026	−0.0002	
A-2	112.0	.0059	.5936	−.0037	−.0013	
A-2	89.2	.0088	.5896	−.0074	−.0050	
A-2	49.1	.0093	.5889	−.0080	−.0056	
B-2	128.4	.0106	.5961	−.0006	+.0018	
A-2	50.9	.0113	.6002	+.0036	+.0060	
D-1	15.0	.0117	.6034	+.0068	+.0092	
B-2	142.3	.0150	.5920	−.0042	−.0018	
				−.0020	±.0039	
C-2	90.9	.0624	.5845	−.0055	−.0031	−0.0028
C-2	48.9	.0757	.5810	−.0073	−.0049	−.0046
A-2	16.0	.0771	.5926	+.0046	+.0070	+.0073
A-2	16.6	.1136	.5833	+.0003	+.0027	+.0030
C-2	47.8	.1722	.5642	−.0098	−.0074	−.0071
A-2	18.5	.1977	.5673	−.0026	−.0002	+.0001
A-2	20.6	.2664	.5601	+.0018	+.0042	+.0045
C-2	48.0	.2742	.5455	−.0114	−.0090	−.0087
B-2	21.6	.3208	.5482	−.0002	+.0022	+.0025
B-2	23.5	.3732	.5386	+.0002	+.0026	+.0029
B-2	26.8	.4438	.5240	+.0007	+.0031	+.0034
B-2	37.3	(.5510)	(.4923)	(−.0061)		
				−.0027	±.0042	±.0043
General means				−.0024	±.0041	

TABLE 21.—*Plate No. 5–6 (Bureau of Standards)*

[D=5.785 ins.; d=1.997 ins.; β=0.3452; throat taps]

Flow nozzle used	Initial pressure p_1 lbs./in.²	$\frac{p_1-p_2}{p_1}=x$	C_1 (obs.)	C_1 (obs.) $-C_1$ (calc.) $=\delta$	$\delta-0.0009$
1	2	3	4	5	6
A-2	213.8	0.0016	0.5864	−0.0117	−0.0126
A-2	209.5	.0026	.5985	−.0021	−.0030
D-1	15.0	.0036	.6159	+.0181	+.0172
D-1	49.9	.0043	.6008	+.0032	+.0023
B-2	213.9	.0073	.5892	−.0082	−.0091
B-2	219.5	.0074	.5952	−.0022	−.0031
D-1	15.0	.0090	.6062	+.0091	+.0082
A-2	88.9	.0108	.5978	+.0008	−.0001
				+.0009	±.0009
B-2	132.1	.0225	(.6326)	(+.0371)	
D-1	16.6	.0250	.5968	+.0015	+.0006
A-2	49.2	.0251	.5947	−.0006	−.0015
D-1	17.4	.0298	.5968	+.0022	+.0013
C-1	84.2	.0401	.5940	+.0006	−.0003
D-1	19.8	.0484	.5888	−.0035	−.0044
A-2	45.6	.0641	.5920	+.0017	+.0008
A-2	21.3	.0665	.5917	+.0018	+.0009
A-2	23.6	.0780	.5903	+.0019	+.0010
C-1	87.5	.0871	.5872	+.0006	−.0003
A-2	28.3	.0923	.5855	−.0009	−.0018
A-2	30.1	.0961	.5853	−.0006	−.0015
A-2	32.7	.1015	.5867	+.0016	+.0007
A-2	34.9	.1051	.5874	+.0022	+.0013
C-2	49.3	.1158	.5859	+.0018	+.0009
B-2	50.0	.1316	.5831	+.0024	+.0015
C-2	49.5	.1752	.5744	+.0002	−.0007
B-2	27.3	.2382	.5642	+.0007	−.0002
C-2	47.2	.2428	.5647	+.0020	+.0011
B-2	30.4	.2578	.5608	+.0007	−.0002
				+.0009	±.0011
General means				+.0009	±.0028

Table 21 contains the data for an orifice of diameter ratio $\beta = 0.3452$. One of the values of C_1 is far out of line with the others and gives a very large δ. We regard this large departure from the mean (+0.0371) as representing a mistake rather than an error, and we omit it from the average. In a few other similar cases we have likewise had no scruples in ignoring isolated points which departed from the general run by several times the average departure of the rest of the points.

The general mean at the foot of column 5 shows that the values of C_1 for this orifice averaged about 0.0009, or something less than 0.2 per cent, higher than the computed values. The mean departure from the mean δ is ± 0.0028 (foot of column 6). This series is one of the very best.

TABLE 22.—*Plate No. 11–6 (Foxboro Company)*

[D=5.785 ins.; d=3.500 ins.; β=0.6050; throat taps]

Flow nozzle used	Initial pressure p_1 lbs./in.²	$\frac{p_1-p_2}{p_1}=x$	C_1 (obs.)	C_1 (obs.) $-C_1$ (calc.) $=\delta$	$\delta-0.0026$	$\delta-0.0011$
1	2	3	4	5	6	7
A–2	49.4	0.0015	0.6148	+0.0059	+0.0033	
C–1	88.6	.0061	.6088	+.0005	−.0021	
A–2	15.1	.0090	.6135	+.0066	+.0040	
C–1	48.8	.0196	.6075	+.0010	−.0016	
				+.0035	±.0027	
B–2	17.4	.0810	.5980	+.0007	−.0019	−0.0006
C–2	18.3	.1110	.5925	+.0002	−.0024	−.0011
C–2	19.5	.1262	.5926	+.0030	+.0004	+.0017
				+.0013	±.0016	±.0011
General means				+.0026	±.0022	

Table 22 contains the data for an orifice of diameter ratio $\beta = 0.605$. The observations cover only a short range of x because it was impossible to reach high differentials with so large an orifice. They are so few in number that averages have little significance, but, judged by the criterion already employed, this is one of the good series. The values of C_1 are, on the whole, about 0.0026, or 0.5 per cent, higher than the computed values.

XXII. COMMENTS ON THE DATA IN TABLES 19 TO 22

For convenience of comparison, some of the mean values from Tables 19 to 22 are brought together in Table 23, which may now be examined.

TABLE 23.—*Summary of values from Tables 19 to 22*

		Table—			
		19	20	21	22
1	Serial number of plate	1–6	5–8	5–6	11–6
2	Diameter ratio, β	0.1083	0.2778	0.3452	0.6050
3	Number of points for $x<0.02$	2	8	8	4
4	Number of points for $x>0.02$	7	11	19	3
5	Mean δ for all points	+.0018	−.0024	+.0009	+.0026
6	Mean δ for $x<0.02$	+.0047	−.0020	+.0009	+.0035
7	Line 6–line 5	+.0029	+.0004	.0000	+.0009
8	Mean δ for $x>0.02$	+.0009	−.0027	+.0009	+.0013
9	Line 8–line 5	−.0009	−.0003	.0000	−.0013
10	Mean scattering for all points	±.0098	±.0041	±.0028	±.0022
11	Mean scattering for $x<0.02$	±.0187	±.0039	±.0069	±.0027
12	Mean scattering for $x>0.02$	±.0095	±.0042	±.0011	±.0016

1. MEAN VALUES OF δ

For each orifice let the curve $C_1=f(x)$ be constructed from equation (30) with the appropriate value of β. Let this curve be raised by the amount shown in line 5 of Table 23, and let the new curve be called "the adjusted curve" for the orifice in question. If points representing the observed values of C_1 are also plotted, they will obviously be, on the average, as much above as below the adjusted curve.

Line 7 shows the average amount by which the observed points are above the adjusted curve for those experiments in which $x<0.02$; that is, in which the downstream static pressure was more than 98 per cent of the upstream pressure. For plate No. 5–6, the best of the series here presented, the mean point for $x<0.02$ lies on the adjusted curve, while for the other three plates it lies higher; but this does not indicate a general rule. For when all the orifices are taken into account the differences corresponding to those in line 7 come out negative about as often as positive, and the mean point for $x<0.02$ is sometimes above and sometimes below the adjusted curve, with no marked preponderance of either direction.

For $x>0.02$ the mean departure of the observed points from the adjusted curve is, of course, of the opposite sign to that for $x<0.02$, as is illustrated by a comparison of lines 9 and 7.

2. SCATTERING OF OBSERVED POINTS

The average distance of a series of points from the adjusted curve, taken without regard to sign, may be called their "mean scattering." As remarked in section 21, this quantity, shown in line 10, may be taken as a rough measure of the "badness" of the series.

If, as before, we treat the two groups of points separately (lines 11 and 12), we find that in three of the four cases the mean scattering

was much greater for $x<0.02$ than for $x>0.02$, though in the fourth case the two were sensibly equal. This does illustrate a rule to which there were few exceptions. In nearly all series which included several points near $x=0$—that is, near $r=1$—these points were much more scattered than points farther out.

XXIII. DISCUSSION OF THE ACCIDENTAL ERRORS

The greater scattering of the values of C_1 obtained from experiments at low values of x might naturally, at first sight, be attributed to the greater percentage errors in reading low differentials; but this explanation is fallacious, for, in the first place, the absolute static pressures varied in the ratio of 15 to 1 and a low value of x did not always mean a low absolute value of the differential.

But there is a more striking piece of evidence. Each reading of the differential between the throat taps was accompanied by readings between the flange and between the pipe taps, all within a short space of time and as nearly as possible under the same working conditions. The accidental errors of the three readings can not have been systematically related, but the three values of C_1 varied together, a high value of C_1 for throat taps being accompanied by high values for the other two combinations, and vice versa.

This parallelism was, of course, not perfect, because the accidental errors of reading the differential gauge were not entirely inappreciable. But for the orifices of the lower diameter ratios the resulting accidental errors in C_1 were of the order of only 0.1 or 0.2 per cent; and the agreement of the three sets of values of C_1, as regards their variations from one experiment to another, proved conclusively that these simultaneous variations were not due to errors of the readings at the orifice but to some other cause which affected all three values of C_1 in the same way.

Three possible explanations suggest themselves—the discharge coefficient may depend on the absolute static pressure, to which no attention has hitherto been given; or the discharge coefficients of the flow nozzles may have been incorrectly determined; or the observations at the flow nozzle may have been affected by large errors. (*a*) If the discharge coefficient of an orifice depended on the absolute static pressure at which the experiment was made, this influence would be revealed by intercomparing all the values of C_1 obtained with the same flow nozzle, and the value of δ would vary systematically with the initial pressure p_1.

Particular series may be picked out where this appears to be the case, especially at low values of x; but in general the hypothesis is not substantiated, and the whole mass of observations indicates that within the range of static pressures covered in these experiments the discharge coefficient of an orifice depends only on the ratio of the two

pressures and is sensibly independent of their absolute values. It would, indeed, be very surprising if any effect of the absolute pressure were observed with a gas so nearly ideal as air.

(*b*) Each of the orifices referred to in Tables 19 to 22 was tested with two or more flow nozzles, and the same was true of nearly all the orifices. If the discharge coefficients of the nozzles had been incorrectly determined relatively to one another, the values of δ would have varied with changes from one nozzle to another, some nozzles giving systematically high values of C_1 and others systematically low values.

Series of values of C_1 for particular orifices may be found which seem to show evidence of this, but here, again, the idea is not confirmed by the aggregate of all the experiments and there is, on the whole, no evidence of errors in the discharge coefficients of the flow nozzles which are at all comparable in magnitude with those required to account for the actual variations in δ.

(*c*) Of the observations made at the flow nozzle, the only one subject to errors of any importance is the reading of the differential by means of the central impact tube; but this was read each time one of the differentials at the orifice upstream was read, and there can have been no systematic connection between the errors of reading the differential gauges at the orifice and at the nozzle. Furthermore, there is no reason to suppose that the errors at the nozzle were of a different order of magnitude from those at the orifice, which have already been shown to be relatively small. It therefore appears that this third explanation of the large accidental errors in C_1 can not be accepted as adequate.

(*d*) The true cause seems to have been the lack of complete steadiness in the rate of flow, due to the impossibility of holding the speed of the compressors perfectly constant or, ultimately, to variations of voltage in the power supply to the motors. There was a large capacity between even the 8-inch orifice station and the flow nozzle, and when the air supply varied there must evidently have been a time lag between the orifices and the nozzle, so that observations made simultaneously at both places did not, in reality, correspond to precisely equal rates of flow.

Any such time lag would be greater the lower the rate of discharge, and its effects on the value of C_1 computed by assuming the flow to be perfectly uniform all along the line would therefore be more likely to be large at low than at high rates of flow. With any one orifice, low rates of flow occur at low values of x. Hence, the effects of variations of compressor speed in producing variations of δ should, on the whole, be more pronounced at low values of x, and, in general, this is just what happened, as was remarked in section 22.

Furthermore, at any given pressure ratio, the absolute rate of flow is lower for small than for large orifices. Hence, if the errors

now in question are really due to the time lag, they will be most marked for the smaller orifices, and this, also, is what was actually found, as is illustrated by Tables 19 to 22, or by the summary in lines 10, 11, and 12 of Table 23.

For any given diameter ratio the orifices are smallest for the 4-inch plates and, other things being equal, the scattering might be expected to be, on the whole, greatest for the 4-inch plates which were, moreover, farthest upstream and separated from the flow nozzle by a somewhat greater capacity than the others. This expectation is also confirmed by an examination of the whole collection of values of C_1.

The voltage, compressor speed, and air supply were, of course, more unsteady at some times than at others, and the statements above are true only on the whole and not in every individual case. But it seems fair to conclude that the greater part of the unexpectedly large accidental errors of the experiments was due to the lack of a perfectly steady power supply, and that even if all our measurements had been absolutely accurate, unavoidable errors would still have been present in the results. The only mitigation of the effects of these accidental errors lies in the multiplication of experiments, by which they are, to a considerable extent, averaged out.

It seems useless to attempt any further quantitative discussion of the accuracy of our results, and the reader must be left to form his own estimate from the specimens given in Tables 19 to 22 and from the remarks which have been presented in this and the two preceding sections.

XXIV. THE EFFECTS OF VISCOSITY

Within the range of working conditions covered by our experiments, the discharge coefficients of square-edged orifices are not appreciably affected by changes in the viscosity of the fluid. The experiments were therefore not adapted to investigating such effects and did not add anything to the experimental information concerning them which has already been published by Hodgson and Daugherty.[12] Nevertheless, the subject is of such importance that it will be discussed briefly here, rather than relegated entirely to an appendix, as would otherwise be more appropriate. It will be treated somewhat further in Appendix C.

Let us suppose that a liquid of low viscosity, such as water, is flowing through an orifice, and that the discharge coefficient is determined from measurements of the differential and rate of discharge. Let the liquid then be replaced, successively, by others of greater and greater viscosity, and in each case let the discharge coefficient

[12] J. L. Hodgson, The Orifice as a Basis of Flow Measurement; Inst. Civ. Eng., Selected Engineering Papers, No. 31; 1925. R. L. Daugherty; Bulletin No. 130, Goulds Pumps (Inc.), Seneca Falls, N. Y.; 1926.

of the orifice be determined at the same volume rate of flow as in the first experiment. Sooner or later the discharge coefficient will begin to increase with the viscosity, the point where this increase first becomes evident depending on the precision of the experiments.

The first effect of increased viscosity is to retard the motion of the liquid over the upstream face of the plate toward the orifice and around the edge. The surface film creeps around the corner more slowly, and the centrifugal force urging it toward the axis of the jet is diminished. Hence, there is less tendency to contraction, the cross section of the vena contracta becomes larger, and the discharge coefficient increases.

But this action can, at most, go only so far as entirely to eliminate contraction; and meanwhile, as the viscosity increases, its retarding effect reaches farther and farther from the edge of the orifice into the jet, so that a higher and higher differential is needed to maintain the given rate of discharge. If the viscosity were increased indefinitely, the differential would evidently also have to be raised indefinitely, and the discharge coefficient would fall toward zero.

The combined result of these two opposing tendencies is that, as the viscosity is progressively increased from low values while the rate of discharge is held constant, the discharge coefficient of the orifice first increases, then passes through a maximum, and thereafter decreases.

The foregoing is an elementary physical interpretation of the observed facts as described by Hodgson and Daugherty in the papers referred to above.

In the absence of viscosity, the only forces called into play in the formation of a jet would be the inertia reactions of the liquid against acceleration, which are proportional to the density; but since no real liquid is entirely free from viscosity, viscous forces are also necessarily developed. The degree to which they modify the motion of the liquid evidently depends, not on their absolute magnitude, which is proportional to the viscosity, but on their relative magnitude in comparison with the inertia forces. Hence, in the present connection, the important characteristic property of the liquid is not simply its viscosity μ but the ratio of viscosity to density or

$$\frac{\mu}{\rho} = \nu \tag{47}$$

which is known as the "kinematic viscosity."

With a given orifice and a given liquid, the viscous resistances increase with the speed of flow, but the kinetic energy and the accompanying inertia reactions increase with the square of the speed. Hence, the influence of viscosity is greater at low than at high speeds, and lowering the rate of discharge has qualitatively the same effect on the discharge coefficient as increasing the kinematic viscosity.

Let us suppose, finally, that without altering either the liquid or the mean linear speed of the jet, experiments are made upon smaller and smaller orifices which are, together with the adjacent parts of the pipe, all geometrically similar to one another or of the same "shape," in the general sense of the term. Reducing the linear dimensions of the apparatus without reducing the linear speed of flow through it increases the transverse gradients of speed, to which the viscous forces are proportional, and the influence of viscosity is therefore greater on small than on large orifices; or reducing the size of the orifice has qualitatively the same effect as increasing the kinematic viscosity of the liquid.

The foregoing conclusions are all consistent with the proposition that for orifices of any one shape the discharge coefficient is determined by the value of the single quantity

$$R=\frac{dS}{\nu}=\frac{dS\rho}{\mu} \tag{48}$$

in which S is the mean linear speed through the orifice, computed from the known diameter d and the observed volume rate of discharge, and R is known as the "Reynolds number."

The proof of this proposition may be deferred to Appendix C, but an important inference may be drawn at once; namely, that for all orifices of any one shape there is a general relation

$$C=f(R) \tag{49}$$

which holds for all liquids, all sizes, and all rates of discharge. According to the reasoning advanced above concerning the effects of varying ν, S, and d separately, the curve representing equation (49) should be qualitatively of the form illustrated in Figure 9, and the experiments of both Hodgson and Daugherty have, in fact, given curves of this form. They show that for all large values of R the discharge coefficient of an orifice has the same sensibly constant value C_0, and that it is not measurably affected by variations of the kinematic viscosity or the rate of discharge unless these are such as to reduce R below some limiting value R_0.

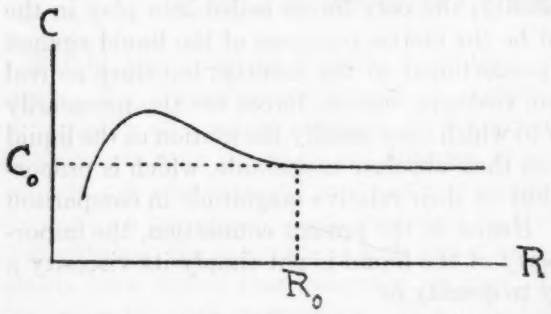

FIG. 9.—*Variation of discharge coefficient with Reynolds number*

The foregoing statements have referred specifically only to liquids, but they are equally applicable to gases when the percentage differen-

tial is small, so that the density is nearly constant; and in Hodgson's experiments the points obtained for air and for various mixtures of water and glycerine all lay indiscriminately along the same smooth curve of the form represented in Figure 9.

The precise form of the curve and the values of C_0 and R_0 depend on the "shape" of the orifice; this term being understood in the most general sense as referring not only to diameter ratio, sharpness of edge, and relative positions of the pressure taps, but to any and all other geometrical peculiarities of the orifice itself or of the channel in which it is installed, which influence the nature of the fluid motion between the two cross sections where the taps are situated. Our present interest is not, however, in the whole curve but only in the horizontal portion of it. It is safer to avoid the effects of viscosity than to attempt to make allowance for them, and what is needed is a simple criterion which will show, in any particular case which may occur in practice, whether the effects of viscosity on the discharge coefficient will be negligible or, if not, how the working conditions may be modified to make them so.

The meaning to be assigned to the term "negligible" obviously depends on the precision of the experiments, so that the value of R_0 is somewhat indefinite at best. Furthermore, the information hitherto published, though drawn from a large number of laborious and painstaking observations, is meager and somewhat conflicting, so that only very rough estimates of the value of R_0 are possible. Nevertheless, such data as are available indicate that for air at ordinary temperatures and for orifice diameter ratios between 0.2 and 0.6 the Reynolds number R will be high enough to make the effects of viscosity negligible in all commercial measurements whenever the relation

$$d^2ph > 10 \qquad (50)$$

is satisfied, d being the diameter of the orifice in inches, p the absolute static pressure in pounds per square inch, and h the differential in inches of water.

Since the process of arriving at the numerical value in (50) involves the use of the density and viscosity of air, the estimate would be different for another gas and, moreover, the value is not independent of the diameter ratio of the orifice. But in the present state of our knowledge it seems useless to attempt further refinements, and we can do no better than to regard the inequality (50) as probably a safe criterion in the commercial metering of natural or other gases which are not widely different from air as regards specific gravity and viscosity.

The condition expressed by (50) is evidently amply satisfied in the great majority of commercial measurements of gas by orifice meters,

for with an orifice of as small diameter as 0.8 inch and an absolute pressure as low as 15 lbs./in.^{2} the differential

$$h=\frac{10}{0.8^2\times 15}=1 \text{ inch}$$

will still be high enough. But in the employment of smaller orifices for the measurement of very low rates of discharge the condition might be violated; and until the subject has been further investigated it seems well to accept (50) as a warning to adopt some other method of metering in these cases, unless the orifice can be standardized under the same working conditions as are to prevail when it is used as a meter.

XXV. GEOMETRICAL SIMILARITY AND THE INFLUENCE OF PIPE DIAMETER

The values of C_1 obtained for the 4-inch plates were, on the average, about 1.5 per cent higher than those found for 6 and 8 inch plates of the same diameter ratio, and this result agrees, qualitatively, with the experience of other experimenters.

Other things being equal, reducing the diameter of the orifice lowers the Reynolds number and will ultimately increase the discharge coefficient, as explained in section 24, and some of the high values obtained with small apparatus have doubtless been due to the disturbing action of viscosity. But many experiments, including our own, have shown a dependence of discharge coefficient on pipe diameter, even when the Reynolds number was much too high to admit of this explanation of the observations.

On the other hand, the theory of dimensions [15] predicts that so long as the effects of viscosity are negligible a mere change of scale will not alter the discharge coefficient, and the validity of the theory has been confirmed experimentally in so many applications to hydro and aerodynamics that deductions from it are no longer open to any reasonable doubt.

The obvious and necessary conclusion is that when, for example, an 8-inch and a 4-inch plate of the same diameter ratio and with similarly situated pressure taps are found to have different discharge coefficients, the change of size has not altered the linear dimensions of all the essential features of the apparatus in the same ratio, but has been accompanied by more or less change of "shape," in the general sense of the term. The two installations are not quite geometrically similar, and the difference of discharge coefficients is caused by this departure from similarity and not directly by the change of absolute size.

[15] See Appendix C.

It is easy to see how this might come about. The most obvious elements of shape are diameter ratio, sharpness of edge, and relative location of pressure taps. To secure an adequate degree of similarity as regards diameter ratio and positions of the taps is a simple matter, because small changes in these elements of shape have very little effect on the discharge coefficient unless the diameter ratio is large. Similarity of edge is much more difficult to attain, as is shown by the considerable differences of behavior exhibited even by carefully made orifices of the same size, installed in identically the same way.

But these three are not the only important elements of shape. For example, it is well known that the introduction of elbows or other pipe fittings, upstream from the orifice, may change the discharge coefficient by several per cent unless the intervening length of straight pipe is sufficient to allow the disturbances produced at the fittings to die out, or unless they are suppressed by means of honeycombs or straightening vanes.

In order that two orifices of different size may be of the same "shape," in the general sense required for the application of dimensional reasoning, all geometrical features of the channel which influence the nature of the fluid motion between the two cross sections where the pressure taps are situated must be reproduced to scale when the size is altered; and in many experimental investigations this condition has not been satisfied.

One point, which becomes of increasing importance as smaller and smaller pipes are employed, is internal roughness. Experiments by Stanton [14] on pipes which were artificially roughened by internal screw threads showed that the roughening caused a considerable modification of the distribution of velocity over the cross section, the speed being diminished near the wall and increased near the axis, for any given average speed. Such an alteration in the distribution of velocity in the stream approaching an orifice would evidently diminish the contraction of the jet and raise the discharge coefficient of the orifice.

But with pipes of any given quality and in equally good condition, the smaller sizes are extremely likely to be relatively, though not absolutely, rougher than the larger ones, so that substituting a small for a large pipe has the same effect on the "shape" of the apparatus as making the large pipe absolutely rougher. It is therefore to be expected that, as a general rule, when ordinary commercial steel pipe is used, the discharge coefficients of orifices of any given diameter ratio will turn out to be highest for the smallest pipes. This is usually found to be the case; but the effect is not due to the change of absolute diameter, except insofar as this is unavoidably accompanied by a change of relative roughness.

[14] T. E. Stanton, Proc. Roy. Soc., **A85**, p. 366; 1911.

In our own experiments each orifice station was preceded by an uninterrupted run of uniform straight pipe at least 120 diameters long, which appears sufficient to eliminate the effects of disturbances produced still farther upstream. But the departure from geometrical similarity which consisted in the greater relative roughness of the 4-inch pipe remained, and it seems probable that the higher discharge coefficients found for the 4-inch plates were due to this.

Other departures from geometrical similarity may also produce an illusory impression that the discharge coefficient of an orifice depends directly on its absolute diameter. For example, in the investigation by Spitzglass [15], orifices were tested in seven sizes of pipe, from 2 to 12 inches in diameter, and the results showed a systematic increase of the discharge coefficient for any given diameter ratio as the diameter of the pipe was decreased; but the run of straight pipe ahead of the orifice was the same for all sizes—namely, 12 feet—instead of some fixed number of pipe diameters. Hence, the condition of geometrical similarity was vary far from satisfied, and no information was obtained regarding the effect of changing the absolute size by itself, but only when accompanied by a simultaneous progressive change in the shape of essential parts of the apparatus. There is no reason to doubt the correctness of the conclusions drawn concerning the effect of changing the pipe diameter in this particular form of installation. But the quantitative result can not be accepted as of general applicability, for it would quite possibly have been different if the entrance length had been 6 or 30 feet instead of 12.

From the published accounts of other investigations in which orifices have been tested in pipes of various sizes, it is often impossible to form any opinion of the degree of geometrical similarity between large and small installations, or of the nature of the departures from similarity, so that it would be useless to attempt any physical interpretation of the results obtained. As a general rule, such experiments have shown higher discharge coefficients for small than for large pipes, as happened in our own work. This is probably usually due, at least in part, to roughness, as explained above; but it may also be due to the manner of preparing the orifices. For any slight rounding off of the entrance corner—for instance, by a light finishing touch with fine emery cloth—raises the discharge coefficient, and any given degree of absolute rounding affects a small orifice more than a large one.

The only general conclusions that can safely be drawn are as follows:

(*a*) So long as the Reynolds number is large enough that viscosity may be ignored, there is no reason to suppose that a uniform change of scale of all the essential parts of the apparatus influences the discharge coefficient at all.

[15] J. M. Spitzglass, Trans. Am. Soc. Mech. Eng., 44, p. 919; 1922.

(*b*) Changes of pipe diameter are, in practice, nearly always accompanied by changes of shape which are such as to make the discharge coefficient of an orifice of given diameter ratio higher in small than in large pipes.

(*c*) The magnitude of this change with pipe diameter depends on the particular form of apparatus used, and the results of one experimenter may differ from those of another by more than the errors of experiment, because the two observers are not measuring the same thing.

(*d*) So far as we know, there are no published data on the variation of discharge coefficient with pipe diameter which can be accepted as generally valid.

XXVI. EQUATIONS FOR USE IN ORIFICE METER COMPUTATIONS

Equations (20) of Section X, in conjunction with (26) of Section XI, make it possible to compute the rate of flow of air through an orifice of known discharge coefficient from observations of the temperature, static pressure, humidity, and differential. They are suited to the purpose of defining discharge coefficients for which they were developed, but in practical computation various other forms of equation are more convenient under various circumstances. It would be impossible to give a complete list of such forms, but the sort of transformation required may be illustrated.

(*a*) It is usually desired that the rate of discharge be expressed in terms of volume, measured at some standard density or under some standard conditions.

Let ρ_s[lb./ft.^{3}] = the standard density adopted

and

V[ft.^{3}/min.] = the rate of discharge measured at ρ_s.

Then the rate in lb./sec. is

$$M = \frac{1}{60} V \rho_s \tag{51}$$

and (20,*C*) assumes the form

$$V = \frac{31.50}{\rho_s} C'_1 d^2 \sqrt{\rho_1 \Delta} \tag{52}$$

in which d is in ins.; Δ in lb./ in.^{2}; and ρ_1 in lb./ft.^{3}

(*b*) The differential is usually measured by a liquid manometer, and it is then convenient to have the equation in such form that the manometer reading may be substituted directly, without being first reduced to lb./in.^{2}

Let

σ = the specific gravity of the liquid at its actual temperature, referred to water at 60° F.;

h[ins.] = the differential as read.

With standard gravity

$$1 \text{ lb./in.}^2 = 27.706 \text{ inches of water at } 60° \text{ F.} \tag{53}$$

so that

$$\Delta[\text{lb./in.}^2] = \frac{\sigma h}{27.706} \tag{54}$$

and the factor $\sqrt{\Delta}$ in (52) is to be replaced by

$$\sqrt{\frac{\sigma h}{27.706}} = 0.1900\sqrt{\sigma h} \tag{55}$$

The resulting equation is

$$V = \frac{5.985\sqrt{\sigma}}{\rho_s} C'_1 d^2 \sqrt{\rho_1 h} \tag{56}$$

(*c*) The density ρ_1 must be computed from the pressure, temperature, and humidity, and it is convenient to embody the computation in the equation, rather than perform it separately and then substitute.

For this purpose equation (26) Section XI may be utilized. In all ordinary commercial metering air may be regarded as following Boyle's law; hence, the correction factor Y may be omitted and the equation simplified to the form

$$\rho = \frac{2.6914p(1-0.38w)}{458+t} \tag{57}$$

in which $w = \pi/p$ is the "vapor fraction"; that is, the partial pressure of the water vapor in the air, expressed as a fraction of the total pressure.

If the value of ρ_1 given by (57) is substituted in (56), the result may be written

$$V = NC'_1 d^2 \sqrt{\frac{p_1 h(1-0.38w)}{458+t}} \tag{58}$$

where

$$N = \frac{9.819\sqrt{\sigma}}{\rho_s} \tag{59}$$

If the standard density is not stated directly but specified by standard conditions, let

p_s [lbs./in.^{2}] = the standard pressure;

t_s [°F.] = the standard temperature;

and

w_s = the standard vapor fraction.

Then by (57)

$$\rho_s = \frac{2.6914p_s(1-0.38w_s)}{458+t_s} \tag{60}$$

and (59) takes the alternative form

$$N = \frac{3.648\sqrt{\sigma}(458+t_s)}{p_s(1-0.38w_s)} \tag{61}$$

The value of the factor N is fixed by the standard density or the standard conditions and the specific gravity σ of the manometer liquid. It is independent of the working conditions at the orifice, and is constant except for small variations in $\sqrt{\sigma}$ which may be caused by variations of the temperature of the manometer liquid. If this remains between 32° and 100° F., the greatest possible variation of N from its mean value is about one-fourth per cent for water and much less for mercury. Such errors are negligible in commercial metering and N may be regarded as sensibly constant. If it is desired to allow for even small variations, the most natural procedure is to use a constant value of N, computed for some fixed temperature of the manometer, and reduce the observed values of h to this temperature before substituting in (58).

(*d*) The operations by which (20, *c*) was transformed into (58) might equally well have been carried out on (20, *a*, *b*, *d*). The results can be obtained from (58) by substituting C'_2, p_2 for C'_1, p_1, or by utilizing the equations

$$C_1 = C'_1\sqrt{1-\beta^4};\ C_2 = C'_2\sqrt{1-\beta^4} \tag{62}$$

The value of N is the same in all four cases and is to be found from (59) or (61).

XXVII. NUMERICAL EXAMPLES

To illustrate the computation of N, let the standard conditions adopted for fixing the standard density be 60°F., 14.65 lb./in.^{2}, and 50 per cent saturation; and let the manometer liquid be carbon tetrachloride of specific gravity $\sigma = 1.58$.

As a preliminary to substitution in (61) it is necessary to find the value of W_s. The pressure of saturated water vapor at 60° F. is found from the steam tables to be 0.256 lb./in.^{2} Hence, for 50 per cent saturation at 60° F. and 14.65 lbs./in.^{2} the value of the vapor fraction is

$$W_s = \frac{0.256}{2\times 14.65} = 0.00874 \tag{63}$$

whence

$$1 - 0.38\ W_s = 0.9967 \tag{64}$$

Equation (61) now gives for N the value

$$N = \frac{3.648\sqrt{1.58}(458+60)}{14.65\times 0.9967} = 162.7 \tag{65}$$

and this is to be substituted in (58) or in whichever of the four equivalent equations may be best suited to the problem in hand.

Since the air must be somewhere between perfectly dry and completely saturated, equation (64) shows that, if the standard tempera-

ture is 60° F., the value of N given by (65) can not be in error by more than ± 0.33 per cent, whatever be the standard vapor fraction. If an uncertainty of this amount in V is regarded as negligible, it is therefore unnecessary to specify any standard humidity and it is sufficient to assume 50 per cent saturation. The uncertainty will be less if a lower standard temperature is adopted, because the saturation pressure of water vapor decreases with the temperature.

To illustrate further, the general equations may be applied to the measurement of air by a particular orifice meter.

Let an orifice of diameter $d=2.50$ ins. be installed in a long, straight pipe of diameter $D=6.90$ ins. and provided with flange taps, the static pressure gauge being connected to the downstream tap.

To avoid useless repetition, it will be supposed that the differential is read in inches of a liquid of specific gravity $\sigma=1.58$, and that the standard conditions for measuring V are those specified above, so that N has the value already computed and given by (65).

Under these circumstances the equation to be used for computing the rate of discharge of air through the orifice is

$$V=162.7\times 2.5^2\times C'_2\sqrt{\frac{p_2 h(1-0.38w)}{458+t}} \tag{66}$$

in which

V[ft.^{3}/min.] = the rate of discharge measured under the specified standard conditions;

p_2[lb./in.^{2}] = the absolute static pressure at the downstream pressure tap;

h [ins.] = the differential as read on a manometer containing a liquid of specific gravity $\sigma=1.58$, referred to water at 60° F.;

t[°F.] = the temperature of the air entering the orifice;

w = its vapor fraction; and

C'_2 = the hydraulic discharge coefficient, based on the downstream static pressure and with the approach factor included, for flange taps.

In applying (66) to the case of a particular measurement of flow, the values of t and h are observed directly and that of p_2 is obtained by allowing for the outside barometric pressure in the usual manner. The value of w will be discussed presently, but we may first specialize further by assuming that the following values have been observed:

$$p_2=25 \text{ lb./in.}^2;\ h=45 \text{ ins.};\ t=80° \text{ F.} \tag{67}$$

When substituted in (66), these values give

$$V=1470\ C'_2\sqrt{1-0.38w} \tag{68}$$

and the value of w is now to be considered.

The value of w depends on the humidity of the air entering the orifice, and this is seldom known, although a knowledge of the circumstances may show that the air must be nearly dry or nearly saturated. But w is almost always so small that a very rough estimate of its value is all that is needed, and it is sufficient to assume that the air is one-half saturated.

In the present example the pressure of saturated water vapor at 80° F. is 0.505 lb./in.^{2}, so that on the assumption of 50 per cent saturation the partial pressure of the water vapor is $\pi = 0.2525$. The total pressure of the air entering the orifice is by (54).

$$p_1 = p_2 + \frac{\sigma h}{27.706} \tag{69}$$

or

$$p_1 = 25 + \frac{1.58 \times 45}{27.706} = 27.57 \text{ lb./in.}^2 \tag{70}$$

Hence

$$0.38w = \frac{0.38 \times 0.2525}{27.57} = 0.0035 \tag{71}$$

and

$$\sqrt{1 - 0.38w} = 0.9982 \tag{72}$$

Since the actual humidity of the air must be between 0 and 100 per cent of saturation, this value can not be in error by more than ±0.18 per cent, and the uncertainty caused by failure to determine the humidity is insignificant.

At higher temperatures or lower static pressures the uncertainty is greater and in extreme cases it might be of some importance, but it is evident that in the great majority of commercial measurements the assumption of 50 per cent saturation is amply accurate, and that in most cases the effect of humidity on the density may be entirely ignored and the factor $\sqrt{1 - 0.38w}$ omitted from the general equation (58), of which (66) and (68) are special forms.

Retaining the value given by (72) reduces (68) to the form

$$V = 1467 C'_2 \tag{73}$$

and it remains only to insert the value of C'_2.

This value must either have been determined by an experimental standardization of the particular orifice, or it must be taken from some standard table. If the edge of the orifice is of the same quality as the average of the orifices used in our experiments, the value of C'_2 may be found from Table 13, Section XVI. The diameter ratio is

$$\beta = \frac{d}{D} = \frac{2.50}{6.90} = 0.362 \tag{74}$$

and the pressure ratio is (see equation (70))

$$r = \frac{p_2}{p_1} = \frac{25.0}{27.57} = 0.907 \tag{75}$$

whence by interpolation in the table we have $C'_2 = 0.623$ and finally, by (73).

$$V = 914 \text{ ft.}^3/\text{min.} \tag{76}$$

It may be noted here that the limiting value given by the table for $r = 1.0$ is $C'_2 = 0.605$, which differs from 0.623 by nearly 3 per cent. The change of discharge coefficient with the pressure ratio is therefore by no means negligible in this example.

XXVIII. REMARKS ON METERING OTHER GASES

For other gases than air, the developments of Section XXVI remain unchanged up to and including equation (56), but from that point onward they must be modified as regards the computation of the density ρ_1, and also of ρ_s, if this is merely specified by stating standard conditions.

If the gas in question obeys Boyle's law as approximately as air does, its specific gravity may be treated as a constant and the modifications needed in the equations are simple and obvious. But if the gas deviates far from Boyle's law as happens with some natural gasses at high pressures, the computation of density is not so simple, for it is to be remembered that ρ_1 in (56) represents the actual density of the fluid in the pipe ahead of the orifice, and this may differ seriously from the density computed by means of Boyle's law from the density at atmospheric pressure. But since the experiments which gave occasion for this paper were concerned with air only, the computations needed for gases that do not follow Boyle's law need not be discussed further here.

As regards numerical values of the discharge coefficients of orifices, it may be said that the limiting values for $r = 1$ will be the same for all gases.[16] For lower values of r—that is, for higher percentage differentials—it is probable that the discharge coefficient will be found to vary slightly with the properties of the gas, especially with its specific heat ratio. It does not, however, seem likely that these variations will be of any importance so long as the pressure ratio is not lower than $r = 0.9$. Further experimental data on this subject are to be desired.

XXIX. SUMMARY OF CONCLUSIONS

Aside from the tables of discharge coefficients which have been given in Sections XIV, XVI, and XVIII, and constitute the quantitative results of the investigation, the following points may be noted:

(*a*) The discharge coefficient of an oriffice for air does not depend on or vary with the absolute static pressure.

[16] See, however, Section XXIV.

(*b*) The hydraulic discharge coefficient based on either upstream or downstream static pressure is not a constant but varies with the ratio of the two pressures. At low static pressures and high differentials these variations may be of serious importance and ignoring them may lead to errors of several per cent in the computed rate of flow. This difficulty may be avoided by using a discharge coefficient based on the mean of the two static pressures.

(*c*) Very slight changes in the condition of the edge of an orifice may have an appreciable effect on its discharge coefficient; and to produce duplicate orifice plates which have the same discharge coefficient within ± 0.5 per cent requires very careful mechanical work, even when the diameter of the orifice is 1 inch or more. The commercial plates loaned to us were quite as good, in this respect, as the plates made at the Bureau of Standards.

(*d*) The difficulty of duplication increases as the size of the orifice is reduced, and if a standard table of discharge coefficients is to be relied upon, and the orifices not tested individually, it is advisable to use the largest orifice practicable within the range of diameter ratios covered by the available tables.

(*e*) The tables given in Sections XIV, XVI, and XVIII represent average results obtained from well-made orifices installed in 6 and 8 inch pipes, with a straight run of at least 120 pipe diameters upstream and 30 downstream. Similar orifices installed in a 4-inch pipe gave higher coefficients; but the experiments were not adequate to the establishment of a general relation between discharge coefficient and pipe diameter, even for this particular mode of installation, and any such relation must be expected to vary with the nature of the installation.

Appendix A. THEORY OF THE FLOW NOZZLE AND THE IMPACT TUBE

In finding the rate at which a gas is discharged through a flow nozzle under observed conditions of pressure and temperature, the first step is to compute the "theoretical" rate M_t which would occur under certain ideally simplified conditions.

With well-made nozzles, suitably designed for the rates to be measured, most of these conditions are nearly satisfied in practice, and in these respects the simplified ideal state of flow through the nozzle is a close approximation to reality. But one of the conditions assumed in the theoretical work is that the speed of the jet is the same near the wall of the nozzle as farther out toward the center of the stream, and since skin friction and retardation at the wall can not be done away with, this condition is not well satisfied in any real jet.

The result of the departure of the actual from the ideal conditions is to make the true rate of discharge a little less than the theoretical rate, and this fact may be expressed by the equation

$$M = CM_t \tag{1}$$

in which C is a correction factor or discharge coefficient by which the computed theoretical rate must be multiplied to give the true rate M. If the nozzle is to be used in this way as a flow meter, the value of C must, of course, be known to the same percentage accuracy as is required in M.

The obvious procedure for finding the value of C is to measure M by some direct method which does not involve any assumptions—by means of a gas holder, for example—and compare the value obtained for M with the value of M_t computed from the observed working conditions. If this has been done, the nozzle may be used as a convenient secondary standard, the primary standard being the method or instrument by which M was measured.

There is abundant experimental evidence to show that under ordinary working conditions the values of C for well-made nozzles are always within a few per cent of unity. But when an accuracy of two or three parts per 1,000 is required we are left in the lurch, so far as large nozzles are concerned, because no method of that accuracy has been developed so as to be available for measuring large rates of discharge directly, for the purpose of standardizing large nozzles. As the matter now stands, if large rates of flow are to be measured with an accuracy of 0.5 per cent or better, it is necessary to treat the nozzle as a primary standard, accepted on its own merits.

What is done is, in effect, to assume that the whole difference between M and M_t is due to the violation, in practice, of the condition that the speed of the jet shall be uniform right out to the wall of the nozzle, the other ideal conditions of the theory being sensibly realized. The effect of the falling off of speed near the wall of the nozzle is then determined by exploration with a fine impact tube, and a suitable correction applied to the computed theoretical rate of discharge M_t. This amounts to determining C by a self-calibration of the nozzle, without reference to any other standard.

To justify this procedure, we have to examine and criticize the assumptions involved in it and satisfy ourselves that they are sufficiently near the truth to make the values obtained for M accurate to much better than "a few per cent." We shall attempt to do this.

The nozzles used in the present investigation were of the converging type, ending in cylindrical throats, and the speed of the jet was always below the speed of sound in the jet. The discussion may therefore be limited to these conditions, and it will not be necessary to consider diverging nozzles or very high speeds. It will also be

supposed that the approach pipe is straight, round, and coaxial with the nozzle, as it was in our apparatus.

It is sometimes convenient to regard the stream of fluid through the nozzle as composed of a bundle of small filaments, each bounded and separated from the adjacent filaments by a tubular surface with its axis everywhere along the direction of the average motion. If the flow is perfectly steady and along fixed stream lines, this conception of stream tubes is evidently legitimate; but more often the flow is somewhat turbulent and the velocity at any fixed point is not quite steady but subject to small, rapid, irregular, fluctuations in both direction and magnitude.

In this general case the direction of the mean velocity at a point may be defined as the direction of a straight line, such that the mass flow through a small closed curve drawn about the point in any plane containing the line, vanishes when integrated over any appreciable interval of time. Since it is characteristic of turbulence that the fluctuations are too rapid to be followed by our ordinary measuring instruments, an "appreciable" interval of time is to be understood as one during which a large number of fluctuations takes place.

With this definition, a system of curves may be drawn in the stream so as to be, at each point, tangent to the direction of the mean velocity at that point; and the stream may be divided into filaments by tubular surfaces generated by the motion of such curves perpendicularly to themselves. On the whole, no fluid enters or leaves such a filament transversely; the mass flow is sensibly constant at any section of the filament and the same for all sections; and the motion is in some respects analogous to flow along a tubular channel with rigid impervious walls.

The magnitude of the mean velocity at any point, or the mean speed there, may be defined by saying that the constant mass flow along an infinitesimal filament containing the point is equal to the product of the mean speed, the density, and the cross sectional area of the filament at the point.

Having disposed of these preliminaries, we may state the assumptions on which the theoretical equations are based and outline the deduction of the equations, after which we shall discuss the assumptions in some detail.

For the sake of brevity the normal section of the approach pipe just ahead of the point where the stream begins to converge toward the nozzle will be denoted by A_o, and the normal section of the emerging jet at the mouth of the nozzle will be denoted by A. The assumed ideal conditions under which the theoretical equations would be true and M exactly equal to M_t may now be described, as follows:

(*a*) The static pressure of the fluid is uniform and constant over A_o.

(*b*) The static pressure in the jet is uniform over A and is equal to the constant pressure of the atmosphere into which the jet is escaping.

(*c*) The temperature of the fluid is uniform and constant over A_o and A.

(*d*) The mean velocity is uniform over A_o and A and parallel to the common axis of the pipe and the nozzle.

(*e*) There is no transmission of heat between the fluid and the nozzle or between different portions of the fluid; that is, the flow from A_o to A is adiabatic.

(*f*) There is no dissipative generation of heat either by the decay of turbulence or by reason of transverse variations of speed, which may occur in the converging stream even though the velocity is uniform and axial at A_o and A.

(*g*) The fluid is an ideal gas.

The following notation will be employed:

D_o, D = the diameters of the sections A_o and A, respectively;

$\beta = D/D_o$ = the "diameter ratio" of the nozzle;

S_o, S = the speeds normal to A_o and A;

p_o, p = the static pressures in the gas at A_o and A;

ρ_o, ρ = the densities of the gas at A_o and A;

θ_o, θ = its absolute thermodynamic temperatures at A_o and A;

ϵ_o, ϵ = the values, at A_o and A, of the internal energy of the gas per unit mass;

T_o, T = the values, at A_o and A, of the kinetic energy of unit mass of gas;

C_v, C_p = the specific heats of the gas at constant volume and constant pressure, respectively;

$\gamma = C_p/C_v$ = the specific heat ratio of the gas;

R = the "gas constant" for unit mass of gas;

M_t = the "theoretical" mass flow or rate of discharge from the nozzle;

M = the actual or true mass flow: M and M_t would be identical if the assumed ideal conditions were realized in practice.

As regards units, quantities of heat and internal energy are to be measured in the same units as kinetic energy and work, and mechanical quantities are to be measured in some set of normal units. For example, if speed is in ft./sec., density in lb./ft.^{3}, and mass flow in lb./sec., then diameters are to be in feet, pressures in poundals per square foot and quantities of energy in foot poundals (1 ft./lb. = 32.2 feet poundals, and 1 lb./in.^{2} = 32.2 × 144 poundals per square foot.)

Units of this sort are most convenient in the theoretical work, but more familiar units will be introduced later when the equations are to be used for numerical computation.

The first law of thermodynamics, as applied to the passage of unit mass of gas through the nozzle from A_o to A, may be expressed by the equation

$$(T+\epsilon)-(T_o+\epsilon_o)=\frac{p_o}{\rho_o}-\frac{p}{\rho}+W+Q \tag{2}$$

in which the first member represents the increase of the total energy of the unit mass, kinetic plus internal, and the terms of the second member have the following meanings:

p_o/ρ_o, or $p_o\times$ the specific volume at A_o, is the work done on the unit mass, as it crosses A_o, by the gas following it;

p/ρ is the work done by the unit mass, in crossing A, on the gas ahead;

W is the work done by outside forces on the unit mass while it is between A_o and A; and

Q is the heat received from outside sources by the unit mass while it is between A_o and A.

In the case of a horizontal nozzle with fixed rigid walls, no work is done by the walls or by gravity and $W=0$. Furthermore, in the ideal state of flow now under discussion, $Q=0$ by assumption (*c*), the flow being adiabatic. Equation (2) may therefore be written in the form

$$T-T_o=\left(\epsilon_o+\frac{p_o}{\rho_o}\right)-\left(\epsilon+\frac{p}{\rho}\right) \tag{3}$$

In perfectly steady stream line motion with the speed uniform, as required by assumption (*d*), the kinetic energy per unit mass is simply $S^2/2$. But if turbulence is superimposed on the steady flow, the kinetic energy of the turbulent motion increases the total kinetic energy by an amount h equal to the quantity of heat that would be generated if the turbulence were all instantaneously dissipated without changing the speed S. We must therefore write, in general,

$$T_o=\frac{S^2_o}{2}+h_o;\quad T=\frac{S^2}{2}+h \tag{4}$$

and

$$T-T_o=\frac{1}{2}(S^2-S^2_o)-(h_o-h) \tag{5}$$

in which the term (h_o-h) represents the amount by which the kinetic energy of turbulence has decreased from A_o to A by dissipation into heat.

In the ideal case, assumption (f) requires that $(h_o - h) = 0$, though it is to be noted that h_o and h are not required to vanish separately; hence we have

$$T - T_o = \frac{1}{2}(S^2 - S^2{}_o) \tag{6}$$

or by (3)

$$\frac{1}{2}(S^2 - S^2{}_o) = \left(\epsilon_o + \frac{p_o}{\rho_o}\right) - \left(\epsilon + \frac{p}{\rho}\right) \tag{7}$$

Since the rate of discharge is constant, the mass flow is the same at A as at A_o and we have

$$M_t = \frac{\pi}{4} D^2{}_o \rho_o S_o = \frac{\pi}{4} D^2 \rho S \tag{8}$$

and after eliminating S_o from (7) and solving for S, we have

$$S = \sqrt{\frac{2\left(\epsilon_o + \frac{p_o}{\rho_o}\right) - \left(\epsilon + \frac{p}{\rho}\right)}{1 - \beta^4 \left(\frac{\rho}{\rho_o}\right)^2}} \tag{9}$$

which holds for the flow of any fluid, subject to conditions (a,.....f), because up to this point no assumption has been made regarding the nature or properties of the fluid.

Since skin friction necessarily retards the flow near the wall of the nozzle, assumption (d), that the speed is uniform over A, implies that there is no skin friction and that the flow is unresisted. By assumptions (e, f) the flow is also adiabatic and free from any internal dissipation; hence the process of expansion and acceleration from A_o to A is isentropic, and in order to go on from (9) we must know how the density and internal energy of the fluid in question vary with the pressure during isentropic changes of state.

These relations become very simple if it is stipulated that the fluid shall be an ideal gas, in accordance with assumption (g). An ideal gas is, by definition, one for which the equations

$$\frac{p}{\rho\theta} = R = \text{constant, and } C_v = \text{constant} \tag{10}$$

are exactly satisfied. For such a gas it is readily shown, by elementary thermodynamics and with no further assumptions, that

$$C_v = \frac{R}{\gamma - 1} \text{ and } \epsilon = C_v\theta + \text{constant} \tag{11}$$

and that during isentropic changes of state between any two pressures p and p_o, the density and temperature change in accordance with the equations

$$\frac{\rho}{\rho_o} = \left(\frac{p}{p_o}\right)^{\frac{1}{\gamma}} \text{ and } \frac{\theta}{\theta_o} = \left(\frac{p}{p_o}\right)^{\frac{\gamma-1}{\gamma}} \tag{12}$$

From (10, 11, 12) we have

$$\left(\epsilon_0+\frac{p_0}{\rho_0}\right)-\left(\epsilon+\frac{p}{\rho}\right)=(R+C_v)(\theta_0-\theta)=\frac{\gamma}{\gamma-1}R\theta\left(\frac{\theta_0}{\theta}-1\right)$$
$$=\frac{\gamma}{\gamma-1}\cdot\frac{p}{\rho}\left[\left(\frac{p_0}{p}\right)^{\frac{\gamma-1}{\gamma}}-1\right] \tag{13}$$

and after substituting from (13) into (9) and eliminating $\frac{\rho}{\rho_0}$ by means of (12) we have

$$S=B\sqrt{\frac{2\gamma}{\gamma-1}\cdot\frac{p}{\rho}\left[\left(\frac{p_0}{p}\right)^{\frac{\gamma-1}{\gamma}}-1\right]} \tag{14}$$

where

$$B=\left[1-\beta^4\left(\frac{p}{p_0}\right)^{\frac{2}{\gamma}}\right]^{-\frac{1}{2}} \tag{15}$$

The mass flow may then be found from (8), one form of the result being

$$M_t=\frac{\pi}{4}D^2B\sqrt{\frac{2\gamma}{\gamma-1}p_0\rho_0\left[\left(\frac{p}{p_0}\right)^{\frac{2}{\gamma}}-\left(\frac{p}{p_0}\right)^{\frac{\gamma+1}{\gamma}}\right]} \tag{16}$$

Equations (14, 15, 16) may, of course, be obtained in various alternative forms by utilizing (11, 12, 13) in different ways, but since the subject is treated in most works on technical thermodynamics the foregoing outline of the reasoning will be sufficient here, and further algebraic details may be dispensed with.

The quantity B, defined by (15), is the "speed-of-approach factor" necessitated by the fact that the gas crosses the section A_0 at the finite speed S_0, instead of starting from rest, as in the case of an orifice in the wall of a large tank. If A_0 is very large compared with A, S^2_0 is negligible in comparison with S^2 and may be omitted from (7). In other words, if β is very small, B is sensibly unity and may be omitted from (14) and (16). The greatest value of β for any of the nozzles used in this investigation was 5/36; and since p was necessarily always less than p_0, the greatest possible value of B was less than 1.00019. The correction for speed of approach was thus entirely negligible, even in the worst case, and B could be omitted from (14, 16).

The assumptions described above define the ideal conditions under which the actual speed and rate of discharge would have precisely the theoretical values given by (14, 16), but the same conditions might have been defined by stating the assumptions somewhat differently. For example, if the fluid were entirely nonconducting and free from viscosity, conditions (*e*) and (*f*) would be satisfied automatically, and these two assumptions might, therefore, be replaced by the two other assumptions, that the fluid was noncon-

ducting and nonviscous. The particular set of assumptions adopted above was chosen, partly because it permits of going as far as equation (9) without imposing any restrictions whatever on the nature of the fluid and partly because it is easier with this choice than with some others to form an estimate of the probable effect of the departures from the ideal conditions which necessarily occur in practice. As they now stand, assumptions (a----f), concerning the general nature of the fluid motion, are more or less interdependent, but the final assumption (g) is quite separate from the others, and it will be convenient to dispose of it first.

No real gas satisfies equations (10) exactly, for departures may always be observed if the experiments cover a wide enough range; but all that is really assumed is that the equations are satisfied over the range of pressure from p_0 to p and over the accompanying range of temperature due to the cooling by rapid expansion from p_0 to p, and if R and C_v are sensibly constant over this range of conditions, the use of equations (10, 11, 12) is justified.

In our work with flow nozzles the initial pressure in the pipe was seldom more than 1 lb./in.^{2} above the outside barometric pressure, but during the calibration of two of the smaller nozzles there were a few cases in which the pressure drop was nearly 2.6 lbs./in.^{2}, so that the pressure fell from 17.3 to 14.7 lbs./in.^{2}. The simultaneous fall of temperature may be found approximately by means of (12), and for initial temperatures in the vicinity of 70° or 80° F. the cooling must have been about 25° F.

Over this range of conditions the variations of R from its mean value are of the order of ± 1 in 25,000. The variations of C_v are nearly ± 1 in 1,300 and those of γ ± 1 in 4700. But a change of this magnitude in γ affects the value of S computed from (14) by only about 1 in 200,000. In view of the foregoing, it seems quite safe to ignore the variations of R and C_v and to accept assumption (g), or equations (10, 11, 12), as sensibly exact under the given experimental conditions.

We proceed to the consideration of assumptions (a) and (b). In a steady stream of gas flowing straight along a uniform pipe the static pressure must be uniform over any normal section, for any departure from this condition would result in transverse currents and be inconsistent with flow parallel to the axis. If the flow is turbulent, it is to be presumed that the static pressure at any point is subject to rapid fluctuations; but if the stream has been freed from permanent eddies, cross currents, or whirl, either by straightening devices or by a sufficient preliminary length of straight pipe, the average static pressure must be the same at all points of a cross section. Assumption (a), therefore, corresponds closely to the actual experimental conditions.

The boundary of a jet of air from a flow nozzle may be made visible by suitable means, and for speeds below that of sound, observation shows that while the boundary gradually loses its sharpness at increasing distances from the end of the nozzle, it starts out as a cylinder and shows no tendency to swell or shrink laterally, as it would necessarily do if the air in the jet were at a different pressure from the surrounding atmosphere. From this it may be concluded that the static pressure is sensibly uniform and equal to the atmospheric back pressure at all points of the exit section A. This agrees with experimental measurements of the static pressure at the center of the mouth of the nozzle, where the pressure, if not uniform, might be expected to differ most from the outside pressure.

It thus appears that assumptions (*a*) and (*b*) are, as nearly as we can tell, satisfied in practice and that, in this regard, the ideal state of affairs is a close approximation to reality, though it is impossible to say just how close.

Turning to assumption (*c*), we find that the first part requires no extended comments, for the temperature in the approach pipe is under experimental control, if necessary, and may without difficulty be made very uniform; but the remaining assumptions are not so readily disposed of, for the assumed conditions are evidently violated in the outer part of the stream close to the wall of the nozzle. Nevertheless, equivalent assumptions sufficient for the validity of (14) may be very nearly true for the central part of the stream at a distance from the wall, and we may consider this possibility.

If the section of the jet at the mouth of the nozzle is explored with a fine impact tube, there is no indication of any systematic variation of the impact pressure with distance from the axis until the tube is moved fairly close to the wall, when the impact pressure begins to fall off rapidly. So far as impact pressure is concerned, and to the limit of accuracy of the apparatus, the jet consists of a uniform core surrounded by a thin nonuniform sheath.

Decreasing the speed of the jet thickens the sheath and diminishes the diameter of the core, and the same effect is produced by increasing the length of the cylindrical throat. Another pertinent fact is that when a steady stream of fluid enters a long, straight pipe from a large space in which the fluid is sensibly at rest the impact pressure is found to be uniform over almost the whole of a cross section near the entrance and does not settle down to its ultimate nonuniform distribution for a long distance.

It takes time for a tangential drag or shearing stress to be propagated from one point to another in a fluid, and the observations cited above show that the uniformity of the core at the mouth of the nozzle is due to the shortness of the time of transit of any given particle of air through the nozzle. The retarding effect of a wall of

given smoothness penetrates the stream only a certain distance before becoming inappreciable, and beyond this distance—the thickness of the sheath—no effect is produced unless the skin friction is increased by roughening the wall or unless, alternatively, the time available is increased, either by slowing down the jet or by lengthening the nozzle. Those filaments of the stream which make up the uniform core observed at the exit section A are too far from the wall to have been appreciably retarded by it, even at the end of their course through the nozzle, and the flow along them goes on in the same way as if there were no skin friction at all.

To this conclusion it might be objected that the impact pressure of a stream depends on density as well as speed, and that constancy of impact pressure does not prove that speed and density are separately constant. Any change of speed due to the proximity of the wall of the nozzle must necessarily be a decrease, but a simultaneous increase of density by the right amount would offset this and keep the impact pressure constant, in spite of the falling off of speed.

In reply, it may be remarked that if the static pressure is constant all the way across the mouth of the nozzle, as it appears to be, an increase of density near the wall would require that the temperature there be lower than farther out in the stream. Now, the air is cooled by its rapid expansion and, in any normal circumstances and in the absence of artificial cooling of the nozzle, it tends to be colder than the nozzle and to be heated by contact with it. Furthermore, the surface layer is most heated by skin friction because it is most rapidly sheared. For both these reasons the air immediately in contact with the wall must be not colder but hotter than the air farther out, and the transverse temperature gradient must be upward toward the wall. Hence, there can be no such compensating increase of density as was postulated above, and we are justified in concluding that the speed at the exit section A is unretarded by skin friction at least as far out from the axis as the impact pressure remains constant.

The increase of temperature due to the flow of heat from the surface layer toward the axis is also confined to the sheath and is imperceptible inside the core, for at constant static pressure an increase of temperature at any point within the core would lower the density and would have to be accompanied by a simultaneous increase of speed in order to keep the impact pressure constant. The nearer the point in question is to the source of heat at the wall the greater will be the rise of temperature and the greater the increase of speed required to compensate it, whereas the speed can only decrease toward the wall, if it changes at all. Hence, the heating must be negligible inside the core where the impact pressure is constant.

It may be noted here, as a side remark, that the propagation of a retarding drag and of a rise in temperature into a stream of gas, from a fixed boundary which is kept hotter than the gas, is the result of a single mechanism, so that the two phenomena are not independent but intimately connected. When two parallel streams of gas are flowing past each other they tend to mix, and the mixing tends to equalize both temperature and velocity. In pure stream line motion the mixing is on a molecular scale by diffusion, which tends to equalize not only the mean longitudinal components of the molecular velocities, but also the mean molecular kinetic energies of translation in all directions indiscriminately, to which the absolute temperatures are proportional. If the motion is turbulent, the mixing occurs on a molar instead of on a molecular scale; the colder but faster moving layer is continually having some of its particles replaced by others from the adjacent layer which are hotter but moving forward more slowly. The substitution of turbulent convection for the slower process of mixing by diffusion accelerates both phenomena, but the parallelism of heating and retardation remains and both effects necessarily increase or decrease together.

To return from this parenthesis, the general conclusion is that the expansion and accelaration of the air that escapes from the nozzle within the region of uniform impact pressure revealed by exploration with the impact tube go on in sensibly the same manner as if the wall of the nozzle were perfectly frictionless and nonconducting. And if we now suppose this inner part or core of the stream to be surrounded by a geometrical surface, reaching from A_o to A and so constructed as to be everywhere tangent to the direction of the mean velocity, the air of the core is discharged through this imaginery nozzle in precisely the same way as if the geometrical surface were a rigid, impervious, frictionless, nonconducting, material nozzle, somewhat smaller in diameter than the actual nozzle but of similar though less sharply curved profile. The conditions which were originally assumed to prevail throughout the stream but which are evidently violated near the wall of the nozzle are much more approximately satisfied in this core from which the nonuniform sheath has been excluded; but some further examination of the circumstances is required before it can be admitted that all the conditions necessary to the validity of (14) are satisfied.

It will first be supposed that the diameter ratio β is so small that S^2_o and, a fortiori, its transverse variations, may be neglected. As already noted, this condition was satisfied by even the largest of the nozzles employed in the present investigation.

The different filaments of the core now all start from A_o at the same static pressure p_o and with the same (negligible) speed S_o, and they all reach A at the same static pressure p and with the same

impact pressure. The question is: Can the flow along each filament be regarded as unresisted, adiabatic, and free from internal dissipation; that is, as isentropic? If so, the speed S attained at A must be the same for all filaments and must have the value given by (14).

The conditions of flow are not quite the same along all the filaments, because the outer ones are longer and more curved than the ones near the axis; and it can not be assumed that there are no transverse gradients of speed and no shearing anywhere in the converging stream, even though there is no skin friction to retard the outer layer. Such shearing will be distributed symmetrically about the axis of the nozzle, but it will be different at different distances from the axis on account of the varying curvature of the filaments.

Let us consider the ring of filaments where this shearing is most rapid, wherever that may be. The resistance to shearing dissipates kinetic energy into heat, lowering the speed and raising the temperature relatively to other filaments where the rate of shear is lower. Hence, where those filaments which have suffered the greatest dissipation arrive at A, over which the static pressure is constant, the impact pressure will be less than it is elsewhere; but in practice no such variation is observed, hence it is to be concluded that the effects of this internal dissipation on the speed of flow are insignificant, and that the speed at A is sensibly uniform throughout the core. Moreover, if this dissipative heating is insignificant, its effects in disturbing the initial uniformity of temperature and causing a flow of heat between adjacent filaments must also be negligible, and the flow along each filament of the core may be regarded as adiabatic.

It remains only to consider the possible effects of the dissipative decay, between A_o and A, of turbulence initially existing at A_o. It is a matter of common observation that the natural turbulence of a stream of water or air decreases with the speed of the stream and may even become quite imperceptible while the general forward speed is still considerable; and it is obvious that, in the absence of artificial stirring or of devices introduced with the special purpose of creating turbulence, the kinetic energy of turbulence in any ordinary slow stream is, at all events, not of a higher order of magnitude than the kinetic energy of the general forward motion.

If the latter supplies only a negligible term to the equations for the speed of the jet, as is now supposed and as was true in our experiments, the term representing heat obtained from the dissipation of an equal amount of kinetic energy of turbulence must also be negligible. Moreover, turbulence does not vanish instantaneously but decays slowly, and it seems probable that only a small fraction of the turbulence existing at A_o is dissipated during the extremely short time of transit through the nozzle. It therefore seems perfectly safe to

assume that under such conditions as existed in our experiments the effects of the dissipation of initial turbulence were entirely negligible.

Accepting the foregoing reasoning as valid within the limitations of accuracy of the experimental observations on which it depends, we may now say that the flow along each filament of the core is unresisted, adiabatic, free from dissipation, and therefore isentropic; hence equation (14) is applicable to each filament separately. And since the initial speed and density and the initial and final static pressures are the same for all, the final speeds and temperatures are also the same, and the final speed of the uniform core at the mouth of the nozzle has the value

$$S=\sqrt{\frac{2\gamma}{\gamma-1}\frac{p}{\rho}\left[\left(\frac{p_0}{p}\right)^{\frac{\gamma-1}{\gamma}}-1\right]} \qquad (17)$$

given by (14) when β is small enough that S^2_0 is negligible.

The ideal conditions required for the validity of (17) thus appear to be very nearly realized in the core of the jet, and under the circumstances of our experiments it seems probable that if the observations of pressure and temperature were exact, equation (17) would give the true speed of the middle part of the jet within ± 1 in 1,000 or better. If the uniform core filled the whole section of the mouth of the nozzle, the mass flow might then be found to the same accuracy by (16); but since the nonuniform sheath is of finite thickness, a correction factor must be introduced, and in default of a method for the absolute measurement of mass flow this factor has to be determined by means of impact tube observations. Hitherto, it has been sufficient to assume, as a familiar qualitative result of experiment, that the impact pressure of a stream of fluid increases with both speed and density, but it now becomes necessary to discuss the quantitative interpretation of measurements of impact pressure.

Let the impact tube be placed, pointing directly upstream, in a current of air of speed S, static pressure p, and density ρ; and let Δ be the observed impact pressure, so that the absolute static pressure of the air in the mouth of the tube is $p+\Delta=p_0$. The values of p and Δ are observed directly, while that of ρ has to be found from an observation of the temperature, together with the value of p and known constants for air. The problem is to find the unknown value of S from the observations of pressure and temperature.

Air approaching from upstream is slowed down and brought sensibly to rest at the mouth of the impact tube, and concurrently with this decrease of kinetic energy the air is compressed and its pressure rises from p to $p+\Delta$. This air may be regarded as flowing along a tubular filament which is initially of very small cross section in the undisturbed stream but which expands laterally as the speed of flow along it decreases, and finally merges into the nearly station-

ary cap of air at the static pressure $p+\Delta$, which covers the mouth of the tube. The equivalent outflow needed to maintain a steady pressure in the mouth of the tube is provided by a continual slow spilling over the edge, this escaping air falling at once to the pressure p and mixing with the general stream past the tube.

If it be assumed that the flow along this central filament is adiabatic, unresisted, and free from dissipation, the process of deceleration and compression is isentropic and thermodynamically reversible and is an exact reversal of adiabatic isentropic expansion from $p+\Delta$ to p, accompanied by acceleration from a negligibly low speed to the final speed S. Hence, on the permissible assumption that air acts sensibly like an ideal gas, the air speed required to set up the observed impact pressure will be given by the equation

$$S=\sqrt{\frac{2\gamma}{\gamma-1}\frac{p}{\rho}\left[\left(\frac{p+\Delta}{p}\right)^{\frac{\gamma-1}{\gamma}}-1\right]} \tag{18}$$

which is identical in form with (17) and deduced by the same theoretical reasoning.

Equation (18), or some more convenient mathematical equivalent, is commonly used for finding the value of S; but since the equation is deduced from assumptions which are evidently not exactly true, this practice requires justification.

In discussing the discharge of air through a nozzle, reasons were advanced for supposing that the conditions are so nearly uniform across the core of the stream that the flow along any filament is sensibly unaffected by interchange of heat or momentum with adjacent filaments; but in the case now under consideration the conditions are evidently different and are less simple. The central filament which leads to the mouth of the impact tube is not surrounded by other filaments which are just like it and so have no effect on it. On the contrary, the surrounding filaments are, on the whole, moving much faster than the central one and must exert a forward drag on it, something like a negative skin friction. Moreover, the air in the central filament is heated by the rapid compression, and must lose heat laterally. The reasons for regarding (17) as accurate for the case of the jet are therefore not sufficient to make (18) appear reliable for interpreting impact tube observations, and some additional evidence is needed before (18) can be trusted.

The best sort of evidence would be furnished by experiments in which the air speed S was measured by an independent absolute method, but such measurements are difficult, and there is not much evidence of this kind available, even for low speeds. Experiments at the National Physical Laboratory [17] showed that up to air speeds of

[17] Bramwell, Relf, and Fage; Rep. Adv. Comm. Aeron., p. 35; 1912-13.

50 ft.-sec. the measured and computed speeds did not differ by more than 1 part in 1,000; and other observers, using various methods for measuring the speed, have also failed to detect any disagreement of measured and computed values greater than the errors of experiment. For higher speeds there are no direct measurements to refer to but there is, fortunately, an important piece of indirect evidence.

Let an impact tube be fixed on the axis of the jet from a flow nozzle a little outside the end of the nozzle, and let it be connected, through a sensitive differential gauge, to a static side hole in the wall of the approach pipe ahead of the nozzle, so that the gauge indicates the excess of the total static pressure in the impact tube over the static pressure of the approaching stream. If the speed of approach is so low that the equivalent impact pressure is below the limit of accuracy of the gauge, the gauge reads sensibly zero, otherwise the reading of the gauge is equal to the impact pressure at the axis of the approaching stream. In any event, the total pressure in the impact tip at the mouth of the nozzle is equal to the total pressure in an impact tip placed in the center of the approaching stream.

This convenient relation, which was pointed out and utilized by Moss[18] in the paper already cited, appears to hold very accurately.

In addition to the experiments of Moss, experiments by the Bureau of Standards with a 2-inch nozzle on the end of an 8-inch pipe have shown that at air speeds slightly below the speed of sound the relation was certainly accurate to within less than 0.001 of the pressure drop through the nozzle, and there is every reason to suppose that it holds more rather than less accurately at lower speeds.[19]

The air in the central filament which strikes the mouth of the impact tube starts from a low or negligible speed in the approach pipe, expands to atmospheric pressure at the mouth of the nozzle, and is accelerated to a high speed there. It is then decelerated and brought to rest at the mouth of the impact tube, and its pressure rises from atmospheric to the pressure in the tube. The relation described above shows that the final pressure of the air when brought to rest is, as nearly as we can tell, exactly equal to the initial static pressure it would have had in the approach pipe if the pipe had been very large and the speed of approach negligible; and that so far as speed and static pressure are concerned the second half of the process is an exact reversal of the first half.

It follows from this that if (17) does, in fact, give the speed of the jet accurately, from observations of the initial and final static pressures and the initial temperature (needed for computing ρ), (18) gives the speed of a stream of air to the same degree of accuracy from obser-

[18] Trans. Am. Soc. Mech. Eng., **38**, p. 761; 1916. See also a recent paper presented at the annual meeting of the society; December, 1927.

[19] Under some very special conditions the relation might be expected to fail, but these conditions would never occur in ordinary practice. See M. Barker; Proc. Roy. Soc., **A-101**, p. 435; Aug. 1, 1922.

vations of the impact pressure Δ and of the static pressure and temperature of the undisturbed stream. Hence, if we admit the force of the reasons set forth above for regarding (17) as accurate for the core of a jet, we must accept (18) as confirmed empirically, without any further discussion of the physics of the impact tube.

There is, however, a quite different way of looking at the matter. Let us ignore the arguments hitherto advanced in favor of the accuracy of (17) and start afresh from the experimental fact that when an impact tube is placed in the jet from the mouth of the nozzle the expansion and acceleration through the nozzle are reversed by the compression and deceleration in front of the impact tube.

This is, of course, just what would happen if the whole process of expansion and recompression were completely reversible and isentropic, for on this condition both (17) and (18) are exact, and the experimental relation necessarily follows; but while this condition is sufficient it is not strictly necessary, for it is conceivable that both parts of the process might be irreversible, and yet the departures from the ideal conditions might happen to offset each other in such a way that both equations were always in error by the same amount and the experimental relation still subsisted.

If the conditions of expansion along a core filament to the end of the nozzle were at all like those of the recompression along the central filament ahead of the impact tube, such a compensation of errors might seem possible; but when we consider the dissimilarity of the two processes it seems almost infinitely improbable that there should be any compensation of this sort. There are obvious causes to prevent either process from being exactly reversible and isentropic, but these causes are so different, while their effects, if any, are the same, that the only rational conclusion to be drawn is that the effects are insignificant in both cases; and from this it follows that the ideal conditions for the validity of (17) and (18) are so nearly realized in practice that the departures from them may be ignored and the equations regarded as sensibly exact.

This second method of justifying the use of the theoretical formulas is much simpler than the former one, and it is based on a single well established experimental fact, namely, the existence of the relation pointed out by Moss, which is known to hold to an accuracy of 1 in 1,000 at worst. Most readers will probably find the argument more satisfactory than the earlier one; but in any event it seems safe to assume, in the absence of convincing experimental proof to the contrary, that, so far as the equations themselves are concerned and aside from errors in the measurements of pressure and temperature, the equations will give the true values of the speeds in question to an accuracy of 1 part in 1,000 or better, and they will henceforth be accepted without further discussion of their accuracy.

The employment of the impact tube in calibrating a nozzle so as to determine the value of its discharge coefficient $C = M/M_t$ will be considered in Appendix B. At present we have only to supplement the theoretical discussion of the flow nozzle by showing how the theoretical mass flow M_t may be computed in practice from the observations of pressure, temperature, and humidity.

Direct substitution of S from (17) into (8) gives us

$$M_t = \frac{\pi}{4} D^2 \sqrt{\frac{2\gamma}{\gamma - 1} p\rho \left[\left(\frac{p_o}{p} \right)^{\frac{\gamma-1}{\gamma}} - 1 \right]} \tag{19}$$

and by (12) we have

$$p\rho = p_o \rho_o \frac{p}{p_o} \cdot \frac{\rho}{\rho_o} = p_o \rho_o \left(\frac{p}{p_o} \right)^{\frac{\gamma+1}{\gamma}} \tag{20}$$

whence by (19)

$$M_t = \frac{\pi}{4} D^2 \sqrt{\frac{2\gamma}{\gamma - 1} p_o \rho_o \left[\left(\frac{p}{p_o} \right)^{\frac{2}{\gamma}} - \left(\frac{p}{p_o} \right)^{\frac{\gamma+1}{\gamma}} \right]} \tag{21}$$

which is the form into which (16) degenerates when β is small, as it was in the present experiments.

For air in the vicinity of atmospheric pressure and temperature the specific heat ratio is very nearly $\gamma = 1.40$, so that (21) reduces to

$$M_t = 2.078 D^2 \sqrt{p_o \rho_o \left[\left(\frac{p}{p_o} \right)^{1.43} - \left(\frac{p}{p_o} \right)^{1.714} \right]} \tag{22}$$

Hitherto, all equations have been given in terms of normal units, so that in (22), if M_t is expressed in lb./sec. and ρ_o in lb./ft.^{3}, D must be measured in feet and p_o and p in poundals/ft.^{2}. If we now express D in inches and p_o and p in lb./in.^{2}, the numerical factor

$$\frac{\sqrt{144 \times 32.174}}{144} = 0.47268$$

must be introduced and (22) becomes, with these new units

$$M_t = 0.98222 D^2 \sqrt{p_o \rho_o \left[\left(\frac{p}{p_o} \right)^{1.43} - \left(\frac{p}{p_o} \right)^{1.714} \right]} \tag{23}$$

The diameter D is a known constant for each nozzle and p_o and p are observed directly, but the value of ρ_o has to be found from the pressure, temperature, and humidity of the air in the approach pipe. The method of computation and the necessary data on air have already been described in Section XI of the body of the paper, and the result is expressed there by equation (26). Since the range of pressure at the nozzle is small, we may set $Y = 1$ and we then have, for our present purpose,

$$\rho_o = 2.6914 \frac{p_o}{458 + t} \left(1 - 0.38 \frac{\pi}{p_o} \right) \tag{24}$$

in which t°F. is the temperature of the approaching air, and π lb./in.^{2} is the partial pressure of the water vapor in it. Upon substituting this value of ρ_o in (23) we get as the final equation for computing M_t

$$M_t = 1.6114 D^2 p_o \sqrt{\frac{1-0.38\frac{\pi}{p_o}}{458+t_o}\left[\left(\frac{p}{p_o}\right)^{\frac{2}{\gamma}} - \left(\frac{p}{p_o}\right)^{\frac{\gamma+1}{\gamma}}\right]} \qquad (25)$$

in which:

M_t[lb./sec.] = the theoretical rate of discharge;
D[ins.] = the throat diameter of the nozzle;
p_o[lb./in.^{2}] = the static pressure in the discharge trunk;
p[lb./in.^{2}] = the pressure of the outside atmosphere;
π[lb./in.^{2}] = the partial pressure of the water vapor in the air in the trunk; and
t[°F.] = the temperature of the air in the trunk.

Appendix B. DISCHARGE COEFFICIENTS OF THE NOZZLES

It has been shown in Appendix A that the theoretical equations (12, 17) may be regarded as giving the actual values of the density and speed, without appreciable error, for all points of the section A within the uniform core of the jet, and these equations lead to the expressions (19, 21, 22, 23, 25) for the "theoretical" rate of discharge which would occur if the core filled the whole throat of the nozzle. But since, in reality, the speed is lower in the immediate vicinity of the wall than farther away, the actual rate of discharge is less than the theoretical rate, and the next problem is to find how the theoretical rate must be corrected to allow for the actual departure from uniformity of conditions near the boundary of the jet.

The only experimental method available for investigating the state of affairs in the variable region consists in observing the impact pressure in a fine impact tube set at various distances from the axis of the jet, and we have now to consider how the results of such observations may be interpreted and utilized.

The walls of the pipe and nozzle formed a surface of revolution, and after the approaching stream had been straightened by passing through the honeycombs, conditions in the jet appeared to be nearly symmetrical about the axis of the nozzle. The arithmetical mean of readings of the impact pressure at a given radius but in several uniformly spaced azimuths was therefore taken to represent the reading that would have been obtained everywhere at that radius if the flow had been completely symmetrical, and we proceed to consider the properties of a symmetrical jet.

In accordance with the notation employed in Appendix A, let ρ_r, S_r, etc., denote the density, speed, etc., in the exit section A at the radius r, and let a be the radius of this section.

The mass flow through a ring shaped element of A, of radius r and width dr, is

$$dM = 2\pi r dr \rho_r S_r \tag{26}$$

whereas if the density and speed at this radius had the theoretical values given by (12, 17) the mass flow would be

$$dM_t = 2\pi r dr \rho S \tag{27}$$

For this element of the area, the ratio of actual to theoretical flow is $\rho_r S_r / \rho S$, and the discharge coefficient of the nozzle is the average value of this ratio for the whole area of the section. We therefore have the equation

$$C = \frac{1}{\pi a^2}\int_0^a 2\pi r \frac{\rho_r S_r}{\rho S} dr = \int_0^1 \frac{\rho_r S_r}{\rho S} d\left(\frac{r}{a}\right)^2 \tag{28}$$

or if we abbreviate by setting

$$\left(\frac{r}{a}\right)^2 = x \text{ and } \frac{\rho_r S_r}{\rho S} = y \tag{29}$$

we have

$$C = \int_0^1 y dx \tag{30}$$

If the values of y can be determined and the curve

$$y = f(x) \tag{31}$$

drawn, the value of C may then be found graphically by measuring the area inclosed by the curve, the axes, and the ordinate at $x = 1$. If ABC in Figure 10 represents the curve, the value of the discharge coefficient is given by

$$C = \text{area } \overline{OABCDO} = 1 - \text{area } \overline{BECB} \tag{32}$$

This procedure cannot be followed strictly, because there is no practicable way of determining the required values of y according to the definition in (29). But approximate values may be obtained from measurements of impact pressure, and under the conditions prevailing in our experiments the approximation is close enough that the foregoing graphical method may be followed without serious error.

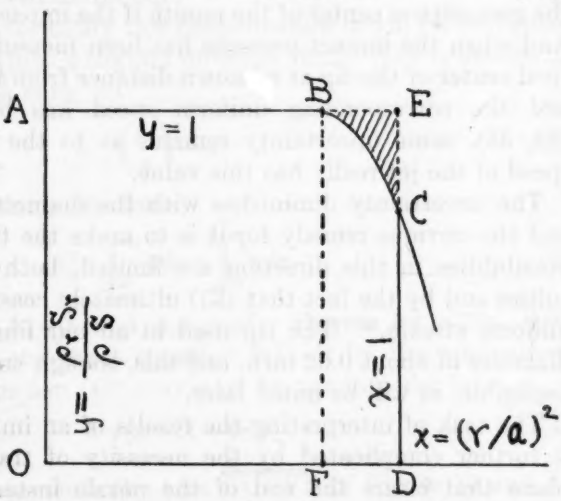

FIG. 10

It was shown in Appendix A that, for an impact tube in a uniform stream of air, equation (18) may be relied on as a sensibly accurate relation connecting the observed impact pressure with the speed, density, and static pressure of the undisturbed stream. With $\gamma = 1.40$, as for air, the equation is

$$S = \sqrt{7\frac{p}{\rho}\left[\left(\frac{p+\Delta}{p}\right)^{\frac{2}{7}} - 1\right]} \tag{33}$$

and after developing $(1+\Delta/p)^{\frac{2}{7}}$ by the binomial theorem, this may be reduced to

$$S = Q\sqrt{\frac{2\Delta}{\rho}} \tag{34}$$

in which

$$Q = \left[1 - \frac{5}{14}\frac{\Delta}{p} + \frac{10}{49}\left(\frac{\Delta}{p}\right)^2 - \frac{95}{686}\left(\frac{\Delta}{p}\right)^3 + \frac{247}{2401}\left(\frac{\Delta}{p}\right)^4 - \cdot - \text{etc.}\right]^{\frac{1}{2}} \tag{35}$$

Equations (34, 35) are usually more convenient than (33) for numerical computation, and they are more suitable to our present purpose.

If the speed of the stream in which the impact tube is placed varies transversely, as it does near the boundary of the jet from a nozzle, and if the observed value of Δ is substituted in (34, 35), the resulting value of S is the speed of a uniform stream, of the given density and static pressure, which would set up the pressure actually observed in the impact tube. This fictitious uniform speed is some sort of average of the speeds upstream from the mouth of the tube and is between the highest and lowest of them; but it is not necessarily equal to the speed that would exist at the present position of the geometrical center of the mouth if the impact tube were removed. And when the impact pressure has been measured with the geometrical center of the tip at a known distance from the axis of the nozzle, and the corresponding uniform speed has been computed from (34, 35), some uncertainty remains as to the radius at which the speed of the jet really has this value.

The uncertainty diminishes with the diameter of the impact tip, and the obvious remedy for it is to make the tip very fine; but the possibilities in this direction are limited, both by mechanical difficulties and by the fact that (33) ultimately ceases to hold, even for a uniform stream.[20] The tip used in all our final calibrations had a diameter of about 0.02 inch, and this, though small, was not entirely negligible, as will be noted later.

The task of interpreting the results of an impact tube calibration is further complicated by the necessity of traversing the tip in a plane that clears the end of the nozzle instead of exactly in the plane A where the cylindrical throat of the nozzle terminates. It

[20] See M. Barker, Proc. Roy. Soc., A **101**, p. 435, Aug. 1, 1922.

did not appear that there was any appreciable spreading of the free jet in the short distance between these planes; but when the impact tube was moved entirely outside the jet, so that its tip faced the flat end of the nozzle, with a clearance of a few thousandths of an inch, there was still a considerable excess pressure in the tube. This can not have been due to direct impact of the jet, and whatever its cause it was spurious as an indication of impact pressure.

We shall start, however, by ignoring the difficulties just mentioned and shall assume that values of Δ_r have been obtained with a tip of negligible diameter in the plane A. The effects of the actual departures from these ideal experimental conditions will be considered subsequently.

For a point at the radius r (34) takes the particular form

$$S_r = Q_r \sqrt{\frac{2\Delta_r}{\rho_r}} \tag{36}$$

in which Q_r is defined by (35) with Δ_r/p_r in place of Δ/p; and from (34, 36) we have, as a new expression for y,

$$y = \frac{\rho_r S_r}{\rho S} = \frac{Q_r}{Q}\sqrt{\frac{\rho_r \Delta_r}{\rho \Delta}} \tag{37}$$

Moreover, it may be shown that under the conditions of our experiments both Q_r/Q and ρ_r/ρ were so nearly unity that the simpler equation

$$y = \sqrt{\frac{\Delta_r}{\Delta}} \tag{38}$$

was an adequate substitute for (37).

Before proceeding to justify this simplification it will be convenient to put equation (30) into a slightly different form. Let r_c denote the radius of the uniform core; let

$$\left(\frac{r_c}{a}\right)^2 = w \tag{39}$$

and let (30) be written in the form

$$C = \int_0^w y dx + \int_w^1 y dx \tag{40}$$

Within the core $\Delta_r = \Delta$ and $\rho_r S_r = \rho S$. Hence, for $x \leqq w$, $y = 1$, whether defined by the exact equation (37) or by the approximate equation (38). Equation (40) may now be put into the form

$$C = w + (1-w)\bar{y} \tag{41}$$

in which $(1-w)\bar{y}$ represents the area $\overline{\text{BCDFB}}$ of Figure 10 and $\bar{y}$ is the mean ordinate of the part of the curve between B and C, which refers to the variable region near the boundary. Any error in the

location of the curve $y=f(x)$ due to using (38) instead of (37) can affect only this outer part of the curve.

We return to the consideration of ρ_r/ρ. In normal operation the mouth of the nozzle is kept somewhat warmer than the cold core of the expanded jet by the flow of heat through the metal from the entrance end which is in contact with the warmer air entering it; and since the temperature of the surface film of air is largely, if not completely, controlled by that of the metal in contact with it, the temperature of the air at the boundary of the jet as it leaves the throat will be somewhere between the initial temperature θ_0 and the temperature θ reached by isentropic expansion in the core.

The greatest conceivable effect of this sort would be to prevent the surface film from cooling at all and make the expansion along the wall isothermal; and since the static pressure is sensibly uniform all over A, the final density at the boundary would then be

$$\rho_a=\rho_0\frac{p}{p_0} \tag{42}$$

The final density in the core, as given by (12) with $\gamma=1.40$, is

$$\rho=\rho_0\left(\frac{p}{p_0}\right)^{\frac{5}{7}} \tag{43}$$

so that in the ideal extreme case we have

$$\sqrt{\frac{\rho_a}{\rho}}=\left(\frac{p}{p_0}\right)^{\frac{5}{7}}<1 \tag{44}$$

At any intermediate radius between $r=r_0$ and $r=a$ the value of $\sqrt{\rho_r/\rho}$ will always be between unity and the extreme lowest value given by (44); and if $d\bar{y}$ denotes the amount by which the mean ordinate $\bar{y}$ is overestimated when the variation of density is ignored, an outside limit for this error is given by

$$\frac{d\bar{y}}{\bar{y}}<1-\sqrt{\frac{\rho_a}{\rho}}=1-\left(\frac{p}{p_0}\right)^{\frac{5}{7}} \tag{45}$$

The resulting positive error in C is then, by (41, 45)

$$dC=(1-w)d\bar{y}<(1-w)\left[1-\left(\frac{p}{p_0}\right)^{\frac{1}{7}}\right]\bar{y} \tag{46}$$

and since $\bar{y}$ is always less than unity, an outside value for the error in C is given by

$$dC<(1-w)\left[1-\left(\frac{p}{p_0}\right)^{\frac{1}{7}}\right] \tag{47}$$

The effect of setting $Q_r = Q$ may be treated in a somewhat similar manner. Equation (35) shows that $Q < 1$, and that as Δ_r decreases toward the boundary of the jet Q_r increases, its limiting value being $Q_a = 1$, if $\Delta_a = 0$. Ignoring this variation and setting $Q_r = Q$ for all values of r results in an underestimate of $\bar{y}$ and of C, and outside limits for these negative errors are given by

$$-\frac{d'\bar{y}}{} < 1 - Q \tag{48}$$

and

$$-d'C < (1-w)\,(1-Q) \tag{49}$$

For numerical values we turn to the experimental data. The greatest pressure drop at which any of the nozzles was calibrated was $\Delta = 2.6$ lb./in.^{2}, and at this rate of flow the observed radius of the uniform core gave $w = 0.95$ for the smallest nozzle. With these values, we find from (47) and from (35, 49)

$$dC < 0.0012; \quad -d'C < 0.0015$$

This same nozzle running at $\Delta = 0.6$ lb./in.^{2} gave $w = 0.93$, whence

$$dC < 0.0006; \quad -d'C < 0.0005$$

At any given pressure drop the larger nozzles gave higher values of w and therefore lower values of dC and $-d'C$.

It thus appears that the greatest conceivable errors in C which could be caused by setting $Q_r = Q$ in (37) are of the same order of magnitude as those caused by setting $\rho_r = \rho$, but of opposite sign, and that both kinds of error are separately very small. The approximation involved in passing from (37) to (38) is therefore amply close and (38) may be used without further scruple.

This point having been established, the first step in finding the discharge coefficient of a nozzle when running at a constant pressure drop Δ, from the values of Δ_r observed during the calibration, was to plot the values of $\sqrt{\Delta_r/\Delta}$ against those of $(r/a)^2$ and to draw, as nearly as possible through the resulting points, a smooth curve

$$\sqrt{\frac{\Delta_r}{\Delta}} = f\left(\frac{r^2}{a^2}\right) \tag{50}$$

such as is represented qualitatively by ABC in Figure 10. This was an approximation to the curve that would have been obtained from perfectly accurate observations, made in the ideal manner with an impact tip of negligible diameter, traversed exactly in the plane of the section A. The area $\overline{\text{BECB}}$ was therefore measured, and a

provisional approximate value of the discharge coefficient of the nozzle was found from the relation

$$C = 1 - \text{area } \overline{\text{BECB}} \tag{51}$$

Figure 11 shows three sample curves drawn from observations on a nozzle of 3.262 inches diameter with the impact tip of 0.02-inch diameter. The positions of the plotted points are subject to the errors of measuring the impact pressure and of setting the tip at the intended radius, the former being halved and the latter doubled. The uncertainty of setting was estimated to be about ± 0.003 inch, and this corresponds in Figure 11 to a horizontal displacement of nearly four of the smallest scale divisions, so that the abscissa of a point representing a single observation might be in error by this amount. Accidental errors were, however, partly eliminated in

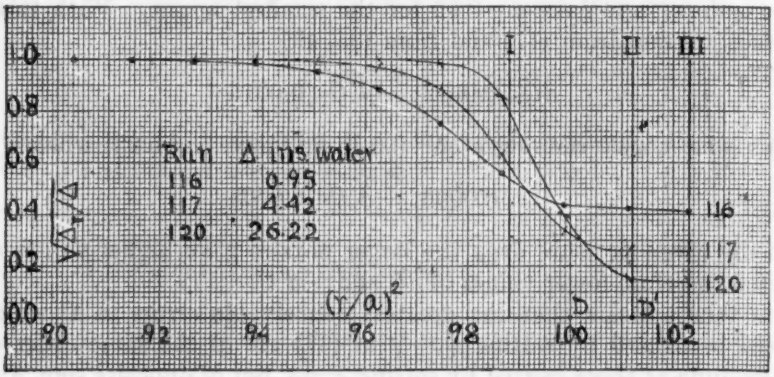

FIG. 11

averaging a number of observations taken in different azimuths at the same nominal radius, and the smoothness of the curves indicates that the remaining accidental errors were small.

But assuming that these errors are very small and that the curves are a sensibly accurate representation of the facts, it is evident that they differ systematically from what might be expected of an ideal calibration; for there can be no doubt that the air adheres to the nozzle, or that the speed of the stream, so long as it is still inside the nozzle, is entirely inappreciable at the wall;[21] and curves obtained from accurate observations made in the ideal manner would all meet at the point ($x=1$, $y=0$) represented by D in Figures 10 and 11. It is the ideal curves that are needed in order that the graphical method described above may give accurate values of C, so we must attempt to interpret the departures of the observed from the ideal curves and apply corrections for them.

[21] In this connection see Stanton, Marshall, and Bryant, Report Adv. Comm. Aeron. (Great Britian), 1919-20, **1**, p. 51.

In a perfect nozzle the plane end would meet the cylindrical throat at a right angle and the section A would be in the plane of the end face instead of a little inside, as it is in any real nozzle because the corner can not be made perfect, even if it is not intentionally rounded off or chamfered to prevent damage in handling.

If the end of the impact tip were ground perfectly flat and set so as, when moved out radially, to slide over the end of the nozzle, making perfect contact, with no clearance, the observations of impact pressure would be made in the plane of A, and the excess pressure in the impact tube would vanish as soon as the tip had been moved entirely outside the jet.

If b denotes the radius of the tip, let

$$\left.\begin{aligned} a-b=r_{\mathrm{I}};\ \left(\frac{a-b}{a}\right)^2=x_{\mathrm{I}} \\ a+b=r_{\mathrm{II}};\ \left(\frac{a+b}{a}\right)^2=x_{\mathrm{II}} \end{aligned}\right\} \tag{52}$$

As long as $x \gtrless x_{\mathrm{I}}$, the whole mouth of the tip is exposed to the impact of the jet; when $x_{\mathrm{I}}<x<x_{\mathrm{II}}$, the mouth is only partly exposed, the outer part being covered; and when $x \gtrless x_{\mathrm{II}}$ the mouth is completely closed. As the tip is moved out through the boundary of the jet, the excess pressure in it must vanish when $r=r_{\mathrm{II}}$, and curves obtained in the way described would all meet at the point ($x=x_{\mathrm{II}}$, $y=0$).

In the case of Figure 11, $a=1.631$ inches and $b=0.01$ inch, so that $x_{\mathrm{I}}=0.988$ and $x_{\mathrm{II}}=1.012$. The lines marked *I* and *II* are drawn at these abscissas. Points on or to the left of *I* represent observations with the tip entirely inside the jet; points between *I* and *II* represent observations with the tip partly outside the geometrical prolongation of the throat of the nozzle; and for points to the right of *II*—for example, points on line *III*—the tip was entirely outside this prolongation.

The condition that the tip should make a perfect fit with the end face of the nozzle was, of course, not satisfied, and the effect of the clearance is very evident from the form of the outer part of the curves. A free jet from a nozzle always entrains the outside air and sets up a circulation in the vicinity. In some way which can not be specified this circulation caused an excess pressure in the slit between the edge of the tip and the end of the nozzle and gave a spurious reading which was not due to the impact of the jet.

This induced circulation is maintained by viscosity, and the effects of viscosity are proportional to the first power of the speed, whereas true impact pressure is proportional to the second power. It is therefore to be expected that the pressure due to the circulation will increase less rapidly with the speed of the jet than does the impact

pressure and will be relatively less pronounced at high than at low speeds. This means that in Figure 11 the observed points on line *III* should be lower as the value of Δ is higher, as they are, in fact. On the other hand, the absolute values of Δ_r for these points should increase with Δ, and this expectation is also confirmed, though it is not at once evident from the figure.

For very low jet speeds it is conceivable that the effects of the induced circulation might even extend inside the prolongation of the throat of the nozzle; but, in general, it is to be expected that when the tip is entirely within this prolongation it will be free from such effects. Accordingly, we find that the observed points to the left of line *I* lie on curves which might, without violence, be made to pass through the point *D'*; and except for the lowest speed this is true also of the points at $x=0.999$, where the tip was nearly half outside the prolongation of the throat.

The question now is, how ought the observed curves to be corrected so as to give values of *C* which are unaffected by the induced circulation and by the size of the tip? A precise answer is impossible, but our actual procedure was as follows:

It was first assumed that if the clearance had been reduced to zero the curves would all have met at the point *D'*. The distance of *D'* from *D* is

$$DD'=2\frac{b}{a}+\left(\frac{b}{a}\right)^2 \tag{53}$$

and if b/a were negligible, the two points would be sensibly coincident. The foregoing assumption means, therefore, that if the effects of induced circulation were eliminated and the diameter of the tip were negligible the curves would meet at *D*. This was accordingly taken to be one point on each corrected curve.

It was then further assumed that as long as the tip was entirely within the prolongation of the throat of the nozzle the effective center of the tip was at its geometrical center. In other words, it was assumed that so long as $r\leqq a-b$ the speed computed from the observed Δ_r by (34, 35) was the true speed at the radius *r*. This means that in Figure 11 the curves were taken to be correct, out as far as the line *I*.

Each curve was then corrected by drawing a straight line from the point where it cut the line *I* to the point *D*. The area between this line and the curve as first drawn was measured, and its value was subtracted from the earlier, approximate value of *C* to give a final corrected value.

With respect to the second of the two assumptions, it may be remarked that when the tip was barely inside the jet, with its geometrical center at $r=a-b$, it was in a region of rapidly varying speed,

and that it is probable that its effective center was slightly displaced toward the axis of the nozzle. If so, the point where the curve cuts line *I* is too high and failure to allow for this makes the correction too small. On the other hand, the curve is doubtless convex throughout, and treating the last part as a straight line makes the correction to *C* too large. The compromise adopted, for want of anything better, gives only a rough estimate of the correction, but the whole value was insignificant in most cases.

The curves given in Figure 11, which have been used for illustration, are fairly typical of the numerous others, though the turnup at the end was often less pronounced and the curves sometimes came closer to the point corresponding to *D*. Consistency in this regard was not to be expected, because the clearance was not always the same, even for the same nozzle, but varied irregularly with the azimuth in which the slide carrying the impact tube was set.

The corrections to *C* obtained from the curves for any one nozzle running at various rates did not differ greatly and an average value was used for each nozzle at all values of Δ. These average values were as given in Table 24.

TABLE 24

Nozzle	Correction (to be subtracted)	Nozzle	Correction (to be subtracted)
D–1	0.0032	A–4	0.0013
A–1	.0018	B–2	.0013
A–2	.0016	C–1	.0011
A–3	.0019	C–2	.0011

In view of the smallness of these corrections, it seems very unlikely that errors in the method of estimating them, described above, can in any case have affected the final value of *C* by as much as ± 0.001.

Figure 12 shows the calibration curves giving the values of the discharge coefficient *C* in terms of the pressure drop through the nozzle in inches of water. The separate points representing the different calibration runs are put in so that the reader may form his own opinion of the consistency of the observations on each nozzle. No curve is given for nozzle B–1, which was used in only one of the orifice tests recorded in this paper.

Nozzles D–1 and A–2 were calibrated at higher differentials, and in each case three more points were obtained, which would be far off the sheet to the right but are entirely consistent with the curves as shown. The highest nozzle differential in any of the orifice tests was about 27 inches of water, so that Figure 12 gives the parts of the curves actually needed in reducing the observations on the orifices.

With the exception of the six points for D–1 and A–2, mentioned above, the points given represent all the calibrations that were made with the exploring tip of 0.02 inch diameter. In the earlier stages of the work a number of calibrations with several exploring tips of larger diameter were carried out and gave points which were considerably more scattered than those shown in the figure, probably because of

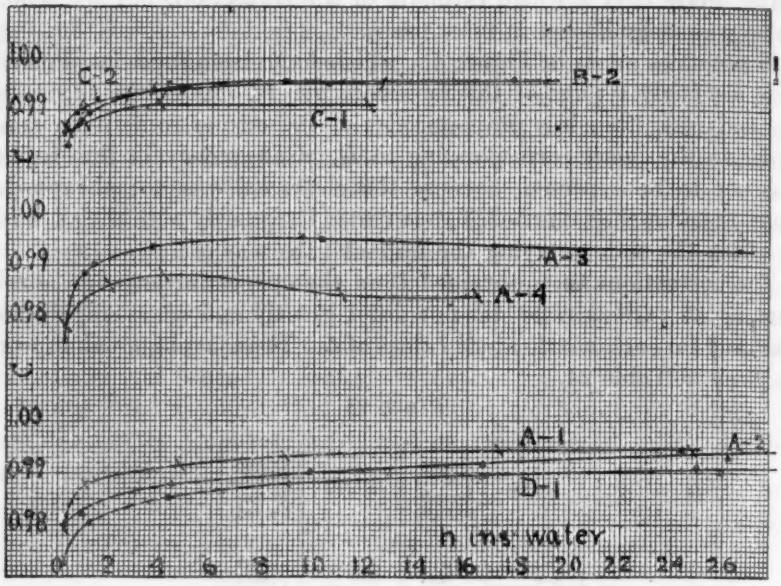

FIG. 12.—*Discharge coefficients of flow nozzles*

lack of experience in the manipulations. All these earlier observations were discarded.

TABLE 25*

Nozzle	Diameter D inches	Times used	Differential at nozzle	
			Greatest h (max.) inches water	Least h (min.) inches water
1	2	3	4	5
D–1	1.764	57	27	0.25
A–1	3.255	5	13	1.12
A–2	3.262	154	18	.16
A–3	3.272	7	26	.26
A–4	3.258	1	17	17
B–2	4.521	62	17	.21
C–1	5.006	16	12	4.1
C–2	5.003	63	12	2.7

The nozzles were not all employed to the same extent nor over the same range of differentials. In Table 25 column 3 gives the number of orifice tests in which each nozzle was used, each such test including observations on three orifices in series. Columns 4 and 5 give approximate values of the greatest and least differentials at the nozzles in the orifice tests. The lowest differentials were measured on an inclined water manometer.

Upon examination of Figure 12 it appears that (*a*) so far as can be judged, the points which determine each curve are consistent among themselves within about ± 0.001 in the values of C; and (*b*) the best determined curves are those for the four nozzles (D–1, A–2, B–2, C–2) which were employed in most of the orifice experiments (336 out of 363).

Whether the different curves are consistent with one another is a question which could not be answered with certainty except by running two or more nozzles in series. We had no facilities for this, but in a great many cases two or more nozzles were used in testing a given orifice. If the discharge coefficients of the nozzles had not been consistent among themselves, the discharge coefficients of the orifice would have shown systematic variations, according to the flow nozzle used; but no such systematic variations were found.

It seems to us probable that the absolute accuracy of the nozzle coefficients read from the curves which are represented on a small scale in Figure 12 was considerably better than ± 0.3 per cent; and we think that under favorable conditions of steadiness in the supply of air or gas, and with sufficient care in calibration by means of a fine impact tube nozzles of this character and of these sizes or larger may be made reliable as primary standard flow meters to within ± 0.1 per cent.

Appendix C. SIMILAR ORIFICES

If a stream of fluid is forced along a pipe line at a fixed rate of discharge, any alteration of the line, such as the introduction of a valve or an elbow into what was previously a straight run of uniform pipe, modifies the motion for an appreciable distance ahead of the place where the change is made, and on the downstream side, eddies or whirls which may be set up are carried along for a considerable distance before dying out. Thus, the distribution of velocity and pressure at any fixed cross section depends on the nature of the line for some distance in both directions, and the discharge coefficient of an orifice installed in the line is influenced by the shape of the nearer parts of the piping, although changes of shape or disturbances set up at sufficiently distant points have no appreciable effect at the orifice.

In treating the discharge coefficient of an orifice as a definite quantity it is therefore implied, and is always to be understood, that the nature of the line in which the orifice is installed is specified out to a sufficient distance in both directions that changes at still greater distances have no further appreciable effect on the discharge coefficient.

It is not necessary that the pipe be either straight or uniform, although that is the simplest shape to describe. What is required is merely that all peculiarities of shape be specified in sufficient detail that, aside from possible mechanical difficulties of construction, they could be reproduced, either on the same scale or on a different one, within such tolerances that the variations still permitted would not change the discharge coefficient by more than the accidental error of an experimental determination of its value.

It is also to be noted that the part of the line that requires specification may be limited to a comparatively short section by installing honeycombs or cellular grids a few pipe diameters before the upstream and after the downstream pressure tap. Such devices tend to protect the intervening region from disturbances which may originate farther away from the orifice, so that the nature of the rest of the line is no longer of any importance. If this plan is adopted, the design and location of the grids must evidently be included in the specification.

To avoid circumlocution, the term "orifice" may be used to connote all these important features of the piping as well as the orifice plate itself, and on this understanding any two "orifices of the same shape" are geometrically similar in all essential respects. If they are also of the same size, they are mere duplicates, and under any given working conditions their discharge coefficients are equal. If they differ in size, their discharge coefficients will be equal under similar working conditions, if the term "similar" is suitably defined, and we have next to consider what meaning is to be assigned to "similar" in this connection.

For any given fluid the working conditions may be defined by the initial pressure and temperature and the rate of discharge; but since an orifice may be tested with various fluids, a general definition of the "working conditions" must include some reference to the properties of the fluid.

To simplify matters, it will first be supposed that the fluid is a liquid, so that its properties are sensibly independent of pressure, and compressibility does not come into the problem.

The discharge coefficient of a particular orifice for a given liquid at a given temperature may vary with the rate of discharge—that is, with the linear speed through the orifice—and if the properties of the liquid are varied, either by altering the temperature or by substituting a different liquid, it may again be found that the discharge coefficient has changed. For present purposes the most obviously important

properties of the liquid are its density and viscosity. Sufficiently precise experiments would doubtless reveal the effects of altering other properties, but under ordinary circumstances these effects are inappreciable and, in practice, the values of density and viscosity may be regarded as constituting a complete characterization of the liquid with respect to flow along pipes or through orifices.

It follows from the foregoing that there is some relation connecting the discharge coefficient C with the speed of flow S, the density of the liquid ρ, and its viscosity μ. In other words, there is some equation

$$C=f(S,\rho,\mu) \tag{54}$$

which holds for this orifice and shows how its discharge coefficient depends on the working conditions specified by the values of S, ρ, and μ.

The mathematical form of the functional symbol or operator f remains entirely unknown until determined by experiment; but it is certain that some such equation exists, because changes of S, ρ, and μ do sometimes affect the value of C, and the list of variables is complete because, so long as the orifice remains unchanged there is nothing else of importance that can be varied independently.

For an orifice of another shape or size the operator f may be of somewhat different form, and an equation which should hold generally for all orifices would evidently have to contain a sufficient number of geometrical quantities to account for all possible variations of shape and size; but if the problem is limited to orifices of any one shape, the only additional independent variable needed is a single linear dimension such as the orifice diameter d, and there is some equation

$$C=F(S,\rho,\mu,d) \tag{55}$$

which holds generally for all orifices of the given shape.

The form of F depends on the shape and can be determined only by experiment, but it is subject to an important restriction which simplifies the experimental problem very much. This is the familiar condition that all the terms of the equation must be of the same dimensions. Now, the discharge coefficient C is dimensionless, or of zero dimensions, for it is a pure ratio, and its value is independent of the unit by which the actual and theoretical rates of discharge are measured. Hence, all the terms in the second member of (55) must also be of zero dimensions, and in order that this may certainly be true, regardless of the still unknown form of the operator F, it is necessary and sufficient that all the operands or quantities operated on should be of zero dimensions.

The quantities S, ρ, μ, d do not satisfy this condition, and they can, therefore, not appear separately but only in combinations, each of which, taken as a whole, is of zero dimensions. The expression

$$\frac{dS\rho}{\mu}=R \tag{56}$$

satisfies this requirement, as is evident upon substitution from the dimensional equations $[d]=[l]$, $[S]=[lt^{-1}]$, $[\rho]=[ml^{-3}]$, and $[\mu]=[ml^{-1}t^{-1}]$, and there is no other such combination. Hence, equation (55) is restricted to the more specific form

$$C=\varphi\left(\frac{dS\rho}{\mu}\right)=\varphi(R) \tag{57}$$

The form of φ still remains to be found from experiment, but there is now only one independent variable R, instead of the four in (55); and when the experiments have been made, the results can be represented within the experimental errors by a plane curve.

The statement made above, that R is the only dimensionless combination of S, ρ, μ, d, is, of course, to be understood as meaning that there is no other combination which is independent of R. Such expressions as R^3 or $\log R$ are also of zero dimensions, but their values are fixed by that of R and can not be varied independently of it. So long as the form of φ remains indeterminate, equation (57) is merely a statement that the value of C is fixed by that of R; and the introduction into the second member of any number of additional quantities, each one of which was itself completely determined by R, would not change the meaning of the equation in any way.

On the other hand, it is entirely permissible to replace R by any other quantity which is determined by R. In other words, in representing the results of experiment by a plane curve with C as ordinate, we may use any convenient function of R as the abscissa in place of R itself.

For example, the mass flow M is connected with the density, the diameter of the orifice, and the mean linear speed through it, by the equation

$$M=\frac{\pi}{4}d^2\rho S \tag{58}$$

so that

$$\frac{M}{d\mu}=\frac{\pi dS\rho}{4\mu} \tag{59}$$

Hence, the quantity

$$\frac{M}{d\mu}=R'=\frac{\pi}{4}R \tag{60}$$

may serve in place of R, and equation (57) is equivalent to an equation

$$C=\psi(R') \tag{61}$$

Since the diameter ratio β is one element of "the given shape," the pipe diameter D is fixed by d and the quantity

$$\frac{M}{D\mu}=R''=\frac{\pi}{4}\beta R \tag{62}$$

is another possible substitute for R. Or if S_o denotes the mean linear speed along the pipe, the quantity

$$\frac{DS_o\rho}{\mu}=R'''=\beta R \tag{63}$$

may also serve as an independent variable; that is, as an abscissa against which observed values of C may be plotted as ordinates.

In discussions of the loss of head in pipes the quantity R''' defined by (63) is commonly called "the Reynolds number," though other expressions derived from it might equally well receive that name, and the same term is often used of the analogous quantities which occur in the investigation of other problems in fluid motion, such as the forces on airplanes. In the case of an orifice it may be applied to any one of the quantities defined by (56), (60), (62), and (63) or to any other quantity which is fixed by them.

In any event, the conclusion reached by the argument from dimensions may be expressed by the statement that, for orifices of any one shape, the discharge coefficient for liquids is a function of the Reynolds number only. The values of C for all orifices of the specified shape, whatever the absolute size of the orifice or the nature of the liquid or the rate of discharge, may be represented by a single curve which pertains to and is fixed by the particular shape in question; and when the curve has been determined by experiment the value of C under any future conditions may be found by computing the value of the Reynolds number for these conditions and reading the value of C from the curve.

If the Reynolds number has the same value in two different experiments on orifices of the given shape, the discharge coefficients will be equal, and the phrase "similar working conditions," which was used earlier, is to be interpreted as meaning "conditions under which the Reynolds number has the same value." This state of affairs—geometrically similar orifices operating under similar working conditions or at the same Reynolds number—is often described by saying that the phenomena are "dynamically similar," and the equality of the discharge coefficients of geometrically similar orifices at equal values of the Reynolds number is a particular result of what is commonly known as the "principle of dynamical similarity."

The foregoing discussion has referred only to liquids, and in order to extend it to gases the additional property of compressibility must be taken into account. This presents no great difficulty, but without any further development of the dimensional reasoning it is sufficiently

obvious that if the fall of pressure at the orifice is only a small fraction of the absolute static pressure the change of density can have only an insignificant effect, and the gas will behave sensibly like a liquid. If the curve $C=\varphi(R)$ has been determined for orifices of a particular shape by experimenting on liquids, the same curve is therefore applicable to gases, provided that the percentage differential is very small. Hodgson's experimental results are in entire agreement with this statement.

Since the purpose here has been merely to present the idea of the Reynolds number and to emphasize its importance for the benefit of readers who are not already familiar with the subject,[22] it is unnecessary to enter upon a detailed discussion of the experimental data which have been published or of the forms of the curves for orifices of different diameter ratios. The data have been examined, and the conclusion drawn from them regarding the effects of viscosity in commercial orifice meter practice has been stated in section 24 of the body of the paper.

WASHINGTON, August 22, 1928.

[22] For further discussion of the dimensional method see E. Buckingham, Model experiments and the forms of empirical equations, Trans. Am. Soc. Mech. Eng., 37, p. 262; 1915.